UNIVERSITA' DEGLI STUDI DI MILANO

Dottorato di Ricerca in Biologia Molecolare e Cellulare

XXXIII ciclo

Characterization of TLS Polymerase η function under replication stress induced by low dNTP pools

Giulia Maria Nava

PhD Thesis

Scientific tutor: Federico Lazzaro

Academic year: 2020-2021

Thesis performed at: Department of Biosciences,
University of Milan,
Milan 20133, Italy

Table of Contents

Abstract in Italian

Durante diversi processi cellulari l'RNA e il DNA possono appaiarsi, portando alla formazione di ibridi RNA:DNA. Sebbene queste strutture abbiano una rilevanza fisiologica, il loro stabile accumulo induce stress replicativo, compromettendo la replicazione del DNA e la stabilità del genoma. Le cellule possiedono due enzimi in grado di processare gli ibridi di RNA:DNA: l'RNasi H1, che taglia solo ribonucleotidi consecutivi, e l'RNasi H2 che processa sia ribonucleotidi singoli che multipli. Mutazioni dell'RNasi H2 sono associate a carcinogenesi e ad una grave malattia auto-infiammatoria chiamata sindrome di Aicardi-Goutières. Nel lievito *S.cerevisiae* l'assenza delle RNase H (*rnh1Δ rnh201Δ*) causa un accumulo di ribonucleotidi nel genoma, e una sensibilità a diversi agenti che inducono stress replicativo, tra cui l'idrossiurea (HU), un composto che riduce la concentrazione di nucleotidi, bloccando le forche replicative. Inaspettatamente, noi abbiamo scoperto che questa sensibilità all'HU è causata dall'attività della DNA polimerasi translesione η (codificata dal gene *RAD30*).

In questo studio, abbiamo dunque caratterizzato questo nuovo ruolo di Pol η in HU, e la tossicità che ne deriva dall'assenza di RNasi H, concentrandoci anche sui possibili meccanismi regolatori. I nostri dati indicano che Pol η lavora a livello delle forche replicative stressate dall'HU, con un reclutamento che sembra dipendere dalla mono-ubiquitinazione di PCNA, e che potrebbe anche essere regolato dai livelli di SUMOilazione di Pol η. Abbiamo dimostrato che l'attività catalitica di Pol η è dannosa in cellule prive di RNasi H, causando l'attivazione del checkpoint del danno al DNA e l'arresto in G2 / M. Questi effetti deleteri si verificano durante il primo ciclo di replicazione in HU, e sembrano derivare dall'incorporazione di tratti di ribonucleotidi promossa da Pol η. In accordo, un mutante di Pol η che incorpora più ribonucleotidi, incrementa ulteriormente la sensibilità all'HU delle cellule prive di RNasi H.

Tutti questi dati sono compatibili con l'idea che Pol η promuova la replicazione del DNA quando le forche sono bloccate dalla carenza di dNTPs, inducendo la formazione o la stabilizzazione d'ibridi RNA: DNA. Questi ibridi potrebbero derivare dall'incorporazione diretta di ribonucleotidi nel DNA, da un'errata maturazione dei frammenti di Okazaki, o dalla stabilizzazione di R-loops. Tuttavia, in uno scenario in cui le RNasi H non riescono a ripristinare il corretto appaiamento DNA:DNA, questi ibridi diventano tossici per le cellule. Infine, eseguendo uno screening genetico (SGA), ho identificato alcuni interattori negativi di *RAD30* che potrebbero compensare la sua funzione a livello delle forche replicative bloccate dall'HU.

Abstract in English

RNA:DNA hybrids are transient physiological intermediates that arise during several cellular processes such as DNA replication. Although these structures have physiological relevance, their stable accumulation perturbs DNA replication, inducing replication stress and genome instability. Cells possess two enzymes that process these structures restoring the correct DNA:DNA sequence: RNase H1, which just handles stretches of multiple rNMPs, and RNase H2 that processes either single or multiple ribonucleotides hybridized with DNA. Mutations in the human RNase H2 lead to carcinogenesis and a severe auto-inflammatory disease known as Aicardi-Goutières syndrome. *S.cerevisiae* yeast cells lacking RNases H enzymes *(rnh1Δ rnh201Δ)* accumulate ribonucleotides in their genome, becoming sensitive to different replication-stress inducing agents such as hydroxyurea (HU), a compound that decreases the dNTP pools, stalling replication forks. Unexpectedly, we found that this HU-sensitivity is completely suppressed by removing the *RAD30* gene, coding for the translesion DNA polymerase η.

In this study, I characterized this novel activity for the yeast Pol η under HU-induced replication stress, and the toxicity observed in RNase H depleted-cells, also focusing on possible regulatory mechanisms. Our data indicate that Pol η acts at HU-stressed replication forks, with recruitment that seems to depend on PCNA mono-Ub, and might also be regulated by the Pol η-SUMOylation levels. We proved that the catalytic reaction performed by Pol η is detrimental for RNase H deficient cells, causing DNA damage checkpoint activation and G2/M arrest. These harmful effects arise during the first replication cycle in HU and seem to be due to the incorporation of stretches of ribonucleotides promoted by Pol η. In agreement, a Pol η mutant allele with enhanced ribonucleotide incorporation further exacerbates the sensitivity to HU of cells lacking RNases H enzymes.

All these data are compatible with a model in which Pol η promotes DNA replication from stalled replication forks, inducing the formation or stabilization of RNA:DNA hybrids. These hybrids could result from either direct incorporation of rNMPs into DNA or incorrect Okazaki fragments maturation or R-loops stabilization. However, in a scenario where RNase H activity fails to restore DNA, these hybrids become toxic for cells. Finally, performing an SGA screening, I identified some negative interactors of *RAD30* that might compensate for the role played by the polymerase at HU-stalled replication forks.

Aim of the Project

Replication stress is defined as slowing or stalling in replication fork progression. This condition, which can arise from several endogenous or exogenous sources, is the main driver of genome instability, leading to tumorigenesis and cancer progression [1]. Conversely, many therapeutic strategies aim to exploit replication stress to generate an unsustainable level of damage in cancer cells, which selectively kill them [2]. Therefore, the growth of precancerous or cancerous cells strongly depends on their ability to tolerate replication stress.

In this regard, a key role is played by translesion synthesis (TLS) DNA polymerases that can deal with many barriers encountered during replication fork progression thanks to their spacious active sites [3]. Among the different TLS polymerases, I am interested in the study of the Y-family translesion DNA Pol η due to its aberrant expression in many cancer types and its broader role in dealing with different replication stress conditions. For decades its activity has been restricted to an accurate DNA translesion synthesis (TLS) opposite UV-induced thymine dimers and other DNA distorting lesions [4,5]. However, It is now starting to emerge that Pol η can deal with many other lesion-independent replication stress conditions (reviewed in [6]). Pol η downregulation is associated with the genetic disease Xeroderma Pigmentosum-Variant (XPV), characterized by sun sensitivity and elevated incidence of skin cancer [7]. On the other hand, high expression of Pol η has been found in several tumors and has been linked to chemoresistance [8–11]. Due to these outcomes, it appears crucial to characterize how different types of replication stress can trigger the activity of Pol η, in order to understand in deep the contribution of Pol η to genome stability.

Working with *S.cerevisiae* yeast cells, we found that Pol η plays a role when replication stress is induced by depletion of nucleotide pools (Hydroxyurea treatment). In particular, this role becomes deleterious in the absence of RNases H enzymes required to process RNA:DNA hybrids in cells, suggesting an intriguing and unexpected role of RNA in these processes. In this view, the aim of my project was to characterize at the molecular level this alternative role played by the yeast Pol η, and how it becomes toxic in RNase H depleted-cells.

Introduction

Endogenous and exogenous sources of DNA damage and replication stress

DNA replication is a fundamental process of the cell that ensures accurate duplication of the genetic information and subsequent transfer to daughter cells. In Eukaryotes, this complicated and tightly regulated process is initiated at multiple replication origins from which two replication forks travel bi-directionally until the entire genome is replicated. Before the S-phase, each origin is "licensed" by a combination of proteins to prepare the chromatin for replication[12]. Synthesis is subsequently initiated at the beginning of the S-phase in a process called origin firing[13]. The parental duplex is unwound by the helicases Cdc45-GINS-MCM2-7 (CMG), allowing access to the replicative DNA polymerases. These include the DNA polymerase α primase (pol α-Pri), and the DNA polymerases ε and δ that synthesize the leading and lagging strands respectively, with the help of the sliding clamp and processivity factor PCNA, RFC, and numerous additional factors. All these proteins together constitute a multi-subunit complex called replisome, which accounts for replication fork progression[13].

However, a variety of obstacles can slow or stall the replication fork progression and/or DNA synthesis, causing replication stress (reviewed in [14])**(Figure 1)**. Among the most commonly recognized sources of replication stress, there are DNA lesions that can distort the DNA helix or induce breaks, hampering the replication fork progression. Exogenous agents that generate DNA lesions include UV light, ionizing radiation, and numerous genotoxic chemicals, while endogenous sources of damage include reactive oxygen species formed as by-products of normal cellular metabolism or abasic sites resulted from hydrolysis of nucleotide residues[15]. Moreover, despite the replicative DNA polymerases are highly accurate, sometimes they introduce errors in the genome such as mismatches, insertion, deletions, or misincorporation of ribonucleotides instead of deoxyribonucleotides [16].

Besides, many DNA sequences are intrinsically challenging for the replication machinery. Examples include trinucleotide repeats that can form secondary DNA structures, G-quadruplexes structures formed in GC-rich DNA, protein-DNA complexes, and Common fragile sites (CFSs), defined as difficult-to-replicate DNA loci present in the human genome that accumulate breaks or gaps in response to mild replication stress[14]. Furthermore, since transcription operates on DNA, this process inevitably interferes with the replication fork progression. Collisions between transcription and replication machinery are indeed an important source of replication stress[17,18]. In addition, during transcription, the nascent RNA can hybridize back to the complementary DNA strand, forming a triplex structure with an RNA:DNA hybrid and a displaced ssDNA that is termed R-loop[19]. Moreover, highly transcribed yeast genes migrate to the nuclear periphery, anchoring the nuclear pore to facilitate RNA export. However, it was reported that the nuclear positioning of transcribed genes generates a topological impediment for incoming replication forks[20].

In general, replication requires several factors, including nucleotides and replication machinery components that, when limiting, can slow replication forks and induce replication stress. Depletion of dNTP pools is a condition typically observed in many types of cancers and can be artificially recapitulated using a compound called hydroxyurea (HU), which selectively inhibits the ribonucleotide reductase enzyme (RNR), preventing the conversion of rNTPs into dNTPs. Aphidicolin (APH) is another compound that inhibiting the B-family DNA polymerases slows down the replication fork progression. Finally, the overexpression or constitutive activation of oncogenes is another emerging source of replication stress[21].

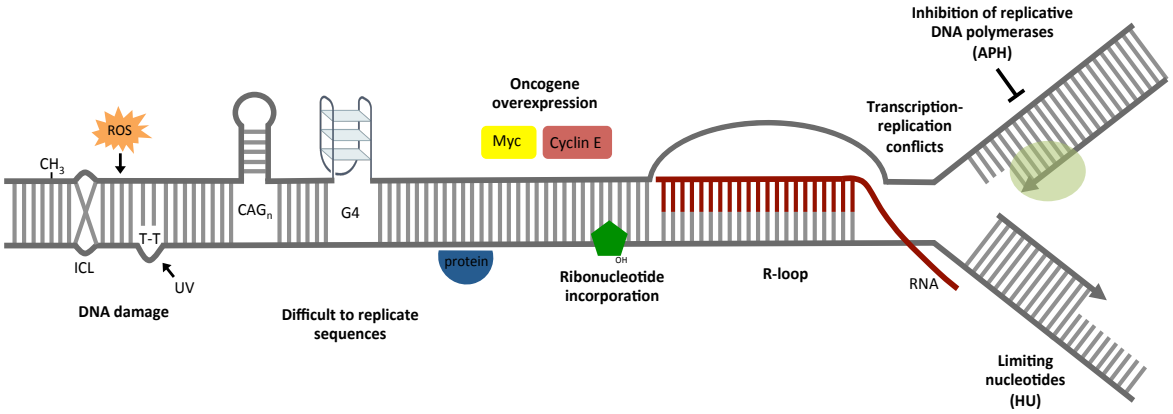

Figure 1. Sources of replication stress.

Replication stress response

Replication through all these obstacles can make the replisome stall, resulting in a condition defined as replication stress. Stalled forks usually expose single-stranded DNA (ssDNA) since replicative helicases continue to unwind for a short tract the parental DNA, while the replicative DNA polymerases are stalled. ssDNA is then coated by the replication protein A (RPA), and this is the signal that activate a surveillance pathway called the DNA replication checkpoint (explained later in the text), and recruits numerous factors that stabilize the stalled replication forks and promote the repair/removal of the obstacles. These multiple interconnecting pathways constitute the so-called Replication Stress Response[14]. Thanks to the existence of this response, stalled replication forks can resume DNA synthesis when replication stress has been relieved. Nevertheless, if replication stress persists or some replication-stress-response components are lost, the fork may fail to restart and collapse. Fork collapse results in replisome disassembly, ssDNA gaps, and DNA breaks, even if the mechanisms by which this occurs are still ambiguous[22,23].

Overall, a defective response to replication stress is the primary cause of genome instability, resulting in gross chromosomal rearrangements (GCRs), chromosome fusions, and chromosome fragmentation and loss. In humans, replication stress and genome instability are common features of most cancer and

precancerous cells and aging[1]. Therefore understand the causes and the consequences of replication stress can increase our comprehension of the early molecular steps involved in tumorigenesis and aging.

The replication checkpoint

At the center of the replication stress response, there is the activation of a signal transduction cascade, called the DNA replication checkpoint (DRC), whose aim is to sustain cell viability and protect genome integrity. Mutations in genes involved in this cascade are frequently found in cancers or genetic syndromes that lead to cancer predisposition. The replication checkpoint constitutes a specialized branch of the DNA damage checkpoint, and it is often referred to as the S phase (or intra-S phase checkpoint)[24–27]. In particular, stalled forks are sensed by protein sensors, and this information is communicated through signal transducers to effectors that mediate the physiological response of the cells. The entire cascade is highly conserved amongst eukaryotes, and here I summarize the yeast *S.cerevisiae* factors. The primary sensor is the apical kinase Mec1 (ATR in mammals), which is recruited to RPA-coated ssDNA exposed at stalled forks together with Ddc2[28]. Mec1 activation depends then on additional factors that include the 9-1-1 complex (Ddc1, Mec3, and Rad17), the replication factors Dpb11 and the DNA helicase/nuclease Dna2[29,30]. Once activated, Mec1 phosphorylates the effector kinase Rad53. This leads to Rad53 activation and subsequent autophosphorylation. Since Rad53 phosphorylation level correlates with its kinase activity and thus with the extent of damages, Rad53 phosphorylation is generally used as a marker of the checkpoint activation in yeast *S.cerevisiae.* Activation of Rad53 also depends upon Mec1 phosphorylating the mediator proteins Rad9 and Mrc1, which binds the FHA domains of Rad53 [31,32].While Rad9 seems to be more important for some types of DNA damage, Mrc1 seems to signal replication stress, since it travels with the replisome[31]. Other factors that emerged as important for the activation of Rad53 are the DNA helicase Sgs1[33,34], the MCM replicative helicases[35], and besides the Rad24-RFC, also the alternative RFC complex (RFC^{Ctf18})[36,37].

Once active, the effector kinase Rad53 acts on various biological processes together with Mec1, which can act both as a sensor and effector of the S-phase checkpoint. A first effect of the checkpoint is to rapidly inhibit DNA synthesis through repression of late and dormant origins[38,39]. Then the classical role of the checkpoint response is to delay progression through mitosis to prevent segregation of damaged DNA or incompletely replicated chromosomes[40–42]. This delay is required to allow DNA repair to occur. Indeed, depending on the obstacles that interfere with the replication fork progression, cells evolved specialized DNA repair pathways (reviewed in [43]). In line with this, another role of the checkpoint kinases is to induce the expression of DNA repair genes and maintain the expression of genes required for DNA replication. Another function of the checkpoint kinases is to up-regulate the dNTP levels, mainly through modulation of the ribonucleotide reductase activity (RNR)[44]. Finally, the

most crucial function of the checkpoint kinases is to protect the fork stability, preserving the ability of the replisome to resume DNA synthesis once the stress is relieved, and preventing fork collapse[23,45,46].

DNA damage tolerance mechanisms

Besides the existence of a plethora of DNA repair pathways that act removing lesions that hamper the replication fork progression, cells evolved specialized mechanisms named DNA damage tolerance (DDT) or post-replication repair (PRR) mechanisms that allow the cell to bypass or "tolerate" lesions encountered during DNA replication, allowing completion of DNA replication. There are two predominant post-replication repair pathways conserved in all the eukaryotic kingdom (reviewed in [47–49]): translesion synthesis (TLS), which involves specialized DNA polymerases able to directly replicate across the lesion and template switching (TS), which is more accurate since it involves recombination to a homologous template, usually the sister chromatid. Several studies support that both pathways are coupled with on-going DNA replication[50–53]. However, the observation that ssDNA gaps can persist into late S/G2, together with the finding that restricting the DTT to G2/M phase does not affect cell viability [54,55] indicates that damage bypass also functions post-replicatively in the G2 phase.

Post-translational modifications of the proliferating cell nuclear antigen (PCNA) play a key role in regulating the choice between the different DTT pathways **(Figure 2)**. PCNA is a homotrimer essential for the processivity of DNA polymerases by tethering polymerases to DNA, but it also represents a loading platform for a variety of proteins that participate in DNA replication and repair [56]. In particular, apart from activating the Replication checkpoint, RPA-coated ssDNA also promotes the recruitment of the E3 Ub-ligase Rad18, which, acting in complex with the E2 Ub-conjugating enzyme Rad6 mono-ubiquitinate PCNA at the conserved residue K164 [57–60]. This is the signal that stimulates TLS activity. Importantly, Rad18 does not seem to be the only enzyme that mono-ubiquitinate PCNA [61–63], and lines of evidence suggested that in some instances TLS can proceed independently on PCNA mono-ubiquitination [64]. K164 mono-ubiquitination can be further extended to K63-linked ubiquitin chain by the E3 ligase Rad5, which acts together with the E2 enzyme Ubc13 and the E2-like enzyme Mms2 [57,65,66]. This poly-ubiquitination of PCNA signals the cell to switch from TLS to TS. However, it was recently proved that Rad5 also has an Mms2-Ubc13 independent role in the TLS pathway [67]. Moreover, apart from having a ubiquitin ligase activity, Rad5 also has an ATPase activity able to catalyze fork reversal [68].

Historically PCNA ubiquitination and DTT pathways have always been related to DNA-Damage bypass. However, it is now clear that DTT can be active also in the absence of DNA lesions. For instance, Ub-PCNA is seen in cells experiencing replication stress induced by hydroxyurea, which depletes dNTPs without generating DNA lesions [60,69]. Ub-PCNA is also seen when there is an overexpression of oncogenes that lead to dysfunctional DNA replication [70], and it was suggested that

PCNA-Ub has a role during normal DNA replication, promoting an efficient lagging-strand DNA synthesis [71,72].

K164 and the nearby K127 of PCNA can also be targeted for SUMOylation. PCNA SUMOylation is observed normally during S-phase or after high dosage of DNA damage and is mediated by the E2-E3 complex Ubc9-Siz1 [57,58]. Although the precise role of this modification is still mysterious, it seems that SUMO-PCNA interacts with the anti-recombinogenic helicase Srs2, which displaces Rad51 from DNA preventing repair through Homologous Recombination in the S phase, thereby facilitating ubiquitin-dependent DDT pathways [69,73]. The ability of Rad18 to target PCNA is indeed strongly enhanced by SUMO-PCNA. Again, PCNA can be the target for other modifications, like ISGylation, acetylation, methylation, and phosphorylation, all involved in regulating its activity during DNA replication and repair (reviewed in [49]).

Since PCNA functions as a trimer, more than one modification can occur on the same clamp. However, whether this happens *in vivo* is still unclear. Moreover, although the main players involved in DDT have been identified, many aspects regarding their coordinate regulation and crosstalk are still obscure. How cell selects TS over TLS, and whether the choice depends on the specific type of damage is still unknown. Answer to those questions can significantly impact the development of chemotherapeutic approaches since players in DDT are frequently defective or overexpressed in different types of cancer[70].

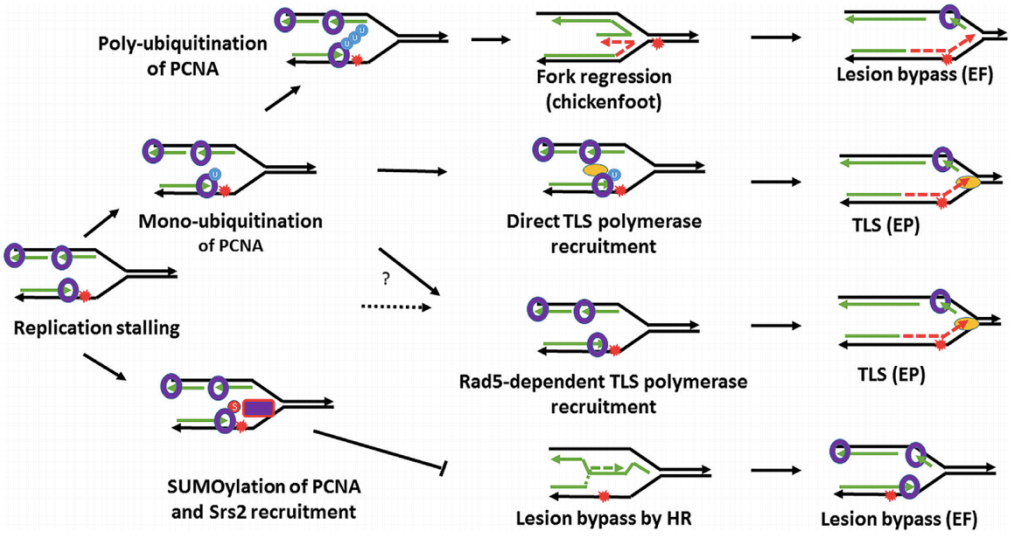

Figure 2. Sub-pathways of the DDT[74].

Template Switching (TS)

The Template Switching is considered an error-free mechanism since it uses the information present in the nascent sister chromatid to bypass stalled replication forks. This mechanism is triggered by the

poly-ubiquitination of PCNA, which in yeast is mediated by Rad5, Mms2, and Ubc13. Poly-ubiquitination is also observed in mammalian cells, where in addition to Mms2 and Ubc13, there are two Rad5 orthologs, which seem to poly-ubiquitinate PCNA via distinct mechanisms: HLTF [75] and SHPRH [76]. Moreover, mouse embryonic fibroblasts lacking both those factors retain the ability to poly-ubiquitinate PCNA, suggesting the existence of another backup E3 ligase [77]. How poly-ubiquitinated PCNA itself signals for TS is still enigmatic, and many aspects regarding the molecular mechanisms used by TS are still obscure.

Anyway, it seems that following PCNA poly-ubiquitination the newly synthesized ssDNA blocked ahead of the DNA lesion present in the template strand, anneals with the daughter's newly synthesized strand forming a three-strand duplex. Homology search and strand invasion seem to be promoted by Rad51, Rad52, Rad54, Rad55, and Rad57 [78–80]. Then, Pol δ extends the DNA by using the daughter's newly synthesized strand as a template. The result is the formation of recombination-like structures called sister chromatic junctions (SCJs) [79], which are preferentially processed by the Sgs1-Top3-Rim1 complex [81]. Other players involved in TS are Pol α primase, Ctf4, and the cohesion complexes that facilitate sister chromatid recombination maintaining nascent sister chromatids nearby [82,83]. In addition, in humans, the Exo1 nuclease and the 9-1-1 (Rad9-Hus1-Rad1) complex were recently implicated in the TS pathway [84].

Besides its Ubiquitin-ligase activity, Rad5 also has an ATPase activity able to promote fork reversal. The result is a structure termed chicken foot, which in theory is a substrate suitable for TS by allowing nascent DNA strands to anneal to provide a template for synthesis past a blockage on the other strand. Besides, reversed forks provide a means to stabilize stalled forks during stress, protecting labile DNA structures from nucleolytic degradation [85].

Translesion synthesis (TLS)

Translesion DNA synthesis utilizes low-fidelity DNA polymerases (TLS) able to replicate directly past the lesions thanks to their large active site, which is flexible enough to accommodate damaged nucleotides[86]. As for the replicative polymerases, also in TLS, we can identify a Palm, Thumb, and Fingers domain. The Palm domain contains the carboxylate residues necessary for the catalysis, while the Fingers and Thumb are shorter compared with the replicative polymerases, making fewer contact with both the template and incoming nucleotide: this contributes to the low fidelity and processivity of TLS[87,88]. These features make worsen by the lack of the 3'-5' exonuclease activity that is characteristic of replicative polymerases[89]. Finally, a TLS-specific additional domain, known as the little-finger domain or polymerase-associated domain (PAD), helps to stabilize TLS polymerases on DNA[88,90,91].

The budding yeast *S.cerevisiae* has three TLS polymerases: Rev1 and Pol η, which belong to the Y family, and Pol ζ, a member of the B family. Later in the text, each of these TLS will be discussed in

detail, paying particular attention to Pol η. Mammals possess two further Y-family polymerases: Pol κ and Pol ι [3] **(Figure 3)**. How the most appropriate TLS is chosen to bypass a specific lesion is still controversial and under extensive studies (reviewed in [92]). Each of these polymerases has indeed one or more cognate lesions, which the enzyme bypasses with relatively high accuracy and efficiency. However, the activity of TLS is generally considered error-prone and mutagenic[93], and TLS overexpression is frequently linked to tumorigenesis and chemotherapy resistance[8–11]. This occurs when TLS bypass the DNA damage caused by the chemotherapy drugs. An example is resistance to cisplatin-inducing treatment, due to the ability of Pol η to bypass the DNA damage adducts caused by the cisplatin-based drugs [10,11]. On the other hand, reduced TLS activity can also lead to cancer predisposition[7]. Therefore, the access of TLS to replication forks must be strictly regulated (reviewed in[94]). A central scaffold for the binding and the recruitment of TLS on DNA is PCNA: interaction with mono-Ub PCNA is mediated by a specific ubiquitin-binding zinc finger (UBZ) or ubiquitin-binding motif (UBM) present in the Y-family polymerases[95]. Additional interaction with PCNA occurs through the canonical PCNA-interacting peptide (PIP) found in all the TLS, except for Rev1 where PCNA-interaction is mediated by its BRCT domain[96,97]. Another level of regulation is posttranslational modifications of the TLS themselves by for instance ubiquitination, phosphorylation, O-GlcNAcylation and SUMOylation [94]. Finally, TLS abundance can also be regulated in a cell-cycle dependent manner. In both *S.cerevisiae* and mammals, for instance, the levels of Rev1 and Polη peak at the G2/M phase relative to G1 and S[98–102]. However, a recent study demonstrated that in presence of UV radiation or hydroxyurea (HU) treatment, which causes replication stress limiting dNTP pools, both Rev1 and Pol η start to accumulate in S-phase [103].

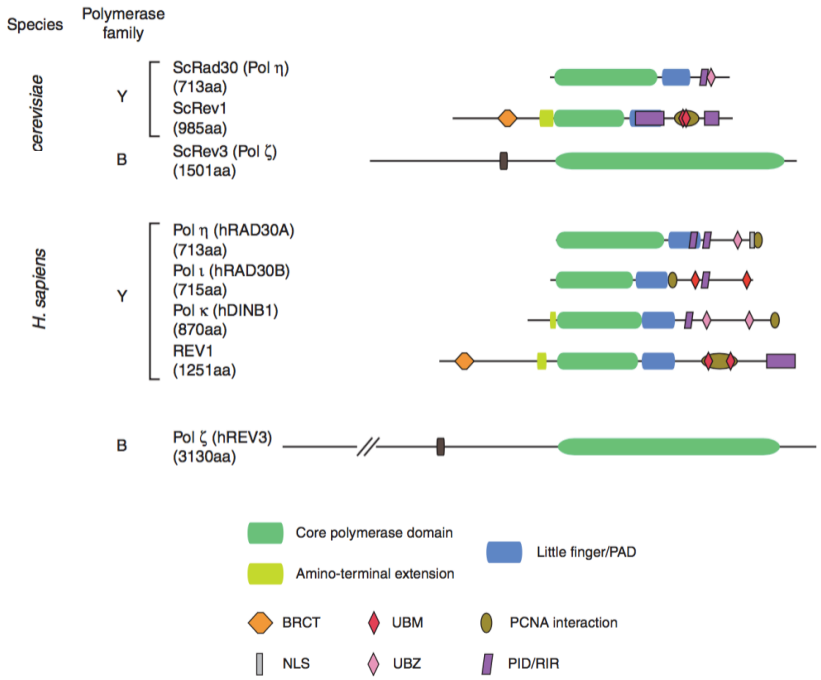

Figure 3. Domain structure of TLS polymerases in *S.cerevisiae* and *Homo sapiens*[104].

Translesion synthesis is thought to occur via two non-mutually exclusive processes: the polymerase switching model and the gap-filling model (reviewed in[105]). The first mechanism takes place during active DNA replication where, after replication fork stalling, replicative DNA polymerases are temporally exchanged with TLS polymerases. Lesion bypass and extension may require the action of one or more TLS polymerases and, finally, a further switch restore an accurate DNA synthesis by replicative polymerases[106–109]. The gap-filling model instead, occurs outside the context of the replication forks during G1 and G2/M phases or in the last stages of the S phase. Here the purpose of TLS is not to restart a stalled replication fork, but rather to fill gaps originated when the DNA replication fork stalled and restarted downstream of the lesion[100,108,110,111]. This lesion-skipping mechanism requires a primase activity to reinitiate DNA synthesis downstream of the damaged site. Interestingly, in human de novo primer synthesis rely on a newly discovered protein called PRImase and DNA-directed POLymerase (PRIMPOL), which possesses both primase and polymerase activities (reviewed in [112]). Orthologs of PRIMPOL are absent in budding yeast, where repriming seems to be promoted by the Pol α primase complex [50,54,113].

Rev1 is a TLS with deoxycytidyl (dCMP) transferase activity[114]. This means that its activity is restricted primarily to introducing dCMP nucleotides preferentially on G template or abasic sites [115]. Interestingly, complete loss of Rev1 compromises the bypass of lesions that are not substrate for its catalytic activity. This can be explained by the fact that besides its catalytic activity, Rev1 plays an important role in coordinating the activity of the other TLS through protein-protein interactions. Its C-terminal domain (CTD) can indeed associate with Y-family polymerases[116–118] and with Pol ζ[119]. This, combined with the interaction between Rev1 and PCNA mediated by the BRCT domain, leads to a model in which Rev1 functions primarily as a molecular "bridge" between PCNA and TLS polymerases, rather than by bypassing lesions directly.

DNA Polymerase ζ is a B-family enzyme related to the replicative polymerases α, ε, and δ, even though its 3'-5' exonuclease domain is inactivated by mutations. It is a heterodimer composed of the Rev3 catalytic subunit and the Rev7 accessory subunits[120]. Interestingly, upon Pol δ stalling at DNA lesions, the catalytic subunit of Pol δ seems to dissociate, while its Pol31 and Pol32 subunits can associate with Rev3/Rev7. The result is a tetrameric enzyme, which exhibits more efficient and processive activity than the Rev3/Rev7 complex alone[121,122]. Pol ζ is generally inefficient at inserting bases opposite lesions but it is very proficient at extending distorted base pairs, such as mismatches that might result from inaccurate base insertion by other TLS polymerases or a base pair involving a bulky DNA lesion[3,123]. Nevertheless, sometimes it can also insert nucleotide across damaged bases, for example, it is capable of single-step bypass of 6-4 photoproducts[124–126], and in budding yeast, it is also able to replicate DNA containing rNMPs [127].

Pol η TLS-dependent functions

DNA polymerase η, encoded by *RAD30* gene in yeast and POLH gene in humans, is a Y-family DNA polymerase able to faithfully bypass several distorting DNA lesions. It is the primary TLS responsible for an error-free bypass of *cis-syn* cyclobutane pyrimidine dimers (CPDs), one of the major lesions resulting from UV radiation [4,128]. Pol η also bypasses oxidative DNA lesions such as 7,8-dihydro-8-oxoguanine (8-oxoG)[5] and thymine glycol (TG)[129], and other lesions such as abasic sites (AP-sites)[130], O^6-methylguanine (O^6-me-G)[131], acetylaminofluorene-adducted guanine[132] and (+)-*trans-anti*-benzo(a)pyrene-N^2-dG[133]. Moreover, it can bypass 1,2-intrastrand d(GpG)-cisplatin adducts [134]. On the other hand, Pol η exhibits low fidelity when copying undamaged DNA. This is consistent with a more open active site compared to the other polymerases that is less specific but better able to accommodate bulky lesions[88].

Several acid residues have been identified as important for the polymerase activity of yeast Pol η: Asp30, Glu39, and Asp155 are essential for Pol η function, since they coordinate the two metal ions necessary for phosphodiester bond formation, while Glu156 seems to participate in nucleotide binding[135]. Recently it was also demonstrated a role for the residues Gln55 and Arg73 in the DNA synthesis among different lesions[136]. Besides, like most DNA polymerases, Pol η has a conserved "steric gate" residue in its active site, which functions to prevent the incorporation of ribonucleotides during DNA synthesis. In *S.cerevisiae* this residue is the Phe35[137], while in humans it is the Phe18, which is stabilized by the Tyr92[138]. Mutations of those residues to alanine increase the propensity to introduce rNMPs over dNMPs into DNA. On the other hand, also WT hPol η can insert rNMPs on undamaged substrates or opposite several DNA lesions[138,139], even if this last condition makes RNase H2-dependent rNMPs removal greatly inefficient[139]. Furthermore, WT hPol η seems capable of synthesizing polyribonucleotide chains, and both yeast and human Pol η can also extend RNA primers incorporating dNMPs or rNMPs [140,141].

Pol η TLS-independent functions

Besides its TLS activity, Pol η also possesses many TLS-independent cellular functions, where the polymerase operates in no DNA-damage context **(Figure 4),** (reviewed in[6]). For instance, Pol η could play a role during HR-mediated DNA repair [142,143]. Pol η can indeed extend DNA synthesis from D-loops recombination intermediates, with an activity that is further stimulated by interaction with Rad51,[143] PALB2 and BRCA2[144]. Since D-loops do not harbour any lesion per se, this role is considered to be TLS independent. Moreover, this D-loop extension capability has a potential role in alleviating replication stress at the ATL telomeres, which strongly rely on recombination-associated DNA synthesis[145]. hPol η is also able to exchange with Pol δ stalled at Common fragile sites (CFSs)[146], and it is required to efficiently replicate these loci, maintaining their stability[147,148]. CFSs are defined as inherently unstable genomic loci exquisitely prone to breakage upon mild replication stress and

recurrently altered in human tumor cells. Consistently, hPol η seems required for S-phase progression during replication stress induced by hydroxyurea (HU), although its activity is proapoptotic[149]. Furthermore, among the variety of factors that induce CFSs instability, there is replication stress resulting from collisions with the transcription machinery[150], and hPol η seems critical for replication to continue upon co-directional collisions with lncRNAs[151].

Moreover, it was recently found that yeast Pol η seems to compete with the replicative DNA polymerases α and δ for the DNA replication of lagging strand[152] and besides this role in DNA replication, Pol η could also function in transcription, probably in the elongation step. Yeast Pol η was found to be enriched in hyper-transcribed regions, and the transcription of several genes was affected by its absence[140]. A transcriptional role is also supported by the fact that, as mentioned above, both yeast and human Pol η can extend RNA primers incorporating rNMPs[140,141]. Pol η also promotes faithful chromosomal segregation participating in the DNA damage-induced cohesion[153], and participates in the IgG diversification during somatic hyper mutation[154]. Furthermore, it is possible that other TLS-independent functions still have to be discovered. Indeed, while more than 20 years of extensive studies support the TLS activity of Pol η, the discovery of all these TLS-independent functions is relatively new. Comprehension of detailed molecular mechanisms is thus still limited and needs further clarification.

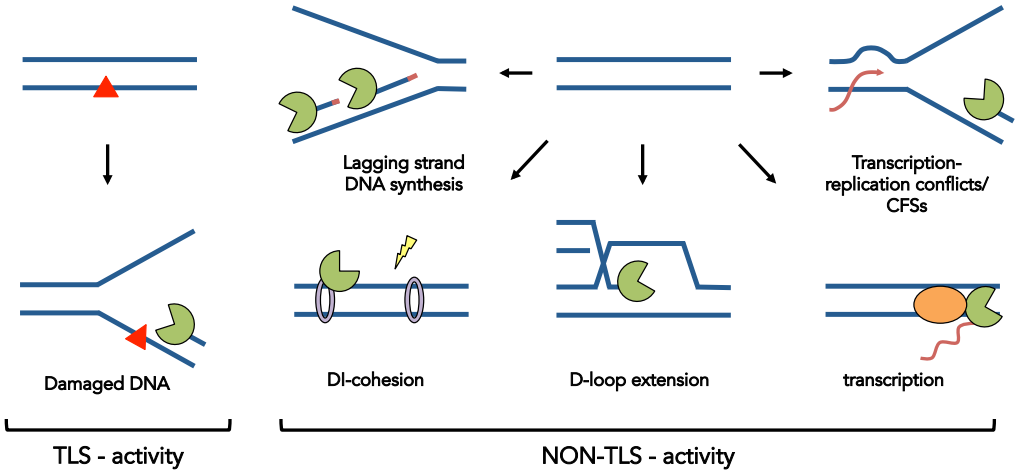

Figure 4. TLS dependent and independent functions of *S.cerevisiae* Polymerase η (modified from[6]).

Pol η regulation

Pol η downregulation is associated with the genetic disease Xeroderma Pigmentosum-Variant (XPV), characterized by sun sensitivity and elevated incidence of skin cancer[7]. On the other hand, since TLS activity can help cancer cells tolerate DNA Damage, high expression of Pol η has been found in

different tumors, including Head and Neck Squamous Cell Carcinomas[8], non-small cell Lung Carcinomas[9] and ovarian stem cells[10] and, Pol η overexpression seems to be responsible to chemoresistance to platinum-based treatments[10,11]. Therefore, it is clear that Pol η activity must be tightly modulated. The picture is further complicated by the plethora of TLS-independent functions of Pol η: cells have to regulate its recruitment in all these different situations.

As discussed above, the abundance of Pol η is regulated in a cell-cycle dependent manner, while PCNA-interactions regulate its recruitment on DNA. These interactions are mediated by the UBZ (ubiquitin-binding zinc finger) domain and the PCNA-interacting peptide (PIP) motif, located at the C-terminal of Pol η that bind to Ub-PCNA and PCNA respectively[155]. In *S.cerevisiae,* it was recently reported that without the UBZ domain, the PIP alone has a minor affinity for Ub-PCNA[156]. Furthermore, it was recently identified a second PIP (PIP2), whose function is maintaining the architecture and the dynamics of the complex[157]. Some conserved residues of the PIP can also bind Rev1, and because of that, they are sometimes referred to as Rev1-interacting region (RIR)[158]. Even if the importance of this C-terminal region of Pol η is still debated, it seems that all these motifs modulate protein localization without affecting the polymerase activity[95,159]. Finally, various post-translational modifications may also regulate Pol η activity. For example, in the absence of DNA damage, the hPol η can be mono-ubiquitinated on one of four lysines present in its PCNA interacting regions [160]. This induces a conformational change in the C-terminal of the protein, which prevents its interaction with chromatin. Then, after UV treatment, a de-ubiquitination event promotes hPol η interaction with PCNA [160]. Removal of hPol η from replication forks is also promoted by its poly-ubiquitination on K462 [161]. Interestingly, this modification is promoted by the O-GlcNAcylation on the adjacent T457 residue [161]. Unlike the inhibitory effect on TLS induced by ubiquitination, full TLS activation seems to be promoted by hPol η phosphorylation on S601 [162,163]. Furthermore, it was recently found that even in the absence of DNA damage, hPol η exists in multiple phosphorylation states, and its phosphorylation changes in a cell cycle-dependent manner [102]. Finally, hPol η can also be SUMOylated. In particular, while multiSUMOylation seems to reduce Pol η interaction with DNA damage sites[164], monoSUMOylation on K163 promotes the association of Pol η at the replication fork during unchallenged S phase[165]. This was the first evidence of a mechanism used to regulate a TLS-independent function of Pol η. Interestingly, the level of SUMOylation increases under lesion-independent replication stress induced by drugs such as hydroxyurea. Thus, it was proposed that mono-SUMOylation regulates the ability of hPol η to replicate common fragile sites (CFSs) in unchallenged S-phase, preventing their breakage, especially upon replication stress.

All these modifications were described for the human Pol η, and it is still not clear if they are also preserved in the yeast protein, where the study and clarification of the biological meaning can be more straightforward. Yeast Pol η seems to be either mono[155] or poly-ubiquitinated[166], and this latter modification seems to targets its proteasome degradation. Moreover, i*n vitro* studies recently found

that yeast Pol η can also be phosphorylated and acetylated[167]. In the same work, it has been proposed that phosphorylation regulates the TLS-independent role of Pol η during the damage-induced cohesion.

RNA in DNA

As described above, RNA into DNA represents an important cause of replication stress. RNA is considered unstable compared to DNA, due to the presence of a reactive 2'-OH group on the sugar moiety, which can attach the sugar-phosphate backbone, generating breaks with genotoxic outcomes [168]. This is the reason why cellular organisms store their genetic information into stable DNA molecules rather than in RNA. Nevertheless, RNA is frequently found in DNA. Examples include single and stretches of ribonucleoside monophosphates (rNMPs) introduced into DNA by DNA polymerases, polyribonucleotide chains synthesized to allow DNA replication priming, transcription bubbles and peculiar three-stranded nucleic acids structures termed R-loops, formed upon re-hybridization of the transcript to its template DNA, RNA:DNA hybrids formed at double-strand breaks (DSBs), etc **(**reviewed in[169]**)(Figure 5).** All these RNA:DNA hybrids contribute to regulate different physiological functions, but they have to be promptly removed to ensure genome integrity and genome stability. Here below, I described in detail origins and consequences of RNA in the genome, as well as pathways involved in their removal.

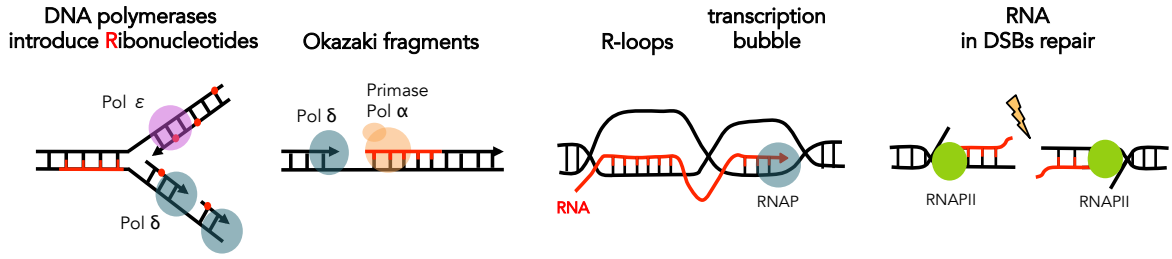

Figure 5. Sources and form of RNA:DNA hybrids present in cells

Ribonucleotides introduced by DNA Polymerases

Within a single round of DNA replication, DNA polymerases frequently incorporate ribonucleosides triphosphate (rNTPs), the normal constituent of RNA, instead of the canonical deoxyribonucleosides triphosphate (dNTPs) [170]. This phenomenon turned out to be extremely conserved from bacteria to humans and occurs more frequently than any other incorporation of abasic, oxidized, and modified nucleotides. It has been estimated that more than 2000, 10000, and 1000000 ribonucleotides are incorporated into bacteria [171], yeast, and mouse genomes respectively, during each cell division, making ribonucleotides the most frequently non-canonical nucleotides incorporated into duplex DNA [172].

Rates of incorporation are influenced by many factors: one of them is the rNTP in question, with rCTP being the most frequently incorporated [173,174]. Another determining factor is the sequence context: different groups using different but related techniques have recently mapped rNMPs locations genome-wide in budding [175–177] and fission yeast [178]. They found that the rNTP distribution is non-random, with more abundant ribonucleotides in the leading strand, and with preferential hotspots in correspondence of mitochondrial DNA, Ty regions, and rDNA locus[174]. The likelihood that rNTPs are mistakenly used instead of dNTPs is also increased by the fact that in physiological conditions there is a great excess of rNTPs over dNTPs (between 30- and 200- fold in *S.cerevisiae*, depending on the nucleotide) [170,179,180]. Consistently, a decrease of dNTP pools (by chemicals such as hydroxyurea (HU) that inhibit the ribonucleotide reductase enzyme) further increases the ribonucleotide incorporation frequency [181]. Finally, incorporation frequency varies depending on the DNA polymerase used. Studies under physiological rNTP:dNTP ratio revealed that *S.cerevisiae* replicative DNA polymerases α, δ, and ε incorporate one ribonucleotide every 625, 5000, or 1250 deoxyribonucleotides respectively [170]. Single ribonucleotides are also incorporated during mtDNA replication by the replicative DNA polymerase ϒ [182,183]. Finally, besides replicative DNA polymerases, an important contribution in ribonucleotides-incorporation is given by all the DNA polymerases involved in reparative DNA synthesis **(Table 1)** (reviewed in [169]). It should be highlighted that those latter are often active outside the S-phase when the concentration of dNTPs can be three-fold lower than in the S phase [44], and thus the rNTPs incorporation can be more relevant.

In order to choose the nucleotide containing the correct sugar, most DNA polymerases use a conserved "steric gate" residue, located at the entrance of their active site that clashes with the 2'OH of the incoming rNTP, physically blocking a nucleotide with the wrong sugar from being incorporated into DNA [184,185]. Residues directly flanking the steric gate also play a role in sugar selectivity [16,186] and recently it was identified an additional polar filter [187]. In B- and Y-family DNA polymerases the steric gate residue is almost always a tyrosine or a phenylalanine [186], and mutations that make the gate more flexible or more rigid, allow higher or lower rate of ribonucleotide misincorporation respectively. For example, in yeast, mutants of the replicative polymerases Pol ε *(pol2-M644G),* Pol δ *(pol3-L612M)*, and Pol α *(pol1-L868M)* incorporate 10, 8, and 15 times more ribonucleotides respectively[16,188,189]. Conversely, the mutant *pol2-M644L* is 3-fold less prone to introduce ribonucleotides [16]. Mutants with decreased sugar selectivity have been selected also for some TLS polymerases as *Scpolη-F35A* [137] and *polι-Y39A* [190].

Although DNA polymerases are mainly responsible for single rNMPs incorporation, under particular circumstances some of them might also incorporate stretches of consecutive rNMPs [169]. For instance, the fact that the *pol2-M644G* mutant becomes synthetic lethal with the simultaneous absence of RNase H1 and H2, suggests that it incorporates stretches of multiples rNMPs, requiring the activity of both

RNases H to be removed [127,169]. Or again, the polη-F35A mutant seems to incorporate stretches of rNMPs at a high rate, leaving a specific 1bp deletion signature, when not removed by RNase H2 [137,152]. Consecutive rNMPs might also be introduced by wild type DNA polymerases: we found that upon replication stress induced by hydroxyurea, *S.cerevisiae* Pol η is recruited at stalled replication forks, where it facilitates the formation of stretches of rNMPs that become highly toxic for cells if not properly repaired with DNA [191]. Again, Pol β seems able to catalyze the incorporation of up to 8 sequential rNMPs [192], *E.coli* polV synthesizes RNA stretches unusually long [193], and finally DinB2 from *Mycobacterium smegmatis* can synthesize even 16 consecutive rNMPs [194]. However, although different techniques can be used to visualize single rNMPs-incorporation to date, multiple embedded rNMPs have never been visualized *in vivo* (reviewed in [169]).

Who	Family	Role in	rNMPs Insertion
pol ε	B	replication/repair	undamaged leading strand
pol δ	B	replication/repair	undamaged lagging strand
pol α	B	replication/repair	undamaged lagging strand
pol ζ	B	TLS mitochondrial replication	rare
pol β	X	repair/TLS	undamaged template, CPDs 8-oxo-Gs
pol λ	X	repair/TLS	8-oxo-Gs
pol μ	X	repair	NHEJ ends
Tdt	X	repair	N-regions of V(D)J ends
pol η	Y	TLS lesion-independent replication stress	undamaged template HU-stalled replication forks 8-oxo-Gs, CPDs, cis-PtGG, 8-methyl-2′-deoxyGs
pol ι	Y	TLS	undamaged template, 8-oxo-Gs, abasic sites
pol κ	Y	TLS	unknown
Rev1	Y	TLS	rare
pol γ	A	mitochondrial replication	rare
pol θ	A	TLS/repair	alt-EJ ends
pol ν	A	TLS/repair	unknown
PrimPol	Archaeo eukaryotic primase superfamily	priming/TLS	undamaged template, 8-oxo-Gs

Table 1. rNMPs insertion by eukaryotic DNA polymerases opposite different DNA templates. Modified from[169]

Consequences of Ribonucleotides into DNA

The abundance and non-random distribution of rNMPs in DNA suggest that their presence may be useful for some biological functions (reviewed in [195]). It has been demonstrated indeed that rNMPs provide a mechanism to mark and initiate Miss Matches Repair (MMR) in eukaryotes [188,196]. While on the lagging strand, nicks from Okazaki fragments allow strand discrimination, it seems that on the leading strand nicks introduced by RNase H2 on rNMPs play this role, ensuring that MMR machinery specifically removes mismatches on the newly synthesized strand. Ribonucleotides promote also an

efficient DSB repair by NHEJ. The Pol μ implicated in the NHEJ pathway has indeed a very low rNTPs/dNTPs discrimination rate and it inserts primarily rNMPs, promoting an effective ligation by the DNA ligase IV [197–199].

Prompt removal of embedded ribonucleotides is anyway required to prevent several negative consequences. Firstly, unrepaired ribonucleotides affect the DNA structure: NMR and X-ray analysis report that a single rNMP within short DNA molecules seems to induce a partial shift from B to A-form conformation [200–202]. Similarly, randomly incorporated rNMPs within long DNA molecules (up to 1 kb in length) induce a shortening and increased elasticity of the DNA backbone [203]. Besides, *in vitro*, and *in silico* analyses report that ribonucleotides adversely affect the nucleosomes assembly [204,205] and once rNMPs are located into nucleosome particles, they seem to be protected by cleavage. rNMPs located in the central part of NPCs are indeed repaired 273-fold less efficiently than those in free dsDNA [206]. It is easy to imagine that all these effects can be even more significant when DNA contains polyribonucleotide tracks instead of single rNMPs. Unrepaired ribonucleotides hamper also DNA replication since replicative DNA polymerases are not very efficient in bypassing them. In *S.cerevisiae*, Pol δ and Pol ε show an efficiency of ≈ 60% on single rNMP bypass, and then they stall proportionally as the number of consecutive rNMPs increases from 1 to 4 [207]. Multiple rNMPs in the nucleus of *S.cerevisiae* are only tolerated thanks to the action of the template-switch and TLS Pol ζ [208]. Moreover, although the impact on DNA polymerases progression is known, an interesting and still unexplored aspect is how ribonucleotides impact the activity of RNA polymerases. In *S.cerevisiae* the expression of 349 genes results indeed altered in the absence of RNase H2, indicating that unrepaired rNMPs cause a transcriptional response [209]. Finally, persistent embedded rNMPs stimulate genomic instabilities (reviewed in [210]), which are manifest as mutagenesis (in terms of deletions in simple repeats to up of 5nt in length) [211], increased recombination, increased loss of heterozygosity (LHO) [212], and increased gross chromosome rearrangements (GCR). While some studies suggest that these phenotypes arise from improper mechanisms that repair single rNMPs in the absence of RNase H2 [213] (reported below), other studies find evidence that problems are mainly caused by multiple tandem rNMPs [214].

Ribonucleotides removal via RNase H

Incorrect bases in DNA are efficiently removed by the 3'- 5' exonuclease activities of the replicative DNA polymerases δ and ε. This mechanism, however, it is quite inefficient in case of an incorrect sugar insertion [215].

Ribonuclease H enzymes (RNase H) instead, are able to initiate rNMPs removal, cleaving DNA at sites of rNMPs incorporation [216]. They are evolutionary conserved, and in eukaryotes, they are divided into two main classes: RNase H1 and RNase H2. RNase H1 is a monomeric enzyme present in the nucleus and mitochondria, and it consists of an N-terminal hybrid binding domain (HBD) and a C-

terminal endonuclease motif, which can only recognize stretched with at least four consecutive rNMPs [217]. RNase H2 is composed of three subunits that in yeast are Rnh201 (catalytic), Rnh202, and Rnh203, (RNase H2A, RNase H2B, RNase H2C in higher eukaryotes, respectively), all essential for the activity of the complex and it can act both on single and consecutive rNMPs. [216] Although overlapping for the RNA:DNA hybrid removal activity, each RNase H enzyme seems to uniquely target specific rNMP stretches [218]. This was confirmed thanks to the development of a separation of function mutant of the RNase H2 enzyme, called rnh201-RED (ribonucleotide excision defective), which loses the ability to remove single rNMPs, but retains a discrete activity on consecutive rNMPs [219]. The two RNase H enzymes seem also to be differently regulated: while RNase H1 is active throughout the cell cycle, the RNase H2 processes its substrates in G2/M phase of the cell cycle [220].

RNase H2 is responsible for the primary pathway of rNMP removal from DNA, named error-free ribonucleotide excision repair (RER) pathway[221] **(Figure 6a).** *In vitro* reconstruction experiments have elucidated the mechanism in detail: single rNMPs are recognized by RNase H2, which cleave the DNA backbone on the 5' side of rNMPs generating a nick whose ends have a 3'OH and a 5'-RNA-DNA junction. The 3'OH is then extended by Pol δ or less efficiently by Pol ε generating a flap, which contains the rNMP. The flap is then processed by the flap endonuclease Fen1 and/or exonuclease Exo1 and the DNA ligase I seals the remaining nick [221]. Interestingly, it was recently found that the DEAD-box RNA helicase DDX3X has RNaseH2-like activity and can support fully reconstituted *in vitro* RER reactions, not only with Pol δ but also with the repair Pols β and λ [222]. Whether the RER pathway also works on consecutive rNMPs has never been proved. Indeed, even if both the RNase H enzymes can recognize tracks of rNMPs embedded into DNA, how the enzymes work *in vivo* on these structures need further clarification, and a detailed molecular mechanism has not been identified yet **(Figure 6d)**.

In bacteria and in yeast cells, both types of RNase H are dispensable for viability, showing an increase in genome instability only upon simultaneous absence of RNase H1 and H2 [208,223]. In higher eukaryotes, both enzymes are essential. Mouse cells *Rnaseh201*$^{-/-}$ accumulate rNMPs that below a certain threshold trigger an innate immune response but are permissive to mouse embryonic development, while above a threshold trigger a p53-induced apoptosis. This lethality was indeed rescued by concomitant inactivation of the p53 gene [224,225]. Death during the embryonic development is also observed in *Rnaseh1*$^{-/-}$ mice, due to incomplete mitochondrial replication [226]. Mutations in any of the three genes encoding human RNase H2 leads to Aicardi-Goutieres syndrome (AGS)[227], a rare inflammatory encephalopathy with infancy onset and characterized by high levels of Type I interferon (IFN alpha) production. Although alterations in different genes have been related to AGS (reviewed in [228]), mutations in the RNase H2 are observed in over 50% of the patients, with the RNaseH2B being the subunit most frequently mutated, and A177T the substitution most commonly observed [229]. RNase H2 dysfunctions have also been associated with systemic lupus erythematosus (SLE) [230] , CLL

(chronic lymphocytic leukemia) and CRPC (castration-resistant prostate cancer) [231]. RNase H2-mutated human cells accumulate rNMPs in their genome and exhibit constitutive post-replication repair (PRR) and DNA damage checkpoint activation [232].

Backup pathways for ribonucleotides removal

The backup strategy used to remove single embedded ribonucleotides in case of faulty RER, is based on Topoisomerase I (Top1)**(Figure 6B),** with an activity that seems to be specific for leading strand-rNMPs [233]. The mechanism starts when Top1 cuts on the 3' side of ribonucleotides, generating a nick containing 5'-OH and cyclic 2'-3' phosphate-terminated ends that require further processing before either ligation or extension is possible [234]. One possibility is that Top1 makes a second incision upstream of the initial one, releasing the rNMP-dNMP, and generating a 2 nt gap which can either be filled in an error-free pathway mediated by Tdp1 [235] or lead to a 2-5bp deletion whether incisions occur within tandem repeat sequences [235,236]. Another possibility is the repair of the nick by Apn2 and Srs2-Exo1 error-free pathway [237,238]. Finally, if Top1 makes a second cut on the complementary strand, the result is a DNA double-strand break (DSB), which can be repaired by either Rad51/52 mediated homologous recombination or by a Top1-mediated illegitimate recombination [239]. It is still unknown what dictates the choice between these different repair pathways and whether they are active also in the presence of RNase H2, collaborating to RER in the removal of rNMPs. While these pathways have been characterized in *S.cerevisiae*, it is now clear that Top1 can cut rNMPs also in RNase H2-mutant human cells [231].

Studies in bacteria identified the nucleotide excision repair (NER) as another backup pathway to remove ribonucleotides from DNA[240]. While in yeast a NER contribution to rNMP removal has been excluded [127], in human it was recently found that NER together with Pol η are involved in the processing of oxidized-ribonucleotides embedded into DNA [241] **(Figure 6C).**

Finally, when ribonucleotides cannot be removed, the activity of the post-replication repair (PRR) pathway becomes critical to tolerate their presence in the chromosomes. Indeed, the coordinate action of the Mms2-dependent template switch and the TLS Pol ζ, becomes crucial in yeast cells lacking both RNase H1 and H2, with Pol ζ which efficiently replicates over 1-4 rNMPs [127] **(Figure 6E)**.

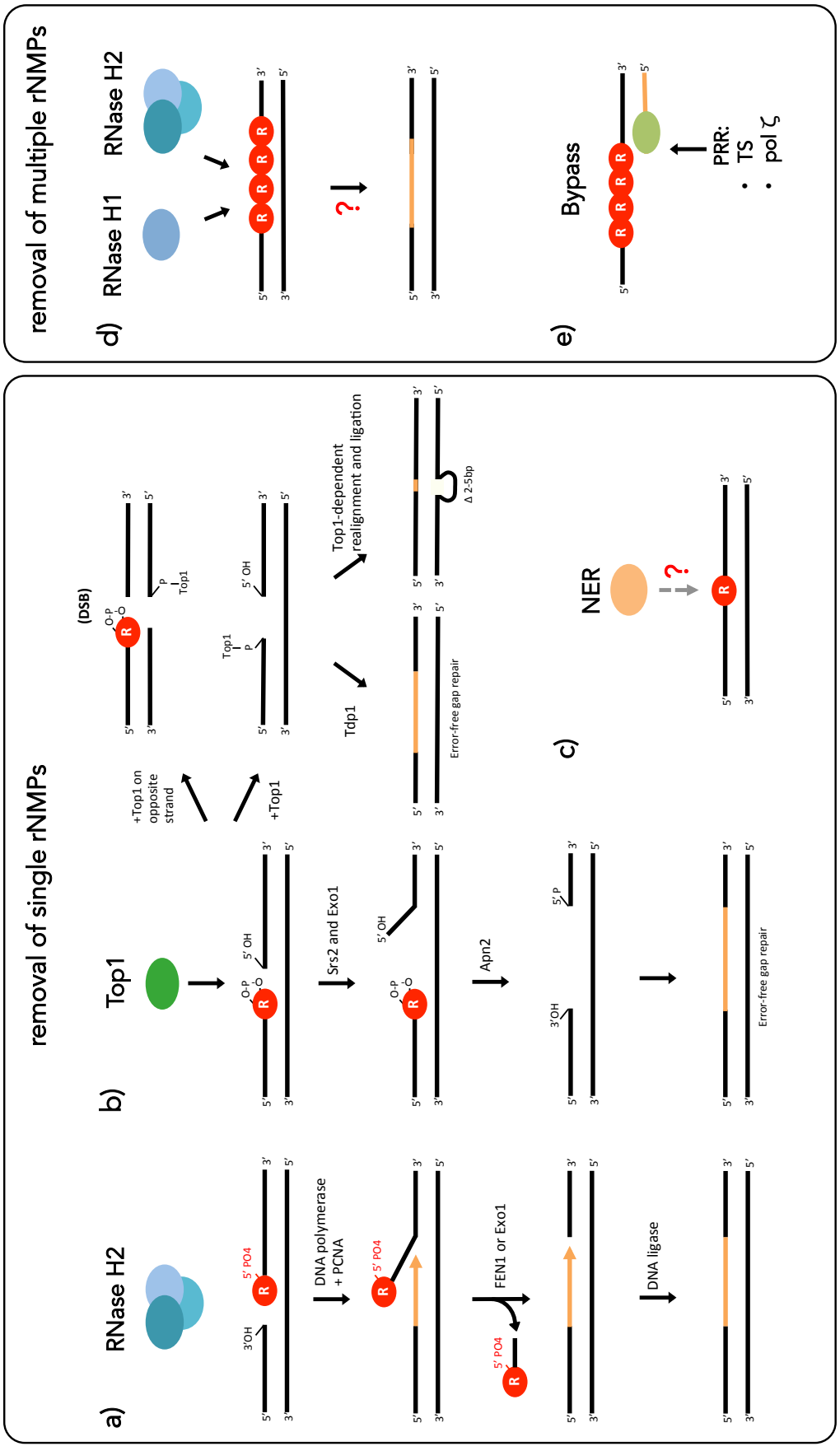

Figure 6. Pathways involved in the removal of single and multiple rNMPs embedded into DNA

RNA:DNA hybrids formed during Okazaki fragments synthesis

The major sources of ribonucleotides introduced into DNA are undoubtedly RNA primers synthesized by the primase activity of Pol α. In eukaryotes, they are approximately 8-10 rNMPs in length, which are repeated at each Okazaki fragment (200nt) on the lagging strand. This means that the replication of the 12Mb *S.cerevisiae* nuclear genome requires the synthesis of about 600000 rNMPs, and the number arrives at 150 million for the human nuclear genome [242]. Besides, we have to consider also RNA chains used to restart stalled replication forks (reviewed in [243]), and RNA primers synthesized by human PrimPol [244,245]. Primer lengths can also vary according to the dNTP pools concentration [246]. To maintain the fidelity of the lagging strand, these ribonucleotides have to be efficiently removed during Okazaki fragments maturation (reviewed in [247]) **(Figure 7),** and it was recently shown that this process can be uncoupled from ongoing DNA synthesis at replication forks [248].

During DNA replication, when the replicative Pol δ encounters the 5' of the downstream Okazaki fragments it can generate a flap of variable length containing the RNA stretch. Short flaps (2-10 nt in length) are processed by Fen1, (with Exo1 as a backup factor) [248–250], while longer flaps are coated by RPA and then processed by Dna2 [251]. Alternatively, the RNA primers can be directly cleaved by RNase H2 (or by RNase H1) up to the final rNMPs, which is then cleaved by Fen1 (Rad27 in S.cerevisiae) [252]. Finally, the generated nicks are sealed by DNA ligase I (Cdc9 in *S.cerevisiae*) [253]. The exact composition and contribution of each pathway are still under investigation, but to date the predominant role seems to be played by Fen1, while the contribution of Dna2 seems to be limited [248].

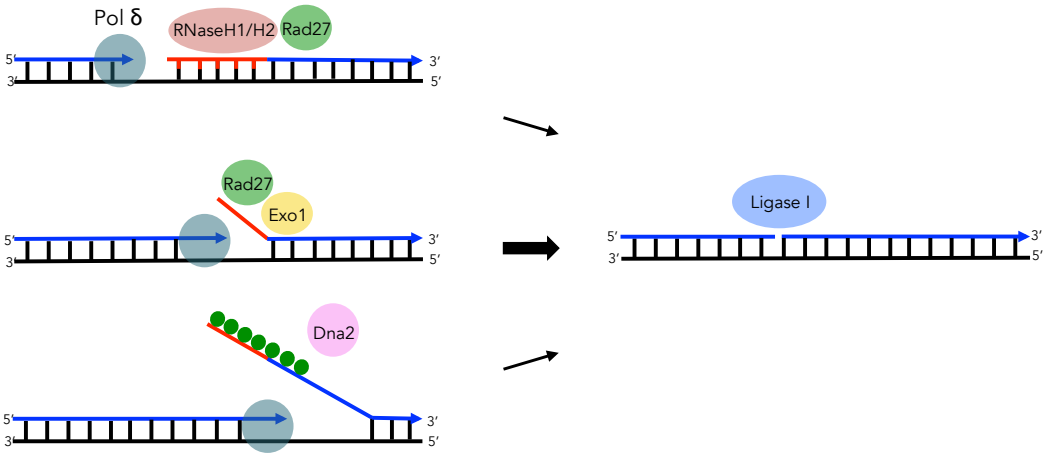

Figure 7. Okazaki Fragments maturation process

Dysfunctions in this process may cause DNA deletions, DNA amplifications, double-strand breaks formation, and even inclusion of RNA stretches into DNA, with deleterious consequences in cells [254]. Different groups linked the RNA primers inclusion in DNA to a genome instability situation [169,191,255], and this seems to occur both in the nucleus and in the mitochondria. For instance, it has been found

that in the absence of RNase H1 the inclusion of RNA primers into mouse mitochondrial genome triggers dramatic effects on mtDNA replication [256]. *S.pombe* uses instead two rNMPs escaped from Okazaki fragments maturation as a system to trigger the recombination events that lead to mating-type switch [257,258].

RNA:DNA hybrids formed during transcription

8bp RNA:DNA hybrids form naturally inside the active site of the RNA polymerase (RNAP) during transcription [259]. Longer hybrids are also able to form when an RNA transcript invades a homologous DNA duplex, which exposes the non-complementary ssDNA strand [19]. These structures called R-loops span 100-2000 bp and occupy a significant portion of the genomes of bacteria, yeast, and higher eukaryotes [260]. R-loops can form co-transcriptionally behind the transcribing RNAP (*in cis*), but can also generate when the transcript hybridizes to any homologous DNA sequence away from the locus of its genesis (*in trans*) [261]. Their stable formation is influenced by high G density, negative supercoiling, and DNA nicks on the template [262]. Besides, due to its G-rich nature, the ssDNA strand can form secondary structures such as G-quadruplexes that further stabilize the RNA:DNA hybrids. R-loops form naturally during *E.coli* plasmid replication [263], mitochondrial DNA replication [264–266], or immunoglobulin class switching [267], and growing evidence suggests that they play important roles in regulating gene expression [268] and chromatin structures [269]. On the other hand, aberrant or excessive R-loops can seriously compromise genome integrity. Recent evidence indeed correlates these structures with several human diseases, including neurological disorders, cancer, and autoimmune diseases (reviewed in [270]). R-loops toxicity can be caused by the exposure of fragile ssDNA, which is prone to transcription-associated mutagenesis (TAM), recombination (TAR), and DSBs [271,272]. R-loops may also promote toxicity by stalling transcription [273], or by directly blocking the progression of DNA replication machinery, causing fork collapse and DSBs [274,275]. In addition, the RNA strand of the R-loops can be used to prime DNA synthesis [276,277]. While this mechanism is normally used in bacterial DNA replication and mitochondrial DNA replication, in *S.cerevisiae* this event has been linked to unscheduled replication in the ribosomal DNA locus, which triggers genome instability [278] .

Maintaining a balance between the positive and a negative effect of R-loops is thus crucial, and to date, many factors have been identified as important in preventing, resolving, but also promoting R-loops formation (reviewed in [279–281])**(Figure 8).** Topoisomerase 1 and 2 enzymes counteract R-loops formation by relieving supercoils in DNA, and also topoisomerase 3B has been found to act at highly expressed genes [282,283]. A role in preventing R-loops formation is also played by factors that act all along the path from the transcription site to the nuclear pore complex (NPC). Indeed, a correct coordination of messenger ribonucleoprotein particle (mRNP) biogenesis and export reduces the ability of RNA transcripts to re-hybridize with the DNA behind RNAPs [284]. Just to mention a few, in

S.cerevisiae it has been found that R-loops accumulate in the absence of Hpr1 protein (involved in mRNA elongation and export), and in the absence of the nuclear basket proteins Mlp1 and Mlp2 [285,286]. Once formed, R-loops can be processed by RNase H1 and H2 which can specifically degrade RNA in RNA:DNA hybrids. In yeast, an increase in R-loops is observed only when both RNases H are inactivated, implying that they can substitute for each other [284]. However, it was then found that RNase H2 seems to act on hybrids genome-wide, while RNase H1 seems to act at a subset of hybrids [218]. Moreover, as mentioned above, the two enzymes are differently regulated during the cell cycle [220]. Hybrids can also be untangled by helicases, like mammalian DHX9 [287], aquarius (AQR) [288], senataxin (Sen1 in yeast) [289], and the ATP-dependent DNA helicase PIF1 [290]. Conversely, it has been found in *S.cerevisiae* that the activity of Rad51 promotes the formation of R-loops *in trans* [261].

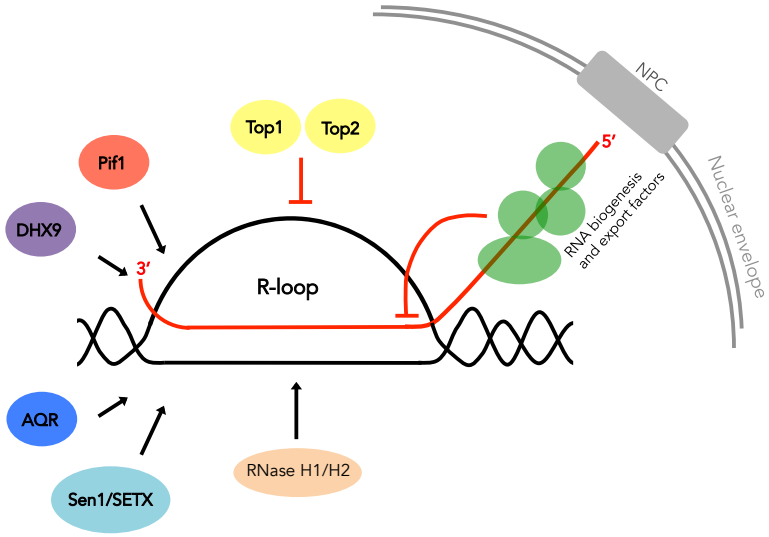

Figure 8. Factors important in preventing and resolving R-loops

RNA:DNA hybrids in DSBs repair

Accumulation of RNA:DNA hybrids have also been observed at the level of DSBs [291–296]. These hybrids could form by de novo transcription [291,293,297,298], or from hybridization of pre-existing nascent transcripts [294,296,299,300]. Anyway, once present at the breaks, they may influence the DNA repair in multiple ways.

First of all, RNA:DNA hybrids seem to impact the efficiency of DNA resection, the process required to create the 3' overhangs needed for DNA recombination. However, while some data indicate that hybrids promote resection [297,299,301], others suggest an anti-resection role [293,300]. RNA:DNA hybrids at the level of the breaks can also impact the repair process: In budding and fission yeast, they seem to promote the repair by HR but not NHEJ [293], while in human cells, they seem to facilitate both types of repair [301]. Moreover, it seems that HR can also occur using the RNA molecule instead of DNA as a

template for the repair [302,303]. On the other hand, persistent hybrids can compromise the binding of some repair factors [304], affect the chromatin structure flanking DSBs [296], and cause an aberrant repair [296,305].

Because of these conflicting data it is clear that many aspects regarding the role of RNA:DNA hybrids in DSBs repair should be more investigated and defined. What is clear is that if not properly removed persistent hybrids may trigger additional DNA damage [293]. Moreover, even if never visualized, also in this case improperly removed RNA stretches might remain embedded at DSB ends, affecting genome stability (reviewed in [169]).

Results & Conclusions

New function for the DNA polymerase η during replication stress

S.cerevisiae cells lacking both RNase H activities (*rnh1*Δ*rnh201*Δ) accumulate rNMPs in their genome, becoming sensitive to different DNA damaging agents such as hydroxyurea (HU) and methyl-methanesulfonate (MMS)[127,306]. Both these agents generate replication stress, acting in different ways: MMS is an alkylating agent, which directly modify DNA by attaching an alkyl group that presents an obstacle to replication fork progression. HU indirectly affects DNA synthesis by reversibly inhibiting ribonucleotide reductase (RNR), the enzyme that converts rNTPs in dNTPs. The consequent depletion of dNTP pools on one hand induces the stalling of replication forks and, on the other hand, makes the incorporation of ribonucleotides into DNA more likely[181]. Noteworthy, it was found that the post replication repair (PRR) pathways become essential for cell survival in the presence of HU since the template switch and the TLS Pol ζ can efficiently bypass rNMPs in the DNA template[127].

Unexpectedly, we found that the deletion of all the yeast TLS polymerases Rev1, Pol ζ and Pol η (*rev1Δ, rev3Δ rev7Δ rad30Δ*) almost completely suppresses the HU sensitivity of *rnh1*Δ*rnh201*Δ cells **(Figure 1A).** By testing the individual contribution of each TLS polymerase, we found that the recovery is fully recapitulated by the single deletion of the DNA polymerase η (encoded by *RAD30* gene) **(Figure 1A).** Interestingly, this recovery is specific for the presence of HU, since it is not observed in the presence of MMS **(Figure 1B).**

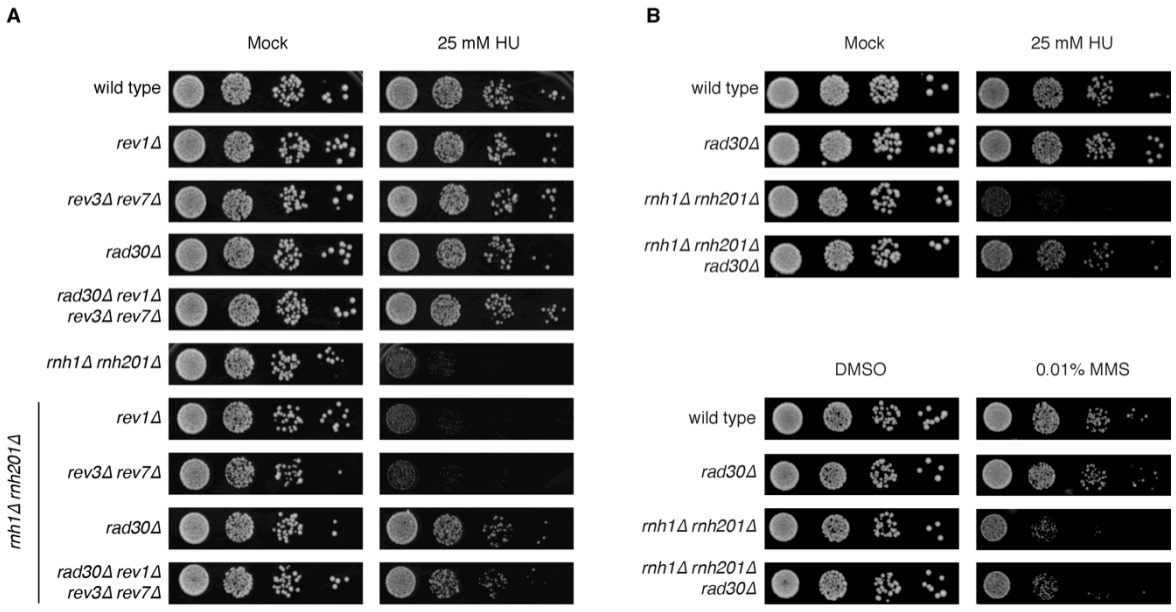

Figure 1. Removal of Pol η rescues the HU sensitivity of cells lacking RNases H activity. 10-fold serial dilution of the indicated strains were plated on **(A)** YEPD and YEPD + 25mM HU and **(B)** on YEPD, YEPD +

25mM HU and YEPD + 0.01% MMS. Plates were incubated at 28°C and pictures were taken after 3 days. Results are representative of four biological replicates [191].

Altogether these data suggest that Pol η plays a role during replication stress induced by nucleotide pool depletion, which turns toxic in the absence of RNase H activity. As already discussed in the introduction, Pol η is a Y-family translesion DNA polymerase, which can face many replication stress conditions: apart from acting on DNA distorting lesions (typical TLS substrate), it is emerging that Pol η can face different lesion-independent replication-stress conditions. In this regard, as already mentioned, the main target of HU is the inhibition of the RNR enzyme, with a consequent depletion in the dNTP pools and stalling of replication forks. In addition, some studies suggest that HU may have other targets that, when inhibited, cause oxidative stress, leading to DNA damage and cell death [307]. However, at the HU concentration in which we appreciate the Pol η toxic role (25mM), the level of oxidative stress generated seems very low. Indeed, a positive control lacking mitochondrial DNA (rho^0) is perfectly able to grow (**Figure 2A**). Moreover, in our lab, it has been seen that *rnh1*Δ*rnh201*Δ cells do not show any sensitivity to agents that generate replication stress, such as H_2O_2 **(Figure 2B).**

These data support the idea that Pol η does not act at DNA lesions generated by oxidative stress, but its activity is related to a condition where the dNTP pools are unbalanced, and replication forks are stalled. We can thus define the role played by Pol η in this condition as a new TLS-independent function of the polymerase. The characterization of this role was the aim of my study.

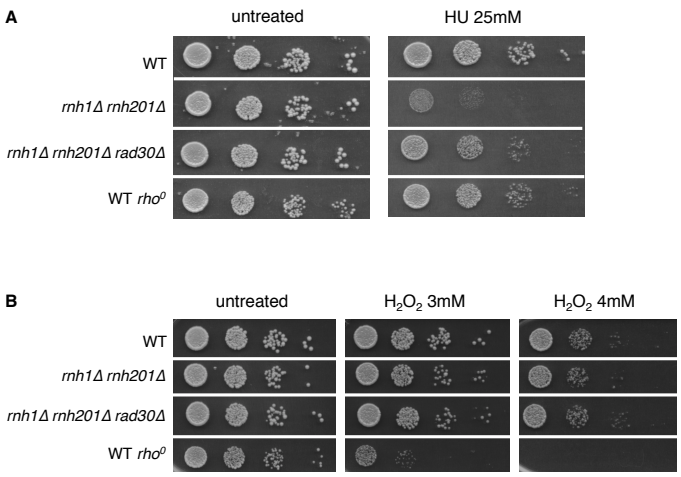

Figure 2. Pol η activity does not seem to be related to the oxidative stress generated by HU. 10-fold serial dilution of the indicated strains were plated on **(A)** YEPD and YEPD + 25mM HU and **(B)** on YEPD, YEPD + 3mM H_2O_2, YEPD + 4mM H_2O_2. Plates were incubated at 28°C and pictures were taken after 2 days.

Characterization of the DNA polymerase η toxicity in RNase H deficient cells

The first step was to characterize the toxic consequences of Pol η activity in cells without RNase H. All the work done for this part has been published in a paper entitled: "RNase H activities counteract a toxic effect of polymerase η in cells replicating with depleted dNTP pools" [191] **(appendix1).**

Therefore, this chapter will summarize the main results present in the manuscript. For the figures and for more details, I remand to the reading of the appendix 1.

Pol η is responsible for DNA damage checkpoint activation and mitotic arrest in RNase H deficient cells

To better understand the phenotypes observed by cell lethality assay, we looked at the effect of Pol η in the cell cycle progression in 25mM HU. It was already known that in the presence of HU, *rnh1Δ rnh201Δ* cells exhibit a prolonged activation of the DNA damage checkpoint; compared to wild-type cells (monitored by looking at the phosphorylation state of Rad53 effector kinase), leading to an arrest of a fraction of cells in G2/M (monitored by FACS analysis)[127]. We found that *RAD30* gene deletion rescues almost completely these HU-induced phenotypes, confirming these abnormalities to be caused by Pol η toxic action **(Figure 2 in [191]).** These phenotypes are also recapitulated, even if with milder phenotypes, with transient exposure to a high HU level (two hours to 200mM HU, followed by a release in fresh medium)**(Figure S2 in [191]).**

Pol η acts at HU-stressed replication forks

As described in the introduction, TLS polymerases can work both at stressed replication forks during the DNA replication or post-replication, in G2/M phase, filling gaps that remained into DNA [105]. To determine when Pol η exerts its toxic activity, we conditionally overexpressed Pol η in *rnh1Δ rnh201Δ rad30Δ* synchronized cell population, at different times following transient exposure to HU. In particular, we induced the expression of Pol η before or after two hours of 200mM HU treatment. Noteworthy, during this acute HU-pulse, cells significantly slow down DNA replication and replication forks stall due to the low dNTP pools. Then, when cells are released, they restore normal DNA replication and divide normally. We found that if Pol η is present during the few replication carried out in the presence of HU, part of the *rnh1Δ rnh201Δ* cells remain blocked in the G2/M phase. On the other hand, when Pol η was induced after the HU-treatment, *rnh1Δ rnh201Δ* cells could re-enter in the next G1 phase without any problem **(Figure 3 in [191]).** This data indicate that Pol η toxic activity starts at the beginning of the S-phase, during active DNA replication under low dNTPs condition.

Pol η toxicity does not depend upon residual rNMPs in the template DNA strand

Since Pol η toxicity is observed only in the absence of RNase H, it is crucial to assess how they relate to each other. One possibility is that the absence of RNases H leads to the accumulation of unprocessed rNMPs that can trigger Pol η activity in the next replication cycle. Conversely, Pol η could act in the first replication cycle in which cells experience HU-induced replication stress. In this case, toxicity could result from the introduction of substrates, possibly rNMPs, which cannot be removed in the absence of RNases H. To discriminate between these two hypotheses, we took advantage of an RNase H2 heterologous conditional system. We used *E.coli* RnhB, which

complements the absence of RNase H1 and H2 in yeast cells, suppressing the HU sensitivity (**Figure S3 in** [191]). Due to its monomeric nature, the RnhB can be easily manipulated, and we placed the gene under transcriptional and translational control.

rnh1Δ rnh201Δ cells carrying the RnhB construct can efficiently remove ribonucleotides from the genome (**Figure S3 in** [191]). RnhB was then turned off in G1 phase, before the release in HU, and cells were collected at different time points to monitor the cell cycle progression and the DDC activation. We found that in presence of RnhB, *rnh1*Δ *rnh201*Δ cells can normally progress through the cell cycle, reaching the next G1 phase, as the wild type. When RnhB is turned off before the HU treatment, *rnh1*Δ *rnh201*Δ cells experience the first replication cycle in which ribonucleotides cannot be removed, and this first cycle is sufficient to trigger the Pol η-dependent phenotypes, similarly to what is observed in *rnh1*Δ *rnh201*Δ cells with the empty plasmid **(Figure 4 in** [191]**).** Altogether, this experiment indicates that Pol η toxicity does not depend upon residual rNMPs in the template strand, but it probably involves the incorporation of rNMPs at HU-stressed replication forks.

Pol η toxicity is related to the insertion of multiple ribonucleotides

The introduction of toxic substrates by Pol η assumes the involvement of the catalytic activity of the polymerase. Moreover, if the toxic substrates are rNMPs in genomic DNA, the expectation is that more rNMPs there are, more harmful the effect should be. In this view, we monitored cell viability in 25mM HU, overexpressing either the wild type allele of *RAD30*, a catalytic-dead (*rad30-D155A-E156A*) allele, or a steric gate mutant with enhanced ribonucleotide incorporation activity *(rad30-F35A)*[137]. Overexpression of all these alleles was achieved at a similar level, and in wild type cells does not compromise the viability both in untreated or in the presence of HU **(Figure 5 in** [191]**).** On the other hand, the overexpression of the wild type Pol η exacerbates the HU sensitivity of *rnh1*Δ *rnh201*Δ cells, suggesting that toxicity is directly related to the level of the protein. The overexpression of the catalytic-dead mutant completely restores normal viability, confirming that toxicity depends on the catalytic activity of the protein. Finally, overexpression of the F35A-mutant exacerbates the cell death of *rnh1*Δ *rnh201*Δ cells on HU compared to the wild type overexpression **(Figure 5 in** [191]**).** This suggests that the toxic function could be the incorporation of ribonucleotides during its synthesis reaction.

We observed Pol η toxicity only upon simultaneous deletion of the two RNase H enzymes, but not in the single mutants **(Figure 6 in** [191]**).** This suggests that problems are caused by the persistency of consecutive ribonucleotides. Indeed, while only RNase H2 can process single rNMPs, both the RNases H can act on stretches longer than four ribonucleotides [216]. To confirm this assumption, we tested a separation-of-function mutant *rnh201-RED* (*rnh201-P45D-Y219A*), which retains the ability to remove stretches of rNMPs, but it is impaired in the processing of single rNMPs [219]. Unlinking these two activities, we confirmed that Pol η is toxic only if RNA:DNA hybrids with more than 4 rNMPs

cannot be processed **(Figure 6 in** [191]**).** This finding suggests that with decreased dNTP pools, Pol η activity may promote the insertion of multiple ribonucleotides in genomic DNA.

Sources of RNA:DNA hybrids

Our data strongly indicate that with depleted dNTP pools, Pol η activity leads to the inclusion of RNA stretches into DNA that result toxic only when both RNases H enzymes are inactive. However, as described in the introduction, RNA:DNA hybrids can arise during different cellular processes [169]. RNA stretches could be directly incorporated by Pol η, or they could result from improper Okazaki fragments processing or R-loops metabolism. Therefore, I deeper investigated these possibilities.

Does Pol η incorporate stretches of RNA into DNA?

Pol η can incorporate rNMPs *in vitro*[138,140]; therefore, RNA stretches could result by direct incorporation of rNMPs by Pol η *in vivo*. This hypothesis is supported by the fact that Pol η activity is observed in HU, where rNMPs are more likely incorporated into DNA [181], and that a steric gate mutated version of Pol η exacerbates the HU sensitivity of *rnh1*Δ *rnh201*Δ cells. I tested multiple approaches to detect rNMPs incorporated by Pol η (among which, the ribonucleotides incorporation assay that we published [308])**(appendix 2).** Unfortunately, these assays were not sensitive enough, probably because they are used to visualize single rNMPs, and cannot discriminate between singles and multiple rNMPs. Indeed, the detection of multiple rNMPs embedded in genomic DNA has never been shown.

Does Pol η compromise the Okazaki fragments processing?

Okazaki fragments synthesis starts from RNA:DNA hybrids that could be stabilized in HU-stalled replication forks. Furthermore, yeast Pol η was recently found to replicate the lagging strand, together with Pol α and δ [152]. Based on this, we hypothesized that Pol η might promote the inclusion of RNA primers into DNA, generating RNA:DNA hybrids that, if not removed, become toxic. To investigate this hypothesis, we generated an unbalance in the different pathways that cooperate in the Okazaki fragments processing. This was done by removing not only the RNases H enzymes but also removing the main player involved in this process, which is Rad27. By genetic crossing, I obtained all the possible combinations of those mutants with or without Pol η. First of all, the absence of RNases H is known to be lethal when combined with *RAD27* deletion, and I verified that this lethality was not caused by *RAD30* **(Figure 3A).** Then, I tested the HU sensitivity to 25 and 50 mM of HU for all the viable combinations of mutants. The expectation was to see a Pol η-dependent lethality not only in the absence of RNases H but also when the Okazaki fragments processing is compromised by the removal of Rad27. However, this does not occur, since the HU sensitivity is appreciated only in *rnh1*Δ *rnh201*Δ cells **(Figure 3B).** In conclusion, compromise the Okazaki fragments processing does not alter the Pol η toxicity, arguing against the involvement of Pol η at the Okazaki fragments level.

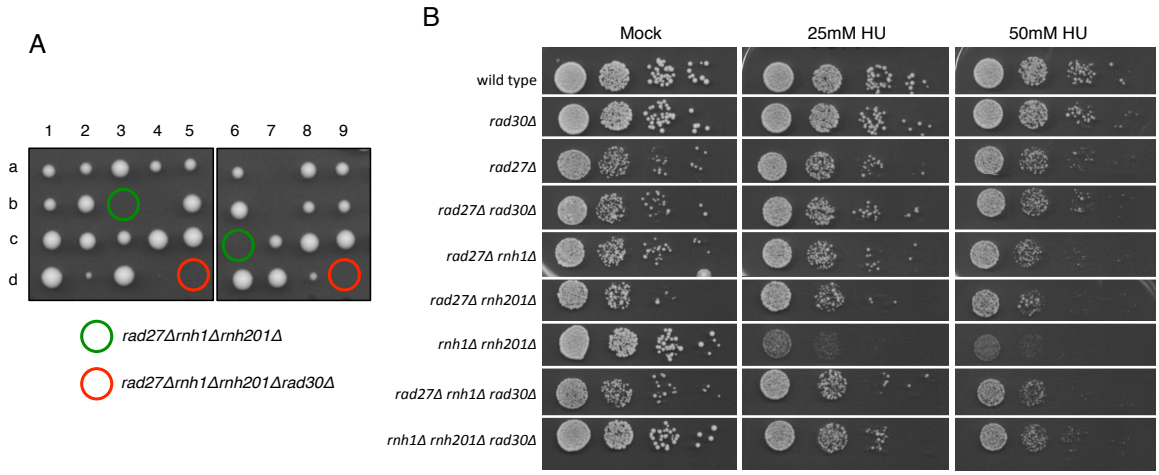

Figure 3. Genetic interactions between Pol η, RNase H1, RNase H2, and Rad27. (A) Tetrads derived from a cross between *rnh1Δ rnh201Δ rad30Δ* MATa and *rad27Δ* MATα strains were dissected on YEPD plates. 9 tetrads are shown. The circles on the figure indicate the position of the original *rnh1Δ rnh201Δ rad27Δ +/- rad30Δ* spores. **(B)** 10-fold serial dilution of the indicated strains are plated on YEPD, YEPD + 25mM HU and YEPD + 50mM HU. Plates were incubated at 28°C and pictures were taken after 3 days. Results are representative of two biological replicates.

Does Pol η act on R-loops?

Another possibility is that Pol η acts extending/stabilizing R-loops that result toxic if not removed by RNases H. This hypothesis is consistent with the discovery that hPol η acts on transcription-replication conflicts, which are characterized by R-loops formation [151] and by the observation that both human and yeast Pol η efficiently extend RNA primers *in vitro* [138,140]. As anticipated in the introduction, R-loops level is regulated by several factors, including RNases H and other players like Topoisomerase 1 and the RNA:DNA helicase Sen1 (reviewed in [281]). I reasoned that if R-loops are the substrates for Pol η activity, I might recapitulate its HU-toxicity even without these other factors. Since *SEN1* is an essential gene, I worked with the temperature-sensitive sen1-1 mutant (G1747D), which carries a mutation in the helicase domain. sen1-1 mutation or *TOP1* deletion cause cell death when combined with the absence of RNases H1 and H2, due to abundant R-loops accumulation [220,309]. I found that this lethality was not caused by the activity of Pol η on R-loops, since *RAD30* deletion does not suppress the lethality **(Figure 4A).** Moreover, deletion of *RAD30* does not affect the HU-sensitivity of *top1Δ* or *sen1-1* strains **(Figure 4B and 4D).** Finally, as reported above, the overexpression of Pol η exacerbates the HU-sensitivity of *rnh1*Δ *rnh201*Δ cells, but it does not have any effect in *top1Δ* or *sen1-1* cells **(Figure 4C and 4E)**.

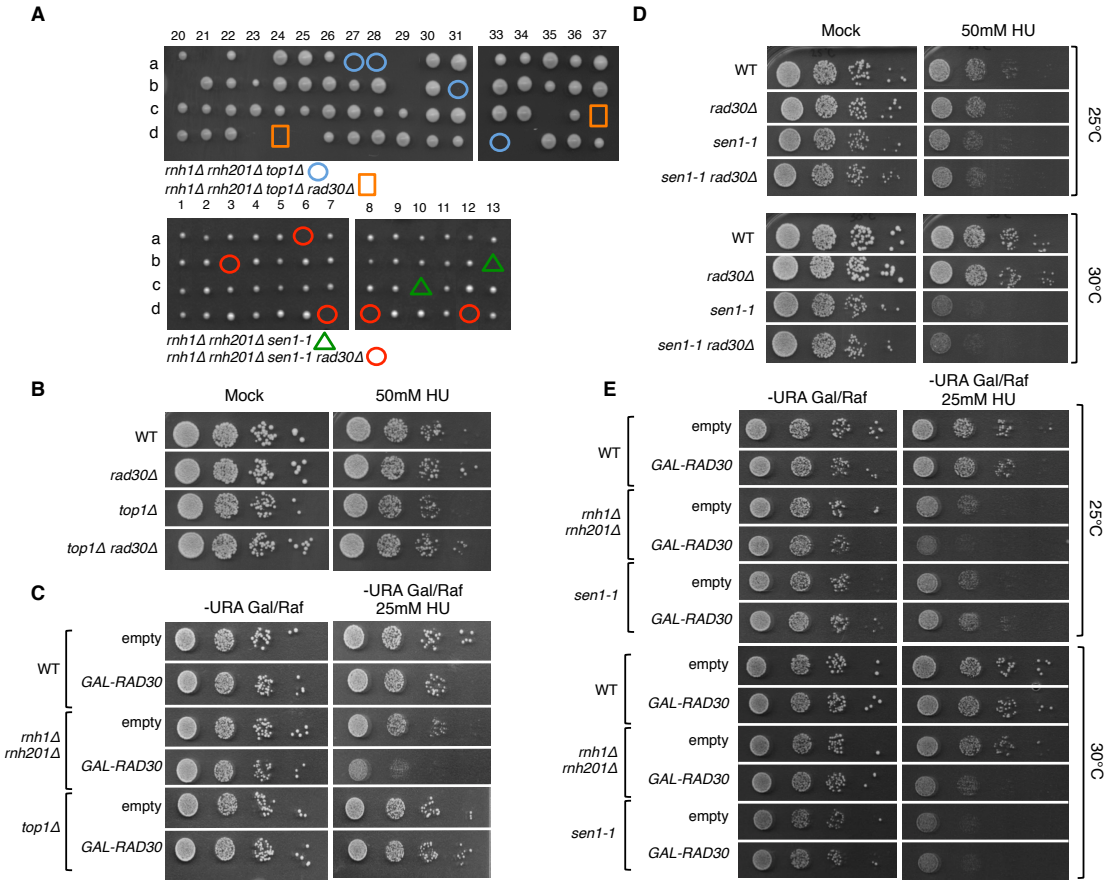

Figure 4. Genetic interactions between Pol η and factors involved in the prevention/removal of R-loops. **(A)** Tetrads derived from a cross between *rnh1Δ rnh201Δ rad30Δ* and *top1Δ* (above), or *rnh1Δ rnh201Δ rad30Δ* and *sen1-1* mutant (below), were dissected on YEPD plates. The different shapes on the figure indicate the position of the original combination of spores that are not viable **(B)(C)** 10-fold serial dilution of the indicated strains are plated on YEPD and YEPD + 25mM HU (B), and on -URA Raffinose 2% Galactose 2% with or without 25mM HU. Rad30 overexpression is obtained through a plasmid carrying *RAD30* gene under the control of a Galactose inducible promoter (C). Plates were incubated at 28°C and pictures were taken after 3 days. Results are representative of two biological replicates. **(D)(E)** 10-fold serial dilution of the indicated strains are plated on YEPD and YEPD + 25mM HU (D), and on -URA Raffinose 2% Galactose 2% with or without 25mM HU (E). Due to the presence of the *sen1-1* temperature-sensitive mutant, plates were incubated at the permissive temperature of 25°C and at the semi-permissive temperature of 30°C. Pictures were taken after 3 days and the results are representative of two biological replicates.

From these results, it seems that Pol η activity is not linked to the presence of R-loops. However, we have to consider that RNases H enzymes are present in both *top1Δ* and *sen1-1* strains since their deletion causes lethality. So, even if Pol η were to act on the hybrids accumulated in these mutants, RNase H activity could still resolve the problem. Therefore, I decided to change the approach: I overexpressed either *TOP1* or *SEN1* in *rnh1*Δ *rnh201*Δ cells. Thanks to their overexpression, those factors should reduce the global level of R-loops present in cells. If Pol η acts on those structures, their reduction should reduce the Pol η-dependent toxicity observed in *rnh1*Δ *rnh201*Δ cells. Unfortunately, the overexpression of *TOP1* appears to be toxic for yeast cells, making it difficult to draw any

conclusion about the Pol η substrates **(Figure 5A).** Interestingly, we found that the overexpression of *SEN1* almost completely suppresses the HU-sensitivity of *rnh1*Δ *rnh201*Δ cells **(Figure 5B).** The same result has been recently obtained also by Appanah et al., [310]. This suppression, which is similar to the one observed upon deletion of *RAD30* leads to the intriguing hypothesis that *SEN1* eliminates the substrates of Pol η, preventing its activity.

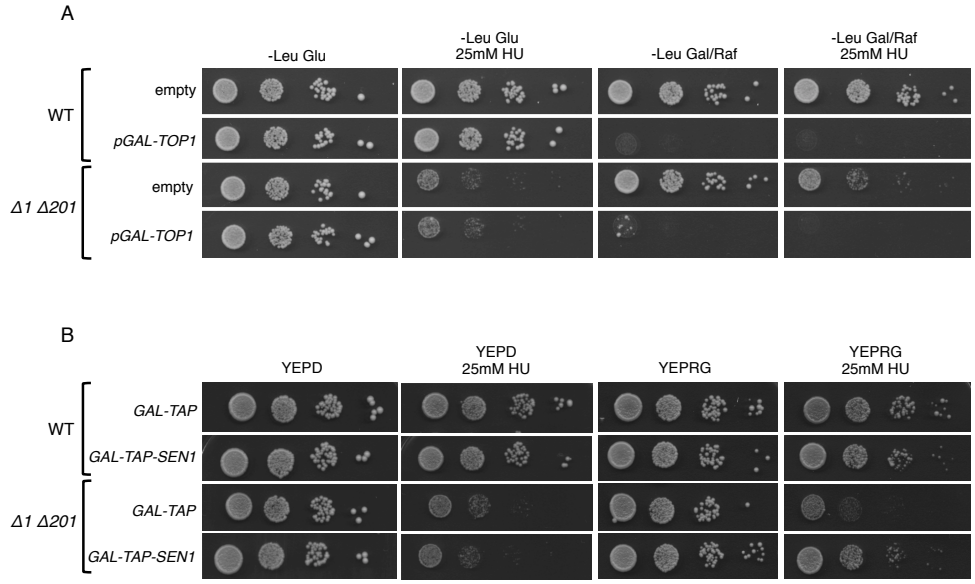

Figure 5. Effect of *TOP1* and *SEN1* overexpression in WT and *rnh1*Δ *rnh201*Δ cells. (A) 10-fold serial dilution of the indicated strains are plated on Sc-Leu +/- 25mM HU and -Leu + Raffinose 2% + Galactose 2% +/- 25mM HU. **(B)** 10-fold serial dilution of the indicated strains are plated on YEPD +/- 25mM HU and YEPD + Raffinose 2% + Galactose 2% +/- 25mM HU. Plates were incubated at 28°C and pictures were taken after 2 days.

As reported above, the HU-sensitivity of *rnh1*Δ *rnh201*Δ cells is directly related to Pol η levels. Indeed, the overexpression of *RAD30* is more toxic than the endogenous variant. In order to link Pol η to R-loops, I tested whether also this sensitivity was suppressed by *SEN1* overexpression **(Figure 6).** Both *SEN1* and the *RAD30* genes were placed under the control of a Galactose inducible promoter, meaning that the presence of Galactose in the media induces the expression of both genes simultaneously. Interestingly, the overexpression of *SEN1* can suppress also the toxicity caused by the overexpression of *RAD30*.

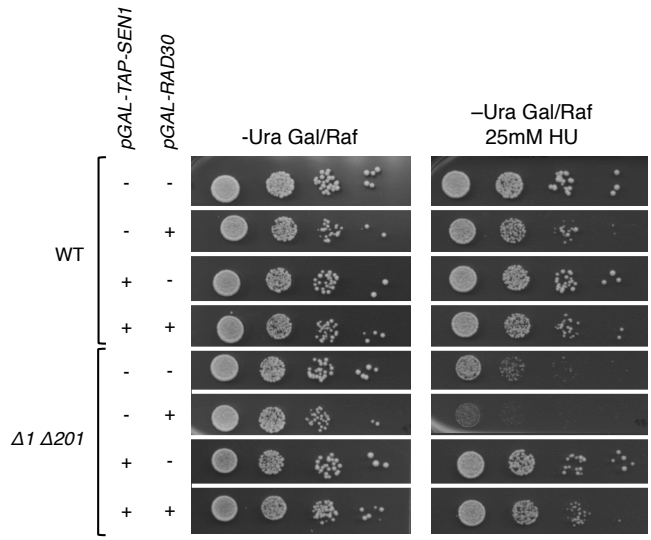

Figure 6. The overexpression of *SEN1* suppresses the toxicity caused by the overexpression of *RAD30*. 10-fold serial dilution of the indicated strains are plated on Sc-Ura + Raffinose 2% + Galactose 2% +/- 25mM HU. Plates were incubated at 28°C and pictures were taken after 3 days.

To conclude, genetic analyses did not prove a correlation between the HU-specific Pol η activity and the Okazaki fragments processing. Besides, due to the lack of an assay capable to detect multiple rNMPs embedded into DNA, we cannot exclude that RNA:DNA hybrids result from the direct incorporation of consecutive rNMPs into DNA by Pol η. On the other hand, the finding that *SEN1* overexpression rescues the HU sensitivity of *rnh1*Δ *rnh201*Δ cells when Pol η is present either at its endogenous level or when it is overexpressed suggests that there might be a link between Pol η activity and R-loops. An intriguing hypothesis is that when HU stalls replication forks, Pol η promotes replication starting from some RNA transcripts, leading to the inclusion of RNA stretches into DNA, removed then by RNases H. Although this phenomenon has been already described both in bacteria and eukaryotic cells [278,311], this is only a speculation that, in the future, will be investigated more in detail.

Characterization of the DNA polymerase η physiological meaning at HU-stalled replication forks

Based on the results reported till now and published in [191], we propose that Pol η actively participates to DNA replication in low dNTPs conditions, leading to the accumulation of stretches of consecutive ribonucleotides in the genome. Although the nature of the RNA:DNA hybrids generated by Pol η is still under investigation, we have characterized the toxic consequences of their presence in cells without RNases H **(appendix 1,[191])**. Nevertheless, the physiological meaning of using Pol η with low dNTP pools is only partially understood.

Contribution of Pol η to DNA replication in low dNTPs concentration, using ribonucleotides as substrates

If it is true that Pol η physiologically contributes to DNA replication in HU, the absence of Pol η should somehow compromise the DNA replication independently on the lack of RNases H enzymes. We compared the viability of wild-type and *rad30Δ* cells at increasing HU concentrations. However, in none of the tested conditions we detected an HU-sensitivity Pol η-dependent **(Figure 7A).** We did not notice any differences, either in sensitivity or cell cycle progression in the presence of a high HU concentration. Wild-type and *rad30Δ* cells synchronized in G1 phase were released in the presence of 150 mM of HU, and we monitored the cell cycle progression at different time points by FACS analysis. Overlapping of the profiles revealed no differences in S-phase progression between the two strains **(Figure 7B).** We thus tested the replication fork progression more in detail using two-dimensional (2D) DNA agarose gel electrophoresis. With this technique, replicating DNA fragments are separated by size and shape through two distinct stages of agarose gel electrophoresis and Southern blot is used to probe the fragment of interest [312]. Results can give powerful information regarding replication kinetic, points of fork stalling, and recombinative intermediates generated **(Figure 7C).** We analysed replication intermediates at some early origin of replication (ARS305, ARS108, and ARS607) in wild-type and *rad30Δ* cells released from a G1 block in the presence of 200mM HU **(Figure 7D)**. Bubble arc represents origins that have been fired bi-directionally (e.g., ARS305), while the asymmetric progression of replication forks generates large Y molecules (e.g., ARS108 and ARS607 profiles, since here origins are located outside the DNA fragment analysed). The absence of *RAD30* does not seem to induce fork stalling or the appearance of recombinative intermediates, and the replication kinetic seems to be the same as wild-type cells. These results indicate that, at least in correspondence of the regions tested; the absence of the *RAD30* per se does not compromise the replication fork progression.

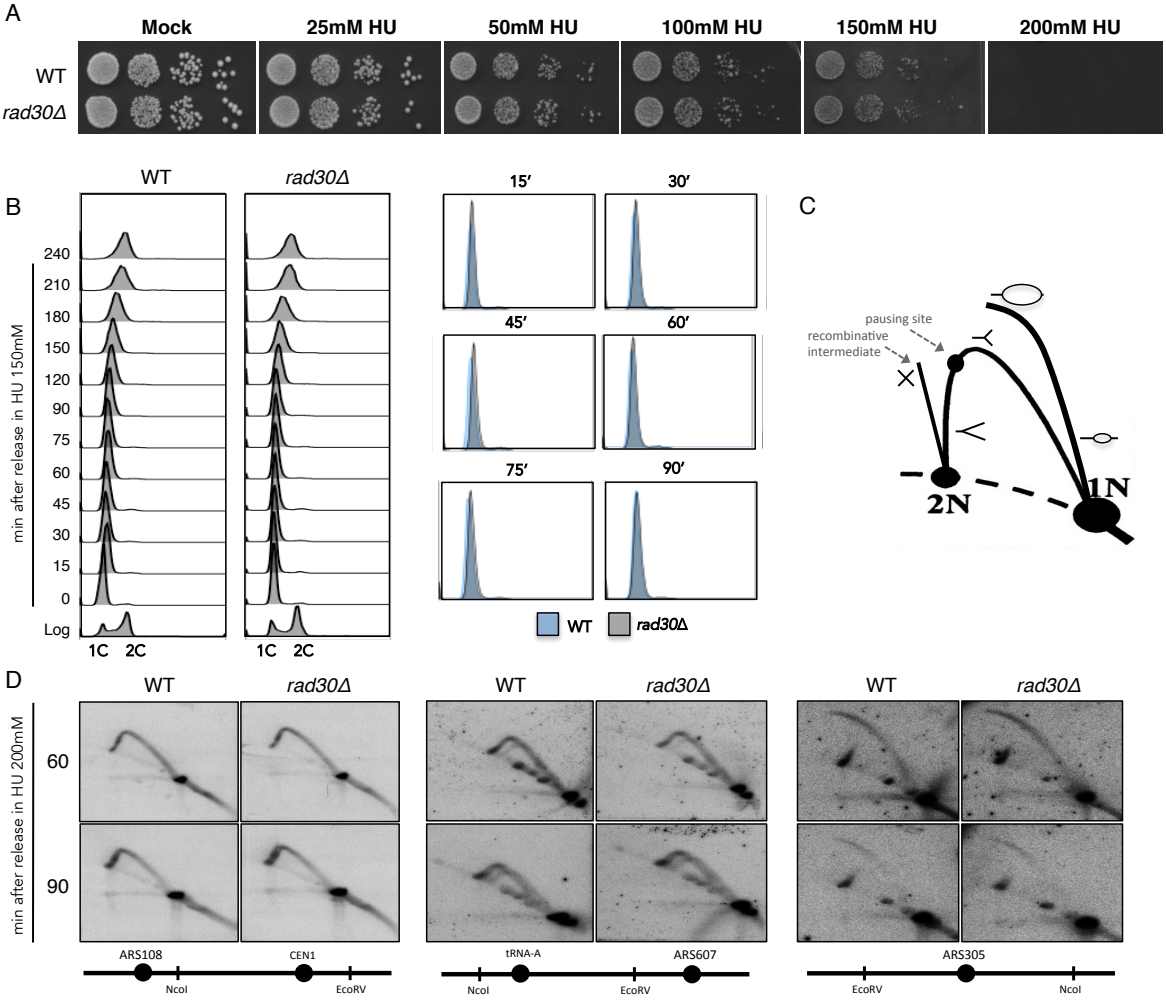

Figure 7. The Absence of Pol η per se does not compromise the replication fork progression in HU. (A) 10-fold serial dilution of the indicated strains are plates on YEPD and YEPD + the indicated increasing HU concentrations **(B)** Exponentially growing cells were synchronized in the G1 phase by α-factor addition (4µg/mL) and then released in YEPD + 150mM HU. Cell cycle progression was followed by flow cytometry (FACS), measuring the DNA content (1C, 2C) at the indicated time points. Overlaps of FACS profiles obtained during the S-phase progression are reports on the right. **(C)** Schematic representation of the replication intermediates discussed in the text. **(D)** Exponentially growing cells were synchronized in the G1 phase by α-factor addition (4µg/mL) and then released in YEPD + 200mM HU. Cell synchronization and release were checked by FACS analysis. DNA was prepared from cells collected at the indicated time points: 10-µg aliquots were cut with restriction enzymes, according to the indicated strategy ad analysed by two-dimensional electrophoresis.

One possible explanation for these phenotypes is the existence of parallel pathways capable to replace the role played by Pol η in HU. To fully characterize this role, is thus important to identify these alternative pathways **(Figure 8).**

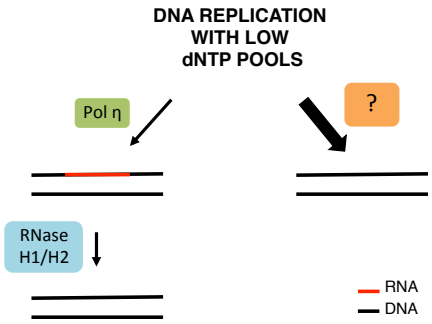

Figure 8. Alternative pathways might replace the role played by Pol η in HU. A possible model that explains why the absence of Pol η alone does not compromise DNA replication in the presence of HU. If unknown pathways can replace its role, only by removing these other factors, we should appreciate HU-specific phenotypes.

SGA to find interactors of the DNA polymerase η under replication stress

Genetic interaction studies are extremely useful to gain knowledge of the role of uncharacterized genes, pathway composition, and connection among these pathways [313]. Genetic interactions occur when mutations in two or more genes result in an unexpected phenotype, not predictable based on the effect of individual gene mutants [314], and a powerful methodology to automate genetic interaction studies is the Synthetic Genetic Array (SGA) methodology. In a typical SGA screen, a query gene deletion mutant is crossed with a library of gene mutants to identify synthetic lethal and synthetic sick genetic interactions, yielding information on the query gene and the genes it interact with [315,316]. Therefore, to identify genes capable of compensating the role played by Pol η in HU, I went to Grant Brown's laboratory in Toronto to perform an SGA in the presence of HU using *RAD30* as a query **(Figure 9A).** Briefly, I crossed yeast cells deleted for *RAD30* with a library consisting of an array of ~5000 non-essential genes mutants and ~1000 temperature-sensitive mutants of essential genes, in which each gene was linked to a selectable marker. From the crossing, I selected heterologous diploids, and I induced their sporulation. Through different steps of growth on synthetic medium, I then selected among all the spores, only the ones containing the query and the array strain mutation simultaneously in haploid condition. I thus obtained a collection of yeast double-mutants in which each gene present in the library was also deleted for *RAD30*. Cells were then grown in YEPD plates with or without 100mM HU, and colony size was used as a proxy for fitness **(Figure 9B)**. Using the SGAtools software (http://sgatools.ccbr.utoronto.ca/), I then selected only the double mutant combinations that deviated from an expected phenotype. I analysed the non-essential (DA) and essential yeast genes (TS) separately, and I performed two independent SGA screenings. Based on the normalization method applied and the threshold selected **(see material and methods),** I defined a list of putative HU-specific negative interactors of *RAD30*. For the non-essential genes, I obtained 293 genetic interactors genes from the SGA 1 and 450 from the SGA 2, with 44 genes common to both my screenings **(Figure 9C, above).** For the essential genes, I obtained 178 positives from the SGA1 and 231 from the SGA 2, with 50 genes common to both my screenings **(Figure 9C, below).** I defined the

44 + 50 genes as the final HITS from the screenings **(Supplementary list 1).** These genes represent the putative synthetic sick and lethal HU-specific interactors of *RAD30.*

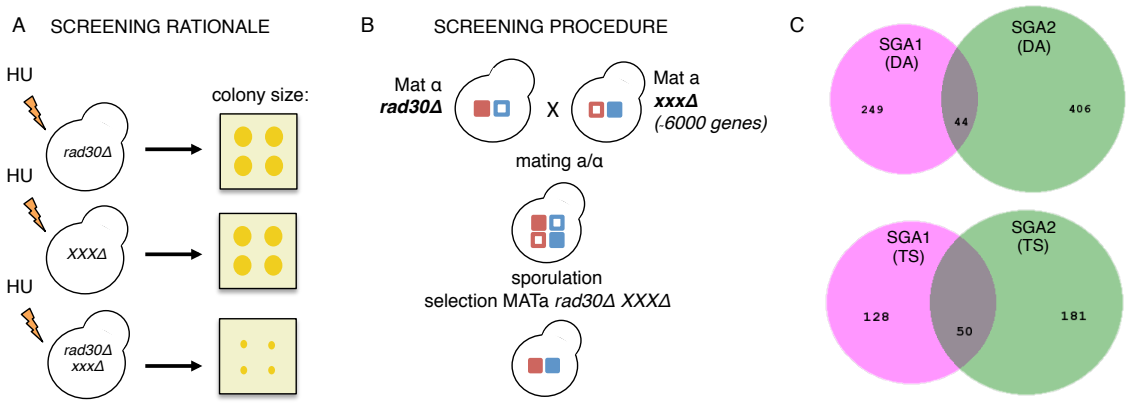

Figure 9. Synthetic genetic array (SGA) methodology to find HU-specific interactors of Pol η. (A) Schematic representation of the screening rational **(B)** Schematic representation of the screening procedure **(C)** Venn diagrams of the candidate HU-specific negative genetic interactors of *RAD30* obtained from the two SGA screenings performed. Non-essential genes (DA) are reported above, essential genes (TS) are reported below.

Serial dilutions of each putative hit were then spotted on YEPD plates with or without HU. In this way, I removed all the false positives genes, and I obtained only the real HU-specific interactors of *RAD30.* I confirmed 14 non-essential genes **(Figure 10A)** and 3 essential genes **(Figure 10B)** (17 genes in total). Gene ontology (GO) enrichment analysis shows that most of those genes are involved in DNA replication and repair, consistently with our observation that during replication stress induced by HU, Pol η is recruited to stalled replication forks **(Figure 10C).**

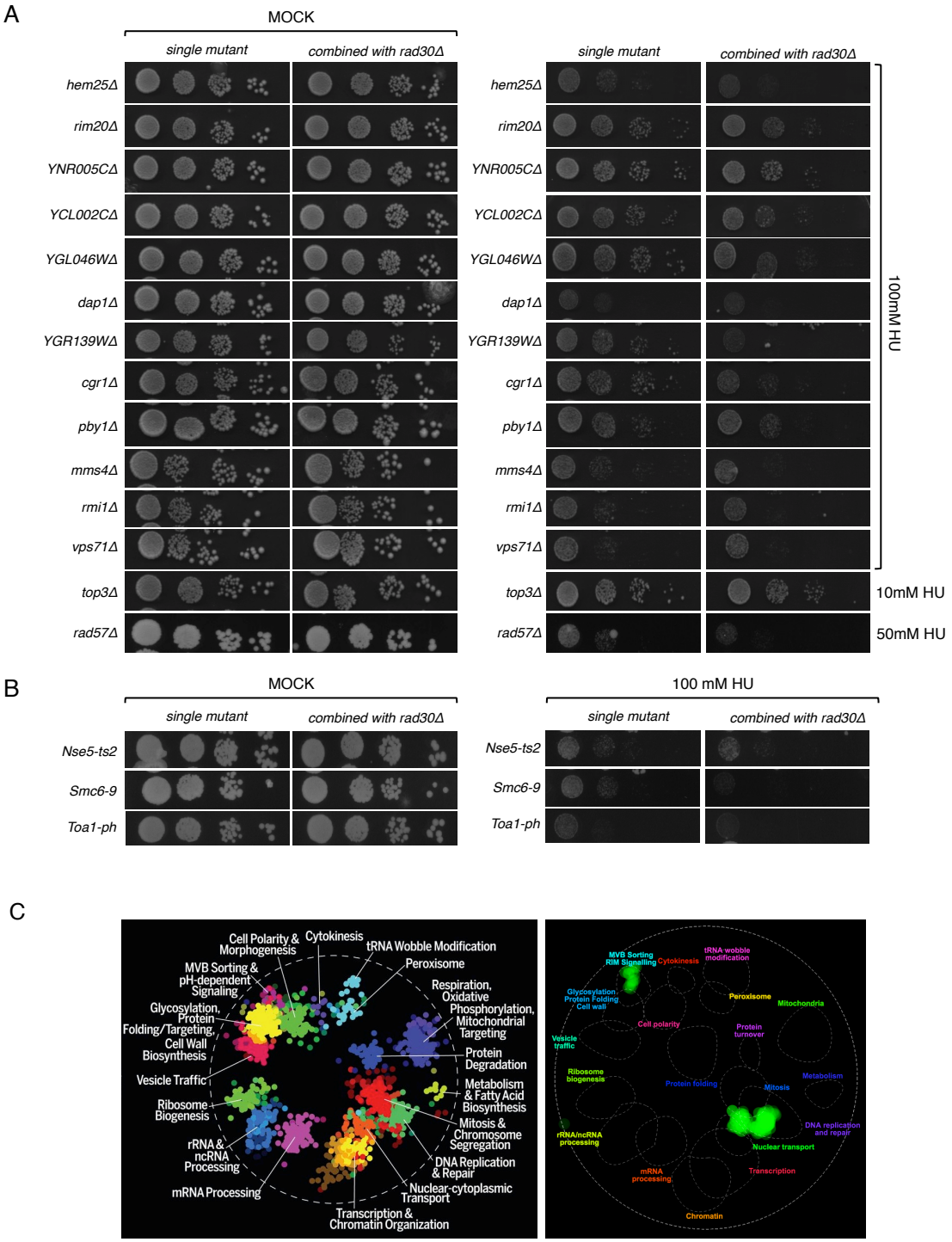

Figure 10. Identification of 17 HU-specific negative interactors of Pol η. (A)(B) The indicated strains +/- *RAD30* deletion were grown in YEPD at the permissive temperature of 25°C O/N. After normalization, 10-fold serial dilution of the indicated strains were then plated on YEPD plates (left) and YEPD plates + the indicated concentration of HU (right). Plates were incubated at the semi permissive temperature of 30°C and pictures were taken after 2 days. Results are representative of two biological replicates. Non-essential genes combined or not with *RAD30* deletion are reported in **(A),** essential genes combined or not with *RAD30* deletion are reported **(B). (C)** On the left, SAFE (Spatial Analysis for Functional Enrichment) analysis was used to identify and color network regions enriched for similar Gene Ontology bioprocess terms [317]. On the right, SAFE analysis of the

validated HU-specific negative interactors of *RAD30* shows enrichment in the DNA replication and repair region of the genetic interaction similarity network.

Interestingly, among the factors annotated in the DNA replication/repair area, there are genes involved in DNA recombination: *MMS4, TOP3, SMC6, NSE5, RMI1, RAD57*. As mentioned in the introduction, recombination factors have an important role in processing stalled replication forks, and all those genes are involved in processing/regulating DNA joint molecules (JM) formed as intermediates during recombinational repair [318]. Further work is now required to demonstrate a link between these recombination factors and the activity played by Pol η at HU-stalled replication forks, which turns toxic in the absence of RNases H enzymes. However, this result is extremely encouraging, and all those genes might be part of the pathway we were looking for.

Regulation of the DNA polymerase η activity

Access of TLS polymerases to damaged DNA templates can be regulated in different ways. As discussed in the introduction, an important role in regulating TLS activity is played by PCNA monoubiquitination. For Pol η, interaction with Ub-PCNA is mediated by the ubiquitin-binding zinc finger (UBZ) domain, and the PCNA-interacting peptide (PIP) located at the C-terminal of the protein [155]. Besides, another significant level of regulation of Pol η activity is represented by post-translational modifications. In this view, we decided to investigate the mechanisms regulating the activity of Pol η under HU induced replication stress.

We found that an endogenous mutant version of *RAD30*, which abolish PCNA interactions thanks to mutations in the UBZ and PIP domains (*rad30-D570A-F627A-F628A*), seems to rescue the HU-sensitivity of RNases H lacking cells **(Figure 11A),** suggesting that PCNA could regulate the activity of yeast Pol η under replication stress, which becomes toxic in the absence of RNases H.

SUMOylation of Pol η

Besides the regulation mediated by PCNA-interaction, human Pol η undergoes different PTM, among which there is SUMOylation. While multiSUMOylation seems to reduce Pol η interaction with DNA damage sites [164], monoSUMOylation of K163 promotes the association of Pol η at the replication forks during unchallenged S-phase and seems to increase under lesion-independent replication stress induced by HU or APH [165]. Thus, this PTM could represent an additional or alternative mechanism to regulate Pol η respect to PCNA monoubiquitination. To examine if yeast Pol η is a SUMO target, we used strains with the endogenous Myc-tagged Rad30 either overexpressing or not the His-tagged Smt3, which is the homolog of SUMO in yeast. SUMOylated proteins were purified on nickel (Ni) beads in denaturing conditions, and the presence of Pol η was tested by western blot using an anti-Myc antibody. We compared untreated cells and cells treated for two hours with 200mM of HU. Unfortunately, there was no SUMOylated Pol η among the SUMO-enriched proteins, neither in untreated nor in the presence of HU **(Figure 11B).** The absence of Pol η-SUMO was not due to

technical problems since western blot against Smt3 confirmed that SUMOylated proteins were correctly enriched, and a positive control, which is known to be hyper-SUMOylated (Gcn5) was properly enriched **(Figure 11B).**

At this point, a possibility is that the fraction of modified-Pol η is too low to be detected or maybe the SUMOylation/deSUMOylation process is extremely rapid. The chance to detect yeast SUMOylated proteins has been shown to increase upon ethanol treatment [319]. The reason is that oxidative stress generated by ethanol causes the oxidation of the cysteine residues of the yeast SUMO-protease Ulp1. This modification results in the loss of its protease activity inducing a global increase of the level of SUMOylated proteins [320]. Therefore, we decided to repeat the experiment treating cells for 1 hour with 10% of ethanol after release from the G1 phase. Interestingly, we detected a slower migrating band in the pull-down, only in the presence of His-Smt3, corresponding to a SUMOylated version of Pol η **(Figure 11C).** The increase of the molecular weight of the polymerase (~11 KDa) suggests that Pol η is mono-SUMOylated. Again, western blot against Smt3 confirmed that SUMOylated proteins were correctly enriched. This time we used PCNA as a positive control since as mentioned in the introduction also this protein is known to be SUMOylated. Conversely to what we expected, replication stress induced by HU seems to decrease the level of SUMOylated Pol η. One possibility might be that, in contrast to what happens in human cells, the activity of yeast Pol η at HU-stalled replication forks might be regulated by a deSUMOylation event. Besides, the difference in the SUMOylation level between humans and yeast could also result from the fact we used an acute treatment of the HU, while in humans it was tested a low dosage of the drug [165].

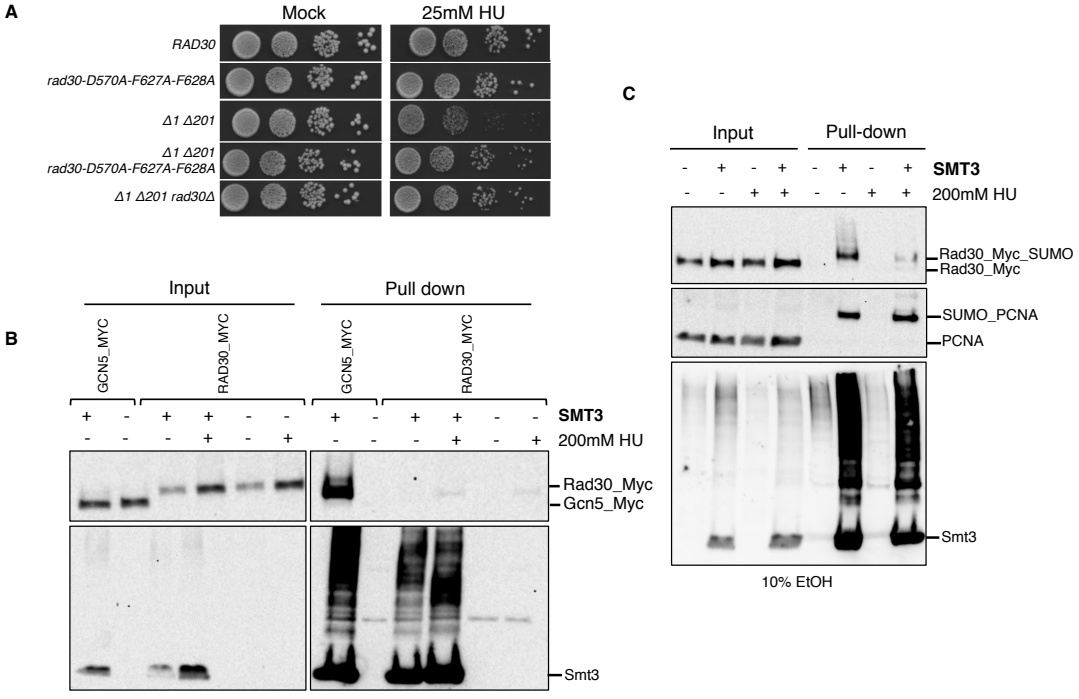

Figure 11. Molecular mechanisms regulating the activity of yeast Pol η during replication stress. (A) Exponentially growing cells of the indicated strains were collected, either prior or after 2h in 200mM HU, for

Ni-NTA pull-down analysis under denaturing conditions on whole cell extracts. Input and pulled-down samples were analysed by western blot using first an anti-Myc antibody (to detect Pol η and the positive control Gcn5), and then using an anti-Smt3 antibody. **(B)** Exponentially growing cells of indicated strains were synchronized in the G1 phase by α-factor (4μg/mL) and released in YEPD + 10% EtOH +/- 200mM HU for 1 hour. Samples were then collected for Ni-NTA pull-down analysis under denaturing conditions on whole cell extracts. Input and pulled-down samples were analysed by western blot using first an anti-Myc antibody to detect Pol η, then an anti-PCNA antibody (to detect PCNA used as positive control), and finally using the anti-Smt3 antibody.

Anyway, to understand if SUMOylation regulates somehow Pol η during replication stress, it is important to map the SUMO modification site(s). We performed an *in silico* analysis with a SUMOylation site-prediction software program named SUMOplot™. This tool predicts the probability for the SUMO consensus sequence, the tetrapeptide motif B-K-x-D/E (where B is a hydrophobic residue, K is the lysine conjugated to SUMO, x is any amino acid (aa), D or E is an acidic residue) to be engaged in SUMO attachment, and scores SUMOylation sites in the protein of interest based on direct amino acid match to SUMO consensus sequence and on possible combinations of consensus amino acids other than lysine. Through this analysis we identified 16 lysines as candidate SUMO acceptor sites **(Figure 12).** We started to mutate the candidate lysines (K) to no longer SUMOylatable arginines (R), through site-directed mutagenesis. Unfortunately, at the moment, even if some lysines have been mutated **(coloured in red in Figure 12),** we still have to find the SUMO acceptor site.
Altogether, even if further work is required to identify the SUMO-acceptor sites in Pol η, we demonstrated for the first time that also the yeast Pol η is a SUMO target. Moreover, the fact that the SUMOylation level decreases when the nucleotide pools is low suggests that a fine regulation of this modification might have a role in regulating the activity of Pol η at HU-stalled replication forks.

Position	sequence	Score
287	VKND	0.93
216	LKFE	0,91
475	LKVG	0,73
96	FKKG	0.68
532	GKED	0.67
299	GKFE	0.67
549	PKLE	0.61
343	LKEF	0.56
140	LKIF	0.56
279	KKPD	0.48
97	KKGE	0.48
546	EKTP	0.39
603	RKRP	0.34
457	RKSG	0.27
68	RKYG	0.27
373	EKLE	0.15

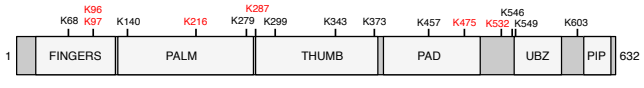

Figure 12. Yeast Pol η lysines candidate for SUMOylation from SUMOplot™ analysis program. Lysines residues candidate for yeast Pol η SUMOylation according to SUMOplot™ analysis are reported in the table, indicating the position of the residues, the sequence context and the score assigned. Briefly, the software predicts the probability for the SUMO consensus sequence to be engaged in SUMO attachment and scores each residue based on two criteria: the direct amino acid match to SUMO consensus sequence and the substitution of the consensus amino acid residues with amino acid residues exhibiting similar hydrophobicity. Residues coloured in

red have already been mutagenized into arginine. On the right it is reported a representation of Pol η and its domains, indicating the 16 lysines candidate as SUMO acceptors sites.

Discussion

It is now well established that RNA frequently hybridizes with DNA, generating RNA:DNA hybrids. These include RNA primers of Okazaki fragments, ribonucleotides introduced by DNA polymerases, R-loops formed during transcription, and many others. (Details regarding origins of single and multiple ribonucleotides present in the genome can be found in the review entitled "One, no one and one hundred thousand: the many forms of ribonucleotides in DNA" [169], that we recently published **(appendix 3)**). In general, although all these RNA:DNA hybrids have been associated with some positive functions [196,321,322], their stable accumulation perturbs DNA replication, inducing replication stress and genome instability [127]. RNA:DNA hybrids are thus processed by Ribonuclease (RNase) H1 and H2, which re-establish the correct DNA:DNA pairing [216,220,323]. *S.cerevisiae* cells lacking these enzymes (*rnh1Δrnh201Δ*) accumulate rNMPs in the genome, becoming sensitive to different replication stress-inducing agents, such as Hydroxyurea (HU), a drug which depletes dNTP pools inducing stalling of replication forks. [127,306]. Unexpectedly we found that this HU-sensitivity is suppressed by deletion of the DNA polymerase η (encoded by *RAD30* gene). Pol η is a Y-family translesion DNA polymerase able to face many replication stress conditions. Apart from acting on DNA-distorting lesions (e.g. UV-induced lesions) [4,128,131], it can also face different lesion-independent replication-stress conditions (reviewed in [6]). In this study, we described a novel involvement of Pol η during DNA replication under decreased nucleotide pools condition, which turns toxic in the absence of RNases H enzymes.

In the presence of HU, RNase H lacking cells activate the DNA damage checkpoint, which causes a cell cycle arrest in G2/M phase [127]. In this study, we proved that by deleting *RAD30*, cells restore their ability to complete the cell cycle by switching off the checkpoint signal. These phenotypes are the result of the Pol η activity at replication forks stressed by dNTP depletion, while no problems arise if Pol η acts later in S phase, once the dNTP pools have been replenished. Importantly, our phenotypes are associated only with the presence of HU, which depleting the dNTP pools enhances the ribonucleotide incorporation [181]. The fact that toxicity does not depend upon residual rNMPs in the template DNA strand, suggests that problems could be caused by ribonucleotides introduced by Pol η itself. In agreement, we have shown that toxicity requires the catalytic activity of the polymerase, and it is exacerbated using a Pol η mutant allele with enhanced ribonucleotide incorporation. Finally, we linked the toxicity to the persistency of RNA:DNA hybrids constituted by at least four consecutive rNMPs. All these results were included in a publication [191] **(appendix 1),** where we proposed that Pol η actively participates to DNA replication in low dNTPs conditions. Its ability to incorporate or extend RNA stretches could enable full-genome duplication at the expense of an accumulation of stretches of consecutive ribonucleotides in the genome **(Figure 13).**

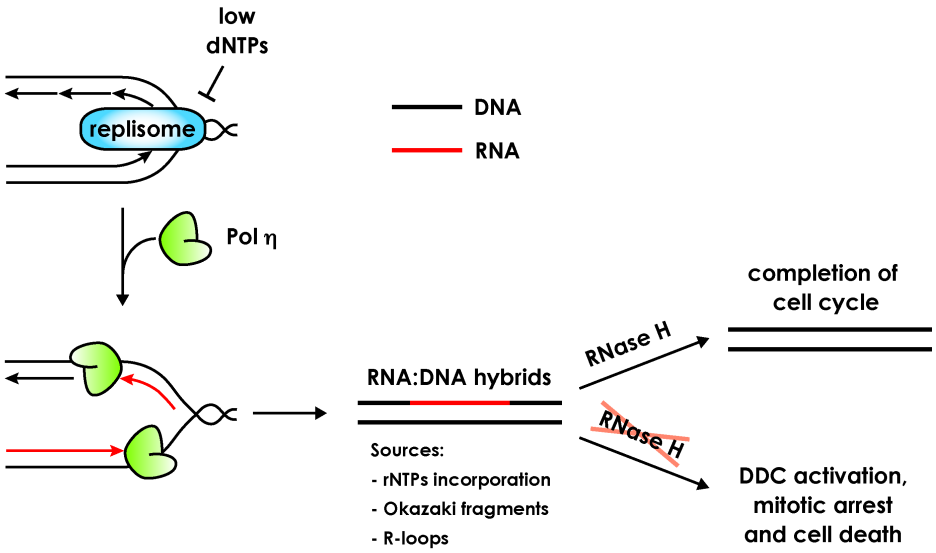

Figure 13. Proposed model of Pol η function during HU-mediated fork stalling [191].

The comprehension of Pol η activity under HU-induced replication stress is far from being complete, and after the publication, I tried to decipher different aspects of this complex picture:

1) The access of Pol η to damaged DNA templates is mainly regulated by PCNA monoubiquitination. However, it is not so clear whether the activity of Pol η under lesion-independent replication stress is regulated by the same mechanism. Our results indicate that PCNA seems to regulate also the recruitment of Pol η at HU-stressed replication forks. Moreover, we demonstrated that yeast Pol η can be mono SUMOylated. Interestingly, the level of SUMOylation decreases in the presence of HU. This indicates that apart from PCNA-monoubiquitination, also this modification might have a role in regulating the activity of Pol η at HU-stalled replication forks. This assumption is consistent with the recent finding that deSUMOylation events are known to promote the resumption of DNA synthesis from arrested forks [324]. We identified different SUMO-acceptor sites within the protein, but after the mutagenesis of the most probable sites, the modified residues are still unknown. An answer can come from coupling Pol η immunoprecipitation (+/- HU) to mass spectrometry analysis. This approach could shed light on the target residues, on how the HU influences this modification, and could also reveal other unscheduled posttranslational modifications that might regulate yeast Pol η.

2) Our data indicate that Pol η acts at HU-stressed replication forks, including RNA:DNA hybrids into DNA. Consistently, previous studies showed that yeast Pol η is enriched in the proximity of some replication origins actively replicated in HU [153,325]. Nevertheless, we still lack a genome-wide view of all the regions where Pol η acts. We recently performed a chromatin immunoprecipitation coupled to deep sequencing (ChIP-seq) in the presence of 200 mM HU, and future data analysis will reveal whether Pol η is recruited genome-wide or if its activity is restricted to specific locations or structures in the genome. In the absence of Pol η however, unknown pathways seem capable to replace its role,

making it difficult to appreciate a contribution of Pol η to DNA replication without removing RNase H enzymes. In collaboration with Grant Brown's lab in Toronto, I performed an SGA screening aimed to identify HU-specific synthetic sick or synthetic lethal interactors of *RAD30*. Interestingly, a bunch of genes validated as negative interactors of *RAD30* in the presence of HU has a role during DNA recombination. An intriguing hypothesis is that some HU-stalled replication forks can be processed through recombination or through a parallel pathway involving *RAD30*, which might act incorporating consecutive ribonucleotides that require the activity of RNases H to be removed. Future analyses need to be done to prove this theory.

3) Our data strongly indicate that Pol η activity leads to the inclusion of RNA stretches into DNA. Pol η is suitable for this function thanks to its ability to extend DNA or RNA primers with either rNTPs or dNTPs [137,140]. Genetic analyses seem to exclude that hybrids originate from the inclusion of RNA primers formed during Okazaki fragments synthesis. Even if it is still possible that rNMPs are directly incorporated by Pol η itself, we have to consider that *SEN1* overexpression rescues the HU sensitivity of *rnh1Δrnh201Δ* cells. This finding leads to the hypothesis that stretches of rNMPs result from the inclusion into DNA of RNA formed during transcription. This is supported by the finding that yeast Pol η is implicated in transcription elongation [140,326], and by *in vitro* studies indicating that when replication forks collide with RNA, transcripts can be used as primers to restart replication [311]. This phenomenon has also been observed in eukaryotic cells [278], and could be the strategy used by Pol η to promote DNA replication when replication forks are stalled by depleted dNTP pools. If this happens, part of the transcript might be included in DNA, generating RNA:DNA hybrids that need to be removed by RNases H enzymes. In this view, the increased toxicity of the ribonucleotide prone mutant of Pol η (F35A) might result from the elongation of transcripts with additional rNMPs, generating longer tracks of RNA:DNA hybrids, that could be more toxic if not resolved. If transcripts are the real substrates of Polη, a global reduction of the transcription levels might correlate with a reduced Pol η activity. Noteworthy, physical detection of multiple embedded rNMPs in DNA is very hard to tackle with the available technology. However, if they are formed by more than 6 consecutive rNMPs, a chance for their detection might come from the DRIP-seq technology [309]. The signal obtained with this technique should overlap with the signal obtained with the Pol η-ChIP-seq.

4) Finally, we proved that hybrids persistency (due to the absence of RNases H) causes cell death. Since hybrids compromise chromatin structure [202,327,328], one possibility is that their incorporation in some critical regions (such as centromeres) affects a proper cell division. This is supported by the finding that deletion of the Spindle Assembly Checkpoint factor *MAD2* partially rescues the HU-sensitivity, the cell cycle arrest, and the DDC activation of *rnh1Δrnh201Δ* cells **(Figure S6 in [191]).** Alternatively, in the absence of RNases H, hybrids could be processed by mutagenic repair mechanisms, such as the ones dependent on Top1, leading to deletions and chromosome breaks [239,329].

In conclusion, although some aspects need further clarification, in this study we described a novel role for the TLS polymerase η during genome duplication under HU-induced replication stress. We also have preliminary data indicating that this role is conserved from yeast to human. Replication stress is a prominent feature of precancerous and cancerous cells and Pol η is aberrantly expressed in several tumor types. Therefore, define the molecular mechanism of Pol η activity under depleted dNTP pools could enhance our knowledge of some tumors, and provide new targets for cancer therapy.

Material and Methods

Table of yeast strains

NAME	GENOTYPE	SOURCE
SY2080	*W303 MATa ade2-1 trp1-1 leu2-3,112 his3-11,15 ura3-1 can1-100 RAD5*	M. Foiani
SY2081	*W303 MATα ade2-1 trp1-1 leu2-3,112 his3-11,15 ura3-1 can1-100 RAD5*	M. Foiani
YFL1213	*(SY2080) MATa rnh1::HIS3 rnh201::KANMX6*	Lazzaro, 2012
YFL1773	*(SY2080) MATa rnh1::HIS3 rnh201::KANMX6 rad30::TRP1*	This Study
YSS21	*(SY2080) MATa rad30::KANMX6*	Giannattasio, 2012
YMG1082	*(SY2080) MATa rad30::KANMX6 rev1::KANMX6 rev3::TRP1 rev7::HIS3*	Giannattasio, 2012
YFL1271	*(SY2080) MATa rad30::KANMX6 rev1::KANMX6 rev3::TRP1 rev7::HIS3 rnh1::HIS3 rnh201::KANMX6*	Lazzaro, 2012
YSS17	*(SY2080) MATa rev1::KANMX6*	This Study
YFL2485	*(SY2080) MATa rev1::HPH rnh1::HIS3 rnh201::KANMX6*	This Study
YMG1096	*(SY2080) MATa rev3::TRP1 rev7::HIS3*	This Study
YFL1389	*(SY2080) MATa rev3::TRP1 rev7::HIS3 rnh1::HIS3 rnh201::KANMX6*	This Study
YFL3192	*(SY2080) MATa rad27::HPH*	This Study
YFL1358/6c	*(SY2081) MATα rnh1::HIS3 rnh201::KANMX6 rad30::KANMX6*	Available in lab
YFL3234/3b	*(SY2080) MATa rad27::HPH rad30::KANMX6*	This Study
YFL3236/2b	*(SY2081) MATα rad27::HPH rnh1::HIS3*	This Study
YFL3240/1a	*(SY2080) MATa rad27::HPH rnh201::KANMX6*	This Study
YFL3239/4b	*(SY2080) MATa rad27::HPH rad30::KANMX6 rnh1::HIS3*	This Study
YFL2852	*(SY2080) MATa top1::HIS3*	Available in lab
YFL3014	*(SY2080) MATa top1::HIS3 rad30::TRP1*	This Study
GH176	*(SY2080) MATa sen1G1747D-NAT1*	G.Liberi
GH292	*(SY2080) MATa sen1G1747D-NAT1 rad30::KANMX6*	G.Liberi
YFL1419	*(SY2080) MATa + pRS426*	This Study
YFL1420	*(SY2080) MATa + pEGUh6-RAD30 [GAL1-6XHIS- RAD30-URA3]*	This Study
YFL1422	*(SY2080) MATa rnh1::HIS3 rnh201::KANMX6 + pRS426*	This Study
YFL1423	*(SY2080) MATa rnh1::HIS3 rnh201::KANMX6 + pEGUh6-RAD30 [GAL1-6XHIS-rad30-URA3]*	This Study
YFL3361	*(SY2080) MATa top1::HIS3 + pRS426*	This Study

YFL3363	*(SY2080) MATa top1::HIS3 + pEGUh6-RAD30 [GAL1-6XHIS-RAD30-URA3]*	This Study
YFL3365	*(SY2080) MATa sen1G1747D-NAT1 + pRS426*	This Study
YFL3367	*(SY2080) MATa sen1G1747D-NAT1 + pEGUh6-RAD30 [GAL1-6XHIS- RAD30-URA3]*	This Study
YFL3803	*(SY2080) MATa + pGREG525*	This Study
YFL3804	*(SY2080) MATa + pFL149.1 [GAL1-13MYC-TOP1-LEU2]*	This Study
YL3805	*(SY2080) MATa rnh1::HIS3 rnh201::KANMX6 + pGREG525*	This Study
YFL3806	*(SY2080) MATa rnh1::HIS3 rnh201::KANMX6 + pFL149.1 [GAL1-13MYC-TOP1-LEU2]*	This Study
YFL3754	*(SY2080) MATa leu2-3,112::GAL1-TAP (LEU2)*	This Study
YFL3755	*(SY2080) MATa leu2-3,112::GAL1-TAP-SEN1 (LEU2)*	This Study
YFL3757	*(SY2080) MATa leu2-3,112::GAL1-TAP (LEU2) rnh1::HIS3 rnh201::KANMX6*	This Study
YFL3758	*(SY2080) MATa leu2-3,112::GAL1-TAP-SEN1 (LEU2) rnh1::HIS3 rnh201::KANMX6*	This Study
YFL3775	*(YFL3754) MATa + pRS426*	This Study
YFL3776	*(YFL3754) MATa + pEGUh6-RAD30 [GAL1-6XHIS- RAD30-URA3]*	This Study
YFL3778	*(YFL3755) MATa + pRS426*	This Study
YFL3779	*(YFL3755) MATa + pEGUh6-RAD30 [GAL1-6XHIS- RAD30-URA3]*	This Study
YFL3781	*(YFL3757) MATa + pRS426*	This Study
YFL3783	*(YFL3757) MATa + pEGUh6-RAD30 [GAL1-6XHIS- RAD30-URA3]*	This Study
YFL3787	*(YFL3758) MATa + pRS426*	This Study
YFL3789	*(YFL3758) MATa + pEGUh6-RAD30 [GAL1-6XHIS- RAD30-URA3]*	This Study
yGWB4990	*(BY4741) MATα ura3Δ::NatMX can1Δ::STE2pr-sp_his5+ leu2Δ0 his3Δ1 met15Δ0 lyp1Δ*	G.Brown
SN1280	*(BY4741) MATα rad30Δ0::natMX can1Δ0::STE2pr-Sp_HIS5 lyp1Δ0 his3Δ1 leu2Δ0 ura3Δ0 met15Δ0 LYS2*	G.Brown
YFL3668	*(SY2080) MATa rad30-D570A-F627A-F628A-13MYC:LEU2*	This Study
YFL3680	*(SY2080) MATa rnh1::HIS3 rnh201::KANMX6 rad30-D570A-F627A-F628A-13MYC:LEU2*	This Study
YFL548	*(SY2080) MATa GCN5-13MYC:KANMX6 + yIPLAC211*	Available in lab
YFL549.3	*(SY2080) MATa GCN5-13MYC:KANMX6 + yIPLAC212*	Available in lab
YFL2977	*(SY2080) MATa RAD30-13MYC:KANMX6 + yIPLAC211*	This Study
YFL3020	*(SY2080) MATa RAD30-13MYC:KANMX6 + yIPLAC212*	This Study

Table of plasmids

NAME	DESCRIPTION	SOURCE
pRS426	*2-micron high copy number yeast vector with URA3 marker*	Available in lab
pEUGh6-RAD30	*2-micron high copy number yeast vector with URA3 marker, GAL1-RAD30-6xHIS*	T.A. Kunkel (Pavlov 2001)
pGREG525	*Centromeric plasmid with LEU2 marker, GAL1-13MYC-Ø*	Available in lab
pFL149.1	*Centromeric plasmid with LEU2 marker, GAL1-13MYC-TOP1*	Available in lab
pCS14	*yeast integrative plasmid with LEU2 marker (pRS305), GAL1-TAP-Ø*	G. De Piccoli (Appanah, 2020)
pCS39	*yeast integrative plasmid with LEU2 marker (pRS305), GAL1-TAP-SEN1*	G. De Piccoli (Appanah, 2020)
YIPLAC211	*yeast integrative plasmid with URA3 marker*	Available in lab
YIPLAC212	*yeast integrative plasmid with URA3 marker, ADH-6xHIS-SMT3*	Available in lab

Yeast strains, plasmids, media and growth conditions

All the strains used in this study are listed in the yeast strains table, except for the strains used in the chapter: Characterization of the DNA polymerase η toxicity in RNase H deficient cells, (results and conclusions) that can be found in the published manuscript [191] , **(appendices 1).** All the strains are derivatives of W303 *RAD5+* background (*trp1-1 his3-11,15 can1-100 ura3-1 leu2-3,112 ade2-1*), with the exception of the query strains used for the SGA (yGWB4990 and SN1280), which are derivatives of BY4742 background (*his3Δ1 leu2Δ0 met15Δ0 ura3Δ0).* Yeast strains were obtained by standard procedures of transformation and tetrad dissection. One-step PCR system was used to delete genes and to tag proteins as described in [330]. YFL2977 and YFL3020 strains were obtained integrating the NcoI-digested YIPLAC211/212 plasmid at the URA3 locus. Proper integration and Smt3 protein level were checked by western blot. YFL3754, YFL3755, YFL3757, and YFL3758 strains were obtained integrating the BsteII-digested pCS14 or pCS39 plasmid at the LEU2 locus. Integration and TAP- Ø / TAP-Sen1 expressions were checked by western blot using the αPAP antibody (1:1500 in 5% milk in TBST).

For all the experiments, cells were grown at 28°C (except for the temperature-sensitive mutants that were grown at the permissive T of 25°C and at the semi-permissive T of 30°C). Cells were grown in YEP medium (1% yeast extract, 2% peptone) containing 2% glucose (YEPD), 2% raffinose (YEPR), or 2% galactose and 2% raffinose (YEPRG). For strains carrying plasmids, cells were grown in Synthetic-Complete (SC) medium supplemented with appropriate sugar(s) and nutrient to maintain the selection. The concentrations of the drugs used are indicated in the figures and in the legends. Hydroxyurea was purchased from US Biological (Salem, MA,USA). MMS was purchased from SIGMA (Saint Louis, MO,USA).

Below are reported all the protocols used in this study. Protocols used for all the experiments reported

in the chapter: Characterization of the DNA polymerase η toxicity in RNase H deficient cells, (results and conclusions) can be found in the published manuscript [191] , **(appendices 1).**

Sensitivity assay

Logarithmically growing yeast cultures or O/N growth yeast cultures were normalized at OD_{600}=0,06. Four 10-fold serial dilutions were prepared and spotted on YEP or selective plates, supplemented with the appropriate sugar and drugs at the indicated concentrations. Plates were incubated at 28°C, (or at 25°C and 30°C in case of the temperature-sensitive mutants), and pictures were taken after 2-4 days.

Tetrads analysis

Parental strains of opposite mating types (*MAT*a and *MAT*α) were crossed on a YEPD plate. After O/N growth and an optional step to specifically enrich MATa/α diploids, cells were transferred on sporulation plates and kept for 3 days at 25°C to induce asci formation (the poor medium-composition and the non-optimal temperature induce sporulation). Asci are then treated for 5 min with zymolyase (0,01mg/mL), to weaken the yeast wall and the 4 spores contained are separated and fixed in known positions on a YEPD plate. This is done through a micromanipulator fixed on an optical microscope (10X). After two days of growth at 28°C (or 25°C in the case of the *sen1-1* mutants), single spore-derived colonies were tested on different selective plates to identify those having the desired combination of selectable markers, and thus the genotype of interest. Genotypes of unviable spores can be deduced by analyzing the three viable spores of the same ascus.

Fluorescence-activated cell-sorting (FACS) Analysis

1mL of cells were centrifuged and fixed O/N in 70% cold ethanol. After centrifugation, cell pellet was resuspended in 0,5mL RNase A solution (1mg/mL in 50mM Tris-HCl p7.5) and incubated 2 hours at 37°C. Then, cells were centrifuged and resuspended in 0,5mL Proteinase K solution (1mg/mL in 50mM Tris-HCl pH7.5) and incubated 2 hours at 42°C. Pellet was resuspended in FACS buffer to keep it stable for few days. For the analysis, DNA was stained with Sytox Green (1:5000M in 50mM Tris-HCl pH7.5) and then the cell-cycle distribution was estimated by cytofluorimetric analysis with a FACScan™. Data were plotted using the FlowJO® Software.

Two-Dimensional agarose gel experiments

Two dimensional agarose gel analysis was carried out essentially as described in [331–333]. More information regarding the technique and the interpretation of the results can be found in [312,334]. For each sample 200mL of ~$1*10^7$ cells were collected, washed, resuspended in 5 mL of sterile water, and placed in 6-multiwell plates on ice. 300 µL of trioxalen solution (0.2mg/mL in 100% ethanol, SIGMA) were added. Cells were incubated for 5 min in the dark and irradiated for ten min with 365 nm UV light. This crosslinking procedure was repeated four times in total. Cells were resuspended in 5 mL

cold NIB Buffer pH 7.2 (17% Glycerol, 50 mM MOPS, 150 mM KAc, 2 mM $MgCl_2$, 0.5 mM Spermidine, 0.15 mM Spermine) and mechanically disrupted by vortexing with glass beads. DNA extraction was performed according to the ‘‘QIAGEN genomic DNA Handbook,’’ using genomic-tip 100/G columns and 10 µg of DNA were digested with NcoI and EcoRV restriction enzymes (according to the strategies described in the results, figure 7). DNA was then precipitated and resuspended in 20 µL of TE 1X. First-dimension gels (0.35% agarose in TBE 1X without EtBr) were run at 75 V for 18 h at room temperature. The low agarose gel concentrations and the low electric field minimize the effects of various molecular shapes and separate replication intermediates mainly according to their different mass. Gel slices containing the fragments of interest and all their replication intermediates are excised and subjected to the second-dimension gel run (0.9% agarose in TBE 1X + 0.3 µg/mL of EtBr). Here, samples were run at 250V for 4.5h at 4°C, supplementing the running buffer with 0.3 mg/mL of EtBr. This high EtBr concentration, agarose gel concentration, and electric field allow resolving replication intermediates according to their different topological structures. Trioxalen crosslinking was then reverted by irradiating gels under 265 nM UV lamps for 10 min. Gels were sequentially washed with 0.25N HCl, milliQ water, denaturing solution (0.5 M NaOH, 1.5M NaCl) and Blot#2 solution (1M $AcNH_4$ 0.02M NaOH). Southern blot was performed overnight on Gene Screen neutral transfer membranes equilibrated in SSC 10X.

25ng of specific DNA probes were labeled with 6000 Ci/mmol of α^{32}P dATP using the Exo-Klenow polymerase (DECAprime™ II by Ambion) and purified by G-50 column (IllustraTM Microspin G-50 Columns, GE Healthcare). Membranes were pre-incubated in hybridization solution (PerfectHyb™ Plus Hybridization Buffer by SIGMA) at 65°C for 1h rotating, then incubated overnight under rotation at 65°C after radioactive probe addition. The next morning, membranes were washed twice with washing solution I (SSC 2X, 1% SDS) pre-heated at 65°C and twice with washing solution II (SSC 0.1X, 0,1% SDS) pre-heated at 42°C. Membranes were dried on air and were exposed to IR-sensitive screens for two days. The radioactive signals were analyzed using a Typhoon™ FLA7000 biomolecular imager (GE Healthcare Life Sciences, Marlborough, MA, USA).

SGA Procedure

Synthetic genetic array (SGA) analysis was carried out as described in [335]. Wild-type (yGWB4990) and *rad30Δ::natMX* (SN1280) Mat α strains were used as query. Their genotype is reported in the strains table. All the steps were performed using a robotic system programmed to manipulate yeast cell arrays. The query strains were grown in 5 mL of YEPD O/N. In the meantime, the 1536-density DMA and TS Mat a strains were replicated to fresh YEPD + G418 plates. The next day each query strain culture was poured over a YEPD plate and cells were grown at 30°C for 1 day. Mating was performed pinning at first the 1536-format query strains onto a fresh YEPD plate and then pinning the DMA/TS on top of the query cells. Mating plates were incubated at room temperature for 2 days and diploids

were selected pinning the Mat a/α zygotes on YEPD + G418/clonNAT plates and incubating plates for 2 days at room temperature. Diploids cells were pinned on sporulation medium, and the sporulation plates were incubated at 23°C for 7 days. The resulting spores were pinned onto SD-His/Arg/Lys+canavanine/thialysine plates to select for Mat a haploid meiotic progeny. The haploid selection plates were incubated at room temperature for 4 days. Canavanine and thialysine are toxic analogues of Arginine and Lysine that allow selecting only haploid Mat a cells, avoiding the selection of recombinogenic events that can generate Mat a/a diploids. For a proper action of these compounds, plates are devoid of Arginine and lysine. Finally, the absence of histidine in the plates allows to specifically select Mat a cells, which express can1Δ::STE2pr-Sp_HIS5. This step of selection onto SD –His / Arg / Lys + canavanine /thialysine plates is repeated a second time and plates are incubated for 2 days at room temperature. The Mat a meiotic progeny is then pinned onto SD -His/Arg/Lys + canavanine/thialysine/G418 plates to select for Mat a meiotic progeny carrying the KanR marker. Plates were incubated at room temperature for 2 days. This step is then repeated pinning cells onto SD - His/Arg/Lys + canavanine/thialysine/G418/clonNAT plates to select the meiotic progeny carrying both KanR and natR markers. Plates were incubated for 3 days at room temperature. Colonies were sequentially pinned on YEPD plates (untreated) and YEPD plates containing 100mM HU. Plates were incubated for 3 days at 30°C, and finally, the double mutants were scored for fitness defects.

Scoring of putative interactions in an SGA Screen

Double mutants SGA Plates (YEPD +/- 100mM HU) were digitally photographed, and colony areas were analysed using the SGA-tools (http://sgatools.ccbr.utoronto.ca/). SGA-tools is a web-based analysis system, which allows to quantify colonies on the agar plates, normalize systematic effects and calculate fitness scores relative to a control experiment. The score is calculated using the multiplicative model, whereby the double mutant fitness is expected to be equal to the product of the corresponding single mutant fitness ($f$ab $= f$a x fb) [336]. When the colony of the double mutant is smaller than expected, it is considered as a negative (synthetic sick or lethal) genetic interaction. If it is larger, it is referred as a positive (e.g. suppression) genetic interaction [337]. From the screenings, I obtained both wild-type and *rad30Δ* cells combined with each gene in the DMA/TS array, either in untreated or in the presence of 100mM HU. Therefore, I applied the following normalization conditions:

First condition: wt-geneX(UT) vs wt-geneX(100mM HU) (negative score corresponded to genes known to be sensitive to HU). **Second condition:** wt-geneX(UT) vs *rad30Δ*-geneX(UT) (the canonical *RAD30*-screening, already published by [338]).

Since I wanted to analyze interactions specific for *RAD30* and for the presence of HU, I focused my attention on genes associated with a score < -0.1 applying a **third condition:** wt-geneX(HU) vs *rad30Δ*-geneX(HU).

I also selected genes associated with a score < -0,1 using the **fourth condition:** *rad30Δ*-geneX (UT) vs *rad30Δ*-geneX (HU), selecting genes where the Δ-score between this condition and the first one was < -0,1. In other words, I compared wt-geneX (UT)vs(HU) to *rad30Δ*-geneX(UT)vs(HU) to find genes that become sensitive to HU only when *RAD30* is deleted, or genes that exacerbate their HU-sensitivity upon deletion of *RAD30*. I analyzed non-essential genes (DA) and essential genes (TS) separately, and I finally compared the two-screenings replicates. Genes selected for further validation were 129 in total, **(supplementary list 1),** including genes common to both the screenings (44 DA + 50 TS), plus some genes associated with a negative score in only one of the SGA. This is because SGA can also generate false-negative results.

Ni-NTA pull-down under denaturing conditions

For each sample, 100 mL of yeast cells were normalized at OD_{600}=0.3 and were collected by centrifugation. Cells were washed with water, resuspended in 150 µL TCA 10% and then transferred in 1.5mL tubes. After glass beads addition, cells were mechanically lysed through FastPrep machine. Lysis was checked under the microscope and the lysate material was transferred into new 1.5mL tubes. After centrifugation, the pellet was sequentially washed with 100% ice-cold acetone, and Tris-Base 1M in order to neutralize eventual residual TCA present in the pellet. Pellet was brought to 1.5 mL total volume in Buffer A pH8.0 (6 M Guanidine HCl, 100 mM NaH_2PO_4, 10 mM Tris-Base) and proteins were solubilized for 3 hours at room temperature under rotation. Cell debris were then removed by centrifugation. 20 µL of protein extracts were collected as input sample. A Ni-pull-down was performed incubating the remaining protein extracts with Ni-nitrilotriacetic (NTA) agarose beads (Qiagen) over-night at room temperature, in presence of 15 mM Imidazole and 0,05% Tween.

Agarose beads were recovered the day after by slow centrifugation and washed two times with Buffer A and three times with Buffer C pH6.3 (8 M Urea, 100 mM NaH_2PO_4, 10 mM Tris-Base), both supplemented with 0,05% Tween 20. Sumoylated proteins were eluted with 50 µl of HU Buffer (8 M Urea, 200 mM Tris-HCl pH 6.8, 1 mM EDTA, 5% SDS, 0,1% bromophenol blue, 0.1M DTT). Input and pull-down samples were run on 4-20% gradient SDS-poly-acrylamide gel (Novex) for western blotting. Pol η and GCN5 modifications were visualized by western blot analysis using αMyc antibodies (mouse monoclonal antibodies, diluted 1:20 in 5% milk in PBST). PCNA was visualized using αPCNA (rabbit, diluted 1:10000 in 5% milk in PBST). 6xHIS-Smt3 expression and protocol success were controlled by incubation with αSMT3 antibody (Rockland Immunochemicals) (rabbit, diluted 1:1000 in 5% milk in TBST).

Supplementary list 1:

ORF	GENE	44 HITS common to the 2 SGAs: F.Score in SGA1 (1st row) and SGA2 (2nd row)				SGD INFO
		30UT_30HU	wtUT_wtHU	Difference	wtHU_30HU	
YBR170C	NPL4	-0,26168	0,03825	-0,29993	-0,30531	Substrate-recruiting cofactor of the Cdc48p-Npl4p-Ufd1p segregase; assists Cdc48p in the dislocation of misfolded, polyubiquitinated ERAD substrates that are subsequently delivered to the proteasome for degradation; also involved in the regulated destruction of resident ER membrane proteins, such as HMG-CoA reductase (Hmg1/2p) and cytoplasmic proteins (Fbp1p); role in mobilizing membrane bound transcription factors by regulated ubiquitin/proteasome-dependent processing (RUP)
		-0,275	-0,04936	-0,22564	-0,12005	
YDR161W	YDR161W	-0,19905	-0,06837	-0,13068	-0,19864	Specific assembly chaperone for ribosomal protein Rpl4a/b; associates co-translationally with a evolutionarily conserved internal loop of nascent Rpl4a/b, and is released only after an the eukaryotic-specific extension of nascent Rpl4a/b mediates nuclear import, incorporation into the pre-ribosome and complex disassembly; role in biogenesis of the 60S ribosomal subunit; transcriptionally co-regulated with rRNA and ribosome biosynthesis genes
		-0,33732	0,00467	-0,34199	-0,38082	
YDL119C	YDL119C	-0,28085	-0,12597	-0,15488	-0,17554	Mitochondrial glycine transporter; required for the transport of glycine into mitochondria for initiation of heme biosynthesis, with YMC1 acting as a secondary transporter; homolog of human SLC25A38, a mitochondrial glycine transporter associated with nonsyndromic autosomal recessive congenital sideroblastic anemia; human SLC25A38 can complement the heme deficiency associated with the null mutant; GFP-fusion protein is induced in response to the DNA-damaging agent MMS
		-0,22574	-0,11063	-0,11511	-0,12232	
YOR275C	RIM20	-0,10916	0,01225	-0,12141	-0,15891	Protein involved in proteolytic activation of Rim101p; part of response to alkaline pH; PalA/AIP1/Alix family member; interaction with the ESCRT-III subunit Snf7p suggests a relationship between pH response and multivesicular body formation
		-0,19533	0,09468	-0,29001	-0,22098	
YNR005C	YNR005C	-0,10539	0,05458	-0,15997	-0,14287	Dubious open reading frame; unlikely to encode a functional protein, based on available experimental and comparative sequence data
		-0,11481	0,23163	-0,34644	-0,24563	
YOR221C	MCT1	-0,31029	-0,15558	-0,15471	-0,13763	Predicted malonyl-CoA:ACP transferase; putative component of a type-II mitochondrial fatty acid synthase that produces intermediates for phospholipid remodeling
		-0,22027	0,01988	-0,24015	-0,31615	
YCL002C	YCL002C	-0,17647	-0,07473	-0,10174	-0,1113	Putative protein of unknown function; YCL002C is not an essential gene
		-0,18053	0,07613	-0,25666	-0,29427	
YPR194C	OPT2	-0,13792	0,00933	-0,14725	-0,14032	Oligopeptide transporter; localized to peroxisomes and affects glutathione redox homeostasis; also localizes to the plasma membrane (PM) and to the late Golgi, and has a role in maintenance of lipid asymmetry between the inner and outer leaflets of the PM; member of the OPT family, with potential orthologs in S. pombe and C. albicans; also plays a role in formation of mature vacuoles and in polarized cell growth
		-0,17772	-0,03326	-0,14446		
YNL142W	MEP2	-0,21593	-0,00783	-0,2081		Ammonium permease involved in regulation of pseudohyphal growth; belongs to Mep-Amt-Rh family of well-conserved ammonium (NH4+) transporters that includes human Rh factors; expression is under the nitrogen catabolite repression regulation; activity is controlled by phospho-silencing; phosphorylation of Mep2 mediated by Npr1; dephosphorylation involves Psr1p and Psr2p
		-0,11009	-0,00468	-0,10541	-0,14642	
YNR032C-A	HUB1	-0,23098	-0,09695	-0,13403		Ubiquitin-like protein modifier; promotes alternative splicing of SRC1 pre-mRNA; binds non-covalently to the HIND domain of Snu66, may function in modification of Sph1p and Hbt1p, functionally complemented by the human or S. pombe ortholog; mechanism of Hub1p adduct formation not yet clear
		-0,20064	0,15431	-0,35495	-0,26823	
YMR021C	MAC1	-0,46435	-0,3363	-0,12805		Copper-sensing transcription factor; involved in regulation of genes required for high affinity copper transport; required for regulation of yeast copper genes in response to DNA-damaging agents; undergoes changes in redox state in response to changing levels of copper or MMS
		-0,39486	-0,22122	-0,17364	-0,20824	
YPR024W	YME1	-0,25218	-0,10733	-0,14485	-0,47102	Catalytic subunit of i-AAA protease complex; complex is located in mitochondrial inner membrane; responsible for degradation of unfolded or misfolded mitochondrial gene products; serves as nonconventional translocation motor to pull PNPase into intermembrane space; also has role in intermembrane space protein folding; mutation causes elevated rate of mitochondrial turnover; human homolog YME1L1 can complement yeast null mutant
					-0,2505	
YOR300W	YOR300W	-0,26216	-0,12538	-0,13678	-0,12343	Dubious open reading frame; unlikely to encode a functional protein, based on available experimental and comparative sequence data; overlaps with verified gene BUD7/YOR299W; mutation affects bipolar budding and bud site selection, though phenotype could be due to the mutation's effects on BUD7
					-0,20495	
YIL006W	YIA6	-0,16965	-0,02511	-0,14454	-0,11904	Mitochondrial NAD+ transporter; involved in the transport of NAD+ into the mitochondria (see also YEA6); member of the mitochondrial carrier subfamily; disputed role as a pyruvate transporter; has putative mouse and human orthologs; YIA6 has a paralog, YEA6, that arose from the whole genome duplication
					-0,10509	
YGL046W	YGL046W				-0,16212	Merged open reading frame; does not encode a discrete protein; YGL046W was originally annotated as an independent ORF, but as a result of a sequence change, it was merged with an adjacent ORF into a single reading frame, designated YGL045W
		-0,10808	0,03178	-0,13986	-0,11226	
YGR269W	YGR269W				-0,13034	Dubious open reading frame; unlikely to encode a functional protein, based on available experimental and comparative sequence data; partially overlaps the uncharacterized ORF HUA1/YGR268C
		-0,11846	0,08567	-0,20413	-0,27914	
YPL046C	ELC1				-0,11834	Elongin C, conserved among eukaryotes; forms a complex with Cul3p that polyubiquitylates monoubiquitylated RNA polymerase II to trigger its proteolysis; plays a role in global genomic repair
		-0,27176	-0,04636	-0,2254	-0,19186	
YCR071C	IMG2				-0,11521	Mitochondrial ribosomal protein of the large subunit; conserved in metazoa, with similarity to human mitochondrial ribosomal protein MRPL49
		-0,27127	-0,14174	-0,12953	-0,19129	
YBR218C	PYC2				-0,11003	Pyruvate carboxylase isoform; cytoplasmic enzyme that converts pyruvate to oxaloacetate; differentially regulated than isoform Pyc1p; mutations in the human homolog are associated with lactic acidosis; PYC2 has a paralog, PYC1, that arose from the whole genome duplication
		-0,22529	-0,01567	-0,20962	-0,1158	
YMR025W	CSI1				-0,10481	Subunit of the Cop9 signalosome; which is required for deneddylation, or removal of the ubiquitin-like protein Rub1p from Cdc53p (cullin); involved in adaptation to pheromone signaling; functional equivalent of canonical Csn6 subunit of the COP9 signalosome
		-0,34621	-0,20577	-0,14044	-0,1088	
YOL041C	NOP12	-0,14207	-0,03759	-0,10448		Nucleolar protein involved in pre-25S rRNA processing; also involved in biogenesis of large 60S ribosomal subunit; contains an RNA recognition motif (RRM); binds to Ebp2; similar to Nop13p and Nsr1p
		-0,14033	-0,02695	-0,11338		

YNL003C	PET8	-0,34295	-0,24044	-0,10251		S-adenosylmethionine transporter of the mitochondrial inner membrane; member of the mitochondrial carrier family; required for biotin biosynthesis and respiratory growth
		-0,46276	-0,33724	-0,12552		
YPL170W	DAP1	-0,67544	-0,53951	-0,13593		Heme-binding protein; involved in regulation of cytochrome P450 protein Erg11p; damage response protein, related to mammalian membrane progesterone receptors; mutations lead to defects in telomeres, mitochondria, and sterol synthesis
		-0,56807	-0,45184	-0,11623		
YER143W	DDI1	-0,17054	0,08908	-0,25962		DNA damage-inducible v-SNARE binding protein; role in suppression of protein secretion; may play a role in S-phase checkpoint control; has ubiquitin-associated (UBA), ubiquitin-like (UBL), and retroviral-like proteinase (RVP) domains
					-0,19592	
YGR093W	YGR093W	-0,12826	-0,00921	-0,11905		Splicing factor that modulates turnover of branched RNAs by Dbr1p; interacts with spliceosomal components and branched RNA splicing products; enhances Dbr1p debranching in vitro; conserved protein with domain organization identical from yeast to human; N-terminal homology to Dbr1p N-terminus, but Dbr1p catalytic residues not conserved; relocalizes to the cytosol in response to hypoxia
					-0,13623	
YML107C	PML39	-0,11246	-0,00614	-0,10632		rotein required for nuclear retention of unspliced pre-mRNAs; required along with Mlp1p and Pml1p; anchored to nuclear pore complex via Mlp1p and Mlp2p; found with the subset of nuclear pores farthest from the nucleolus; may interact with ribosomes
					-0,12371	
YNL045W	LAP2				-0,2016	Leucyl aminopeptidase yscIV with epoxide hydrolase activity; metalloenzyme containing one zinc atom; green fluorescent protein (GFP)-fusion protein localizes to the cytoplasm and nucleus; also known as leukotriene A4 hydrolase
					-0,19833	
YGR139W	YGR139W				-0,18953	Dubious open reading frame; unlikely to encode a functional protein, based on available experimental and comparative sequence data
					-0,24342	
YPR097W	YPR097W				-0,16167	Protein that contains a PX domain and binds phosphoinositides; the authentic, non-tagged protein is detected in highly purified mitochondria in high-throughput studies; PX stands for Phox homology
					-0,10681	
YMR065W	KAR5				-0,15592	Protein required for nuclear membrane fusion during karyogamy; localizes to the membrane with a soluble portion in the endoplasmic reticulum lumen, may form a complex with Jem1p and Kar2p; similar to zebrafish Brambleberry protein; expression of the gene is regulated by pheromone
					-0,10423	
YML090W	YML090W				-0,13689	Dubious open reading frame; unlikely to encode a functional protein, based on available experimental and comparative sequence data; partially overlaps the dubious ORF YML089C; exhibits growth defect on a non-fermentable (respiratory) carbon source
					-0,33497	
YGR242W	YGR242W				-0,13003	Dubious open reading frame; unlikely to encode a functional protein, based on available experimental and comparative sequence data; partially overlaps the verified ORF YAP1802/YGR241C
					-0,20619	
YBR276C	PPS1				-0,12858	Protein phosphatase; has specificity for serine, threonine, and tyrosine residues; has a role in the DNA synthesis phase of the cell cycle
					-0,13596	
YBR082C	UBC4				-0,12201	Ubiquitin-conjugating enzyme (E2); key E2 partner with Ubc1p for the anaphase-promoting complex (APC); mediates degradation of abnormal or excess proteins, including calmodulin and histone H3; regulates levels of DNA Polymerase-{alpha} to promote efficient and accurate DNA replication; interacts with many SCF ubiquitin protein ligases; component of the cellular stress response; UBC4 has a paralog, UBC5, that arose from the whole genome duplication
					-0,24341	
YJL007C	YJL007C				-0,11514	Putative protein of unknown function; conserved among S. cerevisiae strains
					-0,10982	
YPR122W	AXL1				-0,11284	Haploid specific endoprotease of a-factor mating pheromone; performs one of two N-terminal cleavages during maturation of a-factor mating pheromone; required for axial budding pattern of haploid cells
					-0,18943	
YHR066W	SSF1				-0,11202	Constituent of 66S pre-ribosomal particles; required for ribosomal large subunit maturation; functionally redundant with Ssf2p; member of the Brix family; SSF1 has a paralog, SSF2, that arose from the whole genome duplication
					-0,10357	
YOR321W	PMT3				-0,10923	Protein O-mannosyltransferase; transfers mannose residues from dolichyl phosphate-D-mannose to protein serine/threonine residues; acts in a complex with Pmt5p, can instead interact with Pmt1p in some conditions; antifungal drug target; PMT3 has a paralog, PMT2, that arose from the whole genome duplication
					-0,16791	
YDL184C	RPL41A				-0,10719	Ribosomal 60S subunit protein L41A; comprises only 25 amino acids; rpl41a rpl41b double null mutant is viable; homologous to mammalian ribosomal protein L41, no bacterial homolog; RPL41A has a paralog, RPL41B, that arose from the whole genome duplication
					-0,11711	
YOR044W	IRC23				-0,1051	Protein of unknown function; green fluorescent protein (GFP)-fusion localizes to the ER; null mutant displays increased levels of spontaneous Rad52p foci; IRC23 has a paralog, BSC2, that arose from the whole genome duplication
					-0,1296	
YPL073C	YPL073C				-0,10509	Dubious open reading frame; unlikely to encode a functional protein, based on available experimental and comparative sequence data; completely overlaps with verified gene UBP16/YPL072W; may interact with ribosome based on co-purification experiments
					-0,14109	
YJL153C	INO1				-0,10312	Inositol-3-phosphate synthase; involved in synthesis of inositol phosphates and inositol-containing phospholipids; transcription is coregulated with other phospholipid biosynthetic genes by Ino2p and Ino4p, which bind the UASINO DNA element
					-0,10143	
YGL205W	POX1				-0,10038	Fatty-acyl coenzyme A oxidase; involved in the fatty acid beta-oxidation pathway; localized to the peroxisomal matrix
					-0,11276	
YDL071C	YDL071C				-0,10008	Dubious open reading frame; unlikely to encode a functional protein, based on available experimental and comparative sequence data; partially overlaps the verified ORF BDF2/YDL070W
					-0,27421	

19 HITS obtained from only one SGA:

		SGA 1_HITS				
		30UT_vs_30H	/tUT_vs_wtH	30-WT	wtHU_vs_30HU	
Array ORF	Array Nam	filtered score	filtered score	difference	Filtered score	SGD INFO
YGL029W	CGR1	-0,26532	-0,06797	-0,19735	-0,29562	Protein involved in nucleolar integrity and processing of pre-rRNA; has a role in processing rRNA for the 60S ribosome subunit; transcript is induced in response to cytotoxic stress but not genotoxic stress; relocalizes from nucleus to nucleolus upon DNA replication stress
YBR094W	PBY1	-0,35876	-0,03994	-0,31882	-0,29363	Putative tubulin tyrosine ligase associated with P-bodies; may have a role in mRNA metabolism; yeast knockout collection strain identified as a pby1 null mutant is actually wild-type for PBY1 and deleted for mms4
YOR213C	SAS5	-0,13572	0,11729	-0,25301	-0,26354	Subunit of the SAS complex (Sas2p, Sas4p, Sas5p); acetylates free histones and nucleosomes and regulates transcriptional silencing; stimulates Sas2p HAT activity
YBR098W	MMS4	-0,26891	-0,03692	-0,23199	-0,22958	Subunit of structure-specific Mms4p-Mus81p endonuclease; cleaves branched DNA; involved in recombination, DNA repair, and joint molecule formation/resolution during meiotic recombination; phosphorylation of the non-catalytic subunit Mms4p by Cdc28p and Cdc5p during mitotic cell cycle activates the function of Mms4p-Mus81p
YBR231C	SWC5	-0,14265	0,01667	-0,15932	-0,21023	Component of the SWR1 complex; complex exchanges histone variant H2AZ (Htz1p) for chromatin-bound histone H2A; protein abundance increases in response to DNA replication stress; relocalizes to the cytosol in response to hypoxia
YGL080W	FMP37	-0,23439	-0,06773	-0,16666	-0,19917	Highly conserved subunit of mitochondrial pyruvate carrier (MPC); MPC is a mitochondrial inner membrane complex that mediates pyruvate uptake and comprises Mpc1p and Mpc2p during fermentative growth, or Mcp1p and Mpc3p during respiratory growth; null mutant displays slow growth that is complemented by expression of human or mouse ortholog; mutation in human ortholog MPC1 is associated with lactic acidosis and hyperpyruvatemia
YOR179C	SYC1	-0,25499	-0,07557	-0,17942	-0,19042	Subunit of the APT subcomplex of cleavage and polyadenylation factor; may have a role in 3' end formation of both polyadenylated and non-polyadenylated RNAs; SYC1 has a paralog, YSH1, that arose from the whole genome duplication
YOL049W	GSH2	-0,20064	-0,001	-0,19964	-0,17907	Glutathione synthetase; catalyzes the ATP-dependent synthesis of glutathione (GSH) from gamma-glutamylcysteine and glycine; induced by oxidative stress and heat shock
YPL024W	RMI1	-0,36201	-0,15319	-0,20882	-0,16839	Subunit of the RecQ (Sgs1p) - Topo III (Top3p) complex; stimulates superhelical relaxing, DNA catenation/decatenation and ssDNA binding activities of Top3p; involved in response to DNA damage; functions in S phase-mediated cohesion establishment via a pathway involving the Ctf18-RFC complex and Mrc1p; stimulates Top3p DNA catenation/decatenation activity; null mutants display increased rates of recombination and delayed S phase

		SGA 2_HITS				
		30UT_vs_30	WTUT_vs_W	30-wt	wtHU_vs_30HU	
Array ORF	Array Nam	filtered score	filtered score	Difference	filtered score	SGD INFO
YML041C	VPS71	-0,29117	-0,01494	-0,27623	-0,32841	Nucleosome-binding component of the SWR1 complex; SWR1 exchanges histone variant H2AZ (Htz1p) for chromatin-bound histone H2A; required for vacuolar protein sorting
YPL096W	PNG1	-0,25238	0,06579	-0,31817	-0,3186	Conserved peptide N-glycanase; deglycosylating enzyme that cleaves N-glycans that are attached to misfolded ERAD substrate glycoproteins prior to proteasome-dependent degradation; localizes to the cytoplasm and nucleus; activity is enhanced by interaction with Rad23p; human ortholog NGLY1 is associated with a syndrome characterized by developmental delays, epilepsy, absence of tears and liver disease
YLR337C	VRP1	-0,61474	-0,39812	-0,21662	-0,26723	Verprolin, proline-rich actin-associated protein; involved in cytoskeletal organization and cytokinesis; promotes actin nucleation and endocytosis; related to mammalian Wiskott-Aldrich syndrome protein (WASP)-interacting protein (WIP
YPR032W	SRO7	-0,29723	-0,11735	-0,17988	-0,23837	Effector of Rab GTPase Sec4p; forms a complex with Sec4p and t-SNARE Sec9p; involved in exocytosis and docking and fusion of post-Golgi vesicles with plasma membrane; regulates cell proliferation and colony development via the Rho1-Tor1 pathway; homolog of Drosophila lgl tumor suppressor; SRO7 has a paralog, SRO77, that arose from the whole genome duplication
YDL181W	INH1	-0,37112	-0,18693	-0,18419	-0,23772	Protein that inhibits ATP hydrolysis by the F1F0-ATP synthase; inhibitory function is enhanced by stabilizing proteins Stf1p and Stf2p; has a calmodulin-binding motif and binds calmodulin in vitro; INH1 has a paralog, STF1, that arose from the whole genome duplication
YLR079W	SIC1	-0,33078	-0,16533	-0,16545	-0,20916	Cyclin-dependent kinase inhibitor (CKI); inhibitor of Cdc28-Clb kinase complexes that controls G1/S phase transition, preventing premature S phase and ensuring genomic integrity; phosphorylated by Clb5/6-Cdk1 and Cln1/2-Cdk1 kinase which regulate timing of Sic1p degradation; phosphorylation targets Sic1p for SCF(CDC4)-dependent turnover; functional homolog of mammalian Kip1
YDR245W	MNN10	-0,60192	-0,37653	-0,22539	-0,18681	Subunit of a Golgi mannosyltransferase complex; complex mediates elongation of the polysaccharide mannan backbone; membrane protein of the mannosyltransferase family; other members of the complex are Anp1p, Mnn9p, Mnn11p, and Hoc1p
YLR234W	TOP3	-0,54468	-0,36238	-0,1823	-0,18083	DNA Topoisomerase III; conserved protein that functions in a complex with Sgs1p and Rmi1p to relax single-stranded negatively-supercoiled DNA preferentially; DNA catenation/decatenation activity is stimulated by RPA and Sgs1p-Top3p-Rmi1p; involved in telomere stability and regulation of mitotic recombination
YFL003C	MSH4	-0,43083	-0,15786	-0,27297	-0,17897	Protein involved in meiotic recombination; required for normal levels of crossing over, colocalizes with Zip2p to discrete foci on meiotic chromosomes, has homology to bacterial MutS protein
YDR169C	STB3	-0,21434	-0,05079	-0,16355	-0,16917	Ribosomal RNA processing element (RRPE)-binding protein; involved in the glucose-induced transition from quiescence to growth; restricted to nucleus in quiescent cells, released into cytoplasm after glucose repletion; binds Sin3p; relative distribution to the nucleus increases upon DNA replication stress

50 HITS common to the 2 SGAs:

ORF	GENE	Array Annotation	F.Score in SGA1 (1st row) and SGA2 (2nd row) 30UT_30HU	wtUT_wtHU	Difference	wtHU_30HU	SGD INFO
YFL039C	ACT1	act1-125	-0,45656	-0,28992	-0,16664	-0,12998	Actin; structural protein involved in cell polarization, endocytosis, and other cytoskeletal functions
			-0,67393	-0,46542	-0,20851	-0,24762	
YKL022C	CDC16	cdc16-1	-0,12478	-0,00762	-0,11716	-0,14156	Subunit of the anaphase-promoting complex/cyclosome (APC/C); which is a ubiquitin-protein ligase required for degradation of anaphase inhibitors, including mitotic cyclins, during the metaphase/anaphase transition; required for sporulation; relocalizes to the cytosol in response to hypoxia
			-0,20567	-0,08521	-0,12046		
YHR166C	CDC23	cdc23-1	-0,32542	-0,14359	-0,18183	-0,1439	Subunit of the Anaphase-Promoting Complex/Cyclosome (APC/C); APC/C is a ubiquitin-protein ligase required for degradation of anaphase inhibitors, including mitotic cyclins, during the metaphase/anaphase transition
			-0,35647	0,02773	-0,3842	-0,1967	
YDL207W	GLE1	gle1-4	-0,31184	-0,00948	-0,30236	-0,17863	Cytoplasmic nucleoporin required for polyadenylated mRNA export; contains a nuclear export signal; when bound to inositol hexakisphosphate (IP6), functions as an activator for the Dbp5p ATPase activity at the nuclear pore complex during mRNA export; mediates translation initiation; required for efficient translation termination
			-0,32526	-0,16168	-0,16358		
YMR043W	MCM1	mcm1-ph	-0,1024	0,44643	-0,54883	-0,92522	Transcription factor; involved in cell-type-specific transcription and pheromone response; plays a central role in the formation of both repressor and activator complexes; relocalizes to the cytosol in response to hypoxia
						-0,19758	
YFL034C-B	MOB2	mob2-14	-0,30085	-0,16262	-0,13823	-0,2661	Activator of Cbk1p kinase; component of the RAM signaling network that regulates cellular polarity and morphogenesis; activation of Cbk1p facilitates the Ace2p-dependent daughter cell-specific transcription of genes involved in cell separation; similar to Mob1p
			-0,38899	-0,11262	-0,27637	-0,1112	
YFL034C-B	MOB2	mob2-8	-0,94575	-0,70702	-0,23873	-0,19942	Activator of Cbk1p kinase; component of the RAM signaling network that regulates cellular polarity and morphogenesis; activation of Cbk1p facilitates the Ace2p-dependent daughter cell-specific transcription of genes involved in cell separation; similar to Mob1p
			-0,92318	-0,68994	-0,23324	-0,20297	
YML023C	NSE5	nse5-ts2	-0,12882	0,03285	-0,16167	-0,15269	Component of the SMC5-SMC6 complex; this complex plays a key role in the removal of X-shaped DNA structures that arise between sister chromatids during DNA replication and repair
			-0,12772	-0,00049	-0,12723	-0,15442	
YML069W	POB3	pob3-q308k	-0,20114	0,57851	-0,77965	-0,94475	Subunit of the heterodimeric FACT complex (Spt16p-Pob3p); FACT associates with chromatin via interaction with Nhp6Ap and Nhp6Bp, and reorganizes nucleosomes to facilitate access to DNA by RNA and DNA polymerases; protein abundance increases in response to DNA replication stress
			-0,10727	0,32349	-0,43076	-0,14076	
YDR004W	RAD57	/	-0,42513	-0,2567	-0,16843	-0,2268	Protein that stimulates strand exchange; stimulates strand exchange by stabilizing the binding of Rad51p to single-stranded DNA; involved in the recombinational repair of double-strand breaks in DNA during vegetative growth and meiosis; forms heterodimer with Rad55p
			-0,62604	-0,4333	-0,19274	-0,15283	
YLR026C	SED5	sed5-1	-0,30476	0,07529	-0,38005	-0,35985	cis-Golgi t-SNARE syntaxin; required for vesicular transport between the ER and the Golgi complex; binds at least 9 SNARE proteins
			-0,26472	0,00128	-0,266	-0,15564	
YFL034C-B	MOB2	mob2-19	-0,74941	-0,52785	-0,22156		Activator of Cbk1p kinase; component of the RAM signaling network that regulates cellular polarity and morphogenesis; activation of Cbk1p facilitates the Ace2p-dependent daughter cell-specific transcription of genes involved in cell separation; similar to Mob1p
			-0,44352	-0,08953	-0,35399	-0,32845	
YDL147W	RPN5	rpn5-ph	-0,1967	0,00177	-0,19847		Subunit of the CSN and 26S proteasome lid complexes; similar to mammalian p55 subunit and to another S. cerevisiae regulatory subunit, Rpn7p; Rpn5p is an essential protein; the COP9 signalosome is also known as the CSN
			-0,25188	0,13598	-0,38786	-0,33613	
YDR246W	TRS23	trs23-ph	-0,26429	-0,13458	-0,12971		Core component of transport protein particle (TRAPP) complexes I-III; TRAPP complexes are related multimeric guanine nucleotide-exchange factor for the GTPase Ypt1p, regulating ER-Golgi traffic (TRAPPI), intra-Golgi traffic (TRAPPII), endosome-Golgi traffic (TRAPPII and III) and autophagy (TRAPPIII); human homolog is TRAPPC4
						-0,25175	
YNR043W	MVD1	mvd1-1296	-0,40431	-0,28814	-0,11617		Mevalonate pyrophosphate decarboxylase; essential enzyme involved in the biosynthesis of isoprenoids and sterols, including ergosterol; acts as a homodimer
						-0,52103	
YDR064W	RPS13	rps13-ph				-0,54272	Protein component of the small (40S) ribosomal subunit; homologous to mammalian ribosomal protein S13 and bacterial S15
						-0,1077	
YJL074C	SMC3	smc3-42				-0,50589	Subunit of the multiprotein cohesin complex; required for sister chromatid cohesion in mitotic cells; also required, with Rec8p, for cohesion and recombination during meiosis; phylogenetically conserved SMC chromosomal ATPase family member
						-0,15165	
YFL017C	GNA1	gna1-ts				-0,45238	Glucosamine-6-phosphate acetyltransferase; evolutionarily conserved; required for multiple cell cycle events including passage through START, DNA synthesis, and mitosis; involved in UDP-N-acetylglucosamine synthesis, forms GlcNAc6P from AcCoA
						-0,22343	
YGL116W	CDC20	cdc20-2				-0,42886	Activator of anaphase-promoting complex/cyclosome (APC/C); APC/C is required for metaphase/anaphase transition; directs ubiquitination of mitotic cyclins, Pds1p, and other anaphase inhibitors; cell-cycle regulated; potential Cdc28p substrate; relative distribution to the nucleus increases upon DNA replication stress
						-0,14627	
YPR060C	ARO7	/				-0,37752	Chorismate mutase; catalyzes the conversion of chorismate to prephenate to initiate the tyrosine/phenylalanine-specific branch of aromatic amino acid biosynthesis
						-0,43565	
YLR218C	COA4	/				-0,34048	Twin Cx(9)C protein involved in cytochrome c oxidase organization; organization includes assembly or stability; localizes to the mitochondrial intermembrane space via the Mia40p-Erv1p system; interacts genetically with CYC1 and with cytochrome c oxidase assembly factors
						-0,29623	
YLR116W	MSL5	msl5-ph				-0,31258	Component of commitment complex; which defines first step in splicing pathway; essential protein that interacts with Mud2p and Prp40p, forming a bridge between the intron ends; also involved in nuclear retention of pre-mRNA; relocalizes to the cytosol in response to hypoxia
						-0,13359	
YKL113C	RAD27	/				-0,30561	5' to 3' exonuclease, 5' flap endonuclease; required for Okazaki fragment processing and maturation, for long-patch base-excision repair and large loop repair (LLR), ribonucleotide excision repair; member of the S. pombe RAD2/FEN1 family; relocalizes to the cytosol in response to hypoxia
						-0,11557	
YAL038W	CDC19	cdc19-1				-0,25408	Pyruvate kinase; functions as a homotetramer in glycolysis to convert phosphoenolpyruvate to pyruvate, the input for aerobic (TCA cycle) or anaerobic (glucose fermentation) respiration; regulated via allosteric activation by fructose bisphosphate; CDC19 has a paralog, PYK2, that arose from the whole genome duplication
						-0,19899	
YGL045W	RIM8	/				-0,25224	Protein involved in proteolytic activation of Rim101p; part of response to alkaline pH; interacts with ESCRT-1 subunits Stp22p and Vps28p; essential for anaerobic growth; member of the arrestin-related trafficking adaptor family
						-0,44664	
YHR030C	SLT2	/				-0,25097	Serine/threonine MAP kinase; coordinates expression of all 19S regulatory particle assembly-chaperones (RACs) to control proteasome abundance; involved in regulating maintenance of cell wall integrity, cell cycle progression, nuclear mRNA retention in heat shock, septum assembly; required for mitophagy, pexophagy; affects recruitment of mitochondria to phagophore assembly site; plays role in adaptive response of cells to cold; regulated by the PKC1-mediated signaling pathway
						-0,23498	

YGL098W	USE1	use1-ts				-0,23699 -0,384	Essential SNARE protein localized to the ER; involved in retrograde traffic from the Golgi to the ER and Sey1p-independent homotypic ER fusion; required for efficient nuclear fusion during mating; forms a complex with the SNAREs Sec22p, Sec20p and Ufe1p
YML064C	TEM1	tem1-3				-0,23526 -0,15154	GTPase involved in initiation of Mitotic Exit Network (MEN); GTP-binding protein of the Ras superfamily; accumulates at daughter spindle pole body and activates MEN kinase cascade; controls actomyosin and septin dynamics during cytokinesis
YLR383W	SMC6	smc6-9				-0,2343 -0,12717	Component of the SMC5-SMC6 complex; this complex plays a key role in the removal of X-shaped DNA structures that arise between sister chromatids during DNA replication and repair; homologous to S. pombe rad18
YML081C-A	ATP18	/				-0,2258 -0,23245	Subunit of the mitochondrial F1F0 ATP synthase; F1F0 ATP synthase is a large, evolutionarily conserved enzyme complex required for ATP synthesis; termed subunit I or subunit j; does not correspond to known ATP synthase subunits in other organisms
YFR027W	ECO1	eco1-1				-0,22513 -0,10447	Acetyltransferase; required for establishment of sister chromatid cohesion; acetylates Mps3p to regulate nuclear organization; modifies Smc3p at replication forks and Mcd1p in response to dsDNA breaks; phosphorylated by three kinases (Cdc28p, Cdc7p, Mck1p) to generate pair of phosphates spaced precisely for recognition by ubiquitin ligase SCF-Cdc4; mutations in human homolog ESCO2 cause Roberts syndrome; relative distribution to nucleus increases upon DNA replication stress
YFL034C-B	MOB2	mob2-11	-0,87214	-0,70089	-0,17125	-0,20031 -0,15979	Activator of Cbk1p kinase; component of the RAM signaling network that regulates cellular polarity and morphogenesis; activation of Cbk1p facilitates the Ace2p-dependent daughter cell-specific transcription of genes involved in cell separation; similar to Mob1p
YFL005W	SEC4	sec4-8				-0,17523 -0,14551	Rab family GTPase; essential for vesicle-mediated exocytic secretion and autophagy; associates with the exocyst component Sec15p and may regulate polarized delivery of transport vesicles to the exocyst at the plasma membrane
YGR156W	PTI1	pti1-ts1				-0,1715 -0,12614	Essential component of CPF (cleavage and polyadenylation factor); involved in 3' end formation of snoRNA and mRNA; interacts directly with Pta1p; relocalizes to the cytosol in response to hypoxia; similar to mammalian Cleavage-Stimulation Factor CstF-64
YHR030C	SLT2	/				-0,16919 -0,23498	Serine/threonine MAP kinase; coordinates expression of all 19S regulatory particle assembly-chaperones (RACs) to control proteasome abundance; involved in regulating maintenance of cell wall integrity, cell cycle progression, nuclear mRNA retention in heat shock, septum assembly; required for mitophagy, pexophagy; affects recruitment of mitochondria to phagophore assembly site; plays role in adaptive response of cells to cold; regulated by the PKC1-mediated signaling pathway
YDR162C	NBP2	/				-0,16472 -0,28693	Protein involved in the HOG (high osmolarity glycerol) pathway; negatively regulates Hog1p by recruitment of phosphatase Ptc1p to the Pbs2p-Hog1p complex; interacts with Bck1p and down regulates the cell wall integrity pathway; found in the nucleus and cytoplasm; contains an SH3 domain and a Ptc1p binding domain (PBM)
YFL034C-B	MOB2	mob2-24	-0,23651	-0,03703	-0,19948	-0,16417 -0,14785	Activator of Cbk1p kinase; component of the RAM signaling network that regulates cellular polarity and morphogenesis; activation of Cbk1p facilitates the Ace2p-dependent daughter cell-specific transcription of genes involved in cell separation; similar to Mob1p
YKL145W	RPT1	rpt1-1				-0,15661 -0,12474	ATPase of the 19S regulatory particle of the 26S proteasome; one of six ATPases of the regulatory particle; involved in the degradation of ubiquitinated substrates; required for optimal CDC20 transcription; interacts with Rpn12p and Ubr1p; mutant has aneuploidy tolerance
YFL034C-B	MOB2	mob2-38	-0,50428	-0,11162	-0,39266	-0,15495 -0,25143	Activator of Cbk1p kinase; component of the RAM signaling network that regulates cellular polarity and morphogenesis; activation of Cbk1p facilitates the Ace2p-dependent daughter cell-specific transcription of genes involved in cell separation; similar to Mob1p
YOL066C	RIB2	rib2-ph	-0,24613	-0,03117	-0,21496	-0,15425 -0,16134	Bifunctional DRAP deaminase tRNA:pseudouridine synthase; the deaminase catalyzes the third step in riboflavin biosynthesis and the synthase catalyzes formation of pseudouridine at position 32 in cytoplasmic tRNAs; RIB2 has a paralog, PUS9, that arose from the whole genome duplication
YHR065C	RRP3	yhr065c-ph	-0,16919	0,00571	-0,1749	-0,15357 -0,20928	Protein involved in rRNA processing; required for maturation of the 35S primary transcript of pre-rRNA and for cleavage leading to mature 18S rRNA; homologous to eIF-4a, which is a DEAD box RNA-dependent ATPase with helicase activity
YHR036W	BRL1	brl1-c371s				-0,15331 -0,22542	Essential nuclear envelope/ER integral membrane protein; interacts and functions with Apq12p and Brr6p in lipid homeostasis; mutants are defective in nuclear pore complex biogenesis, mRNA nuclear export and are sensitive to sterol biosynthesis inhibitors and membrane fluidizing agents; identified as a dosage suppressor of a temperature sensitive mutation in the major karyopherin, CRM1; homologous to Brr6p
YMR296C	LCB1	lcb1-5				-0,14142 -0,18788	Component of serine palmitoyltransferase; responsible along with Lcb2p for the first committed step in sphingolipid synthesis, which is the condensation of serine with palmitoyl-CoA to form 3-ketosphinganine
YBR026C	ETR1	/				-0,13445 -0,24862	2-enoyl thioester reductase; member of the medium chain dehydrogenase/reductase family; localized to mitochondria, where it has a probable role in fatty acid synthesis; human MECR functionally complements the respiratory growth defect of the null mutant
YGL247W	BRR6	brr6-ph				-0,13311 -0,47194	Essential nuclear envelope integral membrane protein; interacts and functions with Apq12p and Brr1p in lipid homeostasis; mutants are defective in nuclear pore complex biogenesis, nuclear envelope morphology, mRNA nuclear export, and are sensitive to sterol biosynthesis inhibitors and membrane fluidizing agents; exhibits synthetic lethal genetic interactions with genes involved in lipid metabolism; homologous to Brl1p
YJL203W	PRP21	prp21-ts				-0,1303 -0,11701	Subunit of the SF3a splicing factor complex; required for spliceosome assembly
YGR277C	CAB4	cab4-ph				-0,13025 -0,22253	Subunit of the CoA-Synthesizing Protein Complex (CoA-SPC); subunits of this complex are: Cab2p, Cab3p, Cab4p, Cab5p, Sis2p and Vhs3p; involved in histone acylation; probable pantetheine-phosphate adenylyltransferase (PPAT); PPAT catalyzes the fourth step in the biosynthesis of coenzyme A from pantothenate; null mutant lethality is complemented by E. coli coaD (encoding PPAT) and by human COASY
YJL097W	PHS1	phs1-ph				-0,13005 -0,20332	Essential 3-hydroxyacyl-CoA dehydratase of the ER membrane; involved in elongation of very long-chain fatty acids; evolutionarily conserved, similar to mammalian PTPLA and PTPLB; involved in sphingolipid biosynthesis and protein trafficking
YMR168C	CEP3	cep3-1				-0,119 -0,13695	Essential kinetochore protein; component of the CBF3 complex that binds the CDEIII region of the centromere; contains an N-terminal Zn2Cys6 type zinc finger domain, a C-terminal acidic domain, and a putative coiled coil dimerization domain
YLR022C	SDO1	sdo1-vma1-ts				-0,11812 -0,27241	Guanine nucleotide exchange factor (GEF) for Rlp1p; essential protein involved in ribosome maturation; with Rlp1p, promotes release of Tif6p from 60S ribosomal subunits in the cytoplasm so that they can assemble with 40S subunits to generate mature ribosomes; ortholog of the human protein (SBDS) responsible for autosomal recessive Shwachman-Bodian-Diamond Syndrome; highly conserved across archaea and eukaryotes

19 HITS obtained from only one SGA:

			SGA 1				
			30UT_30HU	WTUT_WTH(	30-wt	wtHU_30HU	
Array ORF	Array Name	Array annota	filtered score	filtered score	difference	filtered score	SGD INFO
YLR115W	CFT2	cft2-ph	-0,77769	-0,43819	-0,3395	-0,38824	Subunit of the mRNA cleavage and polyadenlylation factor (CPF); required for pre-mRNA cleavage, polyadenylation and poly(A) site recognition, 43% similarity with the mammalian CPSF-100 protein.
YDL105W	NSE4	nse4-ts1	-0,40429	-0,25239	-0,1519	-0,10848	Component of the SMC5-SMC6 complex; this complex plays a key role in the removal of X-shaped DNA structures that arise between sister chromatids during DNA replication and repai
YGR179C	OKP1	okp1-5	-0,20142	-0,02301	-0,17841	-0,21784	Outer kinetochore protein required for accurate chromosome segregation; component of COMA (Ctf19p, Okp1p, Mcm21p, Ame1p) a kinetochore sub-complex which functions as a platform for kinetochore assembly; orthologous to human centromere constitutive-associated network (CCAN) subunit CENP-Q and fission yeast fta7
YER125W	RSP5	rsp5-sm1	-0,32642	-0,17727	-0,14915	-0,12629	NEDD4 family E3 ubiquitin ligase; regulates processes including: MVB sorting, the heat shock response, transcription, endocytosis and ribosome stability; ubiquitinates Sec23p, Sna3p, Ste4p, Nfi1p, Rpo21p and Sem1p; autoubiquitinates; deubiquitinated by Ubp2p; regulated by SUMO ligase Siz1p, in turn regulates Siz1p SUMO ligase activity; required for efficient Golgi-to-ER trafficking in COPI mutants; mutant tolerates aneuploidy; human homolog implicated in Liddle syndrome
YLR378C	SEC61	sec61-2	-0,21595	-0,09071	-0,12524	-0,15809	Conserved ER protein translocation channel; essential subunit of Sec61 complex (Sec61p, Sbh1p, and Sss1p); forms channel for SRP-dependent protein import; with Sec63 complex allows SRP-independent protein import into ER; involved in posttranslational soluble protein import into the ER, ERAD of soluble substrates, and misfolded soluble protein export from the ER
YDR311W	TFB1	tfb1-6	-0,29869	-0,14195	-0,15674	-0,17796	Subunit of TFIIH and nucleotide excision repair factor 3 complexes; required for nucleotide excision repair, target for transcriptional activators; relocalizes to the cytosol in response to hypoxia
YGR185C	TYS1	tys1-1	-0,41124	-0,14882	-0,26242	-0,34497	Cytoplasmic tyrosyl-tRNA synthetase; required for cytoplasmic protein synthesis; interacts with positions 34 and 35 of the tRNATyr anticodon; mutations in human ortholog YARS are associated with Charcot-Marie-Tooth (CMT) neuropathies; human ortholog YARS functionally complements the heat sensitivity of a ts allele; protein abundance increases in response to DNA replication stress
YPR086W	SUA7	ypr086w-ph	-0,51646	-0,33187	-0,18459	-0,28702	Transcription factor TFIIB; a general transcription factor required for transcription initiation and start site selection by RNA polymerase II

			SGA 2				
			30UT_30HU	WTUT_WTH(	30-wt	wtHU_30HU	
Array ORF	Array Name	Array annota	filtered score	filtered score	difference	filtered score	SGD INFO
YBL074C	AAR2	aar2-ph	-0,21956	0,01249	-0,23205	-0,21417	Component of the U5 snRNP complex; required for splicing of U3 precursors; originally described as a splicing factor specifically required for splicing pre-mRNA of the MATa1 cistron
YGL116W	CDC20	cdc20-1	-0,41067	-0,08225	-0,32842	-0,25815	Activator of anaphase-promoting complex/cyclosome (APC/C); APC/C is required for metaphase/anaphase transition; directs ubiquitination of mitotic cyclins, Pds1p, and other anaphase inhibitors; cell-cycle regulated; potential Cdc28p substrate; relative distribution to the nucleus increases upon DNA replication stress
YDR054C	CDC34	cdc34-1	-0,40012	-0,02591	-0,37421	-0,28742	Ubiquitin-conjugating enzyme (E2); catalytic subunit of SCF ubiquitin-protein ligase complex (together with Skp1p, Rbx1p, Cdc53p, and an F-box protein) that regulates cell cycle progression by targeting key substrates for degradation; protein abundance increases in response to DNA replication stress; human CDC34 functionally complements the thermosensitivity of the cdc34-2 mutant
YDR156W	RPA14	RPA14	-0,24952	0,06559	-0,31511	-0,29961	RNA polymerase I subunit A14
YHR069C	RRP4	rrp4-1	-0,25826	0,22743	-0,48569	-0,58176	Exosome non-catalytic core component; involved in 3'-5' RNA processing and degradation in both the nucleus and the cytoplasm; predicted to contain RNA binding domains; has similarity to human hRrp4p (EXOSC2)
YFR037C	RSC8	rsc8-ts21	-0,27795	-0,07982	-0,19813	-0,24956	Component of the RSC chromatin remodeling complex; essential for viability and mitotic growth; homolog of SWI/SNF subunit Swi3p, but unlike Swi3p, does not activate transcription of reporters
YOR194C	TOA1	toa1-ph	-0,56591	-0,30868	-0,25723	-0,18883	TFIIA large subunit; involved in transcriptional activation, acts as antirepressor or as coactivator; required, along with Toa2p, for ribosomal protein gene transcription in vivo; homologous to largest and second largest subunits of human and Drosophila TFIIA
YLR060W	FRS1	ylr060w-ph	-0,23408	0,03269	-0,26677	-0,26939	Beta subunit of cytoplasmic phenylalanyl-tRNA synthetase; forms a tetramer with Frs2p to generate active enzyme; able to hydrolyze mis-aminoacylated tRNA-Phe, which could contribute to translational quality control

References

1. Gaillard, H., García-Muse, T. & Aguilera, A. Replication stress and cancer. *Nat. Rev. Cancer* **15,** 276–280 (2015).
2. Ubhi, T. & Brown, G. W. Exploiting DNA replication stress for cancer treatment. *Cancer Res.* **79,** 1730–1739 (2019).
3. Prakash, S., Johnson, R. E. & Prakash, L. EUKARYOTIC TRANSLESION SYNTHESIS DNA POLYMERASES: Specificity of Structure and Function. *Annu. Rev. Biochem.* **74,** 317–353 (2005).
4. Johnson, R. E., Prakash, S. & Prakash, L. Efficient bypass of a thymine-thymine dimer by yeast DNA polymerase, Polη. *Science (80-.).* **283,** 1001–1004 (1999).
5. Haracska, L., Yu, S. L., Johnson, R. E., Prakash, L. & Prakash, S. Efficient and accurate replication in the presence of 7,8-dihydro-8-oxoguanine by DNA polymerase η. *Nat. Genet.* **25,** 458–461 (2000).
6. Acharya, N. *et al.* Multifaceted activities of DNA polymerase η: beyond translesion DNA synthesis. *Curr. Genet.* **65,** 649–656 (2019).
7. Masutani, C. *et al.* The XPV (xeroderma pigmentosum variant) gene encodes human DNA polymerase η. *Nature* **399,** 700–704 (1999).
8. Ceppi, P. *et al.* Polymerase η mRNA expression predicts survival of non-small cell lung cancer patients treated with platinum-based chemotherapy. *Clin. Cancer Res.* **15,** 1039–1045 (2009).
9. Zhou, W. *et al.* Expression of DNA translesion synthesis polymerase η in head and neck squamous cell cancer predicts resistance to gemcitabine and cisplatin-based chemotherapy. *PLoS One* **8,** 1–10 (2013).
10. Srivastava, A. K. *et al.* Enhanced expression of DNA polymerase eta contributes to cisplatin resistance of ovarian cancer stem cells. *Proc. Natl. Acad. Sci. U. S. A.* **112,** 4411–4416 (2015).
11. Albertella, M. R., Green, C. M., Lehmann, A. R. & O'Connor, M. J. A role for polymerase η in the cellular tolerance to cisplatin-induced damage. *Cancer Res.* **65,** 9799–9806 (2005).
12. Diffley, J. F. X. The initiation of DNA replication in the budding yeast cell division cycle. *Yeast* **11,** 1651–1670 (1995).
13. Masai, H., Matsumoto, S., You, Z., Yoshizawa-Sugata, N. & Oda, M. Eukaryotic chromosome DNA replication: Where, when, and how? *Annu. Rev. Biochem.* **79,** 89–130 (2010).
14. Zeman, M. K. & Cimprich, K. A. Causes and consequences of replication stress. *Nat. Cell Biol.* **16,** 2–9 (2014).
15. Hoeijmakers, J. H. J. The consequences of DNA injury Genome maintenance mechanisms for preventing cancer. *Nature* **411,** 366–374 (2001).
16. Nick McElhinny, S. A. *et al.* Genome instability due to ribonucleotide incorporation into DNA. *Nat. Chem. Biol.* **6,** 774–781 (2010).
17. Bermejo, R., Lai, M. S. & Foiani, M. Preventing Replication Stress to Maintain Genome Stability: Resolving Conflicts between Replication and Transcription. *Mol. Cell* **45,** 710–718 (2012).
18. Helmrich, A., Ballarino, M., Nudler, E. & Tora, L. Transcription-replication encounters, consequences and genomic instability. *Nat. Struct. Mol. Biol.* **20,** 412–418 (2013).
19. Thomas, M., White, R. L. & Davis, R. W. Hybridization of RNA to double-stranded DNA: formation of R-loops. *Proc. Natl. Acad. Sci.* **73,** 2294–2298 (1976).

20. Bermejo, R. *et al.* The replication checkpoint protects fork stability by releasing transcribed genes from nuclear pores. *Cell* **146,** 233–246 (2011).
21. Primo, L. M. F. & Teixeira, L. K. Dna replication stress: Oncogenes in the spotlight. *Genet. Mol. Biol.* **43,** 1–14 (2020).
22. Cobb, J. A. *et al.* Replisome instability, fork collapse, and gross chromosomal rearrangements arise synergistically from Mec1 kinase and RecQ helicase mutations. *Genes Dev.* **19,** 3055–3069 (2005).
23. Sogo, J. M., Lopes, M. & Foiani, M. Fork reversal and ssDNA accumulation at stalled replication forks owing to checkpoint defects. *Science (80-.).* **297,** 599–602 (2002).
24. Nyberg, K. A., Michelson, R. J., Putnam, C. W. & Weinert, T. A. Toward maintaining the genome: DNA damage and replication checkpoints. *Annu. Rev. Genet.* **36,** 617–656 (2002).
25. Osborn, A. J., Elledge, S. J. & Zou, L. Checking on the fork: the DNA-replication stress-response pathway. *Trends Cell Biol.* **12,** 509–516 (2002).
26. Paulovich, A. G. & Hartwell, L. H. A checkpoint regulates the rate of progression through S phase in S. cerevisiae in Response to DNA damage. *Cell* **82,** 841–847 (1995).
27. Boddy, M. N. & Russell, P. DNA replication checkpoint control. *Front. Biosci.* **4,** 953–956 (1999).
28. Zou, L. & Elledge, S. J. Sensing DNA damage through ATRIP recognition of RPA-ssDNA complexes. *Science (80-.).* **300,** 1542–1548 (2003).
29. Wanrooij, P. H., Tannous, E., Kumar, S., Navadgi-Patil, V. M. & Burgers, P. M. Probing the Mec1ATR checkpoint activation mechanism with small peptides. *J. Biol. Chem.* **291,** 393–401 (2016).
30. Kumar, S. & Burgers, P. M. Lagging strand maturation factor Dna2 is a component of the replication checkpoint initiation machinery. *Genes Dev.* **27,** 313–321 (2013).
31. Alcasabas, A. A. *et al.* Mrc1 transduces signals of DNA replication stress to activate Rad53. *Nat. Cell Biol.* **3,** 958–965 (2001).
32. Pellicioli, A. & Foiani, M. Signal transduction: How Rad53 kinase is activated. *Curr. Biol.* **15,** 769–771 (2005).
33. Cobb, J. A., Bjergbaek, L., Shimada, K., Frei, C. & Gasser, S. M. DNA polymerase stabilization at stalled replication forks requires Mec1 and the RecQ helicase Sgs1. *EMBO J.* **22,** 4325–4336 (2003).
34. Hegnauer, A. M. *et al.* An N-terminal acidic region of Sgs1 interacts with Rpa70 and recruits Rad53 kinase to stalled forks. *EMBO J.* **31,** 3768–3783 (2012).
35. Tsai, F.-L. *et al.* Mcm2-7 Is an Active Player in the DNA Replication Checkpoint Signaling Cascade via Proposed Modulation of Its DNA Gate. *Mol. Cell. Biol.* **35,** 2131–2143 (2015).
36. García-Rodríguez, L. J. *et al.* A conserved Pol ∈ binding module in Ctf18-RFC is required for S-phase checkpoint activation downstream of Mec1. *Nucleic Acids Res.* **43,** 8830–8838 (2015).
37. Kubota, T., Hiraga, S. I., Yamada, K., Lamond, A. I. & Donaldson, A. D. Quantitative proteomic analysis of chromatin reveals that Ctf18 acts in the DNA replication checkpoint. *Mol. Cell. Proteomics* **10,** 1–14 (2011).
38. Santocanale, C. & Diffley, J. F. X. A Mec1- and Rad53-dependent checkpoint controls late-firing origins of DNA replication. *Nature* **395,** 615–618 (1998).
39. Shirahige, K. *et al.* Regulation of DNA-replication origins during cell-cycle progression. *Nature* **395,** 618–621 (1998).
40. Palou, G. *et al.* Cyclin regulation by the S phase checkpoint. *J. Biol. Chem.* **285,** 26431–26440 (2010).

41. Krishnan, V., Nirantar, S., Crasta, K., Cheng, A. Y. H. & Surana, U. DNA replication checkpoint prevents precocious chromosome segregation by regulating spindle behavior. *Mol. Cell* **16,** 687–700 (2004).
42. Putnam, C. D., Jaehnig, E. J. & Kolodner, R. D. Perspectives on the DNA damage and replication checkpoint responses in Saccharomyces cerevisiae. *DNA Repair (Amst).* **8,** 974–982 (2009).
43. Boiteux, S. & Jinks-Robertson, S. DNA repair mechanisms and the bypass of DNA damage in Saccharomyces cerevisiae. *Genetics* **193,** 1025–1064 (2013).
44. Chabes, A. *et al.* Survival of DNA damage in yeast directly depends on increased dNTP levels allowed by relaxed feedback inhibition of ribonucleotide reductase. *Cell* **112,** 391–401 (2003).
45. Lopes, M. *et al.* The DNA replication checkpoint response stabilizes stalled replication forks. *Nature* **412,** 557–561 (2001).
46. Tercero, J. A. & Diffley, J. F. X. Regulation of DNA replication fork progression through damaged DNA by the Mec1/Rad53 checkpoint. *Nature* **412,** 553–557 (2001).
47. Kondratick, C. M., Washington, M. T. & Spies, M. Making choices: DNA replication fork recovery mechanisms. *Semin. Cell Dev. Biol.* (2020). doi:10.1016/j.semcdb.2020.10.001
48. Gao, Y., Mutter-Rottmayer, E., Zlatanou, A., Vaziri, C. & Yang, Y. Mechanisms of post-replication DNA repair. *Genes (Basel).* **8,** (2017).
49. Leung, W., Baxley, R. M., Moldovan, G. L. & Bielinsky, A. K. Mechanisms of DNA damage tolerance: post-translational regulation of PCNA. *Genes (Basel).* **10,** (2019).
50. Lopes, M., Foiani, M. & Sogo, J. M. Multiple mechanisms control chromosome integrity after replication fork uncoupling and restart at irreparable UV lesions. *Mol. Cell* **21,** 15–27 (2006).
51. Branzei, D., Vanoli, F. & Foiani, M. SUMOylation regulates Rad18-mediated template switch. *Nature* **456,** 915–920 (2008).
52. Diamant, N. *et al.* DNA damage bypass operates in the S and G2 phases of the cell cycle and exhibits differential mutagenicity. *Nucleic Acids Res.* **40,** 170–180 (2012).
53. Huang, D., Piening, B. D. & Paulovich, A. G. The Preference for Error-Free or Error-Prone Postreplication Repair in Saccharomyces cerevisiae Exposed to Low-Dose Methyl Methanesulfonate Is Cell Cycle Dependent. *Mol. Cell. Biol.* **33,** 1515–1527 (2013).
54. Daigaku, Y., Davies, A. A. & Ulrich, H. D. Ubiquitin-dependent DNA damage bypass is separable from genome replication. *Nature* **465,** 951–955 (2010).
55. Karras, G. I. & Jentsch, S. The RAD6 DNA damage tolerance pathway operates uncoupled from the replication fork and is functional beyond S phase. *Cell* **141,** 255–267 (2010).
56. Moldovan, G. L., Pfander, B. & Jentsch, S. PCNA, the Maestro of the Replication Fork. *Cell* **129,** 665–679 (2007).
57. Hoege, C., Pfander, B., Moldovan, G. L., Pyrowolakis, G. & Jentsch, S. RAD6-dependent DNA repair is linked to modification of PCNA by ubiquitin and SUMO. *Nature* **419,** 135–141 (2002).
58. Stelter, P. & Ulrich, H. D. Control of spontaneous and damage-induced mutagenesis by SUMO and ubiquitin conjugation. *Nature* **425,** 188–191 (2003).
59. Haracska, L., Torres-Ramos, C. A., Johnson, R. E., Prakash, S. & Prakash, L. Opposing Effects of Ubiquitin Conjugation and SUMO Modification of PCNA on Replicational Bypass of DNA Lesions in Saccharomyces cerevisiae. *Mol. Cell. Biol.* **24,** 4267–4274 (2004).
60. Davies, A. A., Huttner, D., Daigaku, Y., Chen, S. & Ulrich, H. D. Activation of Ubiquitin-Dependent DNA Damage Bypass Is Mediated by Replication Protein A.

Mol. Cell **29,** 625–636 (2008).
61. Terai, K., Abbas, T., Jazaeri, A. A. & Dutta, A. CRL4(Cdt2) E3 ubiquitin ligase monoubiquitinates PCNA to promote translesion DNA synthesis. *Mol. Cell* **37,** 143–9 (2010).
62. Simpson, L. J. *et al.* RAD18-independent ubiquitination of proliferating-cell nuclear antigen in the avian cell line DT40. *EMBO Rep.* **7,** 927–932 (2006).
63. Zhang, S. *et al.* PCNA is ubiquitinated by RNF8. *Cell Cycle* **7,** 3399–3404 (2008).
64. Hendel, A. *et al.* PCNA ubiquitination is important, but not essential for translesion DNA synthesis in mammalian cells. *PLoS Genet.* **7,** (2011).
65. Hofmann, R. M. & Pickart, C. M. Noncanonical MMS2-encoded ubiquitin-conjugating enzyme functions in assembly of novel polyubiquitin chains for DNA repair. *Cell* **96,** 645–53 (1999).
66. Ulrich, H. D. & Jentsch, S. Two RING finger proteins mediate cooperation between ubiquitin-conjugating enzymes in DNA repair. *EMBO J.* **19,** 3388–3397 (2000).
67. Gallo, D. *et al.* Rad5 Recruits Error-Prone DNA Polymerases for Mutagenic Repair of ssDNA Gaps on Undamaged Templates. *Mol. Cell* **73,** 900–914.e9 (2019).
68. Blastyák, A. *et al.* Yeast Rad5 Protein Required for Postreplication Repair Has a DNA Helicase Activity Specific for Replication Fork Regression. *Mol. Cell* **28,** 167–175 (2007).
69. Papouli, E. *et al.* Crosstalk between SUMO and ubiquitin on PCNA is mediated by recruitment of the helicase Srs2p. *Mol. Cell* **19,** 123–133 (2005).
70. Gallo, D. & Brown, G. W. Post-replication repair: Rad5/HLTF regulation, activity on undamaged templates, and relationship to cancer. *Crit. Rev. Biochem. Mol. Biol.* **54,** 301–332 (2019).
71. Becker, J. R. *et al.* Genetic Interactions Implicating Postreplicative Repair in Okazaki Fragment Processing. *PLoS Genet.* **11,** 1–24 (2015).
72. Daigaku, Y. *et al.* PCNA ubiquitylation ensures timely completion of unperturbed DNA replication in fission yeast. *PLoS Genet.* **13,** 1–21 (2017).
73. Pfander, B., Moldovan, G. L., Sacher, M., Hoege, C. & Jentsch, S. SUMO-modified PCNA recruits Srs2 to prevent recombination during S phase. *Nature* **436,** 428–433 (2005).
74. Arbel, M., Liefshitz, B. & Kupiec, M. DNA damage bypass pathways and their effect on mutagenesis in yeast. *FEMS Microbiol. Rev.* 1–11 (2020). doi:10.1093/femsre/fuaa038
75. Unk, I. *et al.* Human HLTF functions as a ubiquitin ligase for proliferating cell nuclear antigen polyubiquitination. *Proc. Natl. Acad. Sci. U. S. A.* **105,** 3768–3773 (2008).
76. Unk, I. *et al.* Human SHPRH is a ubiquitin ligase for Mms2-Ubc13-dependent polyubiquitylation of proliferating cell nuclear antigen. *Proc. Natl. Acad. Sci. U. S. A.* **103,** 18107–18112 (2006).
77. Krijger, P. H. L. *et al.* HLTF and SHPRH are not essential for PCNA polyubiquitination, survival and somatic hypermutation: existence of an alternative E3 ligase. *DNA Repair (Amst).* **10,** 438–44 (2011).
78. Gangavarapu, V., Prakash, S. & Prakash, L. Requirement of RAD52 Group Genes for Postreplication Repair of UV-Damaged DNA in Saccharomyces cerevisiae. *Mol. Cell. Biol.* **27,** 7758–7764 (2007).
79. Vanoli, F., Fumasoni, M., Szakal, B., Maloisel, L. & Branzei, D. Replication and recombination factors contributing to recombination-dependent bypass of DNA lesions by template switch. *PLoS Genet.* **6,** (2010).
80. Zhang, H. & Lawrence, C. W. The error-free component of the RAD6/RAD18 DNA damage tolerance pathway of budding yeast employs sister-strand recombination. *Proc. Natl. Acad. Sci. U. S. A.* **102,** 15954–15959 (2005).

81. Giannattasio, M. *et al.* Visualization of recombination-mediated damage bypass by template switching. *Nat. Struct. Mol. Biol.* **21,** 884–892 (2014).
82. Fumasoni, M., Zwicky, K., Vanoli, F., Lopes, M. & Branzei, D. Error-Free DNA Damage Tolerance and Sister Chromatid Proximity during DNA Replication Rely on the Polα/Primase/Ctf4 Complex. *Mol. Cell* **57,** 812–823 (2015).
83. Branzei, D. & Szakal, B. Priming for tolerance and cohesion at replication forks. *Nucleus* **7,** 8–12 (2016).
84. Karras, G. I. *et al.* Noncanonical Role of the 9-1-1 Clamp in the Error-Free DNA Damage Tolerance Pathway. *Mol. Cell* **49,** 536–546 (2013).
85. Quinet, A., Lemaçon, D. & Vindigni, A. Replication Fork Reversal: Players and Guardians. *Mol. Cell* **68,** 830–833 (2017).
86. Pata, J. D. Structural diversity of the Y-family DNA polymerases. *Biochim. Biophys. Acta - Proteins Proteomics* **1804,** 1124–1135 (2010).
87. Zhou, B. L., Pata, J. D. & Steitz, T. A. Crystal structure of a DinB lesion bypass DNA polymerase catalytic fragment reveals a classic polymerase catalytic domain. *Mol. Cell* **8,** 427–437 (2001).
88. Trincao, J. *et al.* Structure of the Catalytic Core of S. cerevisiae DNA polymerase η: Implications for translesion DNA synthesis. *Mol. Cell* **8,** 417–426 (2001).
89. Reha-Krantz, L. J. DNA polymerase proofreading: Multiple roles maintain genome stability. *Biochim. Biophys. Acta - Proteins Proteomics* **1804,** 1049–1063 (2010).
90. Silvian, L. F., Toth, E. A., Pham, P., Goodman, M. F. & Ellenberger, T. Crystal structure of a DinB family error-prone DNA polymerase from Sulfolobus solfataricus. *Nat. Struct. Biol.* **8,** 984–989 (2001).
91. Ling, H., Boudsocq, F., Woodgate, R. & Yang, W. Crystal Structure of a Y-Family DNA Polymerase in Action. *Cell* **107,** 91–102 (2001).
92. Powers, K. T. & Washington, M. T. Eukaryotic translesion synthesis: Choosing the right tool for the job. *DNA Repair (Amst).* **71,** 127–134 (2018).
93. Friedberg, E. C. Specialized DNA Polymerases, Cellular Survival, and the Genesis of Mutations. *Science (80-.).* **296,** 1627–1630 (2002).
94. Ma, X., Tang, T. S. & Guo, C. Regulation of translesion DNA synthesis in mammalian cells. *Environ. Mol. Mutagen.* **61,** 680–692 (2020).
95. Bienko, M. *et al.* Biochemistry: Ubiquitin-binding domains in Y-family polymerases regulate translesion synthesis. *Science (80-.).* **310,** 1821–1824 (2005).
96. Pustovalova, Y., MacIejewski, M. W. & Korzhnev, D. M. NMR mapping of PCNA interaction with translesion synthesis DNA polymerase Rev1 mediated by Rev1-BRCT domain. *J. Mol. Biol.* **425,** 3091–3105 (2013).
97. Guo, C. *et al.* REV1 Protein Interacts with PCNA: Significance of the REV1 BRCT Domain In Vitro and In Vivo. *Mol. Cell* **23,** 265–271 (2006).
98. Wiltrout, M. E. & Walker, G. C. Proteasomal regulation of the mutagenic translesion DNA polymerase, Saccharomyces cerevisiae Rev1. *DNA Repair (Amst).* **10,** 169–175 (2011).
99. Pabla, R., Rozario, D. & Siede, W. Regulation of Saccharomyces cerevisiae DNA polymerase η transcript and protein. *Radiat. Environ. Biophys.* **47,** 157–168 (2008).
100. Waters, L. S. & Walker, G. C. The critical mutagenic translesion DNA polymerase Rev1 is highly expressed during G2/M phase rather than S phase. *Proc. Natl. Acad. Sci. U. S. A.* **103,** 8971–8976 (2006).
101. Plachta, M., Halas, A., McIntyre, J. & Sledziewska-Gojska, E. The steady-state level and stability of TLS polymerase eta are cell cycle dependent in the yeast S. cerevisiae. *DNA Repair (Amst).* **29,** 147–153 (2015).
102. Bertoletti, F. *et al.* Phosphorylation regulates human polη stability and damage bypass throughout the cell cycle. *Nucleic Acids Res.* **45,** 9441–9454 (2017).

103. Sobolewska, A., Halas, A., Plachta, M., McIntyre, J. & Sledziewska-Gojska, E. Regulation of the abundance of Y-family polymerases in the cell cycle of budding yeast in response to DNA damage. *Curr. Genet.* **66,** 749–763 (2020).
104. Sale, J. E. Translesion DNA Synthesis and Mutagenesis in Eukaryotes. *Cold Spring Harb. Perspect. Biol.* **5,** a012708–a012708 (2013).
105. Waters, L. S. *et al.* Eukaryotic Translesion Polymerases and Their Roles and Regulation in DNA Damage Tolerance. *Microbiol. Mol. Biol. Rev.* **73,** 134–154 (2009).
106. McCulloch, S. D., Kokoska, R. J. & Kunkel, T. A. Efficiency, fidelity and enzymatic switching during translesion DNA synthesis. *Cell Cycle* **3,** 578–581 (2004).
107. Lehmann, A. R. *et al.* Translesion synthesis: Y-family polymerases and the polymerase switch. *DNA Repair (Amst).* **6,** 891–899 (2007).
108. Lehmann, A. R. & Fuchs, R. P. Gaps and forks in DNA replication: Rediscovering old models. *DNA Repair (Amst).* **5,** 1495–1498 (2006).
109. Friedberg, E. C., Lehmann, A. R. & Fuchs, R. P. P. Trading Places: How do DNA polymerases switch during translesion DNA synthesis? *Mol. Cell* **18,** 499–505 (2005).
110. Lehmann, A. R. New functions for Y family polymerases. *Mol. Cell* **24,** 493–495 (2006).
111. McCulloch, S. D. & Kunkel, T. A. The fidelity of DNA synthesis by eukaryotic replicative and translesion synthesis polymerases. *Cell Res.* **18,** 148–161 (2008).
112. Tirman, S., Cybulla, E., Quinet, A., Meroni, A. & Vindigni, A. PRIMPOL ready, set, reprime! *Crit. Rev. Biochem. Mol. Biol.* **56,** 17–30 (2021).
113. Wong, R. P., García-Rodríguez, N., Zilio, N., Hanulová, M. & Ulrich, H. D. *Processing of DNA Polymerase-Blocking Lesions during Genome Replication Is Spatially and Temporally Segregated from Replication Forks*. *Molecular Cell* **77,** (2020).
114. Nelson, J. R., Lawrence, C. W. & Hinkle, D. C. Deoxycytidyl transferase activity of yeast REV1 protein. *Nature* **382,** 729–731 (1996).
115. Haracska, L., Prakash, S. & Prakash, L. Yeast Rev1 protein is a G template-specific DNA polymerase. *J. Biol. Chem.* **277,** 15546–15551 (2002).
116. Guo, C. *et al.* Mouse Rev1 protein interacts with multiple DNA polymerases involved in translesion DNA synthesis. *EMBO J.* **22,** 6621–6630 (2003).
117. Ohashi, E. *et al.* Interaction of hREV1 with three human Y-family DNA polymerases. *Genes to Cells* **9,** 523–531 (2004).
118. Tissier, A. *et al.* Co-localization in replication foci and interaction of human Y-family members, DNA polymerase polη and REVl protein. *DNA Repair (Amst).* **3,** 1503–1514 (2004).
119. Murakumo, Y. *et al.* Interactions in the Error-prone Postreplication Repair Proteins hREV1, hREV3, and hREV7. *J. Biol. Chem.* **276,** 35644–35651 (2001).
120. Nelson, J. R., Lawrence, C. W. & Hinkle, D. C. Thymine-thymine dimer bypass by yeast DNA polymerase zeta. *Science* **272,** 1646–1649 (1996).
121. Makarova, A. V., Stodola, J. L. & Burgers, P. M. A four-subunit DNA polymerase ζ complex containing Pol δ accessory subunits is essential for PCNA-mediated mutagenesis. *Nucleic Acids Res.* **40,** 11618–11626 (2012).
122. Baranovskiy, A. G. *et al.* DNA polymerase δ and ζ switch by sharing accessory subunits of DNA polymerase δ. *J. Biol. Chem.* **287,** 17281–17287 (2012).
123. Lawrence, C. W. Cellular functions of DNA polymerase ζ and REV1 protein. *Adv. Protein Chem.* **69,** 167–203 (2004).
124. Gibbs, P. E. M., McDonald, J., Woodgate, R. & Lawrence, C. W. The relative roles in vivo of Saccharomyces cerevisiae Pol η, Pol ζ, Rev1 protein and Pol32 in the bypass and mutation induction of an abasic site, T-T (6-4) photoadduct and T-T cis-syn cyclobutane dimer. *Genetics* **169,** 575–582 (2005).

125. Szüts, D., Marcus, A. P., Himoto, M., Iwai, S. & Sale, J. E. REV1 restrains DNA polymerase ζ to ensure frame fidelity during translesion synthesis of UV photoproducts in vivo. *Nucleic Acids Res.* **36,** 6767–6780 (2008).
126. Yoon, J. H., Prakash, L. & Prakash, S. Error-free replicative bypass of (6-4) photoproducts by DNA polymerase ζ in mouse and human cells. *Genes Dev.* **24,** 123–128 (2010).
127. Lazzaro, F. *et al.* RNase H and postreplication repair protect cells from ribonucleotides incorporated in DNA. *Mol. Cell* **45,** 99–110 (2012).
128. McCulloch, S. D. *et al.* Preferential cis–syn thymine dimer bypass by DNA polymerase. *Nature* **428,** 97–100 (2004).
129. Kusumoto, R., Masutani, C., Iwai, S. & Hanaoka, F. Translesion synthesis by human DNA polymerase eta across thymine glycol lesions. *Biochemistry* **41,** 6090–6099 (2002).
130. Zhao, B., Xie, Z., Shen, H. & Wang, Z. Role of DNA polymerase η in the bypass of abasic sites in yeast cells. *Nucleic Acids Res.* **32,** 3984–3994 (2004).
131. Haracska, L., Prakash, S. & Prakash, L. Replication past O6-Methylguanine by Yeast and Human DNA Polymerase eta. *Mol. Cell. Biol.* **20,** 8001–8007 (2000).
132. Yuan, F. *et al.* Specificity of DNA lesion bypass by the yeast DNA polymerase η. *J. Biol. Chem.* **275,** 8233–8239 (2000).
133. Zhang, Y. *et al.* Error-prone lesion bypass by human DNA polymerase η. *Nucleic Acids Res.* **28,** 4717–4724 (2000).
134. Alt, A. *et al.* Bypass of DNA lesions generated during anticancer treatment with cisplatin by DNA polymerase eta. *Science* **318,** 967–70 (2007).
135. Kondratick, C. M., Washington, M. T., Prakash, S. & Prakash, L. Acidic Residues Critical for the Activity and Biological Function of Yeast DNA Polymerase . *Mol. Cell. Biol.* **21,** 2018–2025 (2001).
136. Boldinova, E. O., Ignatov, A., Kulbachinskiy, A. & Makarova, A. V. The active site residues Gln55 and Arg73 play a key role in DNA damage bypass by S. cerevisiae Pol η. *Sci. Rep.* **8,** 1–11 (2018).
137. Donigan, K. A. *et al.* Unlocking the steric gate of DNA polymerase η leads to increased genomic instability in Saccharomyces cerevisiae. *DNA Repair (Amst).* **35,** 1–12 (2015).
138. Su, Y., Egli, M. & Guengerich, F. P. Mechanism of ribonucleotide incorporation by human DNA polymerase η. *J. Biol. Chem.* **291,** 3747–3756 (2016).
139. Mentegari, E. *et al.* Ribonucleotide incorporation by human DNA polymerase η impacts translesion synthesis and RNase H2 activity. *Nucleic Acids Res.* **45,** 2600–2614 (2017).
140. Gali, V. K. *et al.* Translesion synthesis DNA polymerase η exhibits a specific RNA extension activity and a transcription-associated function. *Sci. Rep.* **7,** 1–17 (2017).
141. Su, Y., Egli, M., Guengerich, F. P. & Sung, P. Human DNA polymerase η accommodates RNA for strand extension. *J. Biol. Chem.* **292,** 18044–18051 (2017).
142. Kawamoto, T. *et al.* Dual roles for DNA polymerase η in homologous DNA recombination and translesion DNA synthesis. *Mol. Cell* **20,** 793–799 (2005).
143. Mcllwraith, M. J. *et al.* Human DNA polymerase η promotes DNA synthesis from strand invasion intermediates of homologous recombination. *Mol. Cell* **20,** 783–792 (2005).
144. Buisson, R. *et al.* Breast cancer proteins PALB2 and BRCA2 stimulate polymerase η in recombination-associated DNA Synthesis At Blocked Replication Forks. *Cell Rep.* **6,** 553–564 (2014).
145. Garcia-Exposito, L. *et al.* Proteomic Profiling Reveals a Specific Role for Translesion DNA Polymerase η in the Alternative Lengthening of Telomeres. *Cell Rep.* **17,** 1858–

1871 (2016).
146. Barnes, R. P., Hile, S. E., Lee, M. Y. & Eckert, K. A. DNA polymerases eta and kappa exchange with the polymerase delta holoenzyme to complete common fragile site synthesis. *DNA Repair (Amst).* **57,** 1–11 (2017).
147. Bergoglio, V. *et al.* DNA synthesis by pol η promotes fragile site stability by preventing under-replicated DNA in mitosis. *J. Cell Biol.* **201,** 395–408 (2013).
148. Rey, L. *et al.* Human DNA Polymerase η Is Required for Common Fragile Site Stability during Unperturbed DNA Replication. *Mol. Cell. Biol.* **29,** 3344–3354 (2009).
149. De Feraudy, S. *et al.* Pol η is required for DNA replication during nucleotide deprivation by hydroxyurea. *Oncogene* **26,** 5713–5721 (2007).
150. Helmrich, A., Ballarino, M. & Tora, L. Collisions between Replication and Transcription Complexes Cause Common Fragile Site Instability at the Longest Human Genes. *Mol. Cell* **44,** 966–977 (2011).
151. Watanabe, T. *et al.* Impediment of Replication Forks by Long Non-coding RNA Provokes Chromosomal Rearrangements by Error-Prone Restart. *Cell Rep.* **21,** 2223–2235 (2017).
152. Kreisel, K. *et al.* DNA polymerase η contributes to genome-wide lagging strand synthesis. *Nucleic Acids Res.* **47,** 2425–2435 (2019).
153. Enervald, E., Lindgren, E., Katou, Y., Shirahige, K. & Ström, L. Importance of Polη for Damage-Induced Cohesion Reveals Differential Regulation of Cohesion Establishment at the Break Site and Genome-Wide. *PLoS Genet.* **9,** (2013).
154. Franklin, A., Milburn, P. J., Blanden, R. V. & Steele, E. J. Human DNA polymerase-η, an A-T mutator in somatic hypermutation of rearranged immunoglobulin genes, is a reverse transcriptase. *Immunol. Cell Biol.* **82,** 219–225 (2004).
155. Parker, J. L., Bielen, A. B., Dikic, I. & Ulrich, H. D. Contributions of ubiquitin- and PCNA-binding domains to the activity of Polymerase η in Saccharomyces cerevisiae. *Nucleic Acids Res.* **35,** 881–889 (2007).
156. Duong, P. T. M. *et al.* The interaction between ubiquitin and yeast polymerase η C terminus does not require the UBZ domain. *FEBS Lett.* **594,** 1726–1737 (2020).
157. Ripley, B. M., Reusch, D. T. & Washington, M. T. Yeast DNA polymerase η possesses two PIP-like motifs that bind PCNA and Rad6-Rad18 with different specificities. *DNA Repair (Amst).* **95,** 102968 (2020).
158. Boehm, E. M. *et al.* The proliferating cell nuclear antigen (PCNA)-interacting Protein (PIP) motif of DNA polymerase η Mediates Its interaction with the C-terminal domain of Rev1. *J. Biol. Chem.* **291,** 8735–8744 (2016).
159. Plosky, B. S. *et al.* Controlling the subcellular localization of DNA polymerases ι and η via interactions with ubiquitin. *EMBO J.* **25,** 2847–2855 (2006).
160. Bienko, M. *et al.* Regulation of Translesion Synthesis DNA Polymerase η by Monoubiquitination. *Mol. Cell* **37,** 396–407 (2010).
161. Ma, X. *et al.* Polη O-GlcNAcylation governs genome integrity during translesion DNA synthesis. *Nat. Commun.* **8,** (2017).
162. Chen, Y. W. *et al.* Human DNA polymerase η activity and translocation is regulated by phosphorylation. *Proc. Natl. Acad. Sci. U. S. A.* **105,** 16578–16583 (2008).
163. Göhler, T., Sabbioneda, S., Green, C. M. & Lehmann, A. R. ATR-mediated phosphorylation of DNA polymerase η is needed for efficient recovery from UV damage. *J. Cell Biol.* **192,** 219–227 (2011).
164. Guérillon, C., Smedegaard, S., Hendriks, I. A., Nielsen, M. L. & Mailand, N. Multi-site SUMOylation restrains DNA polymerase η interactions with DNA damage sites. *J. Biol. Chem.* jbc.RA120.013780 (2020). doi:10.1074/jbc.RA120.013780
165. Despras, E. *et al.* Rad18-dependent SUMOylation of human specialized DNA polymerase eta is required to prevent under-replicated DNA. *Nat. Commun.* **7,** (2016).

166. Skoneczna, A., McIntyre, J., Skoneczny, M., Policinska, Z. & Sledziewska-Gojska, E. Polymerase eta Is a Short-lived, Proteasomally Degraded Protein that Is Temporarily Stabilized Following UV Irradiation in Saccharomyces cerevisiae. *J. Mol. Biol.* **366,** 1074–1086 (2007).
167. Wu, P., Enervald, E., Joelsson, A. & Palmberg, C. Posttranslational regulation of DNA polymerase η , a connection to damage-induced cohesion in Saccharomyces cerevisiae. (2020).
168. Li, Y. & Breaker, R. R. Kinetics of RNA degradation by specific base catalysis of transesterification involving the 2'-hydroxyl group. *J. Am. Chem. Soc.* **121,** 5364–5372 (1999).
169. Nava, G. M. *et al.* One, No One, and One Hundred Thousand: The Many Forms of Ribonucleotides in DNA. *Int. J. Mol. Sci.* **21,** 1–23 (2020).
170. Nick McElhinny, S. A. *et al.* Abundant ribonucleotide incorporation into DNA by yeast replicative polymerases. *Proc. Natl. Acad. Sci. U. S. A.* **107,** 4949–4954 (2010).
171. Yao, N. Y., Schroeder, J. W., Yurieva, O., Simmons, L. A. & O'Donnell, M. E. Cost of rNTP/dNTP pool imbalance at the replication fork. *Proc. Natl. Acad. Sci. U. S. A.* **110,** 12942–12947 (2013).
172. Caldecott, K. W. Ribose--An Internal Threat to DNA. *Science (80-.).* **343,** 260–261 (2014).
173. Clausen, A. R. *et al.* Tracking replication enzymology in vivo by genome-wide mapping of ribonucleotide incorporation. *Nat. Struct. Mol. Biol.* **22,** 185–191 (2015).
174. Koh, K. D., Balachander, S., Hesselberth, J. R. & Storici, F. Ribose-seq: Global mapping of ribonucleotides embedded in genomic DNA. *Nat. Methods* **12,** 251–257 (2015).
175. Clausen, A. R. *et al.* Tracking replication enzymology in vivo by genome-wide mapping of ribonucleotide incorporation. *Nat. Struct. Mol. Biol.* **22,** 185–191 (2015).
176. Reijns, M. A. M. *et al.* Lagging-strand replication shapes the mutational landscape of the genome. *Nature* **518,** 502–506 (2015).
177. Koh, K. D., Balachander, S., Hesselberth, J. R. & Storici, F. Ribose-seq: Global mapping of ribonucleotides embedded in genomic DNA. *Nat. Methods* **12,** 251–257 (2015).
178. Daigaku, Y. *et al.* A global profile of replicative polymerase usage. *Nat. Struct. Mol. Biol.* **22,** 192–198 (2015).
179. Traut, T. W. Physiological concentrations of purines and pyrimidines. *Mol. Cell. Biochem.* **140,** 1–22 (1994).
180. Ferraro, P., Franzolin, E., Pontarin, G., Reichard, P. & Bianchi, V. Quantitation of cellular deoxynucleoside triphosphates. *Nucleic Acids Res.* **38,** 1–7 (2009).
181. Reijns, M. A. M. *et al.* Enzymatic Removal of Ribonucleotides from DNA Is Essential for Mammalian Genome Integrity and Development. *Cell* **149,** 1008–1022 (2012).
182. Kasiviswanathan, R. & Copeland, W. C. Ribonucleotide discrimination and reverse transcription by the human mitochondrial DNA polymerase. *J. Biol. Chem.* **286,** 31490–31500 (2011).
183. Forslund, J. M. E., Pfeiffer, A., Stojkovič, G., Wanrooij, P. H. & Wanrooij, S. The presence of rNTPs decreases the speed of mitochondrial DNA replication. *PLoS Genet.* **14,** (2018).
184. Joyce, C. M. Choosing the right sugar: How polymerases select a nucleotide substrate. *Proc. Natl. Acad. Sci.* **94,** 1619–1622 (1997).
185. Vaisman, A. & Woodgate, R. Ribonucleotide discrimination by translesion synthesis DNA polymerases. *Crit. Rev. Biochem. Mol. Biol.* **53,** 382–402 (2018).
186. Brown, J. A. & Suo, Z. Unlocking the sugar 'steric gate' of DNA polymerases. *Biochemistry* **50,** 1135–42 (2011).

187. Johnson, M. K., Kottur, J. & Nair, D. T. A polar filter in DNA polymerases prevents ribonucleotide incorporation. *Nucleic Acids Res.* **47,** 10693–10705 (2019).
188. Lujan, S. A., Williams, J. S., Clausen, A. R., Clark, A. B. & Kunkel, T. A. Ribonucleotides are signals for mismatch repair of leading-strand replication errors. *Mol. Cell* **50,** 437–43 (2013).
189. Williams, J. S. *et al.* Evidence that processing of ribonucleotides in DNA by topoisomerase 1 is leading-strand specific. *Nat. Struct. Mol. Biol.* **22,** 291–297 (2015).
190. Donigan, K. A., McLenigan, M. P., Yang, W., Goodman, M. F. & Woodgate, R. The steric gate of DNA polymerase ι regulates ribonucleotide incorporation and deoxyribonucleotide fidelity. *J. Biol. Chem.* **289,** 9136–9145 (2014).
191. Meroni, A. *et al.* RNase H activities counteract a toxic effect of Polymerase eta in cells replicating with depleted dNTP pools. *Nucleic Acids Res.* **47,** 4612–4623 (2019).
192. Bergoglio, V., Ferrari, E., Hübscher, U., Cazaux, C. & Hoffmann, J. S. DNA polymerase β can incorporate ribonucleotides during DNA synthesis of undamaged and CPD-damaged DNA. *J. Mol. Biol.* **331,** 1017–1023 (2003).
193. Vaisman, A. *et al.* Critical amino acids in Escherichia coli UmuC responsible for sugar discrimination and base-substitution fidelity. *Nucleic Acids Res.* **40,** 6144–6157 (2012).
194. Ordonez, H., Uson, M. L. & Shuman, S. Characterization of three mycobacterial DinB (DNA polymerase IV) paralogs highlights DinB2 as naturally adept at ribonucleotide incorporation. *Nucleic Acids Res.* **42,** 11056–11070 (2014).
195. Potenski, C. J. & Klein, H. L. How the misincorporation of ribonucleotides into genomic DNA can be both harmful and helpful to cells. *Nucleic Acids Res.* **42,** 10226–10234 (2014).
196. Ghodgaonkar, M. M. *et al.* Ribonucleotides misincorporated into DNA act as strand-discrimination signals in eukaryotic mismatch repair. *Mol. Cell* **50,** 323–332 (2013).
197. Pryor, J. M. *et al.* breaks by nonhomologous end joining. **361,** 1126–1129 (2019).
198. Martin, M. J., Garcia-Ortiz, M. V., Esteban, V. & Blanco, L. Ribonucleotides and manganese ions improve non-homologous end joining by human Polm. *Nucleic Acids Res.* **41,** 2428–2436 (2013).
199. Nick McElhinny, S. A. & Ramsden, D. A. Polymerase Mu Is a DNA-Directed DNA/RNA Polymerase. *Mol. Cell. Biol.* **23,** 2309–2315 (2003).
200. Jaishree, T. N., Wang, A. H. J., van der Marel, G. A. & van Boom, J. H. Structural Influence of RNA Incorporation in DNA: Quantitative Nuclear Magnetic Resonance Refinement of d(CG)r(CG)d(CG) and d(CG)r(C)d(TAGCG). *Biochemistry* **32,** 4903–4911 (1993).
201. Egli, M., Usman, N. & Rich, A. Conformational Influence of the Ribose 2′-Hydroxyl Group: Crystal Structures of DNA-RNA Chimeric Duplexess. *Biochemistry* **32,** 3221–3237 (1993).
202. Derose, E. F., Perera, L., Murray, M. S., Kunkel, T. A. & London, R. E. Solution structure of the Dickerson DNA dodecamer containing a single ribonucleotide. *Biochemistry* **51,** 2407–2416 (2012).
203. Meroni, A. *et al.* The Incorporation of Ribonucleotides Induces Structural and Conformational Changes in DNA. *Biophys. J.* **113,** 1373–1382 (2017).
204. Hovatter, K. R. & Martinson, H. G. Ribonucleotide-induced helical alteration in DNA prevents nucleosome formation. *Proc. Natl. Acad. Sci. U. S. A.* **84,** 1162–1166 (1987).
205. Fu, I., Smith, D. J. & Broyde, S. Rotational and translational positions determine the structural and dynamic impact of a single ribonucleotide incorporated in the nucleosome. *DNA Repair (Amst).* **73,** 155–163 (2019).
206. Ren, M., Cheng, Y., Duan, Q. & Zhou, C. Transesterification Reaction and the Repair of Embedded Ribonucleotides in DNA Are Suppressed upon the Assembly of DNA into Nucleosome Core Particles †. *Chem. Res. Toxicol.* **32,** 926–934 (2019).

207. Clausen, A. R., Murray, M. S., Passer, A. R., Pedersen, L. C. & Kunkel, T. A. Structure-function analysis of ribonucleotide bypass by B family DNA replicases. *Proc. Natl. Acad. Sci. U. S. A.* **110,** 16802–16807 (2013).
208. Lazzaro, F. *et al.* RNase H and postreplication repair protect cells from ribonucleotides incorporated in DNA. *Mol. Cell* **45,** 99–110 (2012).
209. Arana, M. E. *et al.* Transcriptional responses to loss of RNase H2 in Saccharomyces cerevisiae. *DNA Repair (Amst).* **11,** 933–941 (2012).
210. Klein, H. L. Genome instabilities arising from ribonucleotides in DNA. *DNA Repair* **56,** 26–32 (2017).
211. Kim, N. *et al.* Mutagenic Processing of Ribonucleotides in DNA by Yeast Topoisomerase I. *Science (80-.).* **332,** 1561–1564 (2011).
212. Conover, H. N. *et al.* Stimulation of chromosomal rearrangements by ribonucleotides. *Genetics* **201,** 951–961 (2015).
213. Williams, J. S., Gehle, D. B. & Kunkel, T. A. The role of RNase H2 in processing ribonucleotides incorporated during DNA replication. *DNA Repair (Amst).* **53,** 52–58 (2017).
214. O'Connell, K., Jinks-Robertson, S. & Petes, T. D. Elevated Genome-wide instability in yeast mutants lacking RNase H activity. *Genetics* **201,** 963–975 (2015).
215. Williams, J. S. *et al.* Proofreading of ribonucleotides inserted into DNA by yeast DNA polymerase ε. *DNA Repair (Amst).* **11,** 649–56 (2012).
216. Cerritelli, S. M. & Crouch, R. J. Ribonuclease H: The enzymes in eukaryotes. *FEBS J.* **276,** 1494–1505 (2009).
217. Nowotny, M. *et al.* Structure of Human RNase H1 Complexed with an RNA/DNA Hybrid: Insight into HIV Reverse Transcription. *Mol. Cell* **28,** 264–276 (2007).
218. Zimmer, A. D. & Koshland, D. Differential roles of the RNases H in preventing chromosome instability. *Proc. Natl. Acad. Sci. U. S. A.* **113,** 12220–12225 (2016).
219. Chon, H. *et al.* RNase H2 roles in genome integrity revealed by unlinking its activities. *Nucleic Acids Res.* **41,** 3130–3143 (2013).
220. Lockhart, A. *et al.* RNase H1 and H2 Are Differentially Regulated to Process RNA-DNA Hybrids. *Cell Rep.* **29,** 2890–2900 (2019).
221. Sparks, J. L. *et al.* RNase H2-Initiated Ribonucleotide Excision Repair. *Mol. Cell* **47,** 980–986 (2012).
222. Riva, V. *et al.* Novel alternative ribonucleotide excision repair pathways in human cells by DDX3X and specialized DNA polymerases. *Nucleic Acids Res.* **48,** 11551–11565 (2020).
223. Arudchandran, A. *et al.* The absence of ribonuclease H1 or H2 alters the sensitivity of Saccharomyces cerevisiae to hydroxyurea, caffeine and ethyl methanesulphonate: Implications for roles of RNases H in DNA replication and repair. *Genes to Cells* **5,** 789–802 (2000).
224. Uehara, R. *et al.* Two RNase H2 Mutants with Differential rNMP Processing Activity Reveal a Threshold of Ribonucleotide Tolerance for Embryonic Development. *Cell Rep.* **25,** 1135–1145.e5 (2018).
225. Reijns, M. A. M. *et al.* Enzymatic removal of ribonucleotides from DNA is essential for mammalian genome integrity and development. *Cell* **149,** 1008–1022 (2012).
226. Cerritelli, S. M. *et al.* Failure to Produce Mitochondrial DNA Results in Embryonic Lethality in Rnaseh1 Null Mice. *Mol. Cell* **11,** 807–815 (2003).
227. Crow, Y. J. *et al.* Mutations in genes encoding ribonuclease H2 subunits cause Aicardi-Goutières syndrome and mimic congenital viral brain infection. *Nat. Genet.* **38,** 910–916 (2006).
228. Crow, Y. J. & Manel, N. Aicardi-Goutières syndrome and the type I interferonopathies. *Nat. Rev. Immunol.* **15,** 429–440 (2015).

229. Crow, Y. J. *et al.* Mutations in genes encoding ribonuclease H2 subunits cause Aicardi-Goutières syndrome and mimic congenital viral brain infection. *Nat. Genet.* **38,** 910–916 (2006).
230. Günther, C. *et al.* Defective removal of ribonucleotides from DNA promotes systemic autoimmunity. *J. Clin. Invest.* **125,** 413–424 (2015).
231. Zimmermann, M. *et al.* Europe PMC Funders Group Europe PMC Funders Author Manuscripts CRISPR screens identify genomic ribonucleotides as a source of PARP-trapping lesions. **559,** 285–289 (2019).
232. Pizzi, S. *et al.* Reduction of hRNase H2 activity in Aicardi-Goutières syndrome cells leads to replication stress and genome instability. *Hum. Mol. Genet.* **24,** 649–658 (2015).
233. Williams, J. S. *et al.* Topoisomerase 1-mediated removal of ribonucleotides from nascent leading-strand DNA. *Mol. Cell* **49,** 1010–5 (2013).
234. Sekiguchi, J. A. & Shuman, S. Site-specific ribonuclease activity of eukaryotic DNA topoisomerase I. *Mol. Cell* **1,** 89–97 (1997).
235. Sparks, J. L. & Burgers, P. M. Error-free and mutagenic processing of topoisomerase 1-provoked damage at genomic ribonucleotides. *EMBO J.* **34,** 1259–69 (2015).
236. Huang, S. Y. N., Ghosh, S. & Pommier, Y. Topoisomerase I alone is sufficient to produce short DNA deletions and can also reverse nicks at ribonucleotide sites. *J. Biol. Chem.* **290,** 14068–14076 (2015).
237. Potenski, C. J., Niu, H., Sung, P. & Klein, H. L. Avoidance of rNMP-induced mutations via RNaseH2 and Srs2-Exo1 dependent mechanisms. **73,** 389–400 (2015).
238. Li, F. *et al.* Apn2 resolves blocked 3′ ends and suppresses Top1-induced mutagenesis at genomic rNMP sites. *Nat. Struct. Mol. Biol.* **26,** 155–163 (2019).
239. Huang, S. N., Williams, J. S., Arana, M. E., Kunkel, T. A. & Pommier, Y. Topoisomerase I-mediated cleavage at unrepaired ribonucleotides generates DNA double-strand breaks. *EMBO J.* **36,** 361–373 (2017).
240. Cai, Y., Geacintov, N. E. & Broyde, S. Ribonucleotides as nucleotide excision repair substrates. *DNA Repair (Amst).* **13,** 55–60 (2014).
241. Sassa, A. *et al.* Processing of a single ribonucleotide embedded into DNA by human nucleotide excision repair and DNA polymerase η. *Sci. Rep.* **9,** 1–10 (2019).
242. Williams, J. S., Lujan, S. A. & Kunkel, T. A. Processing ribonucleotides incorporated during eukaryotic DNA replication. *Nat. Rev. Mol. Cell Biol.* **17,** 350–363 (2016).
243. Yeeles, J. T. P., Poli, J., Marians, K. J. & Pasero, P. Rescuing stalled or damaged replication forks. *Cold Spring Harb. Perspect. Biol.* **5,** 1–16 (2013).
244. Wan, L. *et al.* HPrimpol1/CCDC111 is a human DNA primase-polymerase required for the maintenance of genome integrity. *EMBO Rep.* **14,** 1104–1112 (2013).
245. Mourón, S. *et al.* Repriming of DNA synthesis at stalled replication forks by human PrimPol. *Nat. Struct. Mol. Biol.* **20,** 1383–1389 (2013).
246. Hauschka, P. V. Analysis of nucleotide pools in animal cells. *Methods Cell Biol.* **7,** 361–462 (1973).
247. Giannattasio, M. & Branzei, D. DNA Replication Through Strand Displacement During Lagging Strand DNA Synthesis in Saccharomyces cerevisiae. *Genes (Basel).* **10,** 167 (2019).
248. Kahli, M., Osmundson, J. S., Yeung, R. & Smith, D. J. Processing of eukaryotic Okazaki fragments by redundant nucleases can be uncoupled from ongoing DNA replication in vivo. *Nucleic Acids Res.* **47,** 1814–1822 (2019).
249. Bambara, R. A., Murante, R. S. & Henricksen, L. A. Enzymes and reactions at the eukaryotic DNA replication fork. *J. Biol. Chem.* **272,** 4647–50 (1997).
250. Liu, Y., Kao, H.-I. & Bambara, R. A. Flap Endonuclease 1: A Central Component of

DNA Metabolism. *Annu. Rev. Biochem.* **73,** 589–615 (2004).
251. Bae, S. H., Bae, K. H., Kim, J. A. & Seo, Y. S. RPA governs endonuclease switching during processing of Okazaki fragments in eukaryotes. *Nature* **412,** 456–61 (2001).
252. Qiu, J., Qian, Y., Frank, P., Wintersberger, U. & Shen, B. Saccharomyces cerevisiae RNase H(35) functions in RNA primer removal during lagging-strand DNA synthesis, most efficiently in cooperation with Rad27 nuclease. *Mol. Cell. Biol.* **19,** 8361–71 (1999).
253. Johnston, L. H. & Nasmyth, K. Saccharomyces cerevisiae cell cycle mutant cdc9 is defective in DNA ligase. *Nature* **274,** 891–893 (1978).
254. Gordenin, D. A., Kunkel, T. A. & Resnick, M. A. Repeat expansion - All in a flap? *Nat. Genet.* **16,** 116–118 (1997).
255. Epshtein, A., Potenski, C. J. & Klein, H. L. Increased spontaneous recombination in rnase H2-deficient cells arises from multiple contiguous rnmps and not from single rNMP residues incorporated by DNA polymerase epsilon. *Microb. Cell* **3,** 248–254 (2016).
256. Holmes, J. B. *et al.* Primer retention owing to the absence of RNase H1 is catastrophic for mitochondrial DNA replication. *Proc. Natl. Acad. Sci. U. S. A.* **112,** 9334–9339 (2015).
257. Vengrova, S. & Dalgaard, J. Z. The wild-type Schizosaccharomyces pombe mat1 imprint consists of two ribonucleotides. *EMBO Rep.* **7,** 59–65 (2006).
258. Vengrova, S. & Dalgaard, J. Z. RNase-sensitive DNA modification(s) initiates S. pombe mating-type switching. *Genes Dev.* **18,** 794–804 (2004).
259. Westover, K. D., Bushnell, D. A. & Kornberg, R. D. Structural basis of transcription: Nucleotide selection by rotation in the RNA polymerase II active center. *Cell* **119,** 481–489 (2004).
260. Santos-Pereira, J. M. & Aguilera, A. R loops: New modulators of genome dynamics and function. *Nat. Rev. Genet.* **16,** 583–597 (2015).
261. Wahba, L., Gore, S. K. & Koshland, D. The homologous recombination machinery modulates the formation of RNA–DNA hybrids and associated chromosome instability. *Elife* **2,** e00505 (2013).
262. Roy, D., Zhang, Z., Lu, Z., Hsieh, C.-L. & Lieber, M. R. Competition between the RNA Transcript and the Nontemplate DNA Strand during R-Loop Formation In Vitro: a Nick Can Serve as a Strong R-Loop Initiation Site. *Mol. Cell. Biol.* **30,** 146–159 (2010).
263. Itoh, T. & Tomizawa, J. Formation of an RNA primer for initiation of replication of ColE1 DNA by ribonuclease H. *Proc. Natl. Acad. Sci. U. S. A.* **77,** 2450–2454 (1980).
264. Baldacci, G., Chérif-Zahar, B. & Bernardi, G. The initiation of DNA replication in the mitochondrial genome of yeast. *EMBO J.* **3,** 2115–2120 (1984).
265. Pohjoismäki, J. L. O. *et al.* Mammalian mitochondrial DNA replication intermediates are essentially duplex but contain extensive tracts of RNA/DNA hybrid. *J. Mol. Biol.* **397,** 1144–55 (2010).
266. Xu, B. & Clayton, D. A. RNA-DNA hybrid formation at the human mitochondrial heavy-strand origin ceases at replication start sites: An implication for RNA-DNA hybrids serving as primers. *EMBO J.* **15,** 3135–3143 (1996).
267. Roy, D., Yu, K. & Lieber, M. R. Mechanism of R-Loop Formation at Immunoglobulin Class Switch Sequences. *Mol. Cell. Biol.* **28,** 50–60 (2008).
268. Ginno, P. A., Lott, P. L., Christensen, H. C., Korf, I. & Chédin, F. R-Loop Formation Is a Distinctive Characteristic of Unmethylated Human CpG Island Promoters. *Mol. Cell* **45,** 814–825 (2012).
269. Castellano-Pozo, M. *et al.* R loops are linked to histone H3 S10 phosphorylation and chromatin condensation. *Mol. Cell* **52,** 583–590 (2013).

270. Crossley, M. P., Bocek, M. & Cimprich, K. A. R-Loops as Cellular Regulators and Genomic Threats. *Mol. Cell* **73,** 398–411 (2019).
271. Muers, M. Mutation: The perils of transcription. *Nat. Rev. Genet.* **12,** 156 (2011).
272. Wimberly, H. *et al.* R-loops and nicks initiate DNA breakage and genome instability in non-growing Escherichia coli. *Nat. Commun.* **4,** 1–10 (2013).
273. Belotserkovskii, B. P., Shin, J. H. S. & Hanawalt, P. C. Strong transcription blockage mediated by R-loop formation within a G-rich homopurine-homopyrimidine sequence localized in the vicinity of the promoter. *Nucleic Acids Res.* **45,** 6589–6599 (2017).
274. Gan, W. *et al.* R-loop-mediated genomic instability is caused by impairment of replication fork progression. *Genes Dev.* **25,** 2041–2056 (2011).
275. Costantino, L. & Koshland, D. Genome-wide Map of R-Loop-Induced Damage Reveals How a Subset of R-Loops Contributes to Genomic Instability. *Mol. Cell* **71,** 487–497.e3 (2018).
276. Kogoma, T. A novel Escherichia coli mutant capable of DNA replication in the absence of protein synthesis. *J. Mol. Biol.* **121,** 55–69 (1978).
277. Kogoma, T. & Maldonado, R. R. DNA polymerase I in constitutive stable DNA replication in Escherichia coli. *J. Bacteriol.* **179,** 2109–2115 (1997).
278. Stuckey, R., García-Rodríguez, N., Aguilera, A. & Wellinger, R. E. Role for RNA:DNA hybrids in origin-independent replication priming in a eukaryotic system. *Proc. Natl. Acad. Sci. U. S. A.* **112,** 5779–5784 (2015).
279. Costantino, L. & Koshland, D. The Yin and Yang of R-loop biology. *Curr. Opin. Cell Biol.* **34,** 39–45 (2015).
280. Skourti-Stathaki, K. & Proudfoot, N. J. A double-edged sword: R loops as threats to genome integrity and powerful regulators of gene expression. *Genes Dev.* **28,** 1384–1396 (2014).
281. Allison, D. F. & Wang, G. G. R-loops: formation, function, and relevance to cell stress. *Cell Stress* **3,** 38–46 (2019).
282. El Hage, A., French, S. L., Beyer, A. L. & Tollervey, D. Loss of Topoisomerase I leads to R-loop-mediated transcriptional blocks during ribosomal RNA synthesis. *Genes Dev.* **24,** 1546–1558 (2010).
283. Yang, Y. *et al.* Arginine methylation facilitates the recruitment of TOP3B to chromatin to prevent R loop accumulation. *Mol. Cell* **53,** 484–97 (2014).
284. Wahba, L., Amon, J. D., Koshland, D. & Vuica-Ross, M. RNase H and Multiple RNA Biogenesis Factors Cooperate to Prevent RNA:DNA Hybrids from Generating Genome Instability. *Mol. Cell* **44,** 978–988 (2011).
285. García-Benítez, F., Gaillard, H. & Aguilera, A. Physical proximity of chromatin to nuclear pores prevents harmful R loop accumulation contributing to maintain genome stability. *Proc. Natl. Acad. Sci. U. S. A.* **114,** 10942–10947 (2017).
286. Huertas, P. & Aguilera, A. Cotranscriptionally formed DNA:RNA hybrids mediate transcription elongation impairment and transcription-associated recombination. *Mol. Cell* **12,** 711–21 (2003).
287. Chakraborty, P. & Grosse, F. Human DHX9 helicase preferentially unwinds RNA-containing displacement loops (R-loops) and G-quadruplexes. *DNA Repair (Amst).* **10,** 654–665 (2011).
288. Sollier, J. *et al.* Transcription-Coupled Nucleotide Excision Repair Factors Promote R-Loop-Induced Genome Instability. *Mol. Cell* **56,** 777–785 (2014).
289. Mischo, H. E. *et al.* Yeast Sen1 helicase protects the genome from transcription-associated instability. *Mol. Cell* **41,** 21–32 (2011).
290. Boulé, J.-B. & Zakian, V. A. The yeast Pif1p DNA helicase preferentially unwinds RNA DNA substrates. *Nucleic Acids Res.* **35,** 5809–18 (2007).
291. Francia, S. *et al.* Site-specific DICER and DROSHA RNA products control the DNA-

damage response. *Nature* **488,** 231–235 (2012).
292. Li, L. *et al.* DEAD Box 1 Facilitates Removal of RNA and Homologous Recombination at DNA Double-Strand Breaks. *Mol. Cell. Biol.* **36,** 2794–2810 (2016).
293. Ohle, C. *et al.* Transient RNA-DNA Hybrids Are Required for Efficient Double-Strand Break Repair. *Cell* **167,** 1001–1013.e7 (2016).
294. Brustel, J., Kozik, Z., Gromak, N., Savic, V. & Sweet, S. M. M. Large XPF-dependent deletions following misrepair of a DNA double strand break are prevented by the RNA:DNA helicase Senataxin. *Sci. Rep.* **8,** 3850 (2018).
295. D'Alessandro, G. *et al.* BRCA2 controls DNA:RNA hybrid level at DSBs by mediating RNase H2 recruitment. *Nat. Commun.* **9,** 5376 (2018).
296. Cohen, S. *et al.* Senataxin resolves RNA:DNA hybrids forming at DNA double-strand breaks to prevent translocations. *Nat. Commun.* **9,** 533 (2018).
297. Domingo-Prim, J. *et al.* EXOSC10 is required for RPA assembly and controlled DNA end resection at DNA double-strand breaks. *Nat. Commun.* **10,** 2135 (2019).
298. Symington, L. S. Mechanism and regulation of DNA end resection in eukaryotes. *Crit. Rev. Biochem. Mol. Biol.* **51,** 195–212 (2016).
299. Yasuhara, T. *et al.* Human Rad52 Promotes XPG-Mediated R-loop Processing to Initiate Transcription-Associated Homologous Recombination Repair. *Cell* **175,** 558–570.e11 (2018).
300. Alfano, L. *et al.* Depletion of the RNA binding protein HNRNPD impairs homologous recombination by inhibiting DNA-end resection and inducing R-loop accumulation. *Nucleic Acids Res.* **47,** 4068–4085 (2019).
301. Lu, W.-T. *et al.* Drosha drives the formation of DNA:RNA hybrids around DNA break sites to facilitate DNA repair. *Nat. Commun.* **9,** 532 (2018).
302. Keskin, H. *et al.* Transcript-RNA-templated DNA recombination and repair. *Nature* **515,** 436–9 (2014).
303. Mazina, O. M., Keskin, H., Hanamshet, K., Storici, F. & Mazin, A. V. Rad52 Inverse Strand Exchange Drives RNA-Templated DNA Double-Strand Break Repair. *Mol. Cell* **67,** 19–29.e3 (2017).
304. Aguilera, A. & Gómez-González, B. DNA-RNA hybrids: The risks of DNA breakage during transcription. *Nat. Struct. Mol. Biol.* **24,** 439–443 (2017).
305. Amon, J. D. & Koshland, D. RNase H enables efficient repair of R-loop induced DNA damage. *Elife* **5,** 1–20 (2016).
306. Arudchandran, A. *et al.* The absence of ribonuclease H1 or H2 alters the sensitivity of Saccharomyces cerevisiae to hydroxyurea, caffeine and ethyl methanesulphonate: Implications for roles of RNases H in DNA replication and repair. *Genes to Cells* **5,** 789–802 (2000).
307. Singh, A. & Xu, Y. J. The cell killing mechanisms of hydroxyurea. *Genes (Basel).* **7,** (2016).
308. Meroni, A. *et al.* in *Methods in Molecular Biology* **1672,** 319–327 (Humana Press Inc., 2018).
309. El Hage, A., French, S. L., Beyer, A. L. & Tollervey, D. Loss of Topoisomerase I leads to R-loop-mediated transcriptional blocks during ribosomal RNA synthesis. *Genes Dev.* **24,** 1546–1558 (2010).
310. Appanah, R., Lones, E. C., Aiello, U., Libri, D. & De Piccoli, G. Sen1 Is Recruited to Replication Forks via Ctf4 and Mrc1 and Promotes Genome Stability. *Cell Rep.* **30,** 2094–2105.e9 (2020).
311. Pomerantz, R. T. & O'Donnell, M. The replisome uses mRNA as a primer after colliding with RNA polymerase. *Nature* **456,** 762–766 (2008).
312. Dandjinou, A. T., Larrive, M., Wellinger, R. E. & Wellinger, R. J. in *Yeast Protocols* 193–208 (Humana Press, 2006). doi:10.1385/1-59259-958-3:193

313. Boone, C., Bussey, H. & Andrews, B. J. Exploring genetic interactions and networks with yeast. *Nat. Rev. Genet.* **8,** 437–449 (2007).
314. Fisher, R. A. Reproduced by permission of the Royal Society of Edinburgh from Transactions of the Society, vol. 52: 399-433 (1918). *Society* **52,** 399–433 (1918).
315. Tong, A. H. Y. *et al.* Systematic genetic analysis with ordered arrays of yeast deletion mutants. *Science (80-.).* **294,** 2364–2368 (2001).
316. Tong, A. H. Y. Global Mapping of the Yeast Genetic Interaction Network. *Science (80-.).* **303,** 808–813 (2004).
317. Costanzo, M. *et al.* A global genetic interaction network maps a wiring diagram of cellular function. *Science (80-.).* **353,** (2016).
318. Bonner, J. N. & Zhao, X. Replication-associated recombinational repair: Lessons from budding yeast. *Genes (Basel).* **7,** (2016).
319. Zhou, W., Ryan, J. J. & Zhou, H. Global Analyses of Sumoylated Proteins in Saccharomyces cerevisiae. *J. Biol. Chem.* **279,** 32262–32268 (2004).
320. Xu, Z. *et al.* Molecular basis of the redox regulation of SUMO proteases: a protective mechanism of intermolecular disulfide linkage against irreversible sulfhydryl oxidation. *FASEB J.* **22,** 127–137 (2008).
321. Martin, M. J., Garcia-Ortiz, M. V., Esteban, V. & Blanco, L. Ribonucleotides and manganese ions improve non-homologous end joining by human Polμ. *Nucleic Acids Res.* **41,** 2428–36 (2013).
322. Sayrac, S., Vengrova, S., Godfrey, E. L. & Dalgaard, J. Z. Identification of a novel type of spacer element required for imprinting in fission yeast. *PLoS Genet.* **7,** (2011).
323. Sparks, J. L. *et al.* RNase H2-Initiated Ribonucleotide Excision Repair. *Mol. Cell* **47,** 980–986 (2012).
324. Kramarz, K. *et al.* The nuclear pore primes recombination-dependent DNA synthesis at arrested forks by promoting SUMO removal. *Nat. Commun.* **11,** 1–15 (2020).
325. Poli, J. *et al.* dNTP pools determine fork progression and origin usage under replication stress. *EMBO J.* **31,** 883–894 (2012).
326. Balint, E. & Unk, I. Selective Metal Ion Utilization Contributes to the Transformation of the Activity of Yeast Polymerase η from DNA Polymerization toward RNA Polymerization. *Int. J. Mol. Sci.* **21,** 8248 (2020).
327. Egli, M., Usman, N. & Rich, A. Conformational influence of the ribose 2'-hydroxyl group: crystal structures of DNA-RNA chimeric duplexes. *Biochemistry* **32,** 3221–37 (1993).
328. Meroni, A. *et al.* The Incorporation of Ribonucleotides Induces Structural and Conformational Changes in DNA. *Biophys. J.* **113,** 1373–1382 (2017).
329. Yadav, P., Owiti, N. & Kim, N. The role of topoisomerase i in suppressing genome instability associated with a highly transcribed guanine-rich sequence is not restricted to preventing RNA:DNA hybrid accumulation. *Nucleic Acids Res.* **44,** 718–729 (2016).
330. Longtine, M. S. *et al.* Additional modules for versatile and economical PCR-based gene deletion and modification in Saccharomyces cerevisiae. *Yeast* **14,** 953–961 (1998).
331. Doksani, Y., Bermejo, R., Fiorani, S., Haber, J. E. & Foiani, M. A single S phase double-strand break influences replicon dynamics and triggers a Mre11-Tel1/ATM-mediated mechanism controlling terminal fork integrity. *Cell* **137,** 247 (2009).
332. Lopes, M., Cotta-Ramusino, C., Liberi, G. & Foiani, M. Branch Migrating Sister Chromatid Junctions Form at Replication Origins through Rad51/Rad52-Independent Mechanisms. *Mol. Cell* **12,** 1499–1510 (2003).
333. Brewer, B. J. & Fangman, W. L. The localization of replication origins on ARS plasmids in S. cerevisiae. *Cell* **51,** 463–471 (1987).
334. Huberman, J. A. Mapping replication origins, pause sites, and termini by

neutral/alkaline two-dimensional gel electrophoresis. *Methods A Companion to Methods Enzymol.* **13,** 247–257 (1997).
335. Tong, A. H. Y. & Boone, C. 16 High-Throughput Strain Construction and Systematic Synthetic Lethal Screening in S a c c h a r o m y c e s c e r e v i s i a e. *Methods Microbiol.* **36,** (2007).
336. Mani, R., St. Onge, R. P., Hartman IV, J. L., Giaever, G. & Roth, F. P. Defining genetic interaction. *Proc. Natl. Acad. Sci. U. S. A.* **105,** 3461–3466 (2008).
337. Baryshnikova, A. *et al.* Quantitative analysis of fitness and genetic interactions in yeast on a genome scale. *Nat. Methods* **7,** 1017–1024 (2010).
338. Costanzo, M. *et al.* The Genetic Landscape of a Cell. *Science (80-.).* **327,** 425–431 (2010).

Appendices

Published paper I

RNase H activities counteract a toxic effect of Polymerase η in cells replicating with depleted dNTP pools

Alice Meroni[†], **Giulia Maria Nava**[†], Eliana Bianco, Lavinia Grasso, Elena Galati, Maria Cristina Bosio, Daria Delmastro, Marco Muzi-Falconi[*‡] and Federico Lazzaro[*‡]

Dipartimento di Bioscienze, Universita` degli Studi di Milano, via Celoria 26, 20133 Milano, Italy

[†]The authors wish it to be known that, in their opinion, the first two authors should be regarded as Joint First Authors.

Corresponding author: federico.lazzaro@unimi.it

Nucleic Acids Research, 2019, Vol.47, No.9

https://doi:10.1093/nar/gkz165.

Synopsis of the work and specific contributions

In this manuscript, we describe a new role played by the yeast translesion synthesis DNA polymerase η (Pol η) in DNA replication under low deoxyribonucleotides conditions triggered by hydroxyurea. In particular, we found that in this condition, Pol η activity seems to facilitate the formation of RNA:DNA hybrids at stalled replication forks. However, when RNase H activity fails to process these RNA:DNA hybrids, they become highly toxic for cells. We proved that in RNases H lacking cells, the activity of Pol η causes DNA damage checkpoint activation and G2/M arrest. We found that this toxic effect starts in the first replication cycle in the presence of HU, it requires the catalytic activity of Pol η, and it results from the inability to process stretches of at least four consecutive ribonucleotides. We finally found that a Pol η mutant allele with enhanced ribonucleotide incorporation further exacerbates the sensitivity to hydroxyurea of cells lacking RNase H activities.

For what concerns this work, I actively participated in the design and execution of the experiments. I also collaborated to prepare the figures, and I contributed to the revision of the manuscript. Together with Alice Meroni, I am the co-first author of this work.

4612–4623 *Nucleic Acids Research, 2019, Vol. 47, No. 9* *Published online 8 March 2019*
doi: 10.1093/nar/gkz165

RNase H activities counteract a toxic effect of Polymerase η in cells replicating with depleted dNTP pools

Alice Meroni†, Giulia Maria Nava†, Eliana Bianco, Lavinia Grasso, Elena Galati, Maria Cristina Bosio, Daria Delmastro, Marco Muzi-Falconi*,‡ and Federico Lazzaro*,‡

Dipartimento di Bioscienze, Università degli Studi di Milano, via Celoria 26, 20133 Milano, Italy

Received March 28, 2018; Revised February 25, 2019; Editorial Decision February 27, 2019; Accepted March 01, 2019

ABSTRACT

RNA:DNA hybrids are transient physiological intermediates that arise during several cellular processes such as DNA replication. In pathological situations, they may stably accumulate and pose a threat to genome integrity. Cellular RNase H activities process these structures to restore the correct DNA:DNA sequence. Yeast cells lacking RNase H are negatively affected by depletion of deoxyribonucleotide pools necessary for DNA replication. Here we show that the translesion synthesis DNA polymerase η (Pol η) plays a role in DNA replication under low deoxyribonucleotides condition triggered by hydroxyurea. In particular, the catalytic reaction performed by Pol η is detrimental for RNase H deficient cells, causing DNA damage checkpoint activation and G2/M arrest. Moreover, a Pol η mutant allele with enhanced ribonucleotide incorporation further exacerbates the sensitivity to hydroxyurea of cells lacking RNase H activities. Our data are compatible with a model in which Pol η activity facilitates the formation or stabilization of RNA:DNA hybrids at stalled replication forks. However, in a scenario where RNase H activity fails to restore DNA, these hybrids become highly toxic for cells.

INTRODUCTION

The accuracy of genome duplication is mainly guaranteed by the high fidelity of replicative DNA polymerases that insert the correct deoxyribonucleotide respecting the base pairing with the template. Besides discriminating among the different bases, replicative polymerases have also to choose the right sugar moiety (1). In doing so, they are challenged by the intracellular physiologically high concentration of ribonucleotides (rNTPs), which exceed deoxyribonucleotides (dNTPs) by over a hundredfold (2). Specific amino acid residues shape the steric gate in the nucleotide binding site, driving DNA polymerases to select dNTPs, which lack an oxygen at the 2′ carbon of the sugar compared to rNTPs (1). Nonetheless, during DNA replication, a significant number of ribonucleotides is introduced into the nascent strand (2). In yeast, at least 1 rNTP is incorporated every 1000 dNTPs, making rNTPs the most frequent non-canonical nucleotides introduced into the genome (3). Genomic rNMPs play an important physiological role in mismatch repair (4–6) but, if not promptly removed from DNA, they also promote replication stress and genome instability (7–11).

Chromosome embedded ribonucleotides are usually processed by RNase H enzymes, which contribute to the reestablishment of the correct DNA sequence (3): RNase H1 cleaves RNA:DNA hybrids constituted by at least four consecutive ribonucleotides; RNase H2 processes both single and multiple embedded ribonucleotides (12). Noteworthy, dysfunction of the RNase H2 complex is a primary cause of the Aicardi-Goutières syndrome, a rare interferonopathy that mainly affects the brain (13).

Genomic ribonucleotides can also be subjected to mutagenic processing by Topoisomerase 1, leading to the formation of short deletions and ultimately double-strand breaks (14–16). In general, the impaired removal of ribonucleotides leads to severe consequences, as their persistence in DNA

*To whom correspondence should be addressed. Tel: +390 250314827; Fax: +390 250315044; Email: federico.lazzaro@unimi.it
Correspondence may also be addressed to Marco Muzi-Falconi. Email: marco.muzifalconi@unimi.it
†The authors wish it to be known that, in their opinion, the first two authors should be regarded as Joint First Authors.
‡The last two authors should be regarded as Co-last Authors.
Present addresses:
Alice Meroni, Edward A. Doisy Department of Biochemistry and Molecular Biology, Saint Louis University School of Medicine, 1100 South Grand Blvd St. Louis, MO 63104.
Eliana Bianco, Institute of Biochemistry, ETH Zurich, Otto-Stern-Weg 3, CH-8093 Zurich, Switzerland.

distorts the helix structure (17–19) and therefore affects DNA transactions.

Ribonucleotide incorporation is further increased when the cellular dNTP pools are reduced, such as following treatment with the ribonucleotide reductase inhibitor hydroxyurea (HU) (8). Indeed, RNase H deficient cells are hypersensitive to HU (7–9). During replication, genomic rNMPs are not efficiently bypassed by replicative DNA polymerases (7,20–22) and cells rely on post-replication repair mechanisms to overcome these blocks (7). Upon HU treatment, template switching or Pol ζ -mediated translesion synthesis (TLS) are essential to bypass rNMPs in the DNA template and to complete genome duplication (7).

Intriguingly, we found that the increased sensitivity to HU observed in yeast cells lacking RNase H activities (*rnh1Δ rnh201Δ*) is almost totally dependent on the TLS polymerase η (*RAD30*).

Pol η belongs to the Y-family polymerases and has a major role in the bypass of several adducts that halt the progression of replication forks. This versatile polymerase is known for its excellent ability in bypassing thymidine adducts and 8-oxo-guanines in an error-free manner (23–25). In humans, defects in the gene encoding Pol η (*POLH*) lead to the onset of the *xeroderma pigmentosum* variant (XP-V) genetic syndrome (26), characterized by high incidence of skin cancer and sunlight sensitivity, due to the inability to bypass bulky lesions (27). Besides the TLS function, human Pol η has been implicated in class switch recombination (28,29) and common fragile sites (CFSs) stability (30–33). Moreover, yeast Pol η was reported to be recruited at replication forks upon replication stress induction (34). Different studies reported that yeast and human Pol η efficiently utilize rNTPs and extend RNA primers *in vitro* (35–37).

In this work, we describe the involvement of Pol η in genome replication when dNTP pools are low. In particular, we report that in these conditions Pol η catalytic activity becomes harmful when ribonucleotides cannot be removed. The enhanced ribonucleotide incorporation, through a Pol η steric gate mutant (38), further exacerbates this phenotype. In the absence of RNase H activities capable of processing consecutive ribonucleotides, Pol η activity leads to the activation of the DNA damage checkpoint and to cell cycle arrest within a single round of replication in the presence of low dNTPs. We demonstrate that the toxic activity of Pol η is not dependent upon ribonucleotides already present in the template DNA and that RNase H enzymes are essential to resolve the toxic structures promoted by Pol η. We propose a model where Pol η actively participates to DNA replication in low dNTPs conditions. Pol η ability to incorporate rNMPs or extend RNA stretches could be crucial to enable full-genome duplication during replication stress at the expense of an accumulation of longer stretches of consecutive ribonucleotides in the genome. In wild type cells, thanks to RNase H, this is a tolerable compromise. However, this activity of Pol η becomes highly toxic when RNase H enzymes are defective and cells cannot restore the correct DNA composition and structure.

MATERIALS AND METHODS

Yeast strains, plasmids, media and growth conditions

All the strains used in this work are listed in Supplementary Table S1 and are derivatives of the W303 *RAD5*$^{+}$ background. Strains were generated by standard genetic procedures. Deletions were obtained by one-step PCR (39). RNase H2 mutant strains (*rnh201-P45D-Y219A* and r*nh201-D39A*) were obtained by crossing, starting from *MATa sgs1::HIS3 rnh201-D39A* and *MATa sgs1::HIS3 rnh201-P45D-Y219A* (40).

For the indicated experiments, cell cultures were grown at 28°C in YEP medium (1% yeast extract, 2% peptone) containing 2% glucose (YEPD), 2% raffinose (YEPR), or 2% galactose and 2% raffinose (YEPRG). For strains carrying plasmids, cells were grown in Synthetic-Complete (SC) medium supplemented with appropriate sugar(s) and nutrients to maintain the selection. The concentration of drugs/chemicals and their addition to the medium are indicated in the figures and their respective legends.

Hydroxyurea was purchased from US Biological (Salem, MA, USA), Auxin (IAA), Doxycycline (DOXY) and MMS were purchased from Sigma (Saint Louis, MO, USA).

The pEGUh6-RAD30 (*GAL1-6xHIS-RAD30*) and pEGUh6-rad30 D155A D156A (*GAL1-6xHIS-rad30-D155A-E156A*) plasmids were kindly provided by T.A. Kunkel and are described in (41). pFL166.4 (*GAL1-6xHIS-rad30-F35A*) was obtained by site-directed mutagenesis (QuikChange Site-Directed Mutagenesis Kit Thermo Fisher Scientific, Waltham, Massachusetts USA) on pEGUh6-RAD30 using oligos 3′-ACA TAG ATA TGA ATG CCT TTG CTG CAC AGG TTG AGC AGA TGC G-5′ and 3′-CGC ATC TGC TCA ACC TGT GCA GCA AAG GCA TTC ATA TCT ATG T-5′, and then verified by DNA sequencing.

The pFL160.1 plasmid carrying the *rnhB*-3xminiAID-HA under TetOFF promoter (42) was prepared as follows. The *rnhB* gene was amplified from MG1655 *E. coli* strain using primers 3′- TTA ACA TCG ATA GCG GCC GCA TGA TCG AAT TTG TTT ATC CGC ACA CG-5′ and 3′-GAC TTT TGA CAA GAA ACC ATG GAC GCA AGT CCC AGT GCG C-5′. The 3X-miniAID sequence was amplified from the plasmid BYP7432 (43) using primers 3′-GCG CAC TGG GAC TTG CGT CCA TGG TTT CTT GTC AAA AGT C-5′ and 3′-TGC AGG GCC CTA GCG GCC GCT CAC GCA TAG TCA GGA ACA TCG TAT GGG TAT TTA TAC ATT CTC AAG TCT A-5′. The two amplicons were purified and then digested with NotI and PshAI restriction enzymes. Ligation reactions were performed with NotI-digested pCM185 (42). The sequence of the insert and its junction regions was then verified by DNA sequencing (Eurofins Scientific, Luxembourg). Restriction enzymes were provided by New England Biolabs (Ipswich, MA, USA).

Drop test assays

Logarithmically growing yeast cultures were diluted at 2 × 10^6 cells/ml. A series of 10-fold dilutions were prepared,

and 10 μl drops were spotted on YEP or selective plates, supplemented with the appropriate sugar and the indicated drugs. Pictures were taken after incubation at 28°C for 2–4 days.

Sensitivity assay

Exponentially growing cells were synchronized in the G1 phase by adding α-factor (4 μg/ml) (Primm, Milano, Italy). Upon appropriate dilutions, 100 CFU of each strain were plated on YEPRG ± 25 mM HU. After 4 days of incubation, the number of grown colonies was counted and normalized. The standard error of the mean (SEM) was calculated on three independent experiments.

SDS-PAGE and western blot

TCA protein extracts were prepared, and an equal amount of each sample was separated by SDS-PAGE (44). Western blottings were performed with anti-Rad53 (kind gift by C. Santocanale), anti-HIS-tag (70796-3 Novagen, Merck, Darmstadt, Germany) or anti-miniAID-tag (MBL International, Woburn, MA, USA (43)) or anti-Pgk1 (22c5d8 Abcam, Cambridge, UK) antibodies, using standard techniques.

FACS analysis

Cells were fixed in 70% ethanol and treated with RNase A and proteinase K. DNA was stained with Sytox Green (Thermo Fisher Scientific, Waltham, MA, USA), and cell cycle distribution was estimated by cytofluorimetric analysis with a FACScan (BD Biosciences, San Josè, CA, USA). Data were plotted using the FlowJo® Software.

Ribonucleotide incorporation assay

The assay was performed as described in details in (45). Briefly, genomic DNA was isolated using Y-DER (Thermo Fisher Scientific, Waltham, Massachusetts USA) extraction kit according to manufacturer's instruction and treated with *Escherichia coli* RNase HII (NEB, Ipswich, Massachusetts USA), which introduces nicks at every ribonucleotide-containing site. The nicks were then used to radioactively label the site with DNA Polymerase I (NEB, Ipswich, MA, USA) in the presence of unlabeled dA/-dT/-dGTP and α-^{32}P-dCTP (Perkin Elmer, Waltham, MA, USA). Labeled genomic DNA was separated by agarose gel electrophoresis in the presence of ethidium bromide, imaged under UV light and quantified with ImageLab software (Bio-Rad). The gel was successively dried, and the radioactive signal was detected by autoradiography using a Typhoon FLA 7000 (GE Healthcare Life Sciences, Marlborough, MA, USA) and quantified with ImageQuant software (GE Healthcare Life Sciences, Marlborough, MA, USA). The radioactive signal of each sample was normalized on total genomic DNA measured by ethidium bromide staining. The ratio between *in-vitro* RNHII-treated and the untreated sample was expressed as fold change respect to the control sample. The mean of four different experiments ± SEM is reported in the figure.

RESULTS

DNA polymerase η is responsible for HU-induced cell lethality in the absence of RNase H activities

Yeast cells lacking both RNase H activities (*rnh1Δ rnh201Δ*) are sensitive to several genotoxic and replication stress-inducing agents, such as MMS, CPT, and HU (7,46,47). In particular, following HU treatment, the Post Replication Repair (PRR) pathway becomes essential for cell survival, and TLS polymerase ζ is critical to help replicative polymerases bypass the ribonucleotides persisting in the template strand of genomic DNA (7). Unexpectedly, we found that the simultaneous loss of all yeast TLS polymerases, Pol ζ, Pol η and Rev1 (*rev3Δ rev7Δ rad30Δ rev1Δ*) almost completely suppresses the HU sensitivity phenotype of *rnh1Δ rnh201Δ* cells (Figure 1A). By analyzing the individual contribution of each TLS polymerase, we found that the suppression of HU sensitivity is almost completely dependent upon the loss of DNA polymerase η (encoded by *RAD30* gene) (Figure 1A). Furthermore, Pol η affects *rnh1Δ rnh201Δ* cell viability specifically following HU treatment, but not upon treatment with other genotoxic agents impacting on S phase, like MMS (Figure 1B).

Low doses of HU induce a Pol η-dependent DNA damage checkpoint activation and mitotic arrest in RNase H deficient cells

We have previously shown that upon treatment with low doses of HU, RNase H lacking cells exhibit DNA damage checkpoint activation and cell cycle arrest at G2/M phase (7). Given the involvement of Pol η in the HU sensitivity of *rnh1Δ rnh201Δ* cells, we tested its contribution to such checkpoint activation.

The phosphorylation state of the checkpoint effector kinase Rad53 was used as a readout for DNA damage checkpoint (DDC) activation, while cell cycle profiles were analyzed by flow cytometry (48,49). Cells were synchronized in G1 phase with α-factor, released in 25 mM HU, and collected at the indicated time points. At low doses of HU, wild type cells exhibit a mild and transient activation of the DDC in S phase; the checkpoint response is then switched off, and cell cycle progression continues (Figure 2A and B). In *rnh1Δ rnh201Δ* cells, however, Rad53 phosphorylation persists after S phase and cells cannot complete the cell cycle and entry into the next G1 phase is delayed (Figure 2A and B). Consistently with their reduced viability, a fraction of these cells remains in G2/M with 2C DNA content (Figure 2A); no cell cycle defects or Rad53 phosphorylation are observed in the absence of HU (Supplementary Figure S1). Intriguingly, deletion of *RAD30* rescues almost completely all the HU-induced phenotypes observed in RNase H mutants. Indeed, most *rnh1Δ rnh201Δ rad30Δ* cells dephosphorylate Rad53 and exhibit an almost wild type kinetics of cell cycle progression (Figure 2A and B).

It is worth noting that even in the absence of *RAD30* a small proportion of cells remain blocked in G2/M with Rad53 phosphorylated, suggesting that other polymerases may contribute to the HU-induced toxicity.

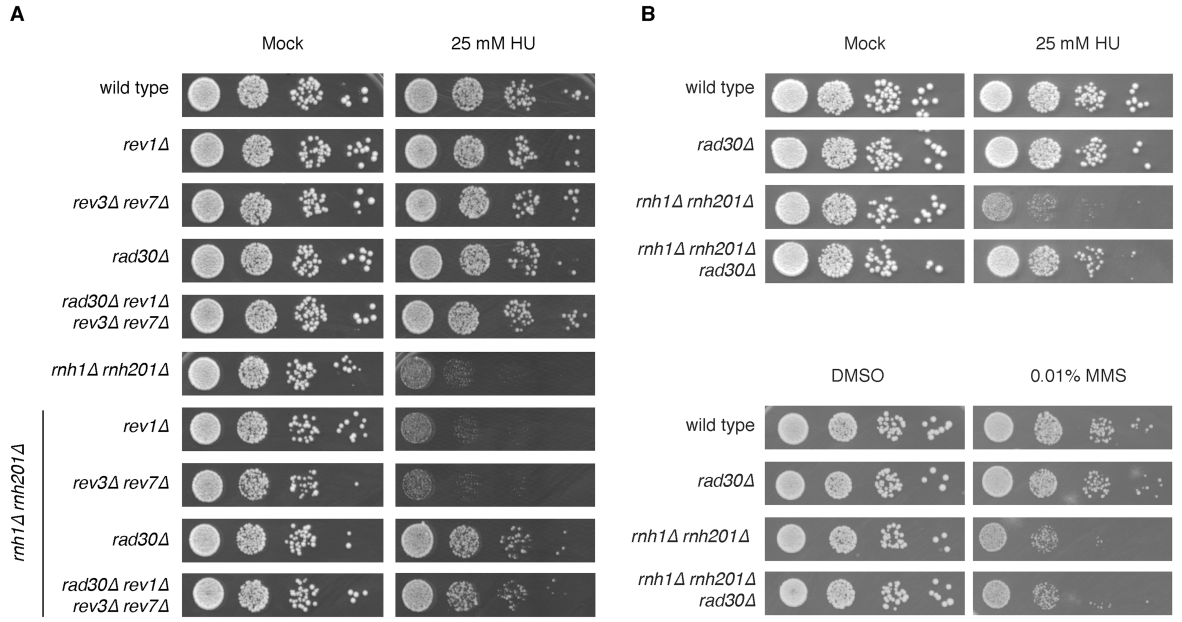

Figure 1. Removal of Pol η rescues the HU sensitivity of cell lacking RNase H activities. 10-fold serial dilutions of the indicated strains were plated on (**A**) YEPD and YEPD + 25 mM HU and (**B**) on YEPD, YEPD + 25 mM HU and YEPD + 0.01% MMS. Plates were incubated at 28°C and pictures were taken after 3 days. Results are representative of four biological replicates.

Pol η acts at HU-stressed replication forks

Hydroxyurea is known to induce replication forks stalling and the formation of ssDNA gaps, which are filled in late S phase mainly by TLS polymerases (50–52). Yeast Pol η was reported to be recruited to the proximity of replication origins during HU-induced stress (34,53). In human cells, Pol η actively participates to CFSs replication, possibly by substituting Pol δ (31–33), and forms nuclear foci upon hydroxyurea exposure (54). Thus, we asked whether the toxic activity of Pol η occurs at the fork during DNA replication under low dNTPs conditions or post-replication, during gap refilling in late S phase/G2.

In order to address this question, we exploited a yeast strain lacking endogenous *RAD30*, where Pol η could be conditionally overexpressed at different times following a transient exposure to HU. We first tested whether an acute exposure to high levels of HU had the same effect as the chronic low dose HU treatment used so far. We exposed α-factor synchronized cells for two hours to 200 mM HU, which was then washed out, rapidly restoring physiological dNTPs level (55–57). Upon release in the cell cycle in the absence of HU, *rnh1Δ rnh201Δ* cells exhibited similar, albeit milder, phenotypes as those reported following a chronic exposure to 25 mM HU (compare Supplementary Figure S2 and Figure 2). Importantly, even though the drug was removed from the medium when cells resumed cell cycle progression, the activation of the DDC and the G2/M cell cycle arrest in *rnh1Δ rnh201Δ* cells was still dependent on Pol η (Supplementary Figure S2).

To determine when Pol η exerts its toxic activity, we synchronized *rnh1Δ rnh201Δ rad30Δ* cultures, and we induced *RAD30* overexpression, before, immediately after or 30′ after the acute HU treatment. In the first case, cells were subjected to nucleotide depletion in the presence of Pol η. In the other samples, cells experienced the HU-induced stress in the absence of Pol η, which was expressed only immediately or 30′ after HU removal. Protein levels were verified by western blotting; cell cycle progression and DDC activation were monitored as previously described. Intriguingly, we observed a strong accumulation of G2/M arrested cells and Rad53 phosphorylation only when Pol η was concomitantly present with hydroxyurea during DNA replication (Figure 3, before HU treatment). In contrast, when Pol η was induced after the removal of HU, most cells did not exhibit cell cycle progression defects or DDC activation (Figure 3, 0 min after HU release, 30 min after HU release). These data indicate that Pol η exerts its toxic effect at replication forks when they are slowed down and challenged by low dNTPs conditions.

Pol η toxicity is independent of ribonucleotides embedded in the DNA replication template

Since Pol η activity becomes toxic only in the absence of RNase H, it is essential to assess how the two are related to each other. Lack of RNase H causes the genome-wide accumulation of unprocessed ribonucleotides, which could stimulate a Pol η activity that becomes toxic when dNTP pools have been depleted. On the other hand, Pol η may be recruited at the HU-stressed replication forks generating a product that becomes toxic in the absence of RNase H. In the first scenario, Pol η would be toxic in the absence of RNase H due to the presence of rNMPs in the template

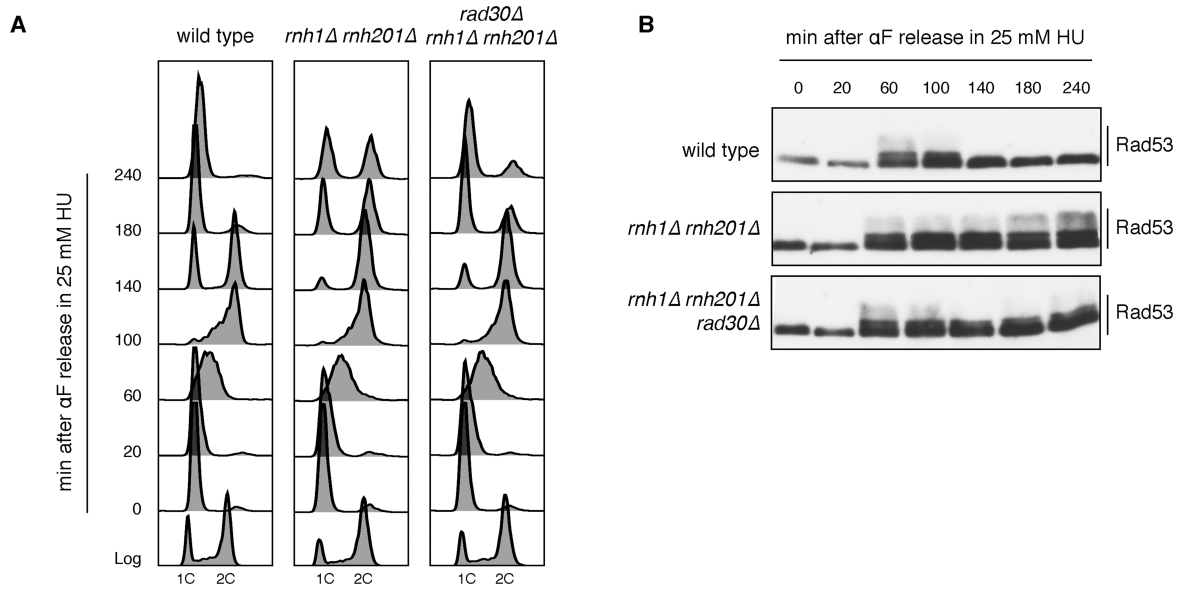

Figure 2. Pol η is responsible for the DNA damage checkpoint activation and G2/M arrest of RNase H deficient cells in low doses of HU. Exponentially growing cells were synchronized in G1 phase by α-factor addition (4 μg/ml) and released in 25 mM HU; α-factor (10 μg/ml) was re-added to the medium 90 min after the release to block cells in the next G1 phase. (**A**) Cell cycle progression was followed by flow cytometry (FACS) measuring DNA content (1C, 2C) at the indicated time points. (**B**) Rad53 phosphorylation was analyzed by western blotting of total cell extracts with anti-Rad53 antibodies. Results are representative of four biological replicates.

strand. In the second case, the inability to process ribonucleotides would be lethal only after Pol η action. To distinguish between these two hypotheses, we evaluated the effects of unprocessed rNMPs within a single cell cycle. We produced a heterologous conditional system, where RNase H2 can be inactivated at different times in a synchronous culture. A yeast strain was generated where we expressed *E. coli rnhB* gene fused to the AID-degron, so that the chimeric protein is degraded following the addition of auxin (IAA) (42,43). The fusion was cloned under the TetOFF promoter so that its expression can be switched off by addition of doxycycline (DOXY). The RNase H2 activity provided by the RnhB-AID fusion protein complemented the simultaneous loss of RNase H1 and H2 in yeast cells, suppressing almost completely the HU sensitivity and the accumulation of ribonucleotides incorporated in genomic DNA (Supplementary Figure S3). Moreover, expression of the *rnhB-AID* construct did not alter cell cycle progression of an otherwise wild type strain (Supplementary Figure S4).

rnh1Δ rnh201Δ cells carrying the conditional *rnhB-AID* construct were grown in the presence of the RnhB (ON), allowing efficient removal of pre-existing ribonucleotides, and arrested with α-factor. RnhB was then turned off (OFF) in α-factor, before the release in 25 mM HU impeding the removal of newly incorporated ribonucleotides. Cells were collected at different time points; cell cycle progression was monitored by FACS analysis (Figure 4A), and DDC activation was evaluated by western blotting (Figure 4B). In the presence of RnhB activity, despite being exposed to a low dose of HU, strains mutated in *RNH1* and *RNH201* progressed throughout the cell cycle and normally reached the next G1 phase, similarly to wild type cells (Figure 4A, panels 1, 3, 6). In these conditions, Rad53 hyperphosphorylation was almost completely absent (Figure 4B, lanes 7, 9, 11). These results further confirm that RnhB-AID efficiently complements the absence of yeast endogenous RNase H activities. When RnhB was turned off before the release in HU, *rnh1Δ rnh201Δ* cells experienced the first round of DNA replication in the presence of hydroxyurea and in the absence of RNase H activities (Figure 4A, lanes 4 and 7). In these conditions, contrary to what observed when RnhB was expressed, cells arrested at G2/M within the first cell cycle (Figure 4A, panel 4) with hyperphosphorylated Rad53 (Figure 4B, lane 10), with a phenotype similar to that of *rnh1Δ rnh201Δ* cells carrying the empty plasmid (Figure 4A, panel 2 and Figure 4B, lane 8). Moreover, deletion of *RAD30* suppressed both the cell cycle arrest and the DDC activation (Figure 4A, panel 7 and Figure 4B, lane 12).

These findings suggest that when Pol η acts at replication forks in low dNTPs, it poses a lethal threat to cells if RNase H activity is missing. This argues against the involvement in the toxic effect of Pol η of pre-existing rNMPs in the template strand.

Pol η toxicity is exerted via its catalytic activity, and it is enhanced by a steric gate mutation that increases rNTPs incorporation

To characterize the mechanism underlying Pol η toxicity, we investigated the involvement of its catalytic activity. HIS-tagged wild type (*RAD30*), catalytic-dead (*rad30-D155A-E156A*) alleles or a steric gate mutant with enhanced ribonucleotide incorporation activity (*rad30-F35A*) (38,58)

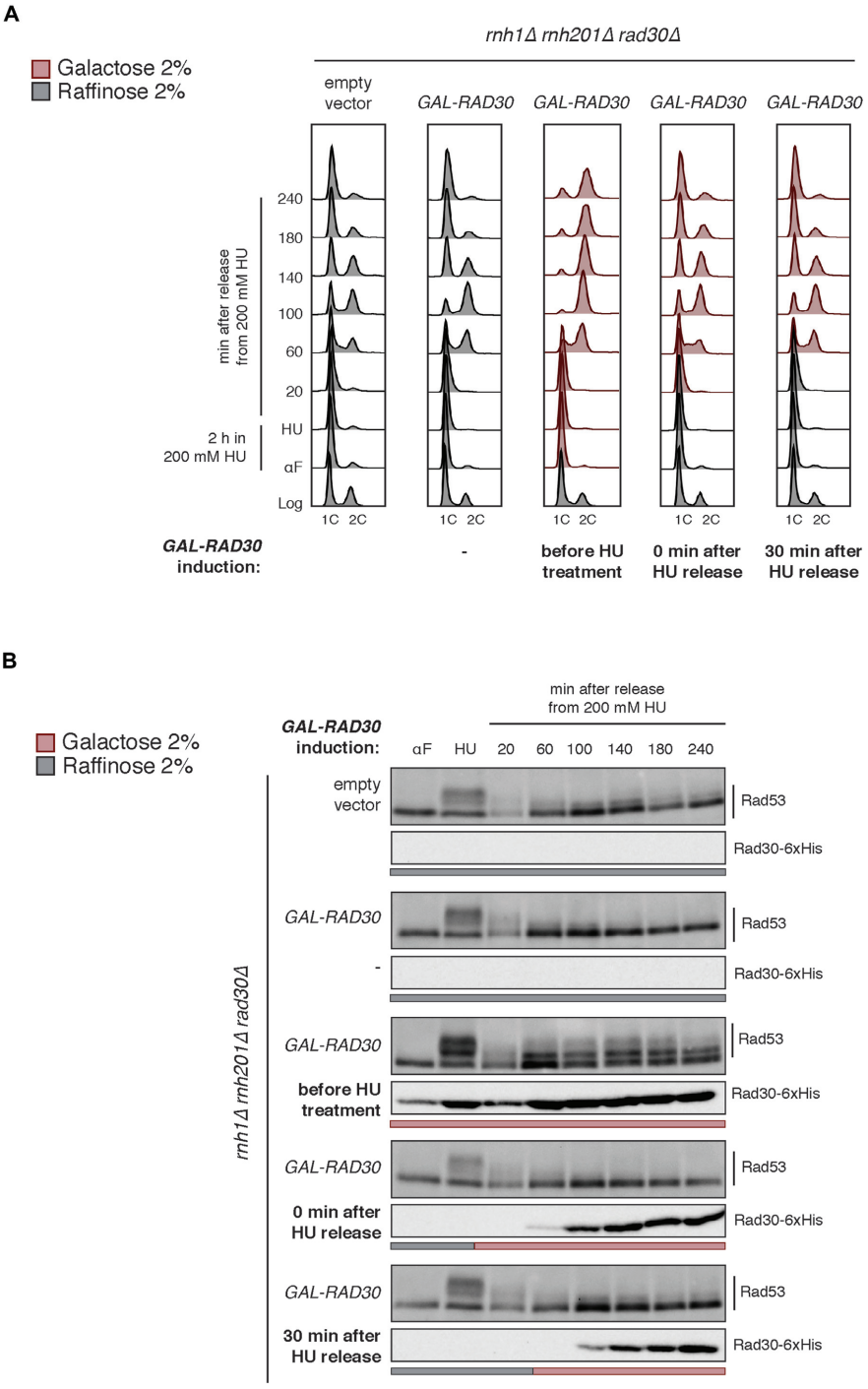

Figure 3. Pol η exerts its toxic activity at HU-stressed DNA replication forks. Cells were grown in SC-URA Raffinose 2%, arrested with α-factor (4 μg/ml) and released from the G1 block by transferring them in SC-URA Raffinose 2% with 200 mM HU for 2 h. HU was then washed out and cells were transferred to fresh medium to allow completion of the cell cycle. α-factor (10 μg/ml) was re-added 90 min after HU wash out to block cells in the next G1 phase. Media were supplemented with Galactose 2% to induce *RAD30* expression, when indicated (red). (**A**) Cell cycle progression was followed by flow cytometry (FACS) measuring DNA content (1C, 2C) at the indicated time points. (**B**) Rad53 phosphorylation and Rad30-6xHis expression were analyzed by western blotting of total cell extracts using appropriate antibodies. Results are representative of three biological replicates.

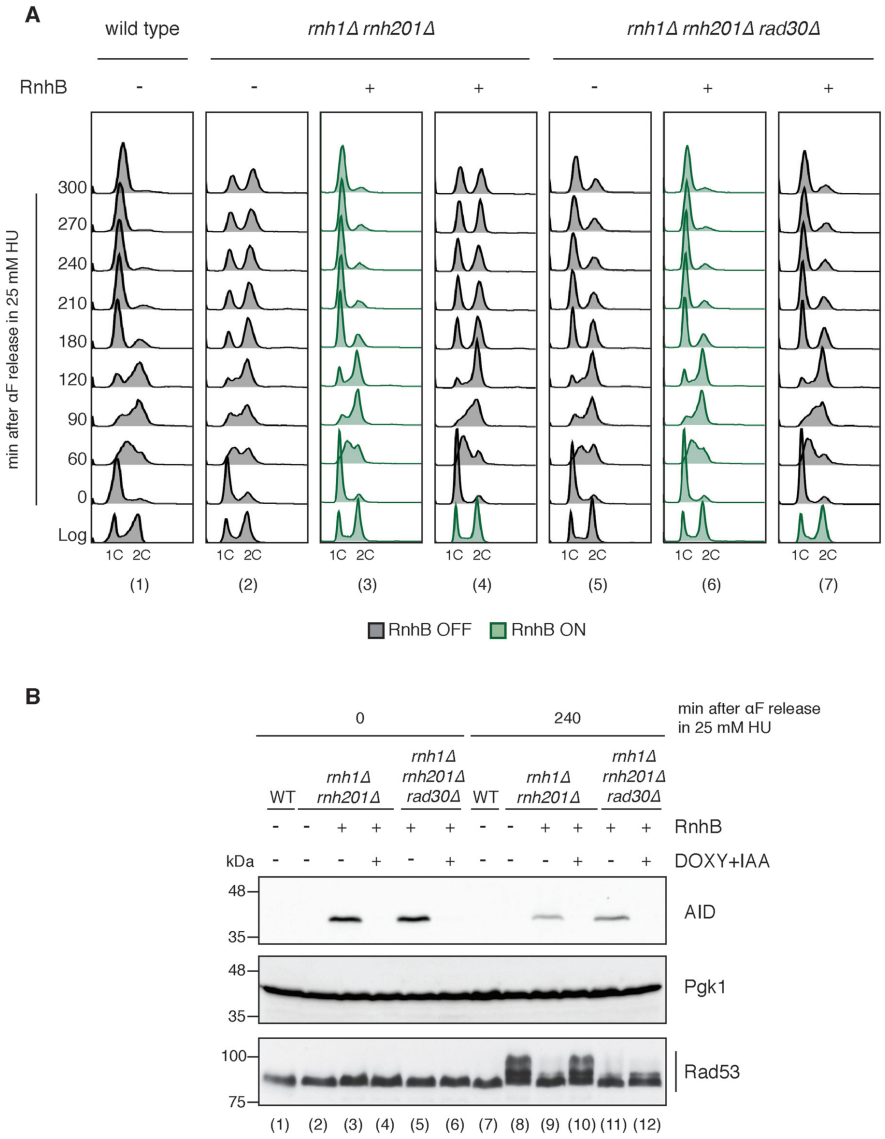

Figure 4. Pol η generates toxic intermediates at stressed replication forks in HU. Exponentially growing cells were synchronized in SC-TRP glucose 2% by α-factor addition (4 μg/ml) and released in YEPD + 25 mM HU. α-factor (10 μg/ml) was re-added 90 min after the release. RnhB was expressed (RnhB ON, in green) and was depleted as needed by addition of 10 μg/ml Doxycycline (DOXY) and 0.5 mM Auxin (IAA) (RnhB OFF, in gray). All the strains host the OsTIR1 gene integrated at the *URA3* locus. (**A**) Cell cycle progression was followed by flow cytometry (FACS) measuring DNA content (1C, 2C) at the indicated time points. (**B**) Rad53 phosphorylation, RnhB-AID and the Pgk1 loading control were analyzed by western blotting of total cell extracts using appropriate antibodies. Results are representative of three biological replicates.

were overexpressed in yeast cells under the control of the *GAL1/10* promoter. Overexpression was necessary because the steric gate mutation although increasing rNTPs incorporation, strongly reduces the catalytic activity of the enzyme. Indeed, a *rad30-F35A* mutant expressed at the endogenous level is catalytically deficient and UV sensitive, while the UV sensitivity is suppressed when overexpressed, likely because enough Pol η catalytic is present (Supplementary Figure S5A and B). Cell viability in 25 mM HU was measured and it is reported in Figure 5A. Overexpression of either wild type or mutant forms of Pol η was achieved at similar levels (Figure 5B) and did not noticeably affect the viability of RNase H wild type cells both in untreated or HU-treated conditions (Figure 5A, grey bars, and Supplementary Figure S5C). In cells lacking RNase H, on the other hand, overexpression of wild type Pol η exacerbated the sensitivity to HU, linking the extent of the toxic activity to the level of Pol η in cells (Figure 5A, black bars). Con-

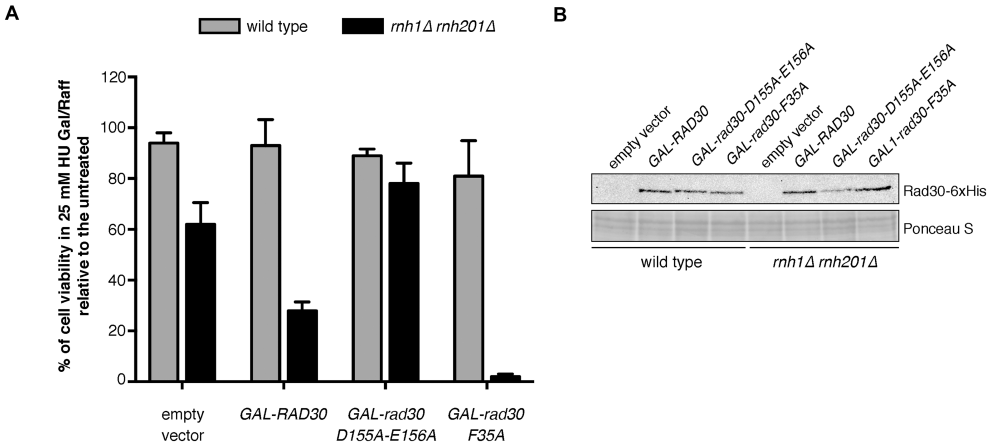

Figure 5. Pol η toxicity depends on its catalytic activity and it is exacerbated if its ribonucleotide-incorporation activity is increased. (**A**) Cells were grown in SC-URA Raffinose 2% and arrested with α-factor. Cultures were then appropriately diluted and plated on SC–URA supplemented with Galactose 2% and Raffinose 2%, either with or without 25 mM HU. Colonies were counted from at least three plates after 4 days at 28°C. Histogram bars represent the ratio between colonies counted on plates with and without hydroxyurea. Error bars represent the standard error of the mean (SEM), calculated on three independent experiments. (**B**) Overexpression levels of wild type and mutant versions of Rad30 were analyzed by western blot with anti-HIS antibodies 4 h after Galactose induction; equal loading was verified by Ponceau S staining.

versely, overexpression of the catalytic-dead mutant (*rad30-D155A-E156A*) suppressed the HU-induced cell lethality restoring viability to levels comparable to those observed in RNase H proficient cells, implying that Pol η catalytic activity is responsible for the HU sensitivity. This was confirmed by the steric gate mutant *rad30-F35A*, which confers enhanced ribonucleotide incorporation activity (37,38) and caused a drastic increase in HU sensitivity to *rnh1Δ rnh201Δ* cells, suggesting that the incorporation of ribonucleotides mediated by Pol η is the cause of cell lethality (Figure 5A, black bars).

To examine whether unprocessed genomic ribonucleotides were responsible for the HU-induced lethality, we analyzed the HU sensitivity imparted by individual *RNH1* (RNase H1) and *RNH201* (RNase H2) deletions, by an RNase H2 catalytic-dead mutant (*rnh201-D39A*) and by a separation of functions mutant *rnh201-RED* (*rnh201-P45D-Y219A*), which has been reported to be able to process multiple consecutive ribonucleotides, while being impaired in the removal of single rNMPs (40) (Figure 6A). The same mutations were then combined with the deletion of *RAD30* to gain an insight into the type of toxic product generated by Pol η (Figure 6B).

The results reveal that HU becomes lethal only when cells cannot process consecutive ribonucleotides (*rnh1Δ rnh201Δ* or *rnh1Δ rnh201-D39A*) but not if consecutive ribonucleotides can be processed by RNase H1 (*rnh201Δ*) or if the ability of RNase H2 to act on multiple rNMPs is preserved (*rnh1Δ rnh201-RED*). Intriguingly, the data shown in Figure 6B also shows that Pol η is toxic only if multiple ribonucleotides cannot be processed, suggesting that when the dNTP pools are decreased Pol η activity may promote the incorporation of stretches of ribonucleotides in the genome.

DISCUSSION

Ribonucleotides are massively incorporated during DNA replication by DNA polymerases, and, if not repaired, they cause genome instability. Depletion of the dNTP pools by hydroxyurea inhibits replicative DNA synthesis. Interestingly, exposure of *rnh1Δ rnh201Δ* cells to even low levels of HU leads to DNA damage checkpoint activation and G2/M arrest. TLS DNA polymerase η is well known for its roles in lesion bypass for the effective completion of DNA synthesis, following exposure to DNA damaging agents (23,24).

We describe a novel involvement of Pol η during genome duplication under replication stress conditions. In particular, we propose that, when canonical DNA polymerases are challenged by deoxyribonucleotide depletion, Pol η facilitates replication fork progression and chromosomal replication favoring the inclusion of consecutive ribonucleotides in newly synthesized genomic DNA. Pol η is suitable for this function thanks to its ability to extend DNA or RNA primers with ribonucleotides (37,38), unlike replicative DNA polymerases, which exhibit lower incorporation capability and are blocked by dNTPs shortage (2,3). Even though this function may be relevant to complete DNA replication and tolerate temporary decreases in the dNTP pools, it presents a potentially lethal challenge when RNase H activities are absent, and chromosome embedded ribonucleotides are excessively accumulated (Figure 7). The genomic sites bound by Pol η in HU-treated cells have been previously mapped and some of them correspond to ARSs (34) that are actively replicated in cells exposed to 200 mM HU (34,53). Moreover, human Pol η is required for S phase progression in hydroxyurea, and its activity induces apoptotic cell death (36,54).

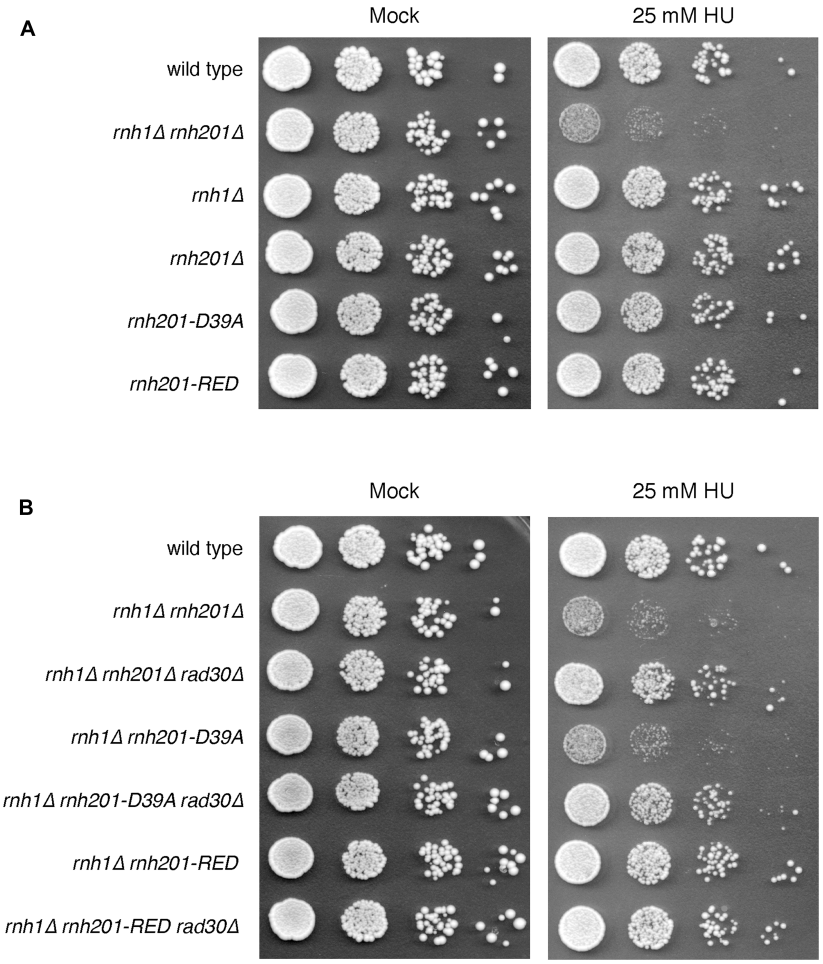

Figure 6. HU sensitivity is due to the failure to process multiple consecutive ribonucleotides. 10-fold serial dilutions of the indicated strains were plated on YEPD and YEPD + 25 mM HU and incubated at 28°C. Pictures were taken after 2 days of incubation. Results are representative of two biological replicates. The D39A mutation inactivates the catalytic function of RNase H2 while the separation of function mutant *rnh201-RED* allows the removal of stretches of rNMPs but is impaired in the removal of single rNMPs.

In this work we show that:

a) When cellular dNTP pools are depleted by exposure to low doses of HU, Pol η catalytic activity promotes the formation of some structures that become toxic only if RNase H activities are lost, while no effect is detected in cells expressing RNase H functions. This strongly suggests a role for ribonucleotides in the Pol η-dependent HU-induced lethality.
b) Such toxic products are generated when Pol η is active at replication forks stressed by dNTPs depletion, while no problem arises if Pol η acts later in S phase, once dNTP pools have been replenished.
c) The formation of the toxic products by Pol η does not depend upon residual rNMPs in the template strand, but it involves ribonucleotides incorporated during the S phase with low dNTP pools, and it elicits a DNA damage checkpoint and G2/M arrest within the same cell cycle.
d) The sensitivity to HU, and thus the formation of the toxic products, is greatly enhanced if cells express a Pol η variant with enhanced rNTPs incorporation ability. Moreover, the HU-induced lethality depends upon the inability in the processing of multiple consecutive ribonucleotides.

Physical detection of multiple rNMPs embedded in genomic DNA has proven to be very hard to tackle with the available technology; no groups to our knowledge were able to address this problem yet. Even if we cannot directly measure the presence of Pol η-dependent multiple ribonucleotides, the data summarized above very strongly support the hypothesis that the phenotypes reported in this work are related to RNA stretches embedded in genomic DNA, which are accumulated only when Pol η is active and the

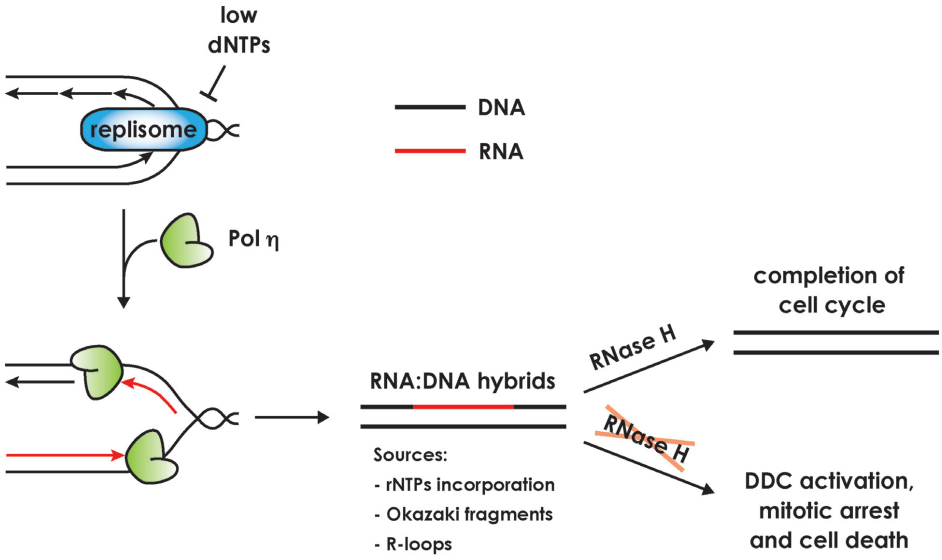

Figure 7. Proposed model of Pol η function during hydroxyurea-mediated fork stalling. Replication forks are stalled by dNTP pools depletion caused by HU, allowing Pol η recruitment. Pol η activity promotes RNA:DNA hybrids formation by either direct incorporation of ribonucleotides in the newly synthesized strand or incorrect Okazaki fragments maturation or R-loops stabilization. These hybrids are later processed by RNase H activities, allowing completion of the cell cycle. In the absence of RNase H, RNA:DNA hybrids are not removed from the genome and lead to DNA damage checkpoint activation, cell cycle arrest and ultimately cell death.

dNTP pools are depleted. Such RNA stretches may arise from the direct incorporation of rNTPs by Pol η, from a Pol η-dependent stabilization of R-loops or impairment of Okazaki fragments processing, consistently with recent evidence showing that Pol η could take part in the replication of the lagging strand (59). Remarkably, following replication with low dNTP pools and active Pol η, if ribonucleotides cannot be processed cells die because they cannot divide (Figure 7). Careful kinetic analyses reveal that, in these conditions, the DDC is switched off after S phase and re-activated when cells reach 2C DNA content in G2/M. Taken together, these observations may correlate RNA:DNA hybrids with chromosome segregation. We propose that RNA:DNA hybrids may compromise chromosomes structure (17–19,60) generating problems that are detected in G2/M and trigger the DDC. Such hybrids may also lead to mutagenic repair mechanisms, such as the one dependent on Top1, leading to deletions and chromosome breaks (15,16). We can also envision that the alteration of chromosome structure due to newly incorporated ribonucleotides may affect particular regions, e.g. centromeres, essential for proper cell division. This hypothesis is supported by the observation that deletion of the Spindle Assembly Checkpoint factor *MAD2* partially rescues the HU sensitivity, cell cycle arrest of cells lacking RNase H and persistent DNA damage checkpoint activation (Supplementary Figure S6).

As mentioned above, such scenario may be conserved in higher eukaryotes as well. This mechanism resembles the one reported in human cells for Chromosome Fragile Sites (CFSs) replication. CFSs are peculiar sequences that assume non-B DNA structures that block replication forks (61,62). Here, Pol η substitutes Pol δ and carries on DNA synthesis, avoiding the formation of breaks and preventing under-replicated DNA from entering mitosis (30–33). As in hydroxyurea, Pol η may act when replication forks are stalled.

In conclusion, this study unravels a novel role of TLS polymerase η and provides evidence of its contribution to the preservation of genome integrity. In the future, it will be interesting to investigate how Pol η can participate to repair synthesis in environments where dNTP pools are physiologically low, such as in neuronal cells.

SUPPLEMENTARY DATA

Supplementary Data are available at NAR Online.

ACKNOWLEDGEMENTS

We thank Prof. P. Plevani and all members of the genome instability and human pathologies lab for critical discussions; C. Santocanale for the Rad53 antibodies, T.A. Kunkel for providing us plasmids, S. Cerritelli and R. Crouch for kindly gifting us RNase H2 mutant strains and L. Ström for kindly gifting us Pol η mutant strains.

Authors Contributions: M.M.-F., F.L. conceived the study, secured funding and revised the manuscript. A.M., G-M.N., E.B., D.D. and F.L. designed and performed experiments. L.G., E.G., M-C.B. contributed to the revision of the manuscript. A.M. wrote the manuscript with input from all authors.

FUNDING

Associazione Italiana per la Ricerca sul Cancro [15631 and 21806 to M.M.F., 15724 to F.L.]; MIUR to M.M.F.; Telethon [GGP15227 to M.M.F.]; Fondazione Cariplo [15724 to F.L., 2013-0798 to F.L.]. Funding for open access charge: Fondazione Telethon [GGP15227].
Conflict of interest statement. None declared.

REFERENCES

1. Joyce,C.M. (1997) Choosing the right sugar: how polymerases select a nucleotide substrate. *Proc. Natl. Acad. Sci. U.S.A.*, **94**, 1619–1622.
2. Nick McElhinny,S.A., Watts,B.E., Kumar,D., Watt,D.L., Lundstrom,E.-B., Burgers,P.M.J., Johansson,E., Chabes,A. and Kunkel,T.A. (2010) Abundant ribonucleotide incorporation into DNA by yeast replicative polymerases. *Proc. Natl. Acad. Sci. U.S.A.*, **107**, 4949–4954.
3. Sparks,J.L., Chon,H., Cerritelli,S.M., Kunkel,T.A., Johansson,E., Crouch,R.J. and Burgers,P.M. (2012) RNase H2-initiated ribonucleotide excision repair. *Mol. Cell*, **47**, 980–986.
4. Shen,Y., Koh,K.D., Weiss,B. and Storici,F. (2012) Mispaired rNMPs in DNA are mutagenic and are targets of mismatch repair and RNases H. *Nat. Struct. Mol. Biol.*, **19**, 98–104.
5. Ghodgaonkar,M.M., Lazzaro,F., Olivera-Pimentel,M., Artola-Borán,M., Cejka,P., Reijns,M.A., Jackson,A.P., Plevani,P., Muzi-Falconi,M. and Jiricny,J. (2013) Ribonucleotides misincorporated into DNA Act as strand-discrimination signals in eukaryotic mismatch repair. *Mol. Cell*, **50**, 323–332.
6. Lujan,S.A., Williams,J.S., Clausen,A.R., Clark,A.B. and Kunkel,T.A. (2013) Ribonucleotides are signals for mismatch repair of leading-strand replication errors. *Mol. Cell*, **50**, 437–443.
7. Lazzaro,F., Novarina,D., Amara,F., Watt,D.L., Stone,J.E., Costanzo,V., Burgers,P.M., Kunkel,T.A., Plevani,P. and Muzi-Falconi,M. (2012) RNase H and postreplication repair protect cells from ribonucleotides incorporated in DNA. *Mol. Cell*, **45**, 99–110.
8. Reijns,M.A.M., Rabe,B., Rigby,R.E., Mill,P., Astell,K.R., Lettice,L.A., Boyle,S., Leitch,A., Keighren,M., Kilanowski,F. *et al.* (2012) Enzymatic removal of ribonucleotides from DNA is essential for mammalian genome integrity and development. *Cell*, **149**, 1008–1022.
9. Pizzi,S., Sertic,S., Orcesi,S., Cereda,C., Bianchi,M., Jackson,A.P., Lazzaro,F., Plevani,P. and Muzi-Falconi,M. (2015) Reduction of hRNase H2 activity in Aicardi-Goutières syndrome cells leads to replication stress and genome instability. *Hum. Mol. Genet.*, **24**, 649–658.
10. Conover,H.N., Lujan,S.A., Chapman,M.J., Cornelio,D.A., Sharif,R., Williams,J.S., Clark,A.B., Camilo,F., Kunkel,T.A. and Argueso,J.L. (2015) Stimulation of chromosomal rearrangements by Ribonucleotides. *Genetics*, **201**, 951–961.
11. Zimmer,A.D. and Koshland,D. (2016) Differential roles of the RNases H in preventing chromosome instability. *Proc. Natl. Acad. Sci. U.S.A.*, **113**, 12220–12225.
12. Cerritelli,S.M. and Crouch,R.J. (2009) Ribonuclease H: the enzymes in eukaryotes. *FEBS J.*, **276**, 1494–1505.
13. Crow,Y.J., Leitch,A., Hayward,B.E., Garner,A., Parmar,R., Griffith,E., Ali,M., Semple,C., Aicardi,J., Babul-Hirji,R. *et al.* (2006) Mutations in genes encoding ribonuclease H2 subunits cause Aicardi-Goutières syndrome and mimic congenital viral brain infection. *Nat. Genet.*, **38**, 910–916.
14. Kim,N., Huang,S.N., Williams,J.S., Li,Y.C., Clark,A.B., Cho,J.-E., Kunkel,T.A., Pommier,Y. and Jinks-Robertson,S. (2011) Mutagenic processing of ribonucleotides in DNA by yeast topoisomerase I. *Science*, **332**, 1561–1564.
15. Yadav,P., Owiti,N. and Kim,N. (2016) The role of topoisomerase I in suppressing genome instability associated with a highly transcribed guanine-rich sequence is not restricted to preventing RNA:DNA hybrid accumulation. *Nucleic Acids Res.*, **44**, 718–729.
16. Huang,S.-Y.N., Williams,J.S., Arana,M.E., Kunkel,T.A. and Pommier,Y. (2016) Topoisomerase I-mediated cleavage at unrepaired ribonucleotides generates DNA double-strand breaks. *EMBO J.*, **36**, e201592426-373.
17. Egli,M., Usman,N. and Rich,A. (1993) Conformational influence of the ribose 2′-hydroxyl group: crystal structures of DNA-RNA chimeric duplexes. *Biochemistry*, **32**, 3221–3237.
18. Jaishree,T.N., van der Marel,G.A., van Boom,J.H. and Wang,A.H. (1993) Structural influence of RNA incorporation in DNA: quantitative nuclear magnetic resonance refinement of d(CG)r(CG)d(CG) and d(CG)r(C)d(TAGCG). *Biochemistry*, **32**, 4903–4911.
19. Meroni,A., Mentegari,E., Crespan,E., Muzi-Falconi,M., Lazzaro,F. and Podestà,A. (2017) The incorporation of Ribonucleotides induces structural and conformational changes in DNA. *Biophys. J.*, **113**, 1373–1382.
20. Williams,J.S., Clausen,A.R., Nick McElhinny,S.A., Watts,B.E., Johansson,E. and Kunkel,T.A. (2012) Proofreading of ribonucleotides inserted into DNA by yeast DNA polymerase ε. *DNA Repair (Amst.)*, **11**, 649–656.
21. Clausen,A.R., Zhang,S., Burgers,P.M., Lee,M.Y. and Kunkel,T.A. (2013) Ribonucleotide incorporation, proofreading and bypass by human DNA polymerase δ. *DNA Repair (Amst.)*, **12**, 121–127.
22. Clausen,A.R., Murray,M.S., Passer,A.R., Pedersen,L.C. and Kunkel,T.A. (2013) Structure-function analysis of ribonucleotide bypass by B family DNA replicases. *Proc. Natl. Acad. Sci. U.S.A.*, **110**, 16802–16807.
23. Johnson,R.E., Prakash,S. and Prakash,L. (1999) Efficient bypass of a thymine-thymine dimer by yeast DNA polymerase, Poleta. *Science*, **283**, 1001–1004.
24. Haracska,L., Prakash,S. and Prakash,L. (2000) Replication past O(6)-methylguanine by yeast and human DNA polymerase eta. *Mol. Cell. Biol.*, **20**, 8001–8007.
25. McCulloch,S.D., Kokoska,R.J., Masutani,C., Iwai,S., Hanaoka,F. and Kunkel,T.A. (2004) Preferential cis-syn thymine dimer bypass by DNA polymerase eta occurs with biased fidelity. *Nature*, **428**, 97–100.
26. Masutani,C., Kusumoto,R., Yamada,A., Dohmae,N., Yokoi,M., Yuasa,M., Araki,M., Iwai,S., Takio,K. and Hanaoka,F. (1999) The XPV (xeroderma pigmentosum variant) gene encodes human DNA polymerase eta. *Nature*, **399**, 700–704.
27. Gratchev,A., Strein,P., Utikal,J. and Sergij,G. (2003) Molecular genetics of Xeroderma pigmentosum variant. *Exp. Dermatol.*, **12**, 529–536.
28. Zeng,X., Winter,D.B., Kasmer,C., Kraemer,K.H., Lehmann,A.R. and Gearhart,P.J. (2001) DNA polymerase eta is an A-T mutator in somatic hypermutation of immunoglobulin variable genes. *Nat. Immunol.*, **2**, 537–541.
29. Faili,A., Aoufouchi,S., Weller,S., Vuillier,F., Stary,A., Sarasin,A., Reynaud,C.-A. and Weill,J.-C. (2004) DNA polymerase eta is involved in hypermutation occurring during immunoglobulin class switch recombination. *J. Exp. Med.*, **199**, 265–270.
30. Rey,L., Sidorova,J.M., Puget,N., Boudsocq,F., Biard,D.S.F., Monnat,R.J., Cazaux,C. and Hoffmann,J.-S. (2009) Human DNA polymerase eta is required for common fragile site stability during unperturbed DNA replication. *Mol. Cell. Biol.*, **29**, 3344–3354.
31. Bergoglio,V., Boyer,A.S., Walsh,E., Naim,V., Legube,G., Lee,M.Y.W.T., Rey,L., Rosselli,F., Cazaux,C., Eckert,K.A. *et al.* (2013) DNA synthesis by Pol η promotes fragile site stability by preventing under-replicated DNA in mitosis. *J. Cell Biol.*, **201**, 395–408.
32. Despras,E., Sittewelle,M., Pouvelle,C., Delrieu,N., Cordonnier,A.M. and Kannouche,P.L. (2016) Rad18-dependent SUMOylation of human specialized DNA polymerase eta is required to prevent under-replicated DNA. *Nat. Commun.*, **7**, 13326.
33. Barnes,R.P., Hile,S.E., Lee,M.Y. and Eckert,K.A. (2017) DNA polymerases Eta and Kappa exchange with the polymerase delta holoenzyme to complete common fragile site synthesis. *DNA Repair (Amst.)*, **57**, 1–11.
34. Enervald,E., Lindgren,E., Katou,Y., Shirahige,K. and Ström,L. (2013) Importance of Polη for Damage-Induced cohesion reveals differential regulation of cohesion establishment at the break site and Genome-Wide. *PLoS Genet.*, **9**, e1003158.
35. Steele,E.J. (2004) DNA polymerase-eta as a reverse transcriptase: implications for mechanisms of hypermutation in innate anti-retroviral defences and antibody SHM systems. *DNA Repair (Amst.)*, **3**, 687–692.
36. Mentegari,E., Crespan,E., Bavagnoli,L., Kissova,M., Bertoletti,F., Sabbioneda,S., Imhof,R., Sturla,S.J., Nilforoushan,A., Hübscher,U.

et al. (2017) Ribonucleotide incorporation by human DNA polymerase η impacts translesion synthesis and RNase H2 activity. *Nucleic Acids Res.*, **45**, 2600–2614.
37. Gali,V.K., Balint,E., Serbyn,N., Frittmann,O., Stutz,F. and Unk,I. (2017) Translesion synthesis DNA polymerase η exhibits a specific RNA extension activity and a transcription-associated function. *Sci. Rep.*, **7**, 1–17.
38. Donigan,K.A., Cerritelli,S.M., McDonald,J.P., Vaisman,A., Crouch,R.J. and Woodgate,R. (2015) Unlocking the steric gate of DNA polymerase η leads to increased genomic instability in *Saccharomyces cerevisiae*. *DNA Repair (Amst.)*, **35**, 1–12.
39. Longtine,M.S., McKenzie,A., Demarini,D.J., Shah,N.G., Wach,A., Brachat,A., Philippsen,P. and Pringle,J.R. (1998) Additional modules for versatile and economical PCR-based gene deletion and modification in *Saccharomyces cerevisiae*. *Yeast*, **14**, 953–961.
40. Chon,H., Sparks,J.L., Rychlik,M., Nowotny,M., Burgers,P.M., Crouch,R.J. and Cerritelli,S.M. (2013) RNase H2 roles in genome integrity revealed by unlinking its activities. *Nucleic Acids Res.*, **41**, 3130–3143.
41. Pavlov,Y.I., Nguyen,D. and Kunkel,T.A. (2001) Mutator effects of overproducing DNA polymerase eta (Rad30) and its catalytically inactive variant in yeast. *Mutat. Res.*, **478**, 129–139.
42. Garí,E., Piedrafita,L., Aldea,M. and Herrero,E. (1997) A set of vectors with a tetracycline-regulatable promoter system for modulated gene expression in *Saccharomyces cerevisiae*. *Yeast*, **13**, 837–848.
43. Nishimura,K., Fukagawa,T., Takisawa,H., Kakimoto,T. and Kanemaki,M. (2009) An auxin-based degron system for the rapid depletion of proteins in nonplant cells. *Nat. Meth.*, **6**, 917–922.
44. Giannattasio,M., Lazzaro,F., Siede,W., Nunes,E., Plevani,P. and Muzi-Falconi,M. (2004) DNA decay and limited Rad53 activation after liquid holding of UV-treated nucleotide excision repair deficient *S. cerevisiae* cells. *DNA Repair (Amst).*, **3**, 1591–1599.
45. Meroni,A., Nava,G.M., Sertic,S., Plevani,P., Muzi-Falconi,M. and Lazzaro,F. (2018) Measuring the levels of ribonucleotides embedded in genomic DNA. *Methods Mol. Biol.*, **1672**, 319–327.
46. Arudchandran,A., Cerritelli,S., Narimatsu,S., Itaya,M., Shin,D.Y., Shimada,Y. and Crouch,R.J. (2000) The absence of ribonuclease H1 or H2 alters the sensitivity of *Saccharomyces cerevisiae* to hydroxyurea, caffeine and ethyl methanesulphonate: implications for roles of RNases H in DNA replication and repair. *Genes Cells*, **5**, 789–802.
47. Stuckey,R., García-Rodríguez,N., Aguilera,A. and Wellinger,R.E. (2015) Role for RNA:DNA hybrids in origin-independent replication priming in a eukaryotic system. *Proc. Natl. Acad. Sci. U.S.A.*, **112**, 5779–5784.
48. Pellicioli,A., Lucca,C., Liberi,G., Marini,F., Lopes,M., Plevani,P., Romano,A., Di Fiore,P.P. and Foiani,M. (1999) Activation of Rad53 kinase in response to DNA damage and its effect in modulating phosphorylation of the lagging strand DNA polymerase. *EMBO J.*, **18**, 6561–6572.
49. Puddu,F., Piergiovanni,G., Plevani,P. and Muzi-Falconi,M. (2011) Sensing of replication stress and Mec1 activation act through two independent pathways involving the 9-1-1 complex and DNA polymerase ε. *PLoS Genet.*, **7**, e1002022.
50. Feng,W., Collingwood,D., Boeck,M.E., Fox,L.A., Alvino,G.M., Fangman,W.L., Raghuraman,M.K. and Brewer,B.J. (2006) Genomic mapping of single-stranded DNA in hydroxyurea-challenged yeasts identifies origins of replication. *Nat. Cell Biol.*, **8**, 148–155.
51. Karras,G.I. and Jentsch,S. (2010) The *RAD6* DNA damage tolerance pathway operates uncoupled from the replication fork and is functional beyond S phase. *Cell*, **141**, 255–267.
52. Daigaku,Y., Davies,A.A. and Ulrich,H.D. (2010) Ubiquitin-dependent DNA damage bypass is separable from genome replication. *Nature*, **465**, 951–955.
53. Poli,J., Tsaponina,O., Crabbé,L., Keszthelyi,A., Pantesco,V., Chabes,A., Lengronne,A. and Pasero,P. (2012) dNTP pools determine fork progression and origin usage under replication stress. *EMBO J.*, **31**, 883–894.
54. de Feraudy,S., Limoli,C.L., Giedzinski,E., Karentz,D., Marti,T.M., Feeney,L. and Cleaver,J.E. (2007) Pol eta is required for DNA replication during nucleotide deprivation by hydroxyurea. *Oncogene*, **26**, 5713–5721.
55. Koç,A., Wheeler,L.J., Mathews,C.K. and Merrill,G.F. (2004) Hydroxyurea arrests DNA replication by a mechanism that preserves basal dNTP pools. *J. Biol. Chem.*, **279**, 223–230.
56. Alvino,G.M., Collingwood,D., Murphy,J.M., Delrow,J., Brewer,B.J. and Raghuraman,M.K. (2007) Replication in hydroxyurea: it's a matter of time. *Mol. Cell Biol.*, **27**, 6396–6406.
57. Singh,A. and Xu,Y.-J. (2016) The cell killing mechanisms of hydroxyurea. *Genes*, **7**, 99.
58. Kondratick,C.M., Washington,M.T., Prakash,S. and Prakash,L. (2001) Acidic residues critical for the activity and biological function of yeast DNA polymerase eta. *Mol. Cell. Biol.*, **21**, 2018–2025.
59. Kreisel,K., Engqvist,M.K.M., Kalm,J., Thompson,L.J., Boström,M., Navarrete,C., McDonald,J.P., Larsson,E., Woodgate,R. and Clausen,A.R. (2018) DNA polymerase η contributes to genome-wide lagging strand synthesis. *Nucleic Acids Res.*, **86**, 417.
60. DeRose,E.F., Perera,L., Murray,M.S., Kunkel,T.A. and London,R.E. (2012) Solution Structure of the Dickerson DNA Dodecamer Containing a Single Ribonucleotide. *Biochemistry*, **51**, 2407–2416.
61. Schwartz,M., Zlotorynski,E. and Kerem,B. (2006) The molecular basis of common and rare fragile sites. *Cancer Lett.*, **232**, 13–26.
62. Ozeri-Galai,E., Lebofsky,R., Rahat,A., Bester,A.C., Bensimon,A. and Kerem,B. (2011) Failure of origin activation in response to fork stalling leads to chromosomal instability at fragile sites. *Mol. Cell*, **43**, 122–131.
63. Giannattasio,M., Follonier,C., Tourrière,H., Puddu,F., Lazzaro,F., Pasero,P., Lopes,M., Plevani,P. and Muzi-Falconi,M. (2010) Exo1 competes with repair synthesis, converts NER intermediates to long ssDNA gaps, and promotes checkpoint activation. *Mol. Cell*, **40**, 50–62.

Figure S1

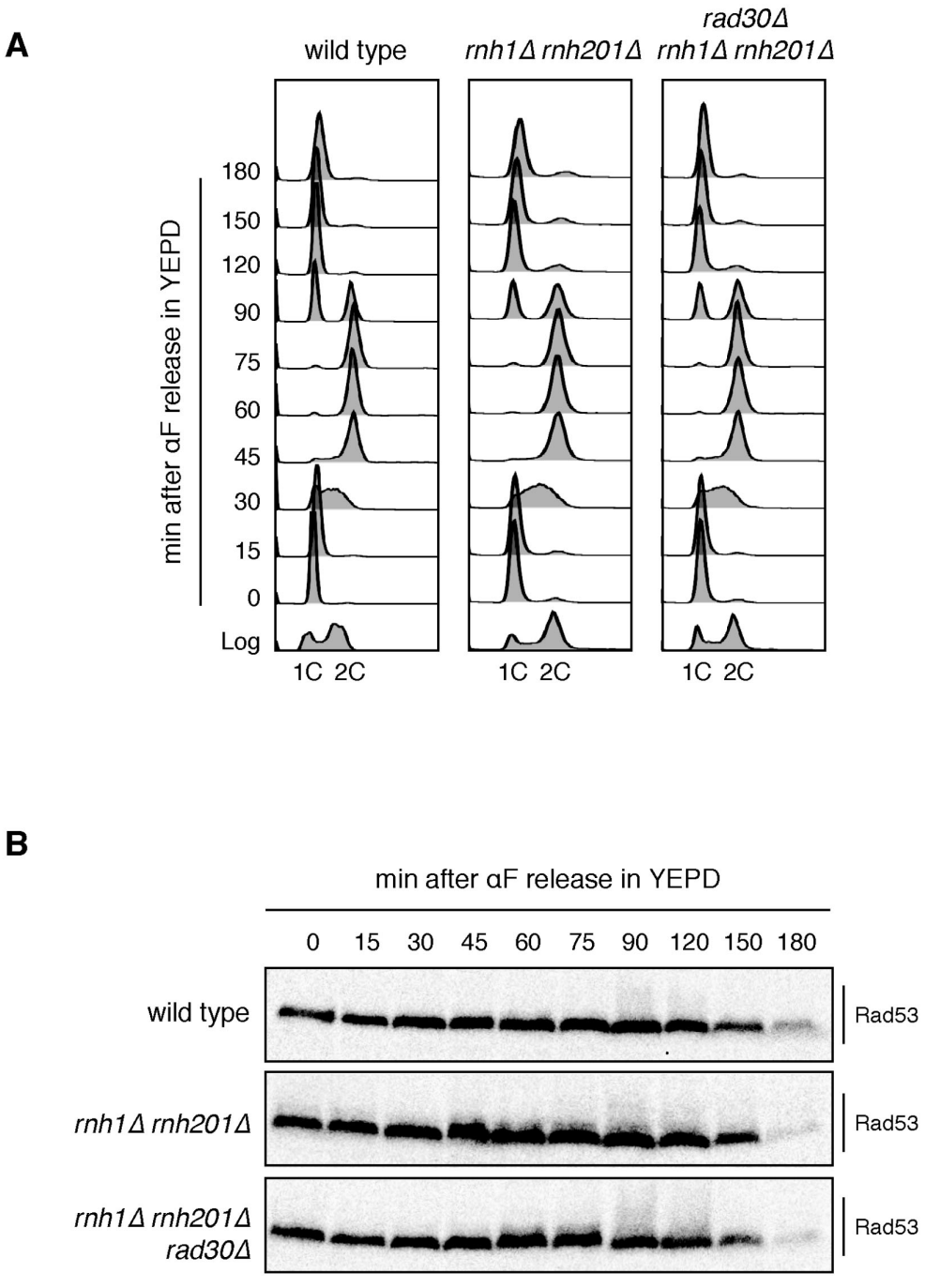

Figure S1. Strains lacking RNase H activity do not exhibit cell cycle delay and DDC activation in untreated conditions.
(A-B) Exponentially growing cells were synchronized in G1 phase by α-factor addition (4 µg/mL) and released in fresh YEPD medium. α-factor (10 µg/mL) was re-added to the medium 90 min after the release to block cells in the next G1 phase. **(A)** Cell cycle progression was followed by flow cytometry (FACS) measuring DNA content (1C, 2C) at the indicated time points. **(B)** Rad53 phosphorylation was analyzed by western blotting of total cell extracts using anti-Rad53 antibodies. Results are representative of two biological replicates.

Figure S2

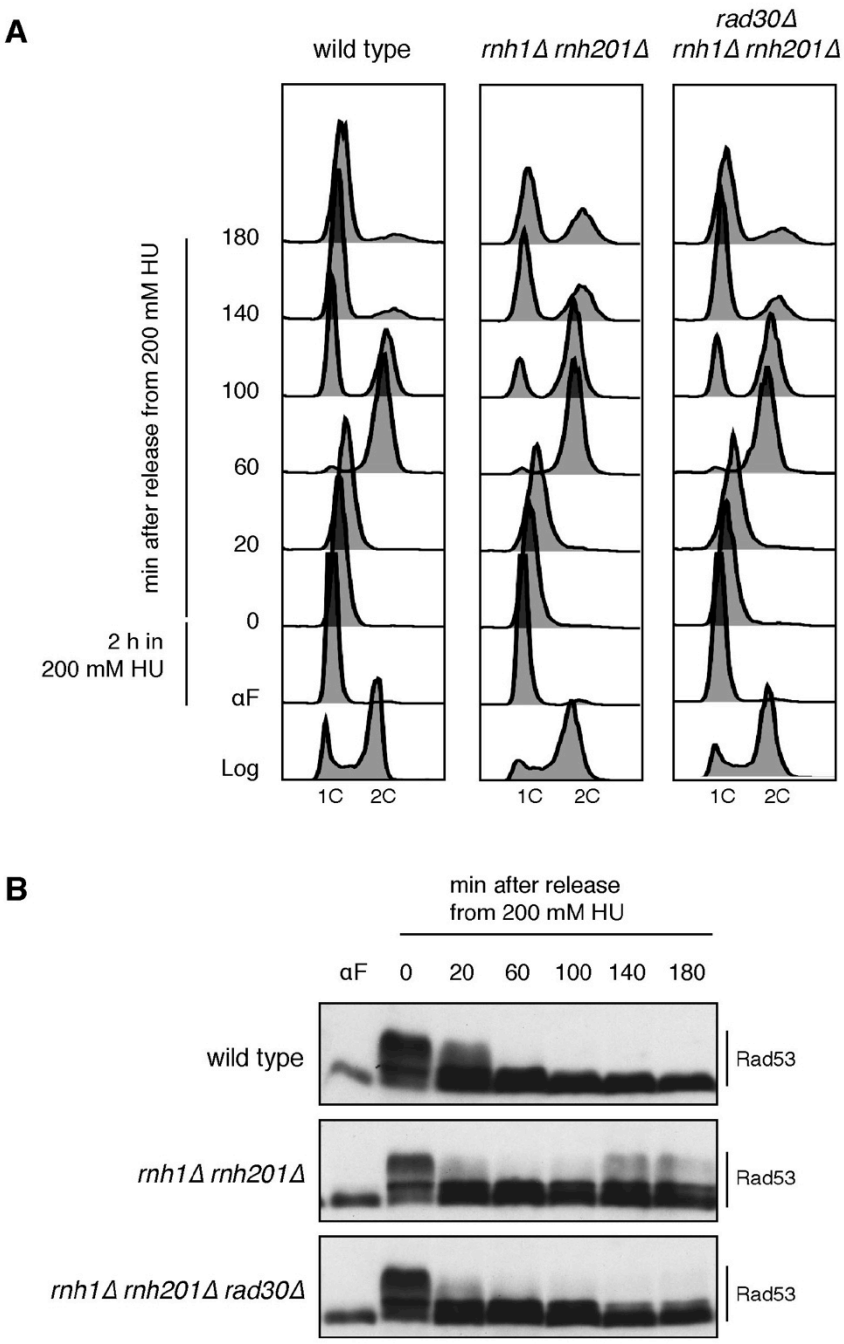

Figure S2. In RNase H deficient cells Pol η promotes DDC activation and G2/M arrest, even after acute HU exposure.
(A-B) Exponentially growing cells were synchronized in G1 phase by α-factor addition (4 µg/mL) and released from the G1 arrest in 200 mM HU for 2 hours. HU was then washed out and cells were transferred to fresh medium to allow completion of the cell cycle. α-factor (10 µg/mL) was then re-added 40 min after the HU wash out to block cells in the next G1 phase. **(A)** Cell cycle progression was followed by flow cytometry (FACS) measuring DNA content (1C, 2C) at the indicated time points.
(B) Rad53 phosphorylation was analyzed by western blotting of total cell extracts using anti-Rad53 antibodies. Results are representative of three biological replicates.

Figure S3

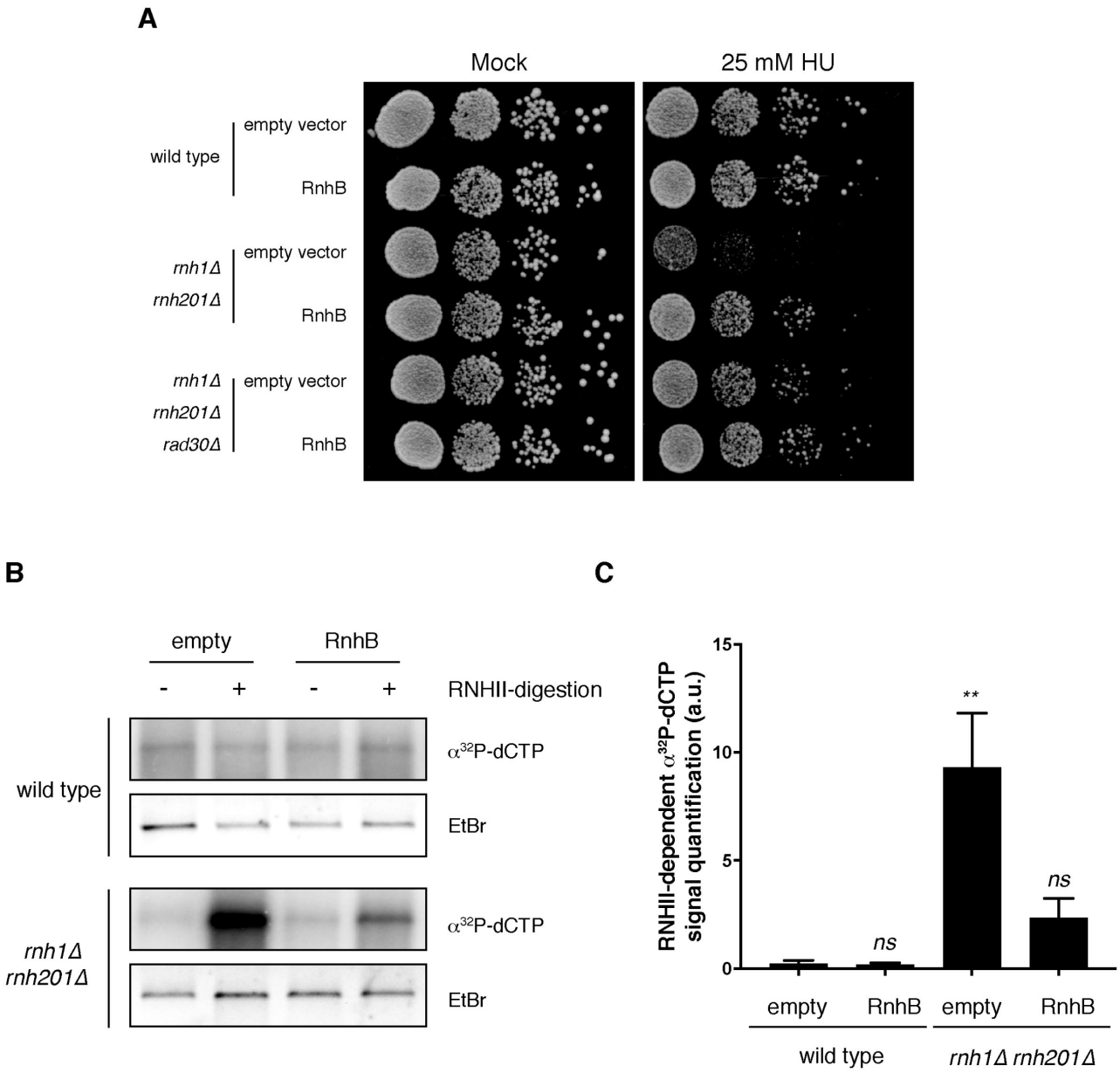

Figure S3. In yeast cells lacking endogenous RNase H enzymes, bacterial RnhB restores the ribonucleotides removal activity.
(A) 10-fold serial dilutions of the indicated strains were plated on SC-TRP and SC-TRP + 25 mM HU and incubated at 28°C. RnhB-AID is constitutively expressed. Pictures were taken after 4 days of incubation. Results are representative of three biological replicates.
(B) Ribonucleotides incorporation assay on genomic DNA extracted from G1 synchronized wild type and *rnh1Δrnh201Δ* cells transformed either with the empty plasmid or the one carrying the RnhB-AID coding gene. All the strains have the *OsTIR1* gene integrated at *URA3* locus.
(C) Ribonucleotides incorporation was quantified and is expressed in arbitrary units as fold change of the RNHII treated sample respect to the untreated. All samples were normalized on the corresponding ethidium bromide signal. The error bars represent the SEM of four independent experiments.
Student t-test is performed relative to the wild type [empty] sample (*ns* = non significative, ** = P ≤ 0.01).

Figure S4

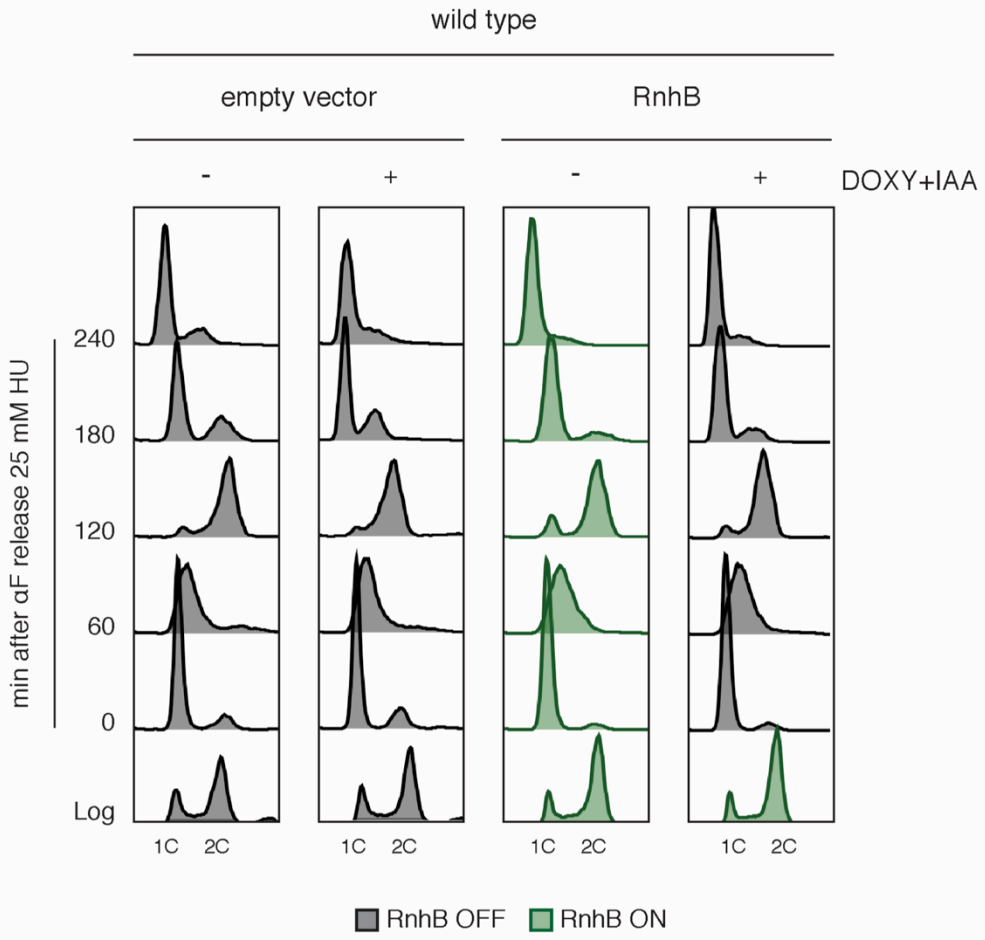

Figure S4. Expression of RnhB does not affect cell cycle progression in wild type cells. Exponentially growing cells were synchronized in SC-TRP Glucose 2% by α-factor addition (4 µg/mL) and released in YEPD + 25 mM HU. α-factor (10 µg/mL) was re-added 90 min after the release. RnhB-AID was expressed (RnhB ON, in green) and was depleted as needed by addition of 10 µg/mL Doxycycline (DOXY) and 0.5 mM Auxin (IAA) (RnhB OFF, in grey). All the strains carry the *OsTIR1* gene integrated at *URA3* locus. Cell cycle progression was followed by flow cytometry (FACS) measuring DNA content (1C, 2C) at the indicated time points. Results are representative of three biological replicates.

Figure S5

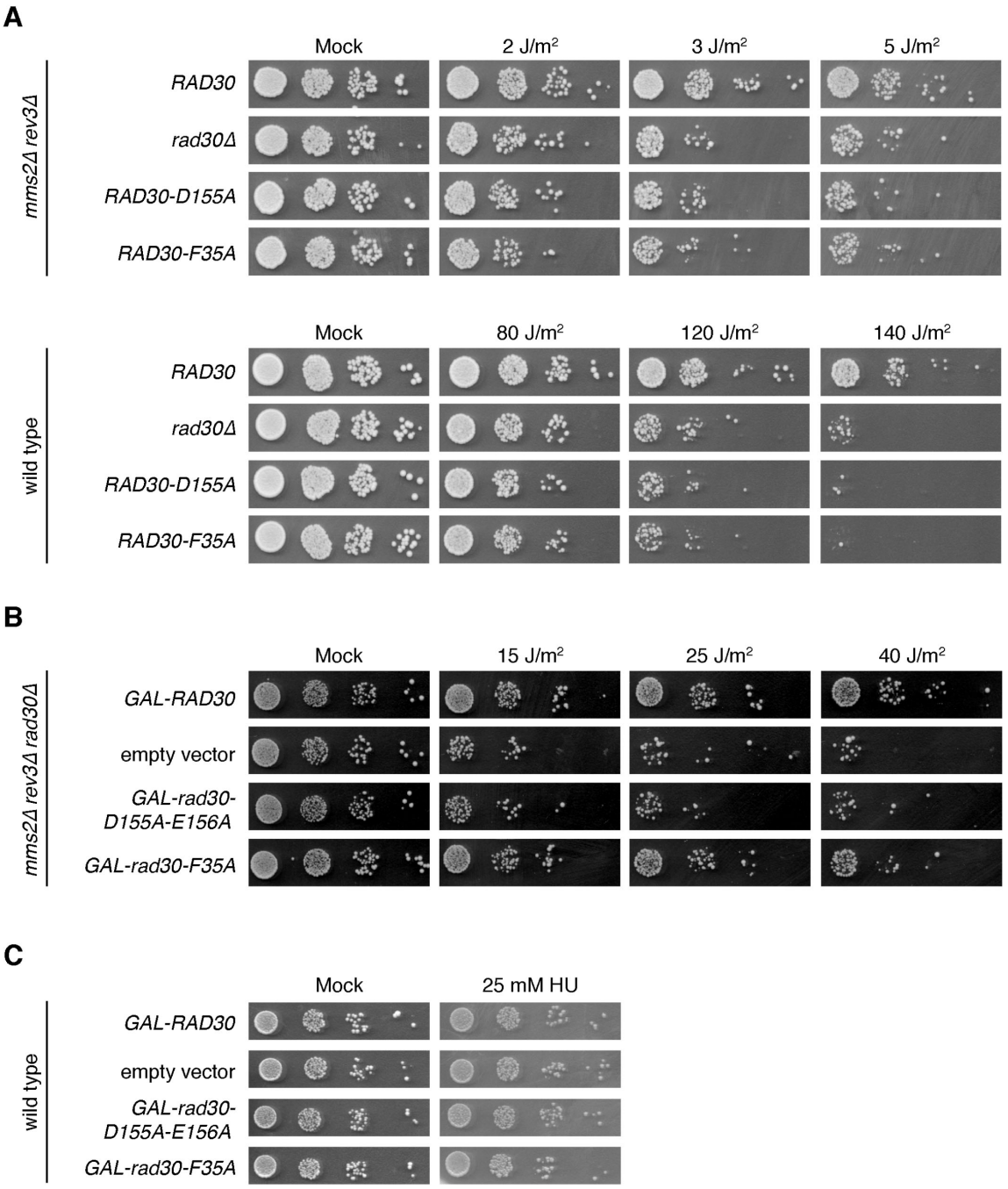

Figure S5. *rad30-F35A* mutant complements UV sensitivity only if overexpressed and wt cell viability is not affected by overexpression of Rad30, *rad30-D155A-E156A* and *rad30-F35A*.
(A)10-fold serial dilutions of the indicated strains were plated on YEPD and UV irradiated.Pictures were taken after 2 days of incubation at 28°C. Results are representative of two biological replicates.
(B)10-fold serial dilutions of the indicated strains were plated on SC-URA, supplemented with Raffinose 2% and Galactose 2% and UV iradiated. Pictures were taken after 3 days of incubation at 28°C. Results are representative of two biological replicates.
(C)10-fold serial dilutions of the indicated strains were plated on SC-URA and SC-URA + 25 mM HU, supplemented with Raffinose 2% and Galactose 2%. Pictures were taken after 3 days of incubation at 28°C. Results are representative of three biological replicates.

Figure S6

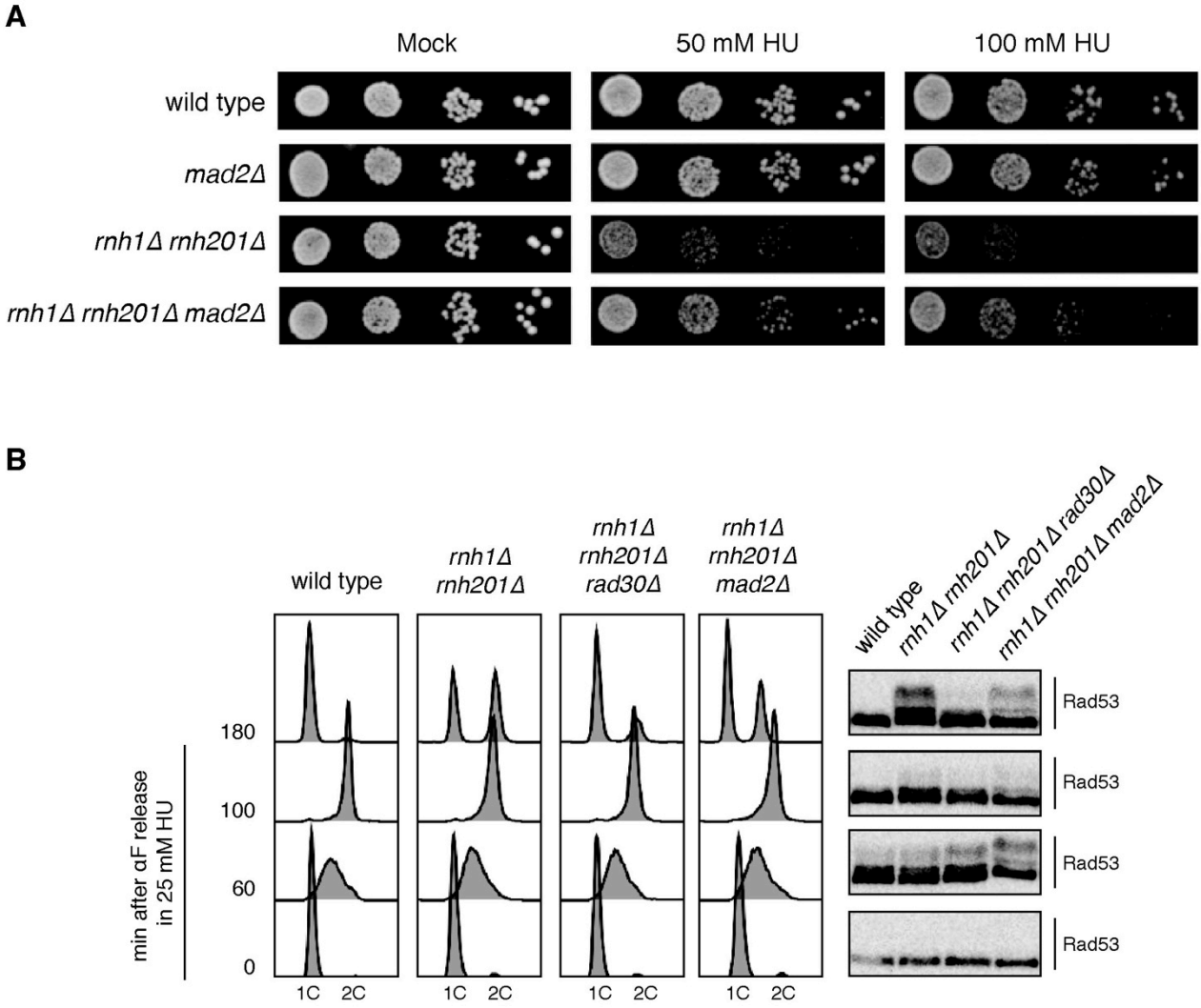

Figure S6. The toxic effect of Pol η is partly dependent upon the spindle assembly checkpoint factor Mad2.
(A) 10-fold serial dilutions of the indicated strains were plated on YEPD and YEPD + 50 mM or 100 mM HU Pictures were taken after 2 days of incubation. **(B)** Exponentially growing cells were synchronized in G1 phase by α-factor addition (4μg/ml) and released in 25 mM HU. α-factor was re-added to the medium 90 min after the release to block cells in the next G1 phase. In the left panel cell cycle progression was followed by flow cytometry (FACS) measuring DNA content (1C, 2C) at the indicated time points. In the right panel Rad53 phosphorylation was analyzed by western blotting of total cell extracts using anti-Rad53 antibodies. Results are representative of two biological replicates.

Table S1

Strain	Genotype	Ref.
SY2080	*W303 MATa ade2-1 trp1-1 leu2-3,112 his3-11,15 ura3-1 can1-100 RAD5*	M. Foiani
YFL1213	*(SY2080) MATa rnh1::HIS3 rnh201::KANMX6*	(7)
YFL1773	*(SY2080) MATa rnh1::HIS3 rnh201::KANMX6 rad30::TRP1*	This Study
YSS21	*(SY2080) MATa rad30::KANMX6*	(63)
YMG1082	*(SY2080) MATa rad30::KANMX6 rev1::KANMX6 rev3::TRP1 rev7::HIS3*	(63)
YFL1271	*(SY2080) MATa rad30::KANMX6 rev1::KANMX6 rev3::TRP1 rev7::HIS3 rnh1::HIS3 rnh201::KANMX6*	(7)
YSS17	*(SY2080) MATa rev1::KANMX6*	This Study
YFL2485	*(SY2080) MATa rev1::HPH rnh1::HIS3 rnh201::KANMX6*	This Study
YMG1096	*(SY2080) MATa rev3::TRP1 rev7::HIS3*	This Study
YFL1389	*(SY2080) MATa rev3::TRP1 rev7::HIS3 rnh1::HIS3 rnh201::KANMX6*	This Study
YFL1419	*(SY2080) MATa + pRS426*	This Study
YFL1420	*(SY2080) MATa + pEGUh6-RAD30 [GAL1-6XHIS-RAD30-URA3]*	This Study
YFL1421	*(SY2080) MATa + pEGUh6-rad30 D155A D156A [GAL1-6XHIS-rad30-D155A-E156A-URA3]*	This Study
YFL2567	*(SY2080) MATa + pFL166.4 [GAL1-6XHIS-rad30-F355A-URA3]*	This Study
YFL1422	*(SY2080) MATa rnh1::HIS3 rnh201::KANMX6 + pRS426*	This Study
YFL1423	*(SY2080) MATa rnh1::HIS3 rnh201::KANMX6 + pEGUh6-RAD30 [GAL1-6XHIS-rad30-URA3]*	This Study
YFL1424	*(SY2080) MATa rnh1::HIS3 rnh201::KANMX6 + pEGUh6-rad30 D155A D156A [GAL1-6XHIS-rad30-D155A-E156A-URA3]*	This Study
YFL2569	*(SY2080) MATa rnh1::HIS3 rnh201::KANMX6 + pFL166.4 [GAL1-6XHIS-rad30-F355A-URA3]*	This Study
YFL2591	*(SY2080) MATa ura3::ADH1-OsTIR1-9MYC:URA3 + pCM185 [TRP]*	This Study
YFL2596	*(SY2080) MATa ura3::ADH1-OsTIR1-9MYC:URA3 rnh1::HIS3 rnh201::KANMX6 + pCM185 [TRP]*	This Study
YFL2603	*(SY2080) MATa ura3::ADH1-OsTIR1-9MYC:URA3 rnh1::HIS3 rnh201::KANMX6 rad30::LEU2 + pCM185 [TRP]*	This Study

YFL2592	*(SY2080) MATa ura3::ADH1-OsTIR1-9MYC:URA3 + pFL160.1 [rnhB-AID-HA-TRP]*	This Study
YFL2598	*(SY2080) MATa ura3::ADH1-OsTIR1-9MYC:URA3 rnh1::HIS3 rnh201::KANMX6 + pFL160.1 [rnhB-AID-HA-TRP]*	This Study
YFL2604	*(SY2080) MATa ura3::ADH1-OsTIR1-9MYC:URA3 rnh1::HIS3 rnh201::KANMX6 rad30::TRP1 + pFL160.1 [rnhB-AID-HA-TRP]*	This Study
YFL3045	*(W303 RAD5) MATa sgs1::HIS3 rnh201-D39A*	(38)
YFL3044	*(W303 RAD5) MATa sgs1::HIS3 rnh201-P45D-Y219A*	(38)
YFL3049/2D	*(SY2080) MATa rnh201-D39A*	This Study
YFL3047/3A	*(SY2080) MATa rnh201-P45D-Y219A*	This Study
YFL1208/2D	*(SY2080) MATa rnh1::HIS3*	(7)
YFL1191/4B	*(SY2080) MATa rnh201::KANMX6*	(7)
YFL3068/2A	*(SY2080) MATa rnh201-D39A rnh1::HIS3*	This Study
YFL3071/3D	*(SY2080) MATa rnh201-D39A rnh1::HIS3 rad30::TRP1*	This Study
YFL3062/2A	*(SY2080) MATa rnh201-P45D-Y219A rnh1::HIS3*	This Study
YFL3066/4A	*(SY2080) MATa rnh201-P45D-Y219 rnh1::HIS3 rad30::TRP1*	This Study
YFL1229/1A	*(SY2080) MATa rnh1::HIS3 rnh201::KANMX6 mad2::TRP1*	This Study
YFL1228/2A	*(SY2080) MATa mad2::TRP1*	This Study
YFL3180	*(SY2080) MATa mms2::HPH rev3::TRP1 rad30::KANMX6 + pRS426*	This Study
YFL3182	*(SY2080) MATa mms2::HPH rev3::TRP1 rad30::KANMX6 + pEGUh6-RAD30 [GAL1-6XHIS-rad30-URA3]*	This Study
YFL3184	*(SY2080) MATa mms2::HPH rev3::TRP1 rad30::KANMX6 + pEGUh6-rad30 D155A D156A [GAL1-6XHIS-rad30-D155A-E156A-URA3]*	This Study
YFL3186	*(SY2080) MATa mms2::HPH rev3::TRP1 rad30::KANMX6 + pFL166.4 [GAL1-6XHIS-rad30-F355A-URA3]*	This Study
YFL3188	*(SY2080) MATa mms2::HPH rev3::TRP1 RAD30-13MYC:KANMX6*	This Study
YFL1496/4a	*(SY2080) MATa mms2::HPH rev3::TRP1 rad30::KANMX6*	This Study
YFL3177/17d	*(SY2080) MATa mms2::HPH rev3::TRP1 rad30-D155A-13MYC:KANMX6*	This Study

YFL3174/12a	*(SY2080) MATa mms2::HPH rev3::TRP1 rad30-F35A-13MYC:KANMX6*	This Study
YSS16	*(SY2080) MATa RAD30-13MYC:KANMX6*	This Study
LS237	*(SY2080) MATa rad30-D155A-13MYC:KANMX6*	(34)
YFL2945	*(SY2080) MATa rad30-F35A-13MYC:KANMX6*	This Study

Published paper II

Measuring the levels of ribonucleotides embedded in genomic DNA

Alice Meroni, **Giulia Maria Nava,** Sarah Sertic, Paolo Plevani, Marco Muzi- Falconi[#*] and Federico Lazzaro.[#*]

Dipartimento di Bioscienze, Università degli Studi di Milano. Milano, Italy

[#] Co-last authors

[*] Corresponding authors: marco.muzifalconi@unimi.it, federico.lazzaro@unimi.it

Book Chapter in **Methods in Molecular Biology Genome instability** (pp. 319–327). Humana Press, New York, NY. (2018)

https://doi.org/10.1007/978-1-4939-7306-4_22

Synopsis of the work and specific contributions

In this Method in Molecular Biology, we described in detail how to measure levels of ribonucleotides embedded in genomic DNA. This protocol was optimized for human and yeast, to compare ribonucleotides levels in different mutants.

This Method is part of a collection of Methods in Molecular Biology, published in the book entitled Genome Instability.

For what concerns this work, I participated in the optimization of the protocol for yeast together with Dott.Alice Meroni, and under the supervision of Dott. Federico Lazzaro.

Chapter 22

Measuring the Levels of Ribonucleotides Embedded in Genomic DNA

Alice Meroni, Giulia M. Nava, Sarah Sertic, Paolo Plevani, Marco Muzi-Falconi, and Federico Lazzaro

Abstract

Ribonucleotides (rNTPs) are incorporated into genomic DNA at a relatively high frequency during replication. They have beneficial effects but, if not removed from the chromosomes, increase genomic instability. Here, we describe a fast method to easily estimate the amounts of embedded ribonucleotides into the genome. The protocol described is performed in *Saccharomyces cerevisiae* and allows us to quantify altered levels of rNMPs due to different mutations in the replicative polymerase ε. However, this protocol can be easily applied to cells derived from any organism.

Key words DNA replication, DNA repair, DNA polymerase, Ribonucleotides incorporation, RNase H, Genome stability, Genomic rNMPs

1 Introduction

During evolution, DNA was selected as the principal molecule to preserve genetic information likely due to its greater stability compared to RNA, whose 3′ hydroxyl group increases its susceptibility to hydrolysis.

At every cell cycle, genomic DNA is duplicated by DNA polymerases, enzymes that are specialized to copy a single-stranded DNA template and polymerize deoxyribonucleotides (dNTPs) accordingly, forming a complementary DNA strand. Given the much greater abundance of rNTPs compared to dNTPs in the nucleus, DNA polymerases evolved a steric gate to help preventing rNTPs from entering the active site [1].

However, recent data revealed that large amounts of rNTPs are incorporated in genomic DNA during replication [2]. The presence of rNMPs in the chromosomes has physiological roles [3–5] and is

M. Muzi-Falconi and F. Lazzaro are co-last authors.

Marco Muzi-Falconi and Grant W. Brown (eds.), *Genome Instability: Methods and Protocols*, Methods in Molecular Biology, vol. 1672, DOI 10.1007/978-1-4939-7306-4_22, © Springer Science+Business Media LLC 2018

normally transient: specific RNase H-based pathways excise them before mitosis [6]. Failure to remove genomic rNMPs causes replication stress and genome instability in yeast and human cells [7–12]. Mutations in the genes coding for RNase H2 in humans are responsible for the rare Aicardi-Goutieres Syndrome (AGS) [13]. Intriguingly, cells derived from AGS patients accumulate rNMPs in their chromosomes and exhibit constitutively activated DNA damage response and post-replication repair mechanisms [8, 10].

To investigate the mechanisms underlying incorporation and removal of ribonucleotides in chromosomes and to determine their effect on genome integrity, it is important to determine rapidly and semiquantitatively the amounts of ribonucleotides present genomic DNA. Here, we describe an experimental strategy based on the approach originally described by Hiller and colleagues [12] and then in [8]. Briefly, genomic DNA is extracted and treated in vitro with bacterial RNase HII, which introduces nicks at every ribonucleotides site. These nicks are radioactively labeled taking advantage of the DNA Polymerase I nick translation capability (Fig. 1). In this chapter, we describe the procedure starting from the preparation of genomic DNA from yeast cells and compare the effect of two mutations affecting the steric gate of pol ε, M644G and M644L, that respectively increase and decrease rNTPs incorporation [9].

2 Materials

1. Eppendorf tubes 1.5 and 2 mL.
2. Pipettes and tips.
3. Glass Pasteur pipette.
4. MilliQ water.
5. 250 mL glass flasks.
6. Stirrer.
7. Gel electrophoresis apparatus.
8. Power supply.
9. UV transilluminator and digital camera.
10. Plastic wrap.
11. Tape.
12. Scalpel.
13. Thermomixer.
14. Geiger counter.
15. Gel dryer.

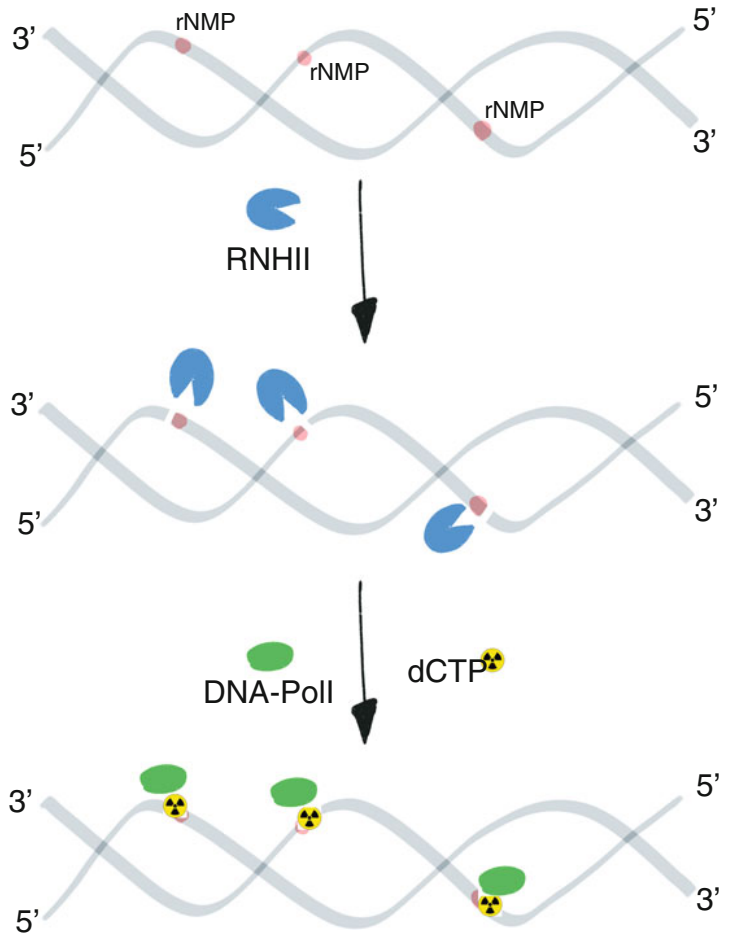

Fig. 1 Representative scheme for ribonucleotides incorporation assay. RNHII recognizes and cleaves ribonucleotides embedded into genomic DNA (*red dot*) leaving 5′ P-ribonucleotide ends. The DNA-PolI enzyme, through nick translation, marks RNHII-induced nicks with radiolabeled dCTP

16. 3 MM Whatman blotting papers.
17. Towel papers.
18. Weight (≥400 g).
19. Phosphorimager and screen.
20. YDER Yeast DNA Extraction kit, materials and reagents listed in the kit instructions (Thermo Scientific).
21. RNase A 10 mg/mL.
22. Phenol:Chloroform:Isoamyl Alcohol 25:24:1 v/v/v (Saturated with 10 mM Tris–HCl, pH 8.0, 1 mM EDTA). Stored at 4 °C.
23. 100% ethanol. Stored at −20 °C.
24. 3 M sodium acetate, pH 7.0. Stored at 4 °C.
25. 70% ethanol. Stored at −20 °C.

26. Agarose powder.
27. 10 mg/mL ethidium bromide (EtBr).
28. TAE 1×: 40 mM Tris–HCl, pH 8.0, 20 mM acetic acid, and 1 mM EDTA. Stored at room temperature.
29. Lambda DNA marker.
30. RNase HII 5000 U/mL.
31. 10× ThermoPol® Reaction Buffer: 200 mM Tris–HCl, 100 mM $(NH_4)_2SO_4$, 100 mM KCl, 20 mM $MgSO_4$, 1% Triton® X-100 (New England Biolabs).
32. 10× dNTPs mix (without dCTP); 200 μM dATP, 200 μM dGTP and 200 μM dTTP.
33. NEBuffer 2; 500 mM NaCl,100 mM Tris–HCl, 100 mM $MgCl_2$, 10 mM DTT (New England Biolabs).
34. DNA Polymerase I 10,000 U/mL.
35. α^{32}P-dCTP, 3000 Ci/mmol.
36. STOP solution: 30% glycerol, 200 mM EDTA, bromophenol blue, in MilliQ water.
37. TCA 30%.
38. Software for quantification and analysis: ImageQuant and Microsoft Excel.

3 Methods

3.1 Genomic DNA Preparation

1. Isolate yeast genomic DNA using the Y-DER extraction Kit according to the manufacturer's instructions. All the steps are performed as described in the kit's instructions, with the following modifications:
   (a) Use 50 mL cultures with an OD_{600} between 0.3 and 0.8.
   (b) RNase A 10 mg/mL is diluted 1:1000 in the Y-PER reagent.
2. Resuspend DNA in 200 μL of MilliQ water and add an equal volume of Phenol:Chloroform:Isoamyl Alcohol 25:24:1 v/v/v saturated with 10 mM Tris–HCl, pH 8.0, 1 mM EDTA (*see* **Note 1**).
3. Vortex vigorously for 15 s.
4. Centrifuge at maximum speed for 10 min at RT.
5. Carefully transfer only the aqueous phase (upper phase) to a new 1.5 mL eppendorf tube. That phase contains DNA. Do not transfer material from the interface or the lower phase. If so, repeat the procedure from **step 2**, adding an equal volume of Phenol:Chloroform:Isoamyl Alcohol 25:24:1 v/v/v saturated with 10 mM Tris–HCl, pH 8.0, 1 mM EDTA.

6. Precipitate DNA by adding three volumes of ice-cold 100% ethanol and 1/10 of the volume of sodium acetate 3 M, pH 7.0. Mix well and keep overnight at −20 °C.
7. Spin down the precipitate at maximum speed for 45′ at 4 °C. Draw off the supernatant.
8. Wash adding 1 mL of ice-cold 70% ethanol. Spin at maximum speed for 30 min at 4 °C. Draw off the supernatant and dry the pellet at 42–44 °C (*see* **Note 2**).
9. Resuspend gently the pellet with 50 μL of MilliQ water.

3.2 Nicking DNA at Ribonucleotide Sites

1. Quantify genomic DNA by loading 2 μL on a 1% agarose gel in TAE (with 0.67 μg/mL EtBr) next to 1 μL of Lambda DNA marker. Run for 10 min at 8–10 V/cm. The genomic DNA band should be compact and easily quantifiable (*see* **Note 3**).
2. Normalize DNA in each sample to 25 ng/μL by adding MilliQ water.
3. Prepare two new 1.5 mL eppendorf tubes per sample. Label the tubes with the sample name plus "−"" and "+" (e.g., Sample 1− and Sample 1+) (*see* **Note 4**), and transfer 20 μL (500 ng) of normalized genomic DNA to each tube.
4. Dilute 1:10 the RNase HII in ThermoPol Buffer 1×. Prepare the two reaction mixtures (mix "−" and mix "+") in new 1.5 mL tubes in excess with respect to the number of samples. Keep the mixtures on ice.
   1× reaction mix recipe (Note that the final reaction volume is 50 μL):

	Mix "−"	**Mix "+"**
ThermoPol Buffer 10×	5 μL	5 μL
RNase HII	/	1 μL
ThermoPol Buffer 1×	1 μL	/
H_2O MilliQ	24 μL	24 μL
Total volume	30 μL	30 μL

5. Vortex briefly and add 30 μL of each mixture to the appropriate labeled tube containing genomic DNA.
6. Incubate at 37 °C with 550 rpm agitation in a thermomixer for 2.30 h.
7. Add 50 μL of MilliQ water and precipitate DNA following **steps 6–8** of section 3.1, consider 100 μL of total volume.
8. Resuspend gently the pellet in 20 μL of MilliQ water.

3.3 Radioactive Labeling of Nicks

1. Quantify and normalize DNA by loading 2 μL on a 1% agarose gel in TAE (with 0.67 μg/mL EtBr) next to 1 μL of Lambda DNA marker. Run for 10 min at 9–10 V/cm (*see* Note for gel preparation).
2. Transfer 300 ng of DNA to a new 1.5 mL tube and add MilliQ water to 15 μL of total volume.
3. Prepare the common DNA Polymerase I reaction mixture, keep it on ice.
   1× DNA Polymerase I reaction mix recipe:

10× dNTPs mix (without dCTP):	2 μL
DNA Pol I 10× buffer NEBuffer 2	2 μL
DNA Pol I 10,000 U/mL	0.5 μL
α^{32}P-dCTP 3000 Ci/mmol	0.3 μL
H_2O MilliQ	0.2 μL

4. Add 5 μL of the DNA Polymerase I reaction mix to the each sample and incubate at 16 °C for 30 min (*see* **Note 5**).
5. Add 4 μL of the STOP solution (*see* **Notes 5** and **6**).
6. Load 20 μL on a 1% agarose gel in TAE (with 0.67 μg/mL EtBr). Here the DNA size marker is dispensable.
7. Run at 7 V/cm for 1.20 h.
8. Cut the gel immediately under the bromophenol blue line (*see* **Note 7**).
9. Examine the gel by UV light and photograph it digitally. This will allow normalization of the radioactive signal with respect to the DNA loaded in the gel.
10. Soak the gel in TCA 30% for half an hour to precipitate the DNA. The bromophenol blue turns yellow.
11. Assemble the sandwich on a glass tray: cover completely the inner part with plastic wrap. Layer three pieces of 3MM Whatman blotting paper larger than the gel. Take out the gel from TCA 30% and place it on the top of the blotting paper. Place in order: three more sheets of blotting paper on the gel, a stack of paper towels, and a weight (0.3–0.5 kg) (Fig. 2).
12. Let the gel dry overnight at room temperature.
13. Remove the paper towels and the blotting papers above the gel. Transfer the desiccated gel on a new 3MM blotting paper.
14. Dry the gel on the blotting paper using a gel dryer for 20 min at 80 °C. Use more than one blotting paper and cover the gel with plastic wrap to avoid radioactive contamination of the instrument.

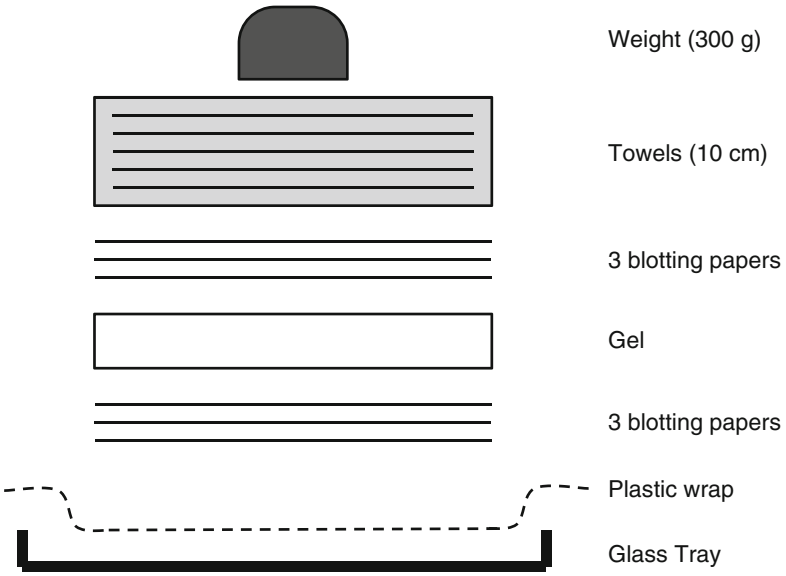

Fig. 2 Scheme to assemble paper sandwich to dry the agarose gel

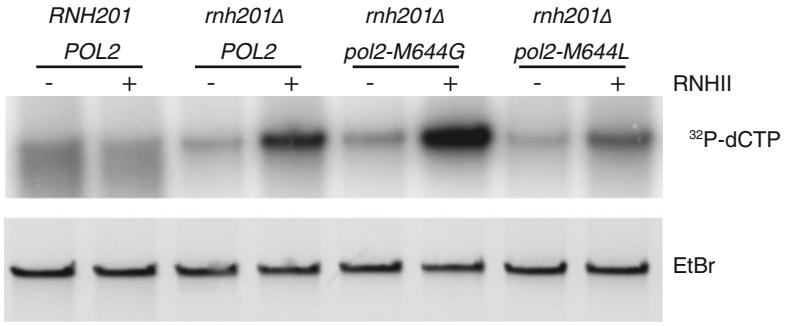

Fig. 3 Visualization of ribonucleotides incorporation assay results. The strains tested are derivatives of a W303 background (*MATa ade2–1 trp1–1 leu2–3112 his3–11,15 ura3–1 can1–100 RAD5*) with a deletion of gene coding for the catalytic subunit of RNase H2 (*rnh201Δ*) combined with wt or mutated *POL2* gene. The *RNH201 POL2* wt strain is used as control. The radiolabeled signal represents the nicks labeled by PolI. The signal dependent upon RNHII treatment is proportional to the genomic ribonucleotides levels. The EtBr panel represents the loading control, acquired before gel dryng and necessary for radioactive quantification

15. Expose the dried gel on a phosphorimager screen for 5–15 min (*see* **Note 8**).
16. Scan the screen in a phophorimager. To quantify the result *see* **Note 9**. An Example is shown in Fig. 3.

4 Notes

1. DNA has to be clean and as little nicked as possible to achieve the best resolution. For these reasons it is strongly recommended to clean DNA through phenol:chloroform extraction and ethanol precipitation. We also found that the YDER preparation yields a genomic DNA with fewer nicks compared with other methods.
2. Draw off as much supernatant as possible with a glass Pasteur pipette, this would ensure removing the majority of the ethanol, and then place the eppendorf tubes in a heater at 42–44 °C. Drying time depends on how much ethanol is left in the samples. Check the samples after 20 min, if the ethanol is still there, leave them in the heater and check later. Note that excessive drying would damage the sample, for this reason keep checking samples every 20 min until the pellet is completely dry.
3. To normalize DNA in the samples take a digital image and use quantifying tools such as ImageQuant or ImageLab (BioRad).
4. Here, each sample is split into two: one half is digested with purified bacterial RNase HII, the other half is left untreated. This allows discrimination between the ribonucleotide-dependent nicks and the nicks generated during DNA preparation.
5. Labeling the nicks is the key step of this protocol. For this reason the procedure needs strict standardization. We suggest proceeding sample by sample adding the reaction mix to each tube every 15–30 s. After 30 min of incubation, repeat this procedure with the STOP solution. In this way, all the samples would be incubated for exactly 30 min at 16 °C.
6. As most DNA polymerases, DNA polymerase I needs magnesium ions. In this case the high concentration of EDTA in the STOP solution will stop the reaction, while the glycerol and the bromophenol blue make the samples ready to be loaded on a gel.
7. Labeled genomic DNA is loaded on the agarose gel together with the DNA Polymerase I reaction mix, including the unincorporated radioactive nucleotides. The nucleotides migrate faster than genomic DNA and the long run ensures complete separation. Free nucleotides migrate immediately below the bromophenol blue; therefore, the gel is cut immediately after the run to avoid their diffusion through the gel. The bromophenol blue is also a pH-indicator, used to monitor the change in the gel pH while soaking in 30% TCA. When it turns yellow

the agarose gel pH has become acid so DNA would be precipitated into it.

8. The exposure time could vary depending on the α^{32}P-dCTP activity. With fresh and fully active α^{32}P-dCTP the signal is saturated in 15 min.
9. Signal quantification. To quantify the resulting signal proceed with the following step. Quantify the bands corresponding to the genomic DNA, including the ones from the EtBr capture. Use the Volume Tool of ImageQuant software drawing a rectangle around the right band. Normalize each radioactive value to the corresponding EtBr value. This would ensure the correct interpretation of the radioactive signal. Then for each sample subtract the "−" signal from the "+" signal as a background normalization.

Acknowledgments

This work was supported by grants from AIRC (n.15631) and Telethon (GGP15227) to M.M.-F., from AIRC and Fondazione Cariplo (TRIDEO 2014 Id. 15724) to F.L., and from Fondazione Cariplo (grant number 2013-0798) to P.P.

References

1. Joyce CM (1997) Choosing the right sugar: how polymerases select a nucleotide substrate. Proc Natl Acad Sci U S A 94:1619–1622
2. McElhinny SAN, Watts BE, Kumar D et al (2010) Abundant ribonucleotide incorporation into DNA by yeast replicative polymerases. Proc Natl Acad Sci U S A 107:4949–4954
3. Ghodgaonkar MM, Lazzaro F, Olivera-Pimentel M et al (2013) Ribonucleotides misincorporated into DNA act as strand-discrimination signals in eukaryotic mismatch repair. Mol Cell 50:323–332
4. Lujan SA, Williams JS, Clausen AR et al (2013) Ribonucleotides are signals for mismatch repair of leading-strand replication errors. Mol Cell 50:437–443
5. Dalgaard JZ (2012) Causes and consequences of ribonucleotide incorporation into nuclear DNA. Trends Genet 28:592–597
6. Sparks JL, Chon H, Cerritelli SM et al (2012) RNase H2-initiated ribonucleotide excision repair. Mol Cell 47:980–986
7. Lazzaro F, Novarina D, Amara F et al (2012) RNase H and postreplication repair protect cells from ribonucleotides incorporated in DNA. Mol Cell 45:99–110
8. Pizzi S, Sertic S, Orcesi S et al (2015) Reduction of hRNase H2 activity in Aicardi-Goutières syndrome cells leads to replication stress and genome instability. Hum Mol Genet 24:649–658
9. Nick McElhinny SA, Kumar D, Clark AB et al (2010) Genome instability due to ribonucleotide incorporation into DNA. Nat Chem Biol 6:774–781
10. Günther C, Kind B, Reijns MAM et al (2014) Defective removal of ribonucleotides from DNA promotes systemic autoimmunity. J Clin Invest 125(1):413–424
11. Reijns MAM, Rabe B, Rigby RE et al (2012) Enzymatic removal of ribonucleotides from DNA is essential for mammalian genome integrity and development. Cell 149:1008–1022
12. Hiller B, Achleitner M, Glage S et al (2012) Mammalian RNase H2 removes ribonucleotides from DNA to maintain genome integrity. J Exp Med 209:1419–1426
13. Crow YJ, Manel N (2015) Aicardi-Goutières syndrome and the type I interferonopathies. Nat Rev Immunol 15(7):429–440

Published paper III

One, No One, and One Hundred Thousand: The Many Forms of Ribonucleotides in DNA

Giulia Maria Nava †, Lavinia Grasso †, Sarah Sertic, Achille Pellicioli , Marco Muzi Falconi * and Federico Lazzaro *

Dipartimento di Bioscienze, Università degli Studi di Milano, via Celoria 26, 20133 Milano, Italy;

Corresponding authors: marco.muzifalconi@unimi.it, federico.lazzaro@unimi.it.

† The authors contributed equally to this work.

International Journal of Molecular Science 2020, 21, 1706

https://doi:10.3390/ijms21051706.

Synopsis of the work and specific contributions

In this review, we discussed the origin of single and multiple ribonucleotides in the genome and the DNA of organelles (mitochondria and chloroplasts). As sources of RNA:DNA hybrids in cells, we describe ribonucleotides that are directly incorporated into DNA by DNA polymerases, primers used in Okazaki fragments synthesis, R-loops formed during transcription, and hybrids formed during DSBs repair. For all these examples, we paid particular attention to situations where the aberrant processing of RNA:DNA hybrids may result in multiple rNMPs embedded in DNA. Indeed, although RNA:DNA hybrids can regulate different physiological functions, their persistence compromises genome integrity and genome stability, so hybrids are usually processed in cells. We concluded the review by providing an overview of the currently available strategies to study the presence of single and multiple ribonucleotides in DNA *in vivo*.

For what concerns this work, I participated in the conceptualization and the writing of the entire manuscript, with Lavinia Grasso and under the supervision of Dott. Federico Lazzaro.

International Journal of
Molecular Sciences

MDPI

Review

One, No One, and One Hundred Thousand: The Many Forms of Ribonucleotides in DNA

Giulia Maria Nava †, Lavinia Grasso †, Sarah Sertic, Achille Pellicioli, Marco Muzi Falconi * and Federico Lazzaro *

Dipartimento di Bioscienze, Università degli Studi di Milano, via Celoria 26, 20133 Milano, Italy; giulia.nava@unimi.it (G.M.N.); lavinia.grasso@unimi.it (L.G.); sarah.sertic@unimi.it (S.S.); achille.pellicioli@unimi.it (A.P.)

* Correspondence: marco.muzifalconi@unimi.it (M.M.F.); federico.lazzaro@unimi.it (F.L.); Tel.: +390250315034 (M.M.F.); +390250314827 (F.L.)

† The authors contributed equally to this work.

Received: 29 January 2020; Accepted: 28 February 2020; Published: 2 March 2020

Abstract: In the last decade, it has become evident that RNA is frequently found in DNA. It is now well established that single embedded ribonucleoside monophosphates (rNMPs) are primarily introduced by DNA polymerases and that longer stretches of RNA can anneal to DNA, generating RNA:DNA hybrids. Among them, the most studied are R-loops, peculiar three-stranded nucleic acid structures formed upon the re-hybridization of a transcript to its template DNA. In addition, polyribonucleotide chains are synthesized to allow DNA replication priming, double-strand breaks repair, and may as well result from the direct incorporation of consecutive rNMPs by DNA polymerases. The bright side of RNA into DNA is that it contributes to regulating different physiological functions. The dark side, however, is that persistent RNA compromises genome integrity and genome stability. For these reasons, the characterization of all these structures has been under growing investigation. In this review, we discussed the origin of single and multiple ribonucleotides in the genome and in the DNA of organelles, focusing on situations where the aberrant processing of RNA:DNA hybrids may result in multiple rNMPs embedded in DNA. We concluded by providing an overview of the currently available strategies to study the presence of single and multiple ribonucleotides in DNA in vivo.

Keywords: rNMPs incorporation; RNA:DNA hybrids; RNase H; replication stress; genome instability

1. Introduction

The presence of single ribonucleotides in DNA has been extensively studied and reported in many excellent reviews [1–4]; here, we just recalled some important details about their sources, effects, and removal. On the other hand, we still lack a complete understanding of the different types of multiple rNMPs that can be found in DNA. Most of the published literature about RNA:DNA hybrids focus on R-loops, but the world of RNA:DNA hybrids is much wider: it also includes RNA primers found at Okazaki fragments, hybrids formed at double-strand breaks (DSBs), polyribonucleotide stretches eventually incorporated by DNA polymerases, etc. In this review, we thus discussed with particular interest the possible sources and consequences of inserting multiple rNMPs into DNA.

2. DNA Polymerases are the Main Source of Single Ribonucleotides Introduced in DNA

2.1. DNA Replication

Most leaving organisms store their genetic information in DNA rather than in RNA, partly because of the inherent chemical instability of the RNA molecule. The DNA, indeed, lacks the reactive 2′-OH

group on the ribose sugar, which can attack the sugar-phosphate backbone, generating breaks with genotoxic outcomes [5]. The DNA must, therefore, be carefully duplicated for proper transmission of the genetic information over many generations, avoiding mutations that can promote genome instability and related human pathologies, like cancer or neurodegenerative diseases [6,7]. The accuracy of DNA replication is ensured not only by the high-fidelity rate of replicative DNA polymerases and their associated proofreading activities but also by numerous other replicative and post-replicative factors and mechanisms, including DNA repair systems [8,9]. Apart from choosing the proper complementary base, replicative DNA polymerases must also discriminate between sugars, ribose in rNTPs versus deoxyribose in dNTPs [10]. This is why replicative DNA polymerases, like most DNA polymerases, are equipped with a special "steric-gate" residue localized in their nucleotide-binding pocket. Steric-gate residues (Tyrosine or Phenylalanine in B-family polymerases) are characterized by a bulky side chain that sterically clashes with the 2′-OH on the ribose ring of incoming rNTPs, thus preventing their incorporation in DNA [11]. Other active site residues are as well necessary to keep the side chain of the steric-gate residue and the incoming nucleotide in the proper orientation to achieve high sugar selectivity; for example, the backbone NH of a highly conserved hydrophobic residue flanking the N-terminus of the steric-gate residue can form a hydrogen bond with a non-bridging oxygen in the β-phosphate of a bound nucleotide [11]. Moreover, it has been recently shown that a polar filter, interacting with the 3′-OH and the triphosphate moiety of the incoming nucleotide, makes the 2′-OH of an rNTP clash with the surface of the fingers domain, limiting the possibility to bind rNTPs in a catalytically competent conformation [12]. The steric and the polar filters fall on nearly perpendicular planes, cooperating for elevated sugar selectivity [12].

However, sugar selectivity is not stringent enough, especially considering that DNA polymerases are constantly challenged by high rNTP concentrations. For example, even if in *Saccharomyces cerevisiae*, the dNTP pools increase of about three-fold upon entry into the S phase respect to G1 [13], and high ribonucleotide reductase (RNR) activity is maintained throughout the S phase [14], the physiological concentrations of the four rNTPs greatly exceed those of dNTPs [15,16]: rNTPs in yeast cells range from 500 to 3000 μM, while dNTPs are in between 12 and 30 μM, with rNTP:dNTP ratios varying from 36:1 for cytosine to 190:1 for adenine [16]. For this reason, pol ε has been estimated to introduce 1 rNMP every 1250 deoxyribonucleoside monophosphates (dNMPs) during leading strand synthesis, while pol δ and pol α, responsible for lagging strand synthesis [17], account for the incorporation of 1 rNMP every 5000 dNMPs and 625 dNMPs, respectively, resulting in more than 13,000 rNMPs inserted into the yeast genome for each replication cycle [16] (Table 1). Such high numbers also result from the reduced ability of pol ε and especially pol δ to proofread rNMPs inserted in DNA [18–20]. Ribonucleotides can thus be considered as the most common non-canonical nucleotides present in the eukaryotic genome [16,21]. The presence of ribonucleotides into genomic DNA has been confirmed in vivo by alkali-sensitivity assays [17], and subsequent studies revealed that the mean frequency of incorporation might be even higher, about 1 rNMP every 700 dNMPs [21]. Single or di-ribonucleotides have been detected in vivo also in mammalian genomic DNA and estimated to generate at least 1,000,000 alkali-sensitive sites per cell [22]. Additionally, different mutations in the active site of the three yeast replicative polymerases, which impact on their sugar selectivity, even induce higher frequencies of rNMPs incorporation. For example, for particular pol ε (*pol2-M644G*), pol δ (*pol3-L612M*), and pol α (*pol1-L868M*) variants, the rNMPs incorporation rate increases 10, 8, and 15 times, respectively [17,23,24].

Table 1. Ribonucleoside monophosphates (rNMPs) insertion by eukaryotic DNA polymerases opposite different DNA templates. Eukaryotic DNA polymerases are classified according to family type and roles in DNA transactions; their ability to synthesize ribonucleotides opposite different types of DNA templates is then reported.

Who	Family	Role In	rNMPs Insertion
pol ε	B	replication/repair	undamaged leading strand [16]
pol δ	B	replication/repair	undamaged lagging strand [16]
pol α	B	replication/repair	undamaged lagging strand [16]
pol ζ	B	translesion synthesis (TLS); mitochondrial replication	rare [25]
pol β	X	repair/TLS	undamaged template, CPDs [26] 8-oxo-Gs [27]
pol λ	X	repair/TLS	8-oxo-Gs [27]
pol μ	X	repair	NHEJ ends [28–30]
Tdt	X	repair	N-regions of V(D)J ends [31]
pol η	Y	TLS; lesion-independent replication stress	undamaged template [32–34]; 8-oxo-Gs, CPDs, cis-PtGG, 8-methyl-2′-deoxyGs [32,33]
pol ι	Y	TLS	undamaged template, 8-oxo-Gs, abasic sites [35]
pol κ	Y	TLS	unknown
Rev1	Y	TLS	rare [36]
pol γ	A	mitochondrial replication	rare [37,38]
pol θ	A	TLS/repair	alt-EJ ends [39]
pol ν	A	TLS/repair	unknown
PrimPol	Archaeo- eukaryotic primase superfamily	priming/TLS	undamaged template, 8-oxo-Gs [40]

2.2. Reparative DNA Synthesis

The activity of pol ε and pol δ is not only restricted to DNA replication. They are indeed involved in repair processes requiring DNA synthesis, in particular, nucleotide excision repair (NER) [41], so they may also introduce rNMPs in such circumstances. Reparative DNA synthesis steps are as well performed by many other specialized polymerases that can contribute to rNMPs incorporation (Table 1) [42].

The X-family polymerases pol β, pol λ, and pol μ are involved in base excision repair (BER), DSBs repair by nonhomologous end-joining (NHEJ), and specialized translesion synthesis (TLS) of oxidative lesions [43,44]. Pol β can place rNMPs opposite cyclobutane pyrimidine dimers (CPDs), and it is even able to synthesize stretches of up to eight rNMPs long in vitro [26]. Moreover, pol β (and, to a lesser extent, pol λ) can introduce ribonucleotides opposite 8-oxo-G lesions under physiological concentrations of metal activators and nucleotides [27]. Due to the lack of a steric gate residue, substituted by a single glycine residue [45], pol μ has a very low rNTPs/dNTPs discrimination rate [28], which allows it to insert rNMPs, promoting efficient DSBs repair by NHEJ [28–30]. The X-family Terminal deoxynucleotidyl transferase (TdT) has been long known to be important for the addition of template-independent nucleotides (N-regions) to gene segment junctions during V(D)J recombination [46,47], and it has as well only a minor preference for dNTPs over rNTPs in vitro, under conditions of in vivo rNTP/dNTP pool imbalance [31]. Y-family polymerases as pol η and pol ι are needed for TLS of many different types of DNA lesions [43,44]. The wild type *S. cerevisiae* pol η just shows a minimal rate of rNMP insertion on undamaged and damaged DNA; by contrast, the steric gate mutant *pol η-F35A* readily incorporates the correct rNMP opposite both templates, and in vivo experiments suggest that it may catalyze the incorporation of stretches of ribonucleotides in DNA [48,49]. Moreover, genetic evidence points towards the idea that under low dNTP conditions, either the wild type pol η or, even more, *pol η-F35A* inserts consecutive ribonucleotides, which become toxic in the absence of RNase H activity [34]. Differently from its yeast counterpart, the wild type human

pol η inserts rNMPs opposite both undamaged and damaged DNA templates, even if maintaining base selectivity [32,33]. Human pol η can incorporate cytidine monophosphate (rCMP) opposite guanine, CPDs, 8-oxo-Gs, 8-methyl-2′-deoxyGs, and cisplatin intra-strand guanine crosslinks (cis-PtGG), and it is also capable of synthesizing polyribonucleotide chains [32,33]. The low sugar selectivity of human pol η may result not only by its extraordinarily spacious active site but also by the absence of the polar filter described above [12]. The human pol ι incorporates and extends ribonucleotides opposite damaged and undamaged bases depending on the sequence context [35]. Contrary to pol η, pol ι readily incorporates rNMPs also opposite abasic sites [35]. The A-family pol θ is a fundamental player in DSBs repair by alternative end-joining (alt-EJ) [50,51]. In vitro studies have demonstrated that, in the presence of Mn^{2+}, pol θ has a robust template-independent terminal transferase activity and it is prone to incorporate rNMPs; this is intriguing, considering that Mn^{2+} is used by the MRX/MRN complex when generating 3′ ssDNA overhangs, which are the substrates of pol θ during alt-EJ [39]. Finally, the DNA-directed primase-polymerase PrimPol, belonging to the archaeo-eukaryotic primase superfamily, is able to use both rNTPs and dNTPs during replication initiation and chain elongation, when activated by Mn^{2+} (the preferred metal cofactor), as well as during the bypass of DNA lesions, even increasing the fidelity of synthesis opposite 8-oxo-G lesions [40]. Interestingly, rCMP paired opposite to damaged templates makes the RNase H2-dependent removal greatly inefficient. This may contribute to the accumulation of rCMP into genomic DNA [33], and it also seems to reduce the efficiency of the human OGG1 and MutYH base excision repair (BER) proteins [52], which may lead to a lack of 8-oxo-Gs removal, resulting in increased mutagenesis.

It should be emphasized that these polymerases are often active outside of the S phase [53–56] when the concentration of dNTPs is even lower than in the S phase [13], which may contribute to more significant incorporation of rNMPs into DNA. We can then speculate that "non-replicative" ribonucleotides may become particularly relevant in post-mitotic cells, such as neurons, where TLS has been recently found to take place [57].

3. Mechanisms of Single Ribonucleotides Removal

The high number of rNMPs incorporated into DNA, together with the observation that steric gate mutations, making replicative polymerases more stringent for sugar discrimination [17], have not been selected through the evolution, suggests that they must have some physiologic meaning. For example, two separate groups have demonstrated how rNMPs provide sites where the genomic DNA can be incised, allowing the mismatch repair machinery to be loaded onto the otherwise continuous leading strand in eukaryotic cells [23,58]. Single chromosome-embedded rNMPs must be anyway promptly removed, as their persistence has several negative consequences. Ribonucleotides left in DNA alter the shape and the conformation of DNA molecules [59–62], the assembly of nucleosomes [63,64], and they may hamper DNA replication since replicative DNA polymerases ε and δ are not efficient in bypassing them [16,18,19,65–68]. However, the most detrimental effects of single rNMPs seem to derive from their improper repair, as reviewed in [3].

To restore the correct DNA:DNA composition, cells have evolved ribonucleases H (RNases H), specialized in the removal of ribonucleotides from DNA. In eukaryotic cells, RNase H2 is composed of three subunits (Rnh201, Rnh202, Rnh203 in yeast; RNaseH2A, RNaseH2B, RNaseH2C in higher eukaryotes), all essential for the activity of the complex, and it cleaves both single and multiple rNMPs paired with DNA [69]. RNase H2 is the initiator of ribonucleotide excision repair (RER), the most common repair pathway for the removal of genomic embedded rNMPs [21]. RER ensures genome integrity and proper development of mouse embryos [22], keeping embedded rNMPs under a threshold of ribonucleotide tolerance [70]. In yeast, the main alternative strategy for processing ribonucleotides in DNA in the case of a faulty RER is based on Topoisomerase 1 (Top1) [71]. Top1-mediated mechanisms act mainly on the leading strand [72] and create unligatable 2′,3′-cyclic phosphate ends [73], which may have mutagenic effects [17,74,75], even resulting in DSBs [76]. Similarly, human Top1 can recognize and incise the DNA at the level of unrepaired rNMPs in RER-defective RNase H2-mutated human

cell lines [77]. RNase H2 mutations are associated with a rare autoinflammatory disorder known as Aicardi–Goutières syndrome (AGS) [78], mainly characterized by early-age onset and chronic overproduction of type I interferon in the absence of infections [79]. Patient-derived cells accumulate rNMPs in their genome and exhibit constitutive post-replication repair (PRR) and DNA damage checkpoint activation [68,80]. The mechanism by which RNase H2 aberrations trigger the disease is still unclear, although over 50% of the studied AGS families are affected by mutations in one of the three RNase H2 genes [81,82]. Moreover, RNase H2 dysfunctions have also been associated with some types of cancer [83–87] and with systemic lupus erythematosus (SLE) [80].

Eukaryotic cells also possess another specialized ribonuclease H, RNase H1, which is a single subunit protein that cleaves stretches of at least four consecutive rNMPs. Its enzymatic activity is essential for mitochondrial DNA replication in mammals [88], while it does not seem to be required during RER [21].

4. Multiple rNMPs Embedded into DNA: One Possible Cause of Genome Instability and Cell Lethality

Although the presence of single ribonucleotides into the chromosomal DNA has been extensively investigated in many organisms, whether the incorporation of consecutive rNMPs is also possible is still unclear. Unlike single rNMPs, which are moderately tolerated up to a certain threshold, multiple rNMPs might be even more detrimental for cellular viability. Indeed, even a few consecutive rNMPs can represent an insuperable obstacle during DNA replication because they cannot be correctly copied by the replicative DNA polymerases δ and ε that progressively stall when encountering four or more rNMPs [66,67]. A similar effect has been observed in mammalian mitochondria, where only RNase H1 activity is present: if multiple rNMPs embedded in mitochondrial DNA (mtDNA) are not properly removed, they cause a block of the replication fork, resulting in breakdown and loss of mtDNA [89]. Additionally, multiple rNMPs in the nucleus of *S. cerevisiae* cells are only tolerated, thanks to the action of the two main pathways of PRR: template-switch and TLS pol ζ [66]. Finally, similarly to single rNMPs, but even more significantly, polyribonucleotide chains may alter the proper conformation of DNA [59,60,62] and interfere with protein binding [63,64], possibly causing catastrophic defects in chromosome segregation and a global alteration of gene expression profiles. For all these reasons, further investigation of multiple rNMPs' metabolism appears very important.

Unfortunately, the study of multiple embedded rNMPs is complicated by the fact that it requires the simultaneous removal of RNase H1 and RNase H2, which can both recognize stretches of more than four consecutive rNMPs. *S. cerevisiae* represents an excellent model organism to this purpose because mutants lacking all RNase H activities are still viable [66]. Nevertheless, RNases H can potentially process any polyribonucleotide tract in DNA (stretches of rNMPs, R-loops, RNA primers found at Okazaki fragments, etc.), so it remains difficult to establish which one of these unprocessed substrates causes the observed effects. Anyway, if stretches of consecutive rNMPs do exist, how they are incorporated (Figure 1) and subsequently removed needs to be clarified. We have discussed below the different possible sources of multiple embedded rNMPs.

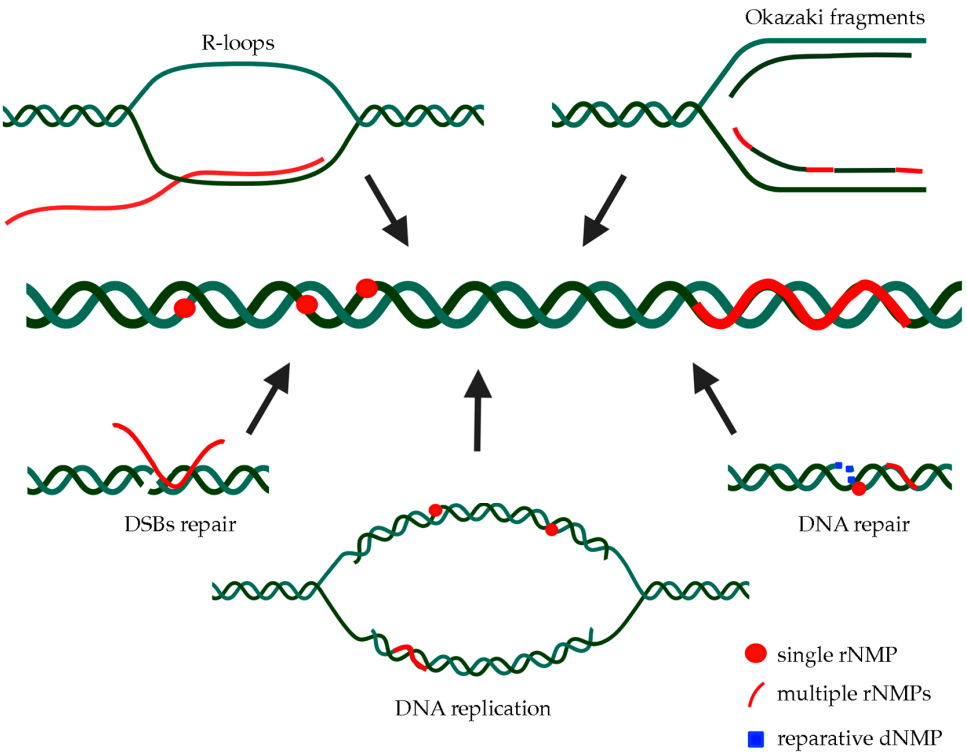

Figure 1. Sources and forms of rNMPs embedded in genomic DNA. Single ribonucleotides are primarily introduced in DNA by several DNA polymerases carrying out genome duplication and/or reparative DNA synthesis; their activity may also result in the direct incorporation of polyribonucleotide chains. Stretches of consecutive ribonucleotides embedded in chromosomal DNA may also derive from the aberrant processing of RNA:DNA hybrid structures, like RNA primers required for Okazaki fragments' synthesis, R-loops, and hybrids at double-strand breaks (DSBs) sites.

4.1. DNA Polymerases

Despite DNA polymerases being primarily responsible for the incorporation of single rNMPs, only mutant variants seem capable of introducing consecutive rNMPs. The pol ε variant *pol2-M644G* mentioned above incorporates rNMPs in DNA at higher frequencies than the wild type pol ε [17]. The fact that this mutant becomes synthetic lethal with the simultaneous absence of RNase H1 and H2 suggests that it incorporates stretches of rNMPs, requiring the activity of both RNases H to be removed [24,66]. On the contrary, pol α and δ variants that incorporate more rNMPs are still viable when combined with RNase H1 and H2 mutants [24]. This could be explained by a low rNMPs density in the lagging strand, possibly correlating with a low probability of introducing consecutive rNMPs [24]. Alternatively, RNase H independent mechanisms may remove single and multiple rNMPs, when incorporated in the discontinuous lagging strand [24].

As already discussed, also the *S. cerevisiae polη-F35A* steric-gate mutant seems to incorporate polyribonucleotide tracts in DNA at a high rate, leaving a specific 1 bp deletion signature, when not removed by RNase H2 [48,49]. Moreover, under particular stress conditions, also wild type replicative and/or reparative DNA polymerases may incorporate consecutive rNMPs. This is what has been suggested for the *S. cerevisiae* pol η. Meroni et al. found that, upon replication stress induced by hydroxyurea, pol η was recruited at stalled replication forks, where it facilitated the formation of stretches of rNMPs that became highly toxic for cells, when not properly replaced with DNA [34].

4.2. Okazaki Fragments

Although the number of rNMPs incorporated during DNA replication is surprisingly large, the main source of genomic ribonucleotides remains by far the replication priming. Replicative DNA polymerases require a piece of RNA initiator (RNAi) of ~8–10 nt in length to properly work and replicate DNA. Considering the discontinuous nature of the lagging strand, this is translated in an average of ~100,000 RNA:DNA hybrids formed at each round of DNA replication in *S. cerevisiae* and in more than 10 millions of hybrids found in human cells [90,91]. RNA:DNA primers must then be removed, and Okazaki fragments (OKFs) joined together, forming a continuous lagging strand. Because of their abundance, it is easy to imagine how just a few defects in their processing may have deleterious consequences in cells. Different pathways cooperate in Okazaki fragments maturation (reviewed in [92]). The dominant pathway seems to be dependent on FEN1 (Rad27 in *S. cerevisiae*), with the additional contribution of Exo1 cleaving the short flaps (2–10 nt in length), generated when the RNAi is displaced through pol δ-mediated DNA synthesis [93–95]. When flaps become longer (>30 nt), the ssDNA generated is coated by RPA, which inhibits the activity of Fen1; the processing of such intermediates requires Dna2 activity [96]. When strand displacement does not occur, also RNase H2 seems to have a role in the direct hydrolysis of RNA:DNA primers [97]. *S. cerevisiae* strains, lacking Rad27 and RNase H2, are sick but become lethal when combined with RNase H1 deletion. This seems to suggest that, besides RNase H2, also RNase H1 has a role in Okazaki Fragments maturation [98]. Finally, the generated nicks are sealed by DNA Ligase I (Cdc9 in *S. cerevisiae*) [99]. The exact composition, crosstalk, and regulation of all these pathways are still largely unknown, but dysfunctions in any of these mechanisms could leave flaps or nicks into the genome, causing deletions, amplification of DNA sequences, and DSBs [100]. Moreover, even if never visualized, dysfunctions could also result in the stable inclusion of RNA stretches into DNA, as suggested by different groups [34,101]. Intriguingly, Holmes et al. [89] found that this also happened in the mouse mitochondrial genome, where, in the absence of RNase H1, the RNA primers were fixed in both template strands of mtDNA, causing dramatic effects on mtDNA replication. The incorporation of an RNA primer into the DNA is also the proposed mechanism for mating-type switching in *Schizosaccharomyces pombe.* During the S phase, two consecutive rNMPs are left by incomplete processing of RNA primer into the lagging strand at the *MAT1* locus; these rNMPs are maintained until the following replication cycle, inducing polymerase stalling, and recombination events, which lead to mating-type switching [102,103].

4.3. R-Loops

Another important source of ribonucleotides in DNA is represented by R-loops, peculiar three-stranded structures formed when a transcribed RNA hybridizes back to the template, leaving the non-template DNA single-stranded [104]. These hybrid regions are longer than the canonical 8 bp hybrids formed by active RNA polymerases (RNAPs) [105], and R-loop-prone regions cover about 8% of the yeast genome [106]. Growing evidence suggests that these structures play important roles in regulating gene expression [107] and chromatin structures [108]. On the other hand, they can compromise genome integrity since R-loops expose patches of ssDNA, which are more susceptible to mutagenesis, recombination, and DNA damage, compared to dsDNA (reviewed in [109]). Moreover, conflicts between the DNA replication machinery and R-loops trigger fork collapse and DSBs [110,111]. Tight R-loop homeostasis must thus be maintained in cells, to prevent their negative outcomes while maintaining positive functions. Understanding how this regulation occurs is a big challenge, and, to date, many factors have been identified as important ones for preventing, resolving, but also promoting R-loops formation (reviewed in [112,113]).

The formation of R-loops is prevented by mRNA biogenesis and processing proteins that reduce the ability of RNA transcripts to re-hybridize with the DNA behind RNAPs [114,115] and by DNA topoisomerases that relax negative supercoils formed behind the transcriptional bubble [116,117]. Once formed, different factors can act to remove R-loops, like RNase H enzymes (H1 and H2), which cleave the RNA moiety of RNA:DNA hybrids [69] and numerous helicases that unwind the hybrids, as

Senataxin (Sen1 in *S. cerevisiae*) [118], the human DHX9 [119], and Pif1-family helicases [120]. Rad51, instead, seems to actively promote R-loops formation [121].

Different situations have been described where the RNA stretch present into R-loops becomes embedded into DNA. In prokaryotic cells, R-loops are frequently associated with origin-independent replication [122,123]. In vitro studies have shown that prokaryotic DNA polymerases can use mRNA as a primer when the replication fork collides with the RNA polymerase [124], and this is also the case for eukaryotic cells. Stuckey et al. [125] found that in *S. cerevisiae*, RNA polymerase I transcription constraints led to persistent R-loops in the ribosomal DNA locus. Here, the RNA present in the R-loop can be used as a primer by DNA polymerases, triggering an origin-independent replication process. Being highly inaccurate, this unscheduled replication can cause genome instability.

4.4. Hybrids at DSBs

The local incorporation of ribonucleotides and the presence of different types of RNA molecules have been shown to have important effects even on DNA DSBs, influencing their repair by nonhomologous end-joining or homologous recombination pathways (reviewed in [126–128]). For example, Pryor et al. recently reported that one or more rNMPs were transiently incorporated at broken DNA ends by pol μ or TdT, enhancing DSB repair by NHEJ mechanisms [30]. Growing evidence shows that also the hybridization of complementary RNA molecules at DSB ends regulates their repair (reviewed in [126–129]); different groups have indeed observed an accumulation of RNA:DNA hybrids at DSB sites [130–140]. The origin of such RNA species is still under investigation. One possibility is that, after DNA damage, RNA polymerase II is recruited at the broken ends, generating newly transcribed RNA, as suggested in [130,132,139,141]. An alternative, which can coexist with the former mechanism, is that the RNA molecules may result from transcripts produced before the formation of the break in active genes [133,134,137,138]. Regardless of the source of RNA:DNA hybrids, the most discussed point is the understanding of their significance when repairing DSBs. Notably, RNA:DNA hybrids seem to contribute to the recruitment of repair factors [131–140] and to the control of DNA end resection [132,137–139], the fundamental process creating 3′ end ssDNA filaments needed for recombination [142]. However, how RNA:DNA hybrids impact on DSB processing and repair is still an open debate [143]. Indeed, while some data indicate that they promote resection [136,137,139], others suggest an anti-resection role [132,138] or no effect at all [134]. More work is thus required to clarify the regulation of this dynamic phenomenon. Furthermore, it has long been known that DSBs repair can proceed through the formation of a cDNA intermediate [144,145]. Perhaps related to those early observations, it has also been discovered that, when RNase H enzymes are not functional, endogenous RNA itself can directly be used as a template for DSBs repair [129].

In conclusion, even if there is now a large body of evidence showing that RNA:DNA hybrids participate in DSBs repair, many aspects should be investigated and defined. Moreover, as mentioned for R-loops, and RNA primers at Okazaki fragments (OFs), it is tempting to speculate that, also in the context of DSBs repair, improperly removed RNA tracts might remain embedded at DSB ends, posing a threat to genome stability.

5. Mechanisms of Multiple Embedded Ribonucleotides Removal

Once defined the different processes that could generate tracts of rNMPs embedded into DNA, the question that arises is: how are these substrates processed in cells? As previously mentioned, single rNMPs are the substrate of RER [21], but whether this pathway also works on multiple rNMPs has never been proved. It is unlikely that the pathways acting on R-loops and OFs could process multiple rNMPs, once embedded into DNA, and thus inaccessible to players like helicases. Since RNase H1 and H2 both process consecutive embedded rNMPs, they represent the main candidates for their removal. Anyway, how the two enzymes work in vivo on these structures needs further clarification. Some progress has been made, thanks to the development of a separation-of-function mutant of the RNase H2 enzyme, called *rnh201-RED* (ribonucleotide excision defective), which loses the ability to

remove single rNMPs, but retains a discrete activity on consecutive rNMPs [146]. This mutant has been extremely useful to enlighten the role of the two functions of RNase H2 (reviewed in [147]). Being still able to remove multiple rNMPs, the *rnh201-RED* mutant alone cannot prove their existence; the development of additional separation-of-function mutants may thus be useful.

6. Ribonucleotides into the DNA of Organelles

Besides being present into the nuclear DNA, ribonucleotides are also found in the DNA contained in two types of eukaryotic organelles: mitochondria [148–150] and chloroplasts [151].

The human mitochondrial DNA (mtDNA) is a circular multicopy molecule of 16.5 kb, composed of two filaments, named heavy (H) strand and light (L) strand, and whose replication mechanism is not completely resolved. Different models for mitochondrial DNA duplication have been proposed, which are well described in recent reviews [152,153]; here, we only summarized the types and the sources of rNMPs that could be found into mtDNA (reviewed in [154]).

Replication primers represent the first source of consecutive rNMPs also in mtDNA. However, they seem to be synthesized by the mitochondrial RNA polymerase POLRMT and not by a replicative primase, as it happens for the nuclear DNA [155]. Such transcripts are stabilized by G-quadruplex structures formed in the non-template DNA strand, resulting in mitochondrial R-loops that act as replication primers [156]. Polyribonucleotide chains could also result from long RNA transcripts, which temporally coat the displaced H-strand, generating RNA:DNA hybrids that function as lagging strands during mtDNA replication, as proposed by one of the models used to explain mtDNA replication called RITOLS (ribonucleotide incorporation throughout the lagging strand). These long RNAs may result from a primase activity or by the hybridization of the displaced DNA with preformed RNA transcripts [157]. RNase H1 is the factor responsible for the removal of multiple rNMPs from mtDNA. The mammalian RNase H1 is recruited into the organelles, thanks to an essential mitochondrial localization domain, and failures in its activity cause mitochondrial dysfunctions. In mouse, when RNase H1 is absent, replication primers are not properly removed, and stretches of RNA remain fixed in both template strands of mtDNA [89]. This is a perfect example of how tracts of embedded rNMPs can compromise genome integrity. Since they cannot be bypassed by the mtDNA polymerase γ, they lead to persistent DNA gaps that are catastrophic for the subsequent round of replication [89]. As a consequence, mice lacking RNase H1 die during embryogenesis [88]. In humans, mutations in RNase H1 have been associated with mitochondrial encephalomyopathy with adult-onset [158]. These examples highlight the importance of removing multiple rNMPs from mtDNA.

Besides stretches of rNMPs, single ribonucleotides are as well incorporated during mtDNA replication. Intriguingly, unlike the nucleus, mitochondria completely lack RNase H2 or other mechanisms for the removal of single rNMPs [159]. As a result, it has been estimated that 30–60 rNMPs persist in each mtDNA molecule of different human and mouse cell lines [38,160]. rNMPs have been mapped in these cells, revealing that they have a random distribution, no strand specificity, and that rAMP is the most frequently found [160,161]. These few single rNMPs may result by the action of the replicative DNA polymerase γ responsible for mtDNA duplication, despite its efficiency in discriminating against rNTPs and in the bypass of previously incorporated rNMPs [37,38]. Anyway, other DNA polymerases seem to contribute to mtDNA replication after DNA damage, like PrimPol [162] pol β, pol ζ, pol η, and pol θ (reviewed in [163]); thus, we cannot exclude a minor contribution of these latter ones in rNMPs incorporation (Figure 2).

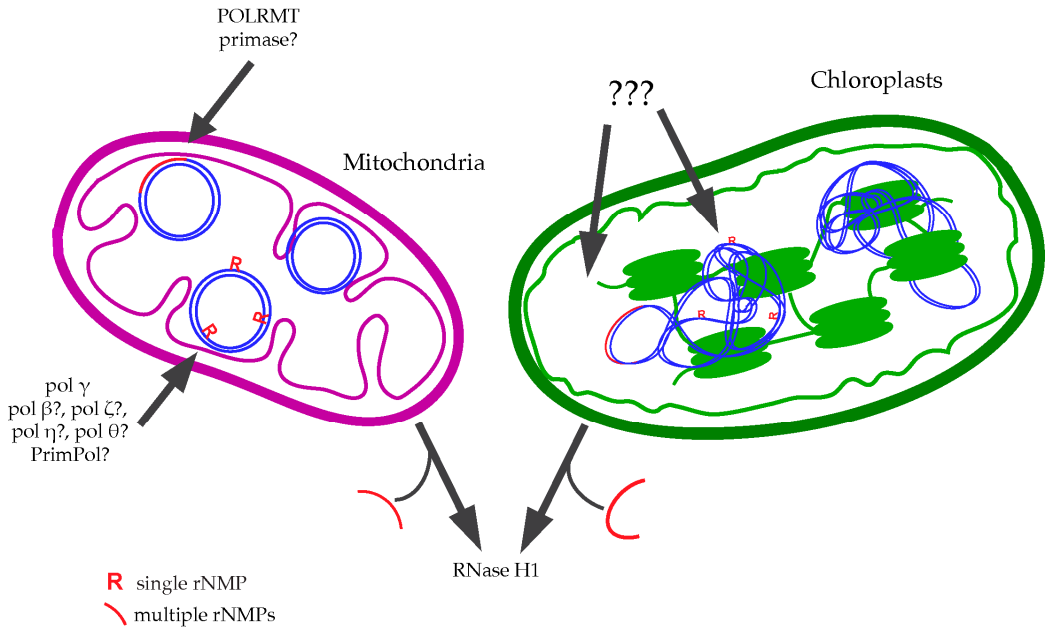

Figure 2. rNMPs incorporation and removal from mitochondrial and chloroplast DNA. Single and multiple ribonucleotides found into the DNA of mitochondria and chloroplasts may result from different sources. Several DNA polymerases might contribute to the incorporation of rNMPs, as demonstrated for pol γ acting on mtDNA. The activity of RNase H1 is essential for processing polyribonucleotide chains synthesized for replication priming, while single rNMPs remain unprocessed due to the absence of RNase H2.

Ribonucleotides have also been observed into the DNA of chloroplasts, the other organelles capable of autonomous replication in plant cells. The chloroplast DNA (cpDNA) consists of linear or circular multicopy molecules of 120–170 kb, which can replicate in different manners (reviewed in [164]). Even if there is still much to learn about rNMPs in the DNA of chloroplasts, it is evident that stretches of multiple rNMPs can compromise cpDNA stability. Apart from RNA tracts used for DNA replication priming, R-loops can be frequently found in these organelles. It has been found that the AtRNaseH1-like protein (RNH1C), together with DNA gyrases, plays a key role in the processing of these hybrids, maintaining chloroplast DNA integrity [165,166]. In addition, also single rNMPs have been observed into the cpDNA of some species of plants, with an estimation of 12–18 rNMPs per molecule [151] (Figure 2). However, the origin, location, and significance of their presence are still unknown, as well as the existence of RNase H2-like enzymes able to remove these structures.

Although rNMPs in mtDNA and cpDNA need to be further explored, their existence in these endosymbiotic organelles is extremely intriguing. This "incorrect" sugar selection comes from ancestral forms of life and is conserved in evolved organisms, suggesting that they have been maintained throughout the evolution to perform physiological functions.

7. Methods to Map and Quantify Ribonucleotides in DNA

At this point, it is clear that RNA can hybridize to DNA in different ways and under different forms, having beneficial but also detrimental effects in cells. It is, therefore, crucial to study and map these structures with precise, quantitative, and reproducible techniques. We have concluded our review with an overview of the most common strategies available for studying in vivo, either single or stretches of rNMPs hybridized with DNA; strong and weak aspects of each method are indicated (Figure 3).

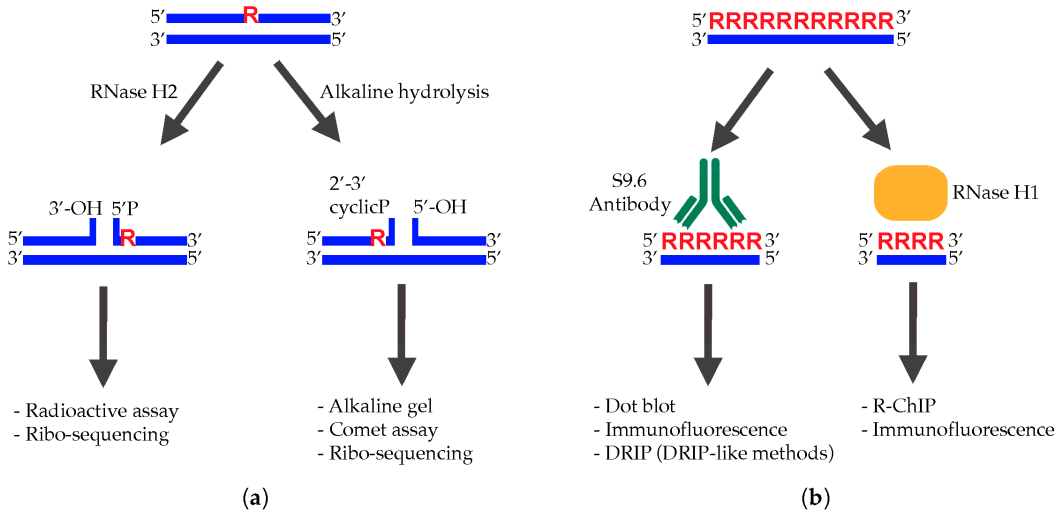

Figure 3. Currently available techniques for studying RNA in DNA. (**a**) The investigation of single ribonucleotides paired with DNA is based on enzymatic or chemical digestion in correspondence of rNMPs to generate single breaks in DNA. Different approaches can then be used to visualize and map the sites of rNMP insertion. (**b**) The main strategies developed to examine stretches of ribonucleotides hybridized with DNA rely on the S9.6 monoclonal antibody or on RNase H1, which allows recognizing RNA:DNA hybrids independently of their sequence. S9.6 binds DNA hybrids of at least 6 bp; RNase H1 detects hybrids of at least 4 bp.

7.1. Single rNMPs Paired with DNA

As mentioned above, the highly reactive 2′-OH group present on the ribose ring of ribonucleotides can attack the adjacent phosphodiester bonds, generating breaks by alkaline hydrolysis [5]. In the presence of a basic solution, the genomic DNA is, therefore, nicked in correspondence of embedded rNMPs, originating fragments that can then be visualized by staining with SYBR Gold or other DNA intercalating dyes, after electrophoresis in alkaline conditions [16,22]. The average size of the fragments correlates with the frequency of rNMPs introduction. Besides this global indication, it is also possible to selectively probe ribonucleotides incorporated into specific regions by Southern blot analysis after digestion with appropriate enzymes. Furthermore, using a strand-specific probe, it is possible to discriminate ribonucleotides incorporated into the leading or lagging replicated-strand [167–169]. Although the alkaline electrophoresis-based approach is widely used, it is very hard to understand whether fragments are exclusively due to embedded rNMPs. Nicks/gaps caused by incomplete replication or nicks generated during DNA manipulation cause the same fragmentation in denaturing conditions. These experiments should, indeed, always be compared with a denaturing condition that does not affect the hydrolysis of ribonucleotides [22].

Similarly, comet assay has also been adapted to measure ribonucleotides embedded into the DNA of human and mouse fibroblasts, as well as in cells collected from patients with SLE and AGS [80]. After nicking the genomic DNA with the bacterial RNase HII, electrophoresis is performed in an alkaline buffer. The migration of the fragmented DNA leads to the formation of comets visualized by fluorescent microscopy after SYBR Gold staining. The length and intensity of the comet tail are proportional to the level of ribonucleotides [170]. Compared to alkaline electrophoresis, the manipulation of the sample is minimal, making the result more reproducible. However, even this technique does not allow distinguishing nicks/gaps from rNMPs.

Hiller et al. [171] were the first to describe another extensively used approach subsequently applied by other groups [68,172]. After extraction, the genomic DNA is treated in vitro with the bacterial RNase HII, which introduces nicks at every site of ribonucleotide incorporation. These nicks

are then radioactively labeled, taking advantage of the DNA polymerase I nick translation capability. The radioactive signal reflects the level of genomic ribonucleotides. With this approach, the advantage is that a comparison of the signals-obtained +/− RNase HII digestion allows discriminating between ribonucleotide-dependent nicks and nicks generated during DNA preparation.

The main limitation of all these approaches, however, is that they are only semi-quantitative and probably only sensitive enough to detect big changes in the ribonucleotide content. Moreover, they sometimes give inconsistent results.

High-throughput sequencing techniques bypassed these limitations, allowing the study of embedded rNMPs with single-nucleotide resolution. This was made possible, thanks to the development of four different strategies: embedded ribonucleotide sequencing (emRiboSeq) [173], hydrolytic end-sequencing (HydEn-seq) [174], ribose-seq [20], and polymerase usage sequencing (Pu-seq) [175]. The genomic DNA is extracted from RNaseH2-defective strains, and it is nicked in the correspondence of the embedded rNMPs. This can be done either enzymatically with RNase H2 [173], or chemically by exploiting alkaline hydrolysis [20,174,175]. Fragments are then ligated to adaptors and sequenced by next generation sequencing (NGS) approaches. Independently of the technique used, raw sequencing data can be analyzed using a novel open-sources software (http://github.com/agombolay/ribose-map) [176]. A similar approach is RADAR-seq (rare damage and repair sequencing) [177]. Here, nicks generated by RNaseH2 are replaced with a patch of modified bases, thanks to a nick translation reaction. The detection of such modified bases by PacBio single molecule, real-time (SMRT) sequencing reveals the location of ribonucleotides [177]. Moreover, by using steric-gate mutants, which incorporate more rNMPs, it has been even possible to assess the precise contribution of replicative and TLS polymerases to DNA replication [20,49,173,174,177]. To date, these approaches have been used in bacteria, archaea, and yeast cells, but they could be adapted to any organism in which RNase H activity can be modulated. They have allowed demonstrating that the rNMPs distribution is non-random and that mitochondrial DNA, Ty regions, and rDNA locus are preferential hotspots [20]. However, all the experiments have been performed in RNase H-deficient strains, where every replication round occurs in the presence of thousands of rNMPs accumulated in the DNA template, which compromises the progression and fidelity of DNA polymerases [19,66]. This could have an influence on the incorporation of rNMPs, masking the real hotspots introduced in a single round of DNA replication. The use of an RNase H conditional mutant [34], which can be switched off just prior to entering the S phase, could be a useful strategy to map the unaffected positions of rNMPs.

Overall, all the strategies described until now exploit the same principle: enzymatic or chemical digestion in correspondence of rNMPs, to generate a single break. This makes it impossible to discriminate between one or several consecutive rNMPs. Indeed, the presence of stretches of embedded ribonucleotides has never been observed. One possibility could be to extract the genomic DNA of RNase H-defective cells and incise only multiple rNMPs with RNase H1 or *RNase H2-RED* [146]. Ribose-sequencing approaches can then be applied. This should avoid the high signal generated by single rNMPs that might mask the signal due to just a few stretches of embedded ribonucleotides.

7.2. Stretches of rNMPs Hybridized with DNA

The main strategies available at the moment to detect multiple ribonucleotides hybridized to DNA rely on the use of the S9.6 monoclonal antibody or on a catalytically inactive version of RNase H1 (reviewed in [178]). Although these tools are massively used to study R-loops, we have to keep in mind that they can recognize any hybrid present in the genome: e.g., R-loops, DNA replication primers, stretches of embedded ribonucleotides, hybrids at DSBs. Moreover, even if with lower affinity, both S9.6 and RNase H1 can also recognize RNA:RNA hybrids [179,180]. In particular, S9.6 binds RNA:DNA hybrids with at least six consecutive ribonucleotides [179], even if the binding affinity seems to be influenced by the sequence context [181]. In addition to S9.6 antibodies, RNA:DNA hybrids can be detected by using the RNase H1 N-terminal hybrid-binding domain (HDB), which can even

recognize stretches made up by just four ribonucleotides [182]. Finally, D5H6 is another antibody able to react with RNA:DNA hybrids [183,184], even if less efficiently, compared to the other systems. Independently of the used tools, treatment with RNase H1 is then essential to prove that the signal obtained is specific for RNA:DNA hybrids.

A first indication about the global level of hybrids present in the genome can be obtained by a dot blot assay [165,185–187], where serial dilutions of genomic DNA are spotted on a membrane and subsequently hybridized with S9.6. Indications about the abundance and localization of RNA:DNA hybrids can also be obtained by immunofluorescence studies. The S9.6 antibody has been extensively used for this purpose [183,188], while Aguilera and colleagues used the HBD of RNase H1 fused with the green fluorescent protein (GFP), forming the so-called HB-GFP [188]. Both these strategies led to the identification of RNA:DNA hybrids in the nucleus of cells, with high intensities detected in the nucleolar region (where the majority of R-loops are formed [117]), as well as in the cytoplasm, possibly because of the abundant RNA:DNA hybrids present in mitochondria.

DNA-RNA immunoprecipitation (DRIP) is currently the most used and accurate technique for mapping genomic RNA:DNA hybrids. It was initially described by the Tollervey's lab [117], and, since then, many variations have been developed (S1-DRIP, bisDRIP, DRIPc, ssDRIP, etc.) [106,189–191]. After chromatin extraction and fragmentation, RNA:DNA hybrids are immunoprecipitated with the S9.6 antibody. The precipitated material is then purified and used for rtPCR reactions, or sequenced, to study the genome-wide distribution of hybrids (DRIP-seq). R-ChIP is a similar approach that uses a catalytically inactive RNase H1, which can still bind hybrids [192,193]. However, the resolution of these techniques depends on the dimension of the immunoprecipitated DNA fragments, and the results obtained are not always reliable. Moreover, probably due to the big number of different protocols available, the results obtained by different groups are sometimes contrasting [194]. Nevertheless, to date, DRIP is considered as the most accurate system to detect and map RNA:DNA hybrids. We have to remember, however, that the latter does not include only R-loops, but any structure in which stretches of RNA anneal to DNA.

8. Concluding Remarks

Although stretches of multiple embedded rNMPs have only been observed in mtDNA, their presence in the nuclear DNA has also been genetically predicted. The persistence of multiple rNMPs in the mitochondrial DNA has been shown to have detrimental effects, and so is suspected for genome-embedded polyribonucleotide chains, with consequences even more severe than those deriving from unprocessed single rNMPs. Different techniques are currently available to study single rNMPs and RNA:DNA hybrids, but further efforts should be made for the development of groundbreaking methods, allowing to isolate only the desired category of RNA:DNA hybrids, and to distinguish sites of single rNMPs insertion from sites with multiple rNMPs. Demonstrating the existence of consecutive embedded rNMPs, and discovering details about their sources and removal, might help to clarify the contribution of the two RNases H in the recognition and processing of all hybrid structures and, importantly, to shed light on the mechanisms linking RNA:DNA hybrid structures, replication stress, genome instability, and severe human pathologies.

Author Contributions: Conceptualization, writing—original draft preparation, G.M.N., L.G., and F.L.; figure preparation S.S.; review and editing, A.P.; supervision and funding acquisition, M.M.F. All authors have read and agreed to the published version of the manuscript.

Funding: The work was supported by ASSOCIAZIONE ITALIANA PER LA RICERCA SUL CANCRO (AIRC), grant number IG21806 to M.M.F. and IG19917 to A.P.; TELETHON, grant number GGP15227 to M.M.F.; and MIUR grant number PRIN-2015LZE994 to A.P. and PRIN-2017KSZZJW_002 to M.M.F.

Acknowledgments: We thank all members of the genome instability and human pathologies lab for critical discussions. Figure 1 was created with BioRender.com.

Conflicts of Interest: The authors declare no conflict of interest.

Abbreviations

AGS	Aicardi–Goutières syndrome
BER	base excision repair
Bis-DRIP	bisulfite DNA:RNA immunoprecipitation
cpDNA	chloroplast DNA
CPDs	cyclobutane pyrimidine dimers
dNMP	deoxyribonucleoside monophosphate
dNTP	deoxyribonucleoside triphosphate
DRIP	DNA:RNA immunoprecipitation sequencing
DRIPc	DNA:RNA Immunoprecipitation followed by cDNA conversion
DSB	double-strand break
emRiboSeq	embedded ribonucleotide sequencing
GFP	green fluorescent protein
HBD	hybrid binding domain
HydEn-seq	hydrolytic end sequencing
mtDNA	mitochondrial DNA
NER	nucleotide excision repair
NHEJ	nonhomologous end-joining
OKFs	Okazaki fragments
PRR	post-replication repair
Pu-seq	polymerase usage sequencing
R-ChIP	R-loop chromatin immunoprecipitation
RADAR-seq	rare damage and repair sequencing
rDNA	ribosomal DNA
RED	ribonucleotide excision defective
RER	ribonucleotide excision repair
RITOLS	ribonucleotide incorporation throughout the lagging strand
RNAi	RNA initiator
RNAPs	RNA polymerases
RNase H	ribonuclease H
rNMP	ribonucleoside monophosphate
RNR	ribonucleotide reductase
rNTP	ribonucleoside triphosphate
S1-DRIP	S1 nuclease DNA:RNA immunoprecipitation
SLE	systemic lupus erythematosus
ssDNA	single-strand DNA
ssDRIP	ssDNA ligation-based library construction from DRIP
TdT	terminal deoxynucleotidyl transferase
TLS	translesion DNA synthesis

References

1. Potenski, C.J.; Klein, H.L. How the misincorporation of ribonucleotides into genomic DNA can be both harmful and helpful to cells. *Nucleic Acids Res.* **2014**, *42*, 10226–10234. [CrossRef]
2. Williams, J.S.; Kunkel, T.A. Ribonucleotides in DNA: Origins, repair and consequences. *DNA Repair (Amst.)* **2014**, *19*, 27–37. [CrossRef]
3. Klein, H.L. Genome instabilities arising from ribonucleotides in DNA. *DNA Repair (Amst.)* **2017**, *56*, 26–32. [CrossRef] [PubMed]
4. Kellner, V.; Luke, B. Molecular and physiological consequences of faulty eukaryotic ribonucleotide excision repair. *EMBO J.* **2019**, e102309. [CrossRef] [PubMed]
5. Li, Y.; Breaker, R.R. Kinetics of RNA degradation by specific base catalysis of transesterification involving the 2′-hydroxyl group. *J. Am. Chem. Soc.* **1999**, *121*, 5364–5372. [CrossRef]
6. Yao, Y.; Dai, W. Genomic Instability and Cancer. *J. Carcinog. Mutagen.* **2014**, *5*, 1–3.

7. Yurov, Y.B.; Vorsanova, S.G.; Iourov, I.Y. Chromosome Instability in the Neurodegenerating Brain. *Front. Genet.* **2019**, *10*. [CrossRef]
8. Kunkel, T.A. DNA Replication Fidelity. *J. Biol. Chem.* **2004**, *279*, 16895–16898. [CrossRef]
9. Yang, W.; Gao, Y. Translesion and Repair DNA Polymerases: Diverse Structure and Mechanism. *Annu. Rev. Biochem.* **2018**, *87*, 239–261. [CrossRef]
10. Joyce, C.M. Choosing the right sugar: How polymerases select a nucleotide substrate. *Proc. Natl. Acad. Sci. USA* **1997**, *94*, 1619–1622. [CrossRef]
11. Brown, J.A.; Suo, Z. Unlocking the sugar "steric gate" of DNA polymerases. *Biochemistry* **2011**, *50*, 1135–1142. [CrossRef] [PubMed]
12. Johnson, M.K.; Kottur, J.; Nair, D.T. A polar filter in DNA polymerases prevents ribonucleotide incorporation. *Nucleic Acids Res.* **2019**, *47*, 10693–10705. [CrossRef] [PubMed]
13. Chabes, A.; Georgieva, B.; Domkin, V.; Zhao, X.; Rothstein, R.; Thelander, L. Survival of DNA damage in yeast directly depends on increased dNTP levels allowed by relaxed feedback inhibition of ribonucleotide reductase. *Cell* **2003**, *112*, 391–401. [CrossRef]
14. Kumar, D.; Viberg, J.; Nilsson, A.K.; Chabes, A. Highly mutagenic and severely imbalanced dNTP pools can escape detection by the S-phase checkpoint. *Nucleic Acids Res.* **2010**, *38*, 3975–3983. [CrossRef]
15. Traut, T.W. Physiological concentrations of purines and pyrimidines. *Mol. Cell. Biochem.* **1994**, *140*, 1–22. [CrossRef] [PubMed]
16. Nick McElhinny, S.A.; Watts, B.E.; Kumar, D.; Watt, D.L.; Lundstrom, E.-B.; Burgers, P.M.J.; Johansson, E.; Chabes, A.; Kunkel, T.A. Abundant ribonucleotide incorporation into DNA by yeast replicative polymerases. *Proc. Natl. Acad. Sci.USA* **2010**, *107*, 4949–4954. [CrossRef]
17. Nick McElhinny, S.A.; Kumar, D.; Clark, A.B.; Watt, D.L.; Watts, B.E.; Lundström, E.B.; Johansson, E.; Chabes, A.; Kunkel, T.A. Genome instability due to ribonucleotide incorporation into DNA. *Nat. Chem. Biol.* **2010**, *6*, 774–781. [CrossRef]
18. Williams, J.S.; Clausen, A.R.; Nick McElhinny, S.A.; Watts, B.E.; Johansson, E.; Kunkel, T.A. Proofreading of ribonucleotides inserted into DNA by yeast DNA polymerase ε. *DNA Repair (Amst.)* **2012**, *11*, 649–656. [CrossRef]
19. Clausen, A.R.; Zhang, S.; Burgers, P.M.; Lee, M.Y.; Kunkel, T.A. Ribonucleotide incorporation, proofreading and bypass by human DNA polymerase δ. *DNA Repair (Amst.)* **2013**, *12*, 121–127. [CrossRef]
20. Koh, K.D.; Balachander, S.; Hesselberth, J.R.; Storici, F. Ribose-seq: Global mapping of ribonucleotides embedded in genomic DNA. *Nat. Methods* **2015**, *12*, 251–257. [CrossRef]
21. Sparks, J.L.; Chon, H.; Cerritelli, S.M.; Kunkel, T.A.; Johansson, E.; Crouch, R.J.; Burgers, P.M. RNase H2-Initiated Ribonucleotide Excision Repair. *Mol. Cell* **2012**, *47*, 980–986. [CrossRef] [PubMed]
22. Reijns, M.A.M.; Rabe, B.; Rigby, R.E.; Mill, P.; Astell, K.R.; Lettice, L.A.; Boyle, S.; Leitch, A.; Keighren, M.; Kilanowski, F.; et al. Enzymatic Removal of Ribonucleotides from DNA Is Essential for Mammalian Genome Integrity and Development. *Cell* **2012**, *149*, 1008–1022. [CrossRef] [PubMed]
23. Lujan, S.A.; Williams, J.S.; Clausen, A.R.; Clark, A.B.; Kunkel, T.A. Ribonucleotides are signals for mismatch repair of leading-strand replication errors. *Mol. Cell* **2013**, *50*, 437–443. [CrossRef] [PubMed]
24. Williams, J.S.; Clausen, A.R.; Lujan, S.A.; Marjavaara, L.; Clark, A.B.; Burgers, P.M.; Chabes, A.; Kunkel, T.A. Evidence that processing of ribonucleotides in DNA by topoisomerase 1 is leading-strand specific. *Nat. Struct. Mol. Biol.* **2015**, *22*, 291–297. [CrossRef]
25. Makarova, A.V.; Nick McElhinny, S.A.; Watts, B.E.; Kunkel, T.A.; Burgers, P.M. Ribonucleotide incorporation by yeast DNA polymerase ζ. *DNA Repair (Amst.)* **2014**, *18*, 63–67. [CrossRef]
26. Bergoglio, V.; Ferrari, E.; Hübscher, U.; Cazaux, C.; Hoffmann, J.S. DNA polymerase β can incorporate ribonucleotides during DNA synthesis of undamaged and CPD-damaged DNA. *J. Mol. Biol.* **2003**, *331*, 1017–1023. [CrossRef]
27. Crespan, E.; Furrer, A.; Rösinger, M.; Bertoletti, F.; Mentegari, E.; Chiapparini, G.; Imhof, R.; Ziegler, N.; Sturla, S.J.; Hübscher, U.; et al. Impact of ribonucleotide incorporation by DNA polymerases β and λ on oxidative base excision repair. *Nat. Commun.* **2016**, *7*, 10805. [CrossRef]
28. Nick McElhinny, S.A.; Ramsden, D.A. Polymerase Mu Is a DNA-Directed DNA/RNA Polymerase. *Mol. Cell. Biol.* **2003**, *23*, 2309–2315. [CrossRef]
29. Martin, M.J.; Garcia-Ortiz, M.V.; Esteban, V.; Blanco, L. Ribonucleotides and manganese ions improve non-homologous end joining by human Polμ. *Nucleic Acids Res.* **2013**, *41*, 2428–2436. [CrossRef]

30. Pryor, J.M.; Conlin, M.P.; Carvajal-Garcia, J.; Luedeman, M.E.; Luthman, A.J.; Small, G.W.; Ramsden, D.A. Ribonucleotide incorporation enables repair of chromosome breaks by nonhomologous end joining. *Science* **2018**, *361*, 1126–1129. [CrossRef]
31. Boulé, J.B.; Rougeon, F.; Papanicolaou, C. Terminal Deoxynucleotidyl Transferase Indiscriminately Incorporates Ribonucleotides and Deoxyribonucleotides. *J. Biol. Chem.* **2001**, *276*, 31388–31393. [CrossRef]
32. Su, Y.; Egli, M.; Guengerich, F.P. Mechanism of ribonucleotide incorporation by human DNA polymerase η. *J. Biol. Chem.* **2016**, *291*, 3747–3756. [CrossRef]
33. Mentegari, E.; Crespan, E.; Bavagnoli, L.; Kissova, M.; Bertoletti, F.; Sabbioneda, S.; Imhof, R.; Sturla, S.J.; Nilforoushan, A.; Hübscher, U.; et al. Ribonucleotide incorporation by human DNA polymerase η impacts translesion synthesis and RNase H2 activity. *Nucleic Acids Res.* **2017**, *45*, 2600–2614. [CrossRef]
34. Meroni, A.; Nava, G.M.; Bianco, E.; Grasso, L.; Galati, E.; Bosio, M.C.; Delmastro, D.; Muzi-Falconi, M.; Lazzaro, F. RNase H activities counteract a toxic effect of Polymerase eta in cells replicating with depleted dNTP pools. *Nucleic Acids Res.* **2019**, *47*, 4612–4623. [CrossRef]
35. Donigan, K.A.; McLenigan, M.P.; Yang, W.; Goodman, M.F.; Woodgate, R. The steric gate of DNA polymerase ι regulates ribonucleotide incorporation and deoxyribonucleotide fidelity. *J. Biol. Chem.* **2014**, *289*, 9136–9145. [CrossRef] [PubMed]
36. Brown, J.A.; Fowler, J.D.; Suo, Z. Kinetic basis of nucleotide selection employed by a protein template-dependent DNA polymerase. *Biochemistry* **2010**, *49*, 5504–5510. [CrossRef] [PubMed]
37. Kasiviswanathan, R.; Copeland, W.C. Ribonucleotide discrimination and reverse transcription by the human mitochondrial DNA polymerase. *J. Biol. Chem.* **2011**, *286*, 31490–31500. [CrossRef] [PubMed]
38. Forslund, J.M.E.; Pfeiffer, A.; Stojkovič, G.; Wanrooij, P.H.; Wanrooij, S. The presence of rNTPs decreases the speed of mitochondrial DNA replication. *PLoS Genet.* **2018**, *14*, e1007315. [CrossRef]
39. Kent, T.; Mateos-Gomez, P.A.; Sfeir, A.; Pomerantz, R.T. Polymerase θ is a robust terminal transferase that oscillates between three different mechanisms during end-joining. *Elife* **2016**, *5*, 1–25. [CrossRef] [PubMed]
40. García-Gómez, S.; Reyes, A.; Martínez-Jiménez, M.I.; Chocrón, E.S.; Mourón, S.; Terrados, G.; Powell, C.; Salido, E.; Méndez, J.; Holt, I.J.; et al. PrimPol, an Archaic Primase/Polymerase Operating in Human Cells. *Mol. Cell* **2013**, *52*, 541–553. [CrossRef]
41. Ogi, T.; Limsirichaikul, S.; Overmeer, R.M.; Volker, M.; Takenaka, K.; Cloney, R.; Nakazawa, Y.; Niimi, A.; Miki, Y.; Jaspers, N.G.; et al. Three DNA Polymerases, Recruited by Different Mechanisms, Carry Out NER Repair Synthesis in Human Cells. *Mol. Cell* **2010**, *37*, 714–727. [CrossRef] [PubMed]
42. Vaisman, A.; Woodgate, R. Ribonucleotide discrimination by translesion synthesis DNA polymerases. *Crit. Rev. Biochem. Mol. Biol.* **2018**, *53*, 382–402. [CrossRef] [PubMed]
43. Hübscher, U.; Maga, G. DNA replication and repair bypass machines. *Curr. Opin. Chem. Biol.* **2011**, *15*, 627–635. [CrossRef] [PubMed]
44. Jain, R.; Aggarwal, A.K.; Rechkoblit, O. Eukaryotic DNA polymerases. *Curr Opin Struct Biol.* **2018**, *53*, 77–87. [CrossRef] [PubMed]
45. Ruiz, J.F.; Juárez, R.; García-Díaz, M.; Terrados, G.; Picher, A.J.; González-Barrera, S.; Fernández de Henestrosá, A.R.; Blanco, L. Lack of sugar discrimination by human Pol μ requires a single glycine residue. *Nucleic Acids Res.* **2003**, *31*, 4441–4449. [CrossRef] [PubMed]
46. Komori, T.; Okada, A.; Stewart, V.; Alt, F. Lack of N regions in antigen receptor variable region genes of TdT-deficient lymphocytes. *Science* **1993**, *261*, 1171–1175. [CrossRef] [PubMed]
47. Gilfillan, S.; Dierich, A.; Lemeur, M.; Benoist, C.; Mathis, D. Mice lacking TdT: Mature animals with an immature lymphocyte repertoire. *Science* **1993**, *261*, 1175–1178. [CrossRef]
48. Donigan, K.A.; Cerritelli, S.M.; McDonald, J.P.; Vaisman, A.; Crouch, R.J.; Woodgate, R. Unlocking the steric gate of DNA polymerase η leads to increased genomic instability in Saccharomyces cerevisiae. *DNA Repair (Amst.)* **2015**, *35*, 1–12. [CrossRef]
49. Kreisel, K.; Engqvist, M.K.M.; Kalm, J.; Thompson, L.J.; Boström, M.; Navarrete, C.; McDonald, J.P.; Larsson, E.; Woodgate, R.; Clausen, A.R. DNA polymerase η contributes to genome-wide lagging strand synthesis. *Nucleic Acids Res.* **2019**, *47*, 2425–2435. [CrossRef]
50. Kent, T.; Chandramouly, G.; McDevitt, S.M.; Ozdemir, A.Y.; Pomerantz, R.T. Mechanism of microhomology-mediated end-joining promoted by human DNA polymerase θ. *Nat. Struct. Mol. Biol.* **2015**, *22*, 230–237. [CrossRef]

51. Zahn, K.E.; Averill, A.M.; Aller, P.; Wood, R.D.; Doublié, S. Human DNA polymerase θ grasps the primer terminus to mediate DNA repair. *Nat. Struct. Mol. Biol.* **2015**, *22*, 304–311. [CrossRef] [PubMed]
52. Cilli, P.; Minoprio, A.; Bossa, C.; Bignami, M.; Mazzei, F. Formation and repair of mismatches containing ribonucleotides and oxidized bases at repeated DNA sequences. *J. Biol. Chem.* **2015**, *290*, 26259–26269. [CrossRef] [PubMed]
53. Mao, Z.; Bozzella, M.; Seluanov, A.; Gorbunova, V. DNA repair by nonhomologous end joining and homologous recombination during cell cycle in human cells. *Cell Cycle* **2008**, *7*, 2902–2906. [CrossRef] [PubMed]
54. Soria, G.; Belluscio, L.; Van Cappellen, W.A.; Kanaar, R.; Essers, J.; Gottifredi, V. DNA damage induced Pol η recruitment takes place independently of the cell cycle phase. *Cell Cycle* **2009**, *8*, 3340–3348. [CrossRef]
55. Diamant, N.; Hendel, A.; Vered, I.; Carell, T.; Reißner, T.; De Wind, N.; Geacinov, N.; Livneh, Z. DNA damage bypass operates in the S and G2 phases of the cell cycle and exhibits differential mutagenicity. *Nucleic Acids Res.* **2012**, *40*, 170–180. [CrossRef]
56. Sertic, S.; Mollica, A.; Campus, I.; Roma, S.; Tumini, E.; Aguilera, A.; Muzi-Falconi, M. Coordinated Activity of Y Family TLS Polymerases and EXO1 Protects Non-S Phase Cells from UV-Induced Cytotoxic Lesions. *Mol. Cell* **2018**, *70*, 34–47. [CrossRef]
57. Zhuo, M.; Gorgun, M.F.; Englander, E.W. Translesion Synthesis DNA Polymerase Kappa Is Indispensable for DNA Repair Synthesis in Cisplatin Exposed Dorsal Root Ganglion Neurons. *Mol. Neurobiol.* **2018**, *55*, 2506–2515. [CrossRef]
58. Ghodgaonkar, M.M.; Lazzaro, F.; Olivera-Pimentel, M.; Artola-Borán, M.; Cejka, P.; Reijns, M.A.; Jackson, A.P.; Plevani, P.; Muzi-Falconi, M.; Jiricny, J. Ribonucleotides misincorporated into DNA act as strand-discrimination signals in eukaryotic mismatch repair. *Mol. Cell* **2013**, *50*, 323–332. [CrossRef]
59. Egli, M.; Usman, N.; Rich, A. Conformational influence of the ribose 2'-hydroxyl group: Crystal structures of DNA-RNA chimeric duplexes. *Biochemistry* **1993**, *32*, 3221–3237. [CrossRef]
60. Derose, E.F.; Perera, L.; Murray, M.S.; Kunkel, T.A.; London, R.E. Solution structure of the Dickerson DNA dodecamer containing a single ribonucleotide. *Biochemistry* **2012**, *51*, 2407–2416. [CrossRef]
61. Chiu, H.-C.; Koh, K.D.; Evich, M.; Lesiak, A.L.; Germann, M.W.; Bongiorno, A.; Riedo, E.; Storici, F. RNA intrusions change DNA elastic properties and structure. *Nanoscale* **2014**, *6*, 10009–10017. [CrossRef] [PubMed]
62. Meroni, A.; Mentegari, E.; Crespan, E.; Muzi-Falconi, M.; Lazzaro, F.; Podestà, A. The Incorporation of Ribonucleotides Induces Structural and Conformational Changes in DNA. *Biophys. J.* **2017**, *113*, 1373–1382. [CrossRef] [PubMed]
63. Hovatter, K.R.; Martinson, H.G. Ribonucleotide-induced helical alteration in DNA prevents nucleosome formation. *Proc. Natl. Acad. Sci. USA* **1987**, *84*, 1162–1166. [CrossRef] [PubMed]
64. Fu, I.; Smith, D.J.; Broyde, S. Rotational and translational positions determine the structural and dynamic impact of a single ribonucleotide incorporated in the nucleosome. *DNA Repair (Amst.)* **2019**, *73*, 155–163. [CrossRef] [PubMed]
65. Watt, D.L.; Johansson, E.; Burgers, P.M.; Kunkel, T.A. Replication of ribonucleotide-containing DNA templates by yeast replicative polymerases. *DNA Repair (Amst.)* **2011**, *10*, 897–902. [CrossRef] [PubMed]
66. Lazzaro, F.; Novarina, D.; Amara, F.; Watt, D.L.; Stone, J.E.; Costanzo, V.; Burgers, P.M.; Kunkel, T.A.; Plevani, P.; Muzi-Falconi, M. RNase H and postreplication repair protect cells from ribonucleotides incorporated in DNA. *Mol. Cell* **2012**, *45*, 99–110. [CrossRef]
67. Clausen, A.R.; Murray, M.S.; Passer, A.R.; Pedersen, L.C.; Kunkel, T.A. Structure-function analysis of ribonucleotide bypass by B family DNA replicases. *Proc. Natl. Acad. Sci. USA* **2013**, *110*, 16802–16807. [CrossRef]
68. Pizzi, S.; Sertic, S.; Orcesi, S.; Cereda, C.; Bianchi, M.; Jackson, A.P.; Lazzaro, F.; Plevani, P.; Muzi-Falconi, M. Reduction of hRNase H2 activity in Aicardi-Goutières syndrome cells leads to replication stress and genome instability. *Hum. Mol. Genet.* **2015**, *24*, 649–658. [CrossRef]
69. Cerritelli, S.M.; Crouch, R.J. Ribonuclease H: The enzymes in eukaryotes. *FEBS J.* **2009**, *276*, 1494–1505. [CrossRef]
70. Uehara, R.; Cerritelli, S.M.; Hasin, N.; Sakhuja, K.; London, M.; Iranzo, J.; Chon, H.; Grinberg, A.; Crouch, R.J. Two RNase H2 Mutants with Differential rNMP Processing Activity Reveal a Threshold of Ribonucleotide Tolerance for Embryonic Development. *Cell Rep.* **2018**, *25*, 1135–1145. [CrossRef]

71. Potenski, C.J.; Niu, H.; Sung, P.; Klein, H.L. Avoidance of ribonucleotide-induced mutations by RNase H2 and Srs2-Exo1 mechanisms. *Nature* **2014**, *511*, 251–254. [CrossRef] [PubMed]
72. Williams, J.S.; Smith, D.J.; Marjavaara, L.; Lujan, S.A.; Chabes, A.; Kunkel, T.A. Topoisomerase 1-Mediated Removal of Ribonucleotides from Nascent Leading-Strand DNA. *Mol. Cell* **2013**, *49*, 1010–1015. [CrossRef] [PubMed]
73. Sekiguchi, J.A.; Shuman, S. Site-specific ribonuclease activity of eukaryotic DNA topoisomerase I. *Mol. Cell* **1997**, *1*, 89–97. [CrossRef]
74. Kim, N.; Huang, S.-y. N.; Williams, J.S.; Li, Y.C.; Clark, A.B.; Cho, J.-E.; Kunkel, T.A.; Pommier, Y.; Jinks-Robertson, S. Mutagenic Processing of Ribonucleotides in DNA by Yeast Topoisomerase I. *Science* **2011**, *332*, 1561–1564. [CrossRef]
75. Sparks, J.L.; Burgers, P.M. Error-free and mutagenic processing of topoisomerase 1-provoked damage at genomic ribonucleotides. *EMBO J.* **2015**, *34*, 1259–1269. [CrossRef]
76. Cho, J.E.; Huang, S.Y.N.; Burgers, P.M.; Shuman, S.; Pommier, Y.; Jinks-Robertson, S. Parallel analysis of ribonucleotide-dependent deletions produced by yeast Top1 in vitro and in vivo. *Nucleic Acids Res.* **2016**, *44*, 7714–7721. [CrossRef]
77. Zimmermann, M.; Murina, O.; Reijns, M.A.M.; Agathanggelou, A.; Challis, R.; Tarnauskaitė, Ž.; Muir, M.; Fluteau, A.; Aregger, M.; McEwan, A.; et al. CRISPR screens identify genomic ribonucleotides as a source of PARP-trapping lesions. *Nature* **2018**, *559*, 285–289. [CrossRef]
78. Crow, Y.J.; Leitch, A.; Hayward, B.E.; Garner, A.; Parmar, R.; Griffith, E.; Ali, M.; Semple, C.; Aicardi, J.; Babul-Hirji, R.; et al. Mutations in genes encoding ribonuclease H2 subunits cause Aicardi-Goutières syndrome and mimic congenital viral brain infection. *Nat. Genet.* **2006**, *38*, 910–916. [CrossRef]
79. Livingston, J.; Crow, Y. Neurologic Phenotypes Associated with Mutations in TREX1, RNASEH2A, RNASEH2B, RNASEH2C, SAMHD1, ADAR1, and IFIH1: Aicardi–Goutières Syndrome and Beyond. *Neuropediatrics* **2016**, *47*, 355–360.
80. Günther, C.; Kind, B.; Reijns, M.A.M.; Berndt, N.; Martinez-Bueno, M.; Wolf, C.; Tüngler, V.; Chara, O.; Lee, Y.A.; Hübner, N.; et al. Defective removal of ribonucleotides from DNA promotes systemic autoimmunity. *J. Clin. Invest.* **2015**, *125*, 413–424. [CrossRef]
81. Rice, G.; Patrick, T.; Parmar, R.; Taylor, C.F.; Aeby, A.; Aicardi, J.; Artuch, R.; Montalto, S.A.; Bacino, C.A.; Barroso, B.; et al. Clinical and molecular phenotype of Aicardi-Goutières syndrome. *Am. J. Hum. Genet.* **2007**, *81*, 713–725. [CrossRef] [PubMed]
82. Crow, Y.J.; Livingston, J.H. Aicardi-Goutières syndrome: An important Mendelian mimic of congenital infection. *Dev. Med. Child Neurol.* **2008**, *50*, 410–416. [CrossRef] [PubMed]
83. Shah, S.P.; Morin, R.D.; Khattra, J.; Prentice, L.; Pugh, T.; Burleigh, A.; Delaney, A.; Gelmon, K.; Guliany, R.; Senz, J.; et al. Mutational evolution in a lobular breast tumour profiled at single nucleotide resolution. *Nature* **2009**, *461*, 809–813. [CrossRef]
84. Williams, K.A.; Lee, M.; Hu, Y.; Andreas, J.; Patel, S.J.; Zhang, S.; Chines, P.; Elkahloun, A.; Chandrasekharappa, S.; Gutkind, J.S.; et al. A Systems Genetics Approach Identifies CXCL14, ITGAX, and LPCAT2 as Novel Aggressive Prostate Cancer Susceptibility Genes. *PLoS Genet.* **2014**, *10*, e1004809. [CrossRef] [PubMed]
85. Mottaghi-Dastjerdi, N.; Soltany-Rezaee-Rad, M.; Sepehrizadeh, Z.; Roshandel, G.; Ebrahimifard, F.; Setayesh, N. Identification of novel genes involved in gastric carcinogenesis by suppression subtractive hybridization. *Hum. Exp. Toxicol.* **2015**, *34*, 3–11. [CrossRef]
86. Dai, B.; Zhang, P.; Zhang, Y.; Pan, C.; Meng, G.; Xiao, X.; Wu, Z.; Wang, J.; Zhang, J.; Zhang, L. RNaseH2A is involved in human gliomagenesis through the regulation of cell proliferation and apoptosis. *Oncol. Rep.* **2016**, *36*, 173–180. [CrossRef]
87. Beyer, U.; Brand, F.; Martens, H.; Weder, J.; Christians, A.; Elyan, N.; Hentschel, B.; Westphal, M.; Schackert, G.; Pietsch, T.; et al. Rare ADAR and RNASEH2B variants and a type I interferon signature in glioma and prostate carcinoma risk and tumorigenesis. *Acta Neuropathol.* **2017**, *134*, 905–922. [CrossRef]
88. Cerritelli, S.M.; Frolova, E.G.; Feng, C.; Grinberg, A.; Love, P.E.; Crouch, R.J. Failure to Produce Mitochondrial DNA Results in Embryonic Lethality in Rnaseh1 Null Mice. *Mol. Cell* **2003**, *11*, 807–815. [CrossRef]
89. Holmes, J.B.; Akman, G.; Wood, S.R.; Sakhuja, K.; Cerritelli, S.M.; Moss, C.; Bowmaker, M.R.; Jacobs, H.T.; Crouch, R.J.; Holt, I.J. Primer retention owing to the absence of RNase H1 is catastrophic for mitochondrial DNA replication. *Proc. Natl. Acad. Sci. USA.* **2015**, *112*, 9334–9339. [CrossRef]

90. Jin, Y.H.; Ayyagari, R.; Resnick, M.A.; Gordeni, D.A.; Burgers, P.M.J. Okazaki fragment maturation in yeast: II. Cooperation between the polymerase and 3′-5′-exonuclease activities of Pol δ in the creation of a ligatable nick. *J. Biol. Chem.* **2003**, *278*, 1626–1633. [CrossRef]
91. Balakrishnan, L.; Bambara, R.A. Okazaki Fragment Metabolism. *Cold Spring Harb. Perspect. Biol.* **2013**, *5*, a010173. [CrossRef] [PubMed]
92. Giannattasio, M.; Branzei, D. DNA Replication Through Strand Displacement During Lagging Strand DNA Synthesis in Saccharomyces cerevisiae. *Genes (Basel)* **2019**, *10*, 167. [CrossRef] [PubMed]
93. Bambara, R.A.; Murante, R.S.; Henricksen, L.A. Enzymes and reactions at the eukaryotic DNA replication fork. *J. Biol. Chem.* **1997**, *272*, 4647–4650. [CrossRef] [PubMed]
94. Liu, Y.; Kao, H.-I.; Bambara, R.A. Flap Endonuclease 1: A Central Component of DNA Metabolism. *Annu. Rev. Biochem.* **2004**, *73*, 589–615. [CrossRef] [PubMed]
95. Kahli, M.; Osmundson, J.S.; Yeung, R.; Smith, D.J. Processing of eukaryotic Okazaki fragments by redundant nucleases can be uncoupled from ongoing DNA replication in vivo. *Nucleic Acids Res.* **2019**, *47*, 1814–1822. [CrossRef] [PubMed]
96. Bae, S.H.; Bae, K.H.; Kim, J.A.; Seo, Y.S. RPA governs endonuclease switching during processing of Okazaki fragments in eukaryotes. *Nature* **2001**, *412*, 456–461. [CrossRef] [PubMed]
97. Liu, B.; Hu, J.; Wang, J.; Kong, D. Direct visualization of RNA-DNA primer removal from okazaki fragments provides support for flap cleavage and exonucleolytic pathways in eukaryotic cells. *J. Biol. Chem.* **2017**, *292*, 4777–4788. [CrossRef]
98. Chang, E.Y.-C.; Tsai, S.; Aristizabal, M.J.; Wells, J.P.; Coulombe, Y.; Busatto, F.F.; Chan, Y.A.; Kumar, A.; Dan Zhu, Y.; Wang, A.Y.-H.; et al. MRE11-RAD50-NBS1 promotes Fanconi Anemia R-loop suppression at transcription–replication conflicts. *Nat. Commun.* **2019**, *10*, 4265. [CrossRef]
99. Johnston, L.H.; Nasmyth, K. Saccharomyces cerevisiae cell cycle mutant cdc9 is defective in DNA ligase. *Nature* **1978**, *274*, 891–893. [CrossRef]
100. Gordenin, D.A.; Kunkel, T.A.; Resnick, M.A. Repeat expansion-All in a flap? *Nat. Genet.* **1997**, *16*, 116–118. [CrossRef]
101. Epshtein, A.; Potenski, C.J.; Klein, H.L. Increased spontaneous recombination in rnase H2-deficient cells arises from multiple contiguous rnmps and not from single rNMP residues incorporated by DNA polymerase epsilon. *Microb. Cell* **2016**, *3*, 248–254. [CrossRef] [PubMed]
102. Vengrova, S.; Dalgaard, J.Z. RNase-sensitive DNA modification(s) initiates S. pombe mating-type switching. *Genes Dev.* **2004**, *18*, 794–804. [CrossRef]
103. Vengrova, S.; Dalgaard, J.Z. The wild-type Schizosaccharomyces pombe mat1 imprint consists of two ribonucleotides. *EMBO Rep.* **2006**, *7*, 59–65. [CrossRef] [PubMed]
104. Thomas, M.; White, R.L.; Davis, R.W. Hybridization of RNA to double-stranded DNA: Formation of R-loops. *Proc. Natl. Acad. Sci. USA* **1976**, *73*, 2294–2298. [CrossRef] [PubMed]
105. Westover, K.D.; Bushnell, D.A.; Kornberg, R.D. Structural basis of transcription: Nucleotide selection by rotation in the RNA polymerase II active center. *Cell* **2004**, *119*, 481–489. [CrossRef] [PubMed]
106. Wahba, L.; Costantino, L.; Tan, F.J.; Zimmer, A.; Koshland, D. S1-DRIP-seq identifies high expression and polyA tracts as major contributors to R-loop formation. *Genes Dev.* **2016**, *30*, 1327–1338. [CrossRef] [PubMed]
107. Ginno, P.A.; Lott, P.L.; Christensen, H.C.; Korf, I.; Chédin, F. R-Loop Formation Is a Distinctive Characteristic of Unmethylated Human CpG Island Promoters. *Mol. Cell* **2012**, *45*, 814–825. [CrossRef] [PubMed]
108. Castellano-Pozo, M.; Santos-Pereira, J.; Rondón, A.G.; Barroso, S.; Andújar, E.; Pérez-Alegre, M.; García-Muse, T.; Aguilera, A. R loops are linked to histone H3 S10 phosphorylation and chromatin condensation. *Mol. Cell* **2013**, *52*, 583–590. [CrossRef]
109. Hamperl, S.; Cimprich, K.A. The contribution of co-transcriptional RNA: DNA hybrid structures to DNA damage and genome instability. *DNA Repair (Amst.)* **2014**, *19*, 84–94. [CrossRef]
110. Gan, W.; Guan, Z.; Liu, J.; Gui, T.; Shen, K.; Manley, J.L.; Li, X. R-loop-mediated genomic instability is caused by impairment of replication fork progression. *Genes Dev.* **2011**, *25*, 2041–2056. [CrossRef]
111. Costantino, L.; Koshland, D. Genome-wide Map of R-Loop-Induced Damage Reveals How a Subset of R-Loops Contributes to Genomic Instability. *Mol. Cell* **2018**, *71*, 487–497. [CrossRef] [PubMed]
112. Skourti-Stathaki, K.; Proudfoot, N.J. A double-edged sword: R loops as threats to genome integrity and powerful regulators of gene expression. *Genes Dev.* **2014**, *28*, 1384–1396. [CrossRef]

113. Costantino, L.; Koshland, D. The Yin and Yang of R-loop biology. *Curr. Opin. Cell Biol.* **2015**, *34*, 39–45. [CrossRef] [PubMed]
114. Huertas, P.; Aguilera, A. Cotranscriptionally formed DNA:RNA hybrids mediate transcription elongation impairment and transcription-associated recombination. *Mol. Cell* **2003**, *12*, 711–721. [CrossRef] [PubMed]
115. García-Benítez, F.; Gaillard, H.; Aguilera, A. Physical proximity of chromatin to nuclear pores prevents harmful R loop accumulation contributing to maintain genome stability. *Proc. Natl. Acad. Sci. USA* **2017**, *114*, 10942–10947. [CrossRef] [PubMed]
116. Tuduri, S.; Crabbé, L.; Conti, C.; Tourrière, H.; Holtgreve-Grez, H.; Jauch, A.; Pantesco, V.; De Vos, J.; Thomas, A.; Theillet, C.; et al. Topoisomerase I suppresses genomic instability by preventing interference between replication and transcription. *Nat. Cell Biol.* **2009**, *11*, 1315–1324. [CrossRef]
117. El Hage, A.; French, S.L.; Beyer, A.L.; Tollervey, D. Loss of Topoisomerase I leads to R-loop-mediated transcriptional blocks during ribosomal RNA synthesis. *Genes Dev.* **2010**, *24*, 1546–1558. [CrossRef]
118. Mischo, H.E.; Gómez-González, B.; Grzechnik, P.; Rondón, A.G.; Wei, W.; Steinmetz, L.; Aguilera, A.; Proudfoot, N.J. Yeast Sen1 helicase protects the genome from transcription-associated instability. *Mol. Cell* **2011**, *41*, 21–32. [CrossRef]
119. Chakraborty, P.; Grosse, F. Human DHX9 helicase preferentially unwinds RNA-containing displacement loops (R-loops) and G-quadruplexes. *DNA Repair (Amst.)* **2011**, *10*, 654–665. [CrossRef]
120. Boulé, J.-B.; Zakian, V.A. The yeast Pif1p DNA helicase preferentially unwinds RNA DNA substrates. *Nucleic Acids Res.* **2007**, *35*, 5809–5818. [CrossRef]
121. Wahba, L.; Gore, S.K.; Koshland, D. The homologous recombination machinery modulates the formation of RNA–DNA hybrids and associated chromosome instability. *Elife* **2013**, *2*, e00505. [CrossRef] [PubMed]
122. Kogoma, T. A novel Escherichia coli mutant capable of DNA replication in the absence of protein synthesis. *J. Mol. Biol.* **1978**, *121*, 55–69. [CrossRef]
123. Kogoma, T.; Maldonado, R.R. DNA polymerase I in constitutive stable DNA replication in Escherichia coli. *J. Bacteriol.* **1997**, *179*, 2109–2115. [CrossRef] [PubMed]
124. Pomerantz, R.T.; O'Donnell, M. The replisome uses mRNA as a primer after colliding with RNA polymerase. *Nature* **2008**, *456*, 762–766. [CrossRef]
125. Stuckey, R.; García-Rodríguez, N.; Aguilera, A.; Wellinger, R.E. Role for RNA:DNA hybrids in origin-independent replication priming in a eukaryotic system. *Proc. Natl. Acad. Sci. USA* **2015**, *112*, 5779–5784. [CrossRef]
126. Puget, N.; Miller, K.M.; Legube, G. Non-canonical DNA/RNA structures during Transcription-Coupled Double-Strand Break Repair: Roadblocks or Bona fide repair intermediates? *DNA Repair (Amst.)* **2019**, *81*, 102661. [CrossRef]
127. Jimeno, S.; Prados-Carvajal, R.; Huertas, P. The role of RNA and RNA-related proteins in the regulation of DNA double strand break repair pathway choice. *DNA Repair (Amst.)* **2019**, *81*, 102662. [CrossRef]
128. Bader, A.S.; Hawley, B.R.; Wilczynska, A.; Bushell, M. The roles of RNA in DNA double-strand break repair. *Br. J. Cancer* **2020**, 613–623. [CrossRef]
129. Meers, C.; Keskin, H.; Storici, F. DNA repair by RNA: Templated, or not templated, that is the question. *DNA Repair (Amst.)* **2016**, *44*, 17–21. [CrossRef]
130. Francia, S.; Michelini, F.; Saxena, A.; Tang, D.; De Hoon, M.; Anelli, V.; Mione, M.; Carninci, P.; D'adda Di Fagagna, F. Site-specific DICER and DROSHA RNA products control the DNA-damage response. *Nature* **2012**, *488*, 231–235. [CrossRef]
131. Li, L.; Germain, D.R.; Poon, H.-Y.; Hildebrandt, M.R.; Monckton, E.A.; McDonald, D.; Hendzel, M.J.; Godbout, R. DEAD Box 1 Facilitates Removal of RNA and Homologous Recombination at DNA Double-Strand Breaks. *Mol. Cell. Biol.* **2016**, *36*, 2794–2810. [CrossRef] [PubMed]
132. Ohle, C.; Tesorero, R.; Schermann, G.; Dobrev, N.; Sinning, I.; Fischer, T. Transient RNA-DNA Hybrids Are Required for Efficient Double-Strand Break Repair. *Cell* **2016**, *167*, 1001–1013. [CrossRef] [PubMed]
133. Brustel, J.; Kozik, Z.; Gromak, N.; Savic, V.; Sweet, S.M.M. Large XPF-dependent deletions following misrepair of a DNA double strand break are prevented by the RNA:DNA helicase Senataxin. *Sci. Rep.* **2018**, *8*, 3850. [CrossRef] [PubMed]
134. Cohen, S.; Puget, N.; Lin, Y.L.; Clouaire, T.; Aguirrebengoa, M.; Rocher, V.; Pasero, P.; Canitrot, Y.; Legube, G. Senataxin resolves RNA:DNA hybrids forming at DNA double-strand breaks to prevent translocations. *Nat. Commun.* **2018**, *9*, 533. [CrossRef]

135. D'Alessandro, G.; Whelan, D.R.; Howard, S.M.; Vitelli, V.; Renaudin, X.; Adamowicz, M.; Iannelli, F.; Jones-Weinert, C.W.; Lee, M.; Matti, V.; et al. BRCA2 controls DNA:RNA hybrid level at DSBs by mediating RNase H2 recruitment. *Nat. Commun.* **2018**, *9*, 5376. [CrossRef]
136. Lu, W.-T.; Hawley, B.R.; Skalka, G.L.; Baldock, R.A.; Smith, E.M.; Bader, A.S.; Malewicz, M.; Watts, F.Z.; Wilczynska, A.; Bushell, M. Drosha drives the formation of DNA:RNA hybrids around DNA break sites to facilitate DNA repair. *Nat. Commun.* **2018**, *9*, 532. [CrossRef]
137. Yasuhara, T.; Kato, R.; Hagiwara, Y.; Shiotani, B.; Yamauchi, M.; Nakada, S.; Shibata, A.; Miyagawa, K. Human Rad52 Promotes XPG-Mediated R-loop Processing to Initiate Transcription-Associated Homologous Recombination Repair. *Cell* **2018**, *175*, 558–570. [CrossRef]
138. Alfano, L.; Caporaso, A.; Altieri, A.; Dell'Aquila, M.; Landi, C.; Bini, L.; Pentimalli, F.; Giordano, A. Depletion of the RNA binding protein HNRNPD impairs homologous recombination by inhibiting DNA-end resection and inducing R-loop accumulation. *Nucleic Acids Res.* **2019**, *47*, 4068–4085. [CrossRef]
139. Domingo-Prim, J.; Endara-Coll, M.; Bonath, F.; Jimeno, S.; Prados-Carvajal, R.; Friedländer, M.R.; Huertas, P.; Visa, N. EXOSC10 is required for RPA assembly and controlled DNA end resection at DNA double-strand breaks. *Nat. Commun.* **2019**, *10*, 2135. [CrossRef]
140. Burger, K.; Schlackow, M.; Gullerova, M. Tyrosine kinase c-Abl couples RNA polymerase II transcription to DNA double-strand breaks. *Nucleic Acids Res.* **2019**, *47*, 3467–3484. [CrossRef]
141. Pessina, F.; Giavazzi, F.; Yin, Y.; Gioia, U.; Vitelli, V.; Galbiati, A.; Barozzi, S.; Garre, M.; Oldani, A.; Flaus, A.; et al. Functional transcription promoters at DNA double-strand breaks mediate RNA-driven phase separation of damage-response factors. *Nat. Cell Biol.* **2019**, *21*, 1286–1299. [CrossRef] [PubMed]
142. Symington, L.S. Mechanism and regulation of DNA end resection in eukaryotes. *Crit. Rev. Biochem. Mol. Biol.* **2016**, *51*, 195–212. [CrossRef] [PubMed]
143. Marini, F.; Rawal, C.C.; Liberi, G.; Pellicioli, A. Regulation of DNA Double Strand Breaks Processing: Focus on Barriers. *Front. Mol. Biosci.* **2019**, *6*, 55. [CrossRef] [PubMed]
144. Moore, J.K.; Haber, J.E. Capture of retrotransposon DNA at the sites of chromosomal double-strand breaks. *Nature* **1996**, *383*, 644–646. [CrossRef] [PubMed]
145. Teng, S.C.; Kim, B.; Gabriel, A. Retrotransposon reverse-transcriptase-mediated repair of chromosomal breaks. *Nature* **1996**, *383*, 641–644. [CrossRef] [PubMed]
146. Chon, H.; Sparks, J.L.; Rychlik, M.; Nowotny, M.; Burgers, P.M.; Crouch, R.J.; Cerritelli, S.M. RNase H2 roles in genome integrity revealed by unlinking its activities. *Nucleic Acids Res.* **2013**, *41*, 3130–3143. [CrossRef] [PubMed]
147. Cerritelli, S.M.; Crouch, R.J. RNase H2-RED carpets the path to eukaryotic RNase H2 functions. *DNA Repair (Amst.)* **2019**, *84*, 102736. [CrossRef]
148. Grossman, L.I.; Watson, R.; Vinograd, J. The Presence of Ribonucleotides in Mature Closed-Circular Mitochondrial DNA. *Proc. Natl. Acad. Sci. USA* **1973**, *70*, 3339–3343. [CrossRef]
149. Wong-Staal, F.; Mendelsohn, J.; Goulian, M. Ribonucleotides in closed circular mitochondrial DNA from HeLa cells. *Biochem. Biophys. Res. Commun.* **1973**, *53*, 140–148. [CrossRef]
150. Miyaki, M.; Koide, K.; Ono, T. RNase and alkali sensitivity of closed circular mitochondrial DNA of rat ascites hepatoma cells. *Biochem. Biophys. Res. Commun.* **1973**, *50*, 252–258. [CrossRef]
151. Kolodner, R.; Warner, R.C.; Tewari, K.K. The presence of covalently linked ribonucleotides in the closed circular deoxyribonucleic acid from higher plants. *J. Biol. Chem.* **1975**, *250*, 7020–7026. [PubMed]
152. Falkenberg, M. Mitochondrial DNA replication in mammalian cells: Overview of the pathway. *Essays Biochem.* **2018**, *62*, 287–296. [PubMed]
153. Yasukawa, T.; Kang, D. An overview of mammalian mitochondrial DNA replication mechanisms. *J. Biochem.* **2018**, *164*, 183–193. [CrossRef] [PubMed]
154. Wanrooij, P.H.; Chabes, A. Ribonucleotides in mitochondrial DNA. *FEBS Lett.* **2019**, *593*, 1554–1565. [CrossRef] [PubMed]
155. Wanrooij, S.; Fusté, J.M.; Farge, G.; Shi, Y.; Gustafsson, C.M.; Falkenberg, M. Human mitochondrial RNA polymerase primes lagging-strand DNA synthesis in vitro. *Proc. Natl. Acad. Sci. USA* **2008**, *105*, 11122–11127. [CrossRef] [PubMed]
156. Wanrooij, P.H.; Uhler, J.P.; Shi, Y.; Westerlund, F.; Falkenberg, M.; Gustafsson, C.M. A hybrid G-quadruplex structure formed between RNA and DNA explains the extraordinary stability of the mitochondrial R-loop. *Nucleic Acids Res.* **2012**, *40*, 10334–10344. [CrossRef]

157. Yasukawa, T.; Reyes, A.; Cluett, T.J.; Yang, M.Y.; Bowmaker, M.; Jacobs, H.T.; Holt, I.J. Replication of vertebrate mitochondrial DNA entails transient ribonucleotide incorporation throughout the lagging strand. *EMBO J.* **2006**, *25*, 5358–5371. [CrossRef]
158. Reyes, A.; Melchionda, L.; Nasca, A.; Carrara, F.; Lamantea, E.; Zanolini, A.; Lamperti, C.; Fang, M.; Zhang, J.; Ronchi, D.; et al. RNASEH1 Mutations Impair mtDNA Replication and Cause Adult-Onset Mitochondrial Encephalomyopathy. *Am. J. Hum. Genet.* **2015**, *97*, 186–193. [CrossRef]
159. Wanrooij, P.H.; Engqvist, M.K.M.; Forslund, J.M.E.; Navarrete, C.; Nilsson, A.K.; Sedman, J.; Wanrooij, S.; Clausen, A.R.; Chabes, A. Ribonucleotides incorporated by the yeast mitochondrial DNA polymerase are not repaired. *Proc. Natl. Acad. Sci. USA* **2017**, *114*, 12466–12471. [CrossRef]
160. Berglund, A.-K.; Navarrete, C.; Engqvist, M.K.M.; Hoberg, E.; Szilagyi, Z.; Taylor, R.W.; Gustafsson, C.M.; Falkenberg, M.; Clausen, A.R. Nucleotide pools dictate the identity and frequency of ribonucleotide incorporation in mitochondrial DNA. *PLoS Genet.* **2017**, *13*, e1006628. [CrossRef] [PubMed]
161. Moss, C.F.; Rosa, I.D.; Hunt, L.E.; Yasukawa, T.; Young, R.; Jones, A.W.E.; Reddy, K.; Desai, R.; Virtue, S.; Elgar, G.; et al. Aberrant ribonucleotide incorporation and multiple deletions in mitochondrial DNA of the murine MPV17 disease model. *Nucleic Acids Res.* **2017**, *45*, 12808–12815. [CrossRef] [PubMed]
162. Torregrosa-Muñumer, R.; Forslund, J.M.E.; Goffart, S.; Pfeiffer, A.; Stojkovič, G.; Carvalho, G.; Al-Furoukh, N.; Blanco, L.; Wanrooij, S.; Pohjoismäki, J.L.O. PrimPol is required for replication reinitiation after mtDNA damage. *Proc. Natl. Acad. Sci. USA* **2017**, *114*, 11398–11403. [CrossRef] [PubMed]
163. Krasich, R.; Copeland, W.C. DNA polymerases in the mitochondria A critical review of the evidence. *Front. Biosci.* **2017**, *22*, 692–709.
164. Morley, S.A.; Ahmad, N.; Nielsen, B.L. Plant organelle genome replication. *Plants* **2019**, *8*, 358. [CrossRef] [PubMed]
165. Yang, Z.; Hou, Q.; Cheng, L.; Xu, W.; Hong, Y.; Li, S.; Sun, Q. RNase H1 cooperates with DNA gyrases to restrict R-loops and maintain genome integrity in arabidopsis chloroplasts. *Plant Cell* **2017**, *29*, 2478–2497. [CrossRef] [PubMed]
166. Kuciński, J.; Kmera, A.; Rowley, M.J.; Khurana, P.; Nowotny, M.; Wierzbicki, A.T. Functional characterization of RNase H1 proteins in Arabidopsis thaliana. *bioRxiv* **2019**, 662080. [CrossRef]
167. Miyabe, I.; Kunkel, T.A.; Carr, A.M. The Major Roles of DNA Polymerases Epsilon and Delta at the Eukaryotic Replication Fork Are Evolutionarily Conserved. *PLoS Genet.* **2011**, *7*, e1002407. [CrossRef]
168. Clausen, A.R.; Williams, J.S.; Kunkel, T.A. Measuring ribonucleotide incorporation into DNA in vitro and in vivo. *Methods Mol. Biol.* **2015**, *1300*, 123–139.
169. Zhou, Z.-X.; Williams, J.S.; Kunkel, T.A. Studying Ribonucleotide Incorporation: Strand-specific Detection of Ribonucleotides in the Yeast Genome and Measuring Ribonucleotide-induced Mutagenesis. *J. Vis. Exp.* **2018**, *137*, e58020. [CrossRef]
170. Kind, B.; Wolf, C.; Engel, K.; Rapp, A.; Cristina Cardoso, M.; Lee-Kirsch, M.A. Single Cell Gel Electrophoresis for the Detection of Genomic Ribonucleotides. *Methods Mol. Biol.* **2018**, *1672*, 311–318.
171. Hiller, B.; Achleitner, M.; Glage, S.; Naumann, R.; Behrendt, R.; Roers, A. Mammalian RNase H2 removes ribonucleotides from DNA to maintain genome integrity. *J. Exp. Med.* **2012**, *209*, 1419–1426. [CrossRef]
172. Meroni, A.; Nava, G.M.; Sertic, S.; Plevani, P.; Muzi-Falconi, M.; Lazzaro, F. Measuring the Levels of Ribonucleotides Embedded in Genomic DNA. *Methods Mol. Biol.* **2018**, *1672*, 319–327. [PubMed]
173. Reijns, M.A.M.; Kemp, H.; Ding, J.; Marion de Procé, S.; Jackson, A.P.; Taylor, M.S. Lagging-strand replication shapes the mutational landscape of the genome. *Nature* **2015**, *518*, 502–506. [CrossRef] [PubMed]
174. Clausen, A.R.; Lujan, S.A.; Burkholder, A.B.; Orebaugh, C.D.; Williams, J.S.; Clausen, M.F.; Malc, E.P.; Mieczkowski, P.A.; Fargo, D.C.; Smith, D.J.; et al. Tracking replication enzymology in vivo by genome-wide mapping of ribonucleotide incorporation. *Nat. Struct. Mol. Biol.* **2015**, *22*, 185–191. [CrossRef] [PubMed]
175. Daigaku, Y.; Keszthelyi, A.; Müller, C.A.; Miyabe, I.; Brooks, T.; Retkute, R.; Hubank, M.; Nieduszynski, C.A.; Carr, A.M. A global profile of replicative polymerase usage. *Nat. Struct. Mol. Biol.* **2015**, *22*, 192–198. [CrossRef] [PubMed]
176. Gombolay, A.L.; Vannberg, F.O.; Storici, F. Ribose-Map: A bioinformatics toolkit to map ribonucleotides embedded in genomic DNA. *Nucleic Acids Res.* **2019**, *47*. [CrossRef]
177. Zatopek, K.M.; Potapov, V.; Maduzia, L.L.; Alpaslan, E.; Chen, L.; Evans, T.C.; Ong, J.L.; Ettwiller, L.M.; Gardner, A.F. RADAR-seq: A RAre DAmage and Repair sequencing method for detecting DNA damage on a genome-wide scale. *DNA Repair (Amst.)* **2019**, *80*, 36–44. [CrossRef]

178. Vanoosthuyse, V. Strengths and Weaknesses of the Current Strategies to Map and Characterize R-Loops. *Non-Coding RNA* **2018**, *4*, 9. [CrossRef]
179. Phillips, D.D.; Garboczi, D.N.; Singh, K.; Hu, Z.; Leppla, S.H.; Leysath, C.E. The sub-nanomolar binding of DNA-RNA hybrids by the single-chain Fv fragment of antibody S9.6. *J. Mol. Recognit.* **2013**, *26*, 376–381. [CrossRef]
180. Hartono, S.R.; Malapert, A.; Legros, P.; Bernard, P.; Chédin, F.; Vanoosthuyse, V. The Affinity of the S9.6 Antibody for Double-Stranded RNAs Impacts the Accurate Mapping of R-Loops in Fission Yeast. *J. Mol. Biol.* **2018**, *430*, 272–284. [CrossRef]
181. König, F.; Schubert, T.; Längst, G. The monoclonal S9.6 antibody exhibits highly variable binding affinities towards different R-loop sequences. *PLoS ONE* **2017**, *12*, e0178875. [CrossRef] [PubMed]
182. Nowotny, M.; Cerritelli, S.M.; Ghirlando, R.; Gaidamakov, S.A.; Crouch, R.J.; Yang, W. Specific recognition of RNA/DNA hybrid and enhancement of human RNase H1 activity by HBD. *EMBO J.* **2008**, *27*, 1172–1181. [CrossRef] [PubMed]
183. Molès, J.-P.; Griez, A.; Guilhou, J.-J.; Girard, C.; Nagot, N.; Van de Perre, P.; Dujols, P. Cytosolic RNA:DNA Duplexes Generated by Endogenous Reverse Transcriptase Activity as Autonomous Inducers of Skin Inflammation in Psoriasis. *PLoS ONE* **2017**, *12*, e0169879. [CrossRef]
184. Shen, W.; Sun, H.; De Hoyos, C.L.; Bailey, J.K.; Liang, X.H.; Crooke, S.T. Dynamic nucleoplasmic and nucleolar localization of mammalian RNase H1 in response to RNAP I transcriptional R-loops. *Nucleic Acids Res.* **2017**, *45*, 10672–10692. [CrossRef] [PubMed]
185. Stork, C.T.; Bocek, M.; Crossley, M.P.; Sollier, J.; Sanz, L.A.; Chédin, F.; Swigut, T.; Cimprich, K.A. Co-transcriptional R-loops are the main cause of estrogen-induced DNA damage. *Elife* **2016**, *5*, e17548. [CrossRef] [PubMed]
186. Manzo, S.G.; Hartono, S.R.; Sanz, L.A.; Marinello, J.; De Biasi, S.; Cossarizza, A.; Capranico, G.; Chedin, F. DNA Topoisomerase I differentially modulates R-loops across the human genome. *Genome Biol.* **2018**, *19*, 100. [CrossRef] [PubMed]
187. Lockhart, A.; Pires, V.B.; Bento, F.; Kellner, V.; Luke-Glaser, S.; Yakoub, G.; Ulrich, H.D.; Luke, B. RNase H1 and H2 Are Differentially Regulated to Process RNA-DNA Hybrids. *Cell Rep.* **2019**, *29*, 2890–2900. [CrossRef] [PubMed]
188. Bhatia, V.; Barroso, S.I.; García-Rubio, M.L.; Tumini, E.; Herrera-Moyano, E.; Aguilera, A. BRCA2 prevents R-loop accumulation and associates with TREX-2 mRNA export factor PCID2. *Nature* **2014**, *511*, 362–365. [CrossRef]
189. Dumelie, J.G.; Jaffrey, S.R. Defining the location of promoter-associated R-loops at near-nucleotide resolution using bisDRIP-seq. *Elife* **2017**, *6*, 1–39. [CrossRef]
190. Sanz, L.A.; Hartono, S.R.; Lim, Y.W.; Steyaert, S.; Rajpurkar, A.; Ginno, P.A.; Xu, X.; Chédin, F. Prevalent, Dynamic, and Conserved R-Loop Structures Associate with Specific Epigenomic Signatures in Mammals. *Mol. Cell* **2016**, *63*, 167–178. [CrossRef]
191. Xu, W.; Xu, H.; Li, K.; Fan, Y.; Liu, Y.; Yang, X.; Sun, Q. The R-loop is a common chromatin feature of the Arabidopsis genome. *Nat. Plants* **2017**, *3*, 704–714. [CrossRef] [PubMed]
192. Chen, L.; Chen, J.Y.; Zhang, X.; Gu, Y.; Xiao, R.; Shao, C.; Tang, P.; Qian, H.; Luo, D.; Li, H.; et al. R-ChIP Using Inactive RNase H Reveals Dynamic Coupling of R-loops with Transcriptional Pausing at Gene Promoters. *Mol. Cell* **2017**, *68*, 745–757. [CrossRef] [PubMed]
193. Chen, J.Y.; Zhang, X.; Fu, X.D.; Chen, L. R-ChIP for genome-wide mapping of R-loops by using catalytically inactive RNASEH1. *Nat. Protoc.* **2019**, *14*, 1661–1685. [CrossRef] [PubMed]
194. Halász, L.; Karányi, Z.; Boros-Oláh, B.; Kuik-Rózsa, T.; Sipos, É.; Nagy, É.; Mosolygó-L, Á.; Mázló, A.; Rajnavölgyi, É.; Halmos, G.; et al. RNA-DNA hybrid (R-loop) immunoprecipitation mapping: An analytical workflow to evaluate inherent biases. *Genome Res.* **2017**, *27*, 1063–1073.